PYROLYSIS PROCESS OPTIMISATION TO MAXIMISE LIMONENE PRODUCTION FROM WASTE TYRES

by

Ntandoyenkosi Malusi Mkhize

Dissertation presented for the Degree

of

DOCTOR OF PHILOSOPHY

(Chemical Engineering)

in the Faculty of Engineering

at Stellenbosch University

Supervisor

Professor Johann Ferdinand Görgens

Co-Supervisors

Professor Percy van der Gryp

Doctor Bart Danon

March 2018

Declaration

By submitting this dissertation electronically, I declare that the entirety of the work contained therein is my own, original work, that I am the sole author thereof (save to the extent explicitly otherwise stated), that reproduction and publication thereof by Stellenbosch University will not infringe any third-party rights and that I have not previously in its entirety or in part submitted it for obtaining any qualification.

Date: March 2018

This dissertation includes four original papers published in peer reviewed journals and two unpublished publication as well a patent. The development and writing of the papers (published and unpublished) were the principal responsibility of myself and, for each of the cases where this is not the case, a declaration is included in the dissertation indicating the nature and extent of the contributions of co-authors.

Abstract

Globally, increasing waste tyre generation is a major economic and environmental challenge. Economic challenges include depleting natural resources and rising crude oil prices from which synthetic rubbers are derived. Environmental problems are mainly associated with large piles of the waste tyres. Waste tyres are characterised by resistance to degradation under typical environmental conditions, high pollution emissions from fires, soil and water pollutants leakage, breeding grounds for venomous insects, such as, snakes and spiders.

Among conventional methods used to reduce waste tyre stock piles include: i) blending the tyre crumb with asphalt for civil works, such as, road construction, ii) combustion for generation of the electricity and/or steam, iii) and reuse in manufacturing of plastic and rubber products, such as, filler. However, the rate of waste tyre generation surpasses consumption capacity by these techniques. Moreover, these techniques are yet to be commercialised as they are fraught with economic and environmental challenges. These challenges include capital and operating costs of the production facilities and toxic compound emissions elimination requirements. One of the promising processing methods for waste tyres valorisation is to produce valuable chemicals (mainly DL-limonene) through increasing their content in the tyre derived oil (TDO) and then use remaining TDO for energy recovery.

In the current study modification of the existing waste tyre pyrolysis processes, and development of the novel methods critical to maximising the DL-limonene yield in the pyrolysis oil, was achieved. Additionally, improvement in the total TDO yield and quality [high quality characterised by high DL-limonene content but less heteroatom compounds (nitrogen-, oxygen- and sulphur-compounds, mainly benzothiazole)] was observed. DL-limonene is a natural occurring compound and its composition is high in citrus fruit peels derived-oil at more than 80 wt.%. The market price of the DL-limonene ranges between 2.5 and 30 US$/kg depending on the purity. DL-limonene is an important component in the industrial formulations of solvents, resins, and adhesives. While benzothiazole is a main component in the processing additives used in the manufacturing of the tyres.

The approach of the current study entails investigating i) various means to maximise DL-limonene yield in the pyrolysis reactor, ii) improving the DL-limonene yield from condensation of the hot pyrolysis volatiles, and iii) substantially reducing the production of most of the heteroatom compounds (nitrogenous, oxygenous and sulphurous containing compounds) to obtain TDO consisting high amounts of DL-limonene. This approached allowed study of the effect of i) temperature, ii) heating rate, iii) residence time of the hot volatiles in the hot reaction zones, and iv) condensation type and cooling

rate of the hot volatiles. These operating conditions parameters were varied by interchanging slow, and flash pyrolysis reactor as well as tube-and-shell condenser and quenching condenser.

Iqoqa

Emhlabeni jikelele, ukukhiqizeka kwemfucuza yamathayi kuyinselelo enkulu yezomnotho, kanjalo nesimo semvelo. Izinselelo zomnotho zihlanganisa ukufinyelela esiphethweni kwamagugu emvelo nokukhuphuka kwamanani amafutha ambiwa emajukujukwini omhlaba ayisisekelo ekwakheni imikhiqizo ehlukahlukene yenjoloba. Ukwanda komthamo wemfucuza yamathayi iyona mbangela enkulu ezingqinambeni zesimo semvelo. Imfucuza yamathayi ayivuthuluki ngokwemvelo ngaphansi kwesimo esijwayelekile, uma yokheleka ngomlilo kukhiqizeka imisizi engcolisa umoya, kumunceke imisizi eyingozi enhlabathi nasemanzi, aba ikhaya lokukhosela lezinambuzane ezonobuthi, njengezinyoka nezicabucabu.

Phakathi kwezinqubo ezivamile ezisetshenziselwa ukwehliswa imithamo yemfucuza yamathayi kufaka: i) ukumbandakanya amathayi acoyiselekile (akhishwe ingxenye ewocingo nesakotini) nemikhiqizo ewomgogodla esetstenziswa emisebenzini yezakhiwo, njengokwakhiwa kwemigwaqo, ii) ukushiswa ekuvulelekeni ukuze kukhiqizwe ugesi nomusi, iii) kanye nokusetshenziswa njengesisekelo ekukhiqizeni amathayi, njengesisekelo somkhiqizo. Kodwa-ke, isivinini sokukhiqizwa kwemfucuza yamathayi singaphezu kwengqalasisinda yokuwamumatha nxa kusetshenziswa lezi zindlela esezibaluliwe. Ngaphezu kwalokho, lezi zindlela kusamele ziphucululwe ukuze zimelane nemithamo emikhulukazi njengoba zisabandanyeka ezinselelweni zezomnotho nezemvelo. Lezi zinselelo zibandakanya izindleko zokwakha kanjalo nokuqinisekisa ukusebenza kwengqalasizinda kanye nezidingo sokuvimbela ukusabalala kwemisizi enobuthi. Enye yezindlela enesasasa elikhulu ekuphenduleni imfucuza yamathayi ekubeni imikhiqizo eletha inzuzo ukuba kukhiqizwe imisizi eyigugu (njenge DL-limonene) ngokuba kwenyuswe inani lawo kumkhiqizo osaluketshezi wethayi (TDO) bese kusetshenziswa i-TDO esele njengesiphehli mandla.

Kulolu cwaningo kube impumelelo ukuguqula izindlela ezijwayelekile zokushisa imfucuza yamathayi endaweni evalelekile, kanjalo nokusungula izindlela ezintsha eziwumgogodla ekwandisweli kokukhiqizwa kwe-DL-limonene. Okunye okuqasheliwe, ukuthuthukiswa komkhiqizo we-TDO kanye nokucwengeka kwayo [ukucwengeka kungamataniswa nobuningi bengxenye ye-DL-limonene kwi-TDO kodwa ibe semazingeni aphansi imisizi enyama nambana (imisizi enesakhiwo se-nitrogen, -oksijini, kanye nesibabule, kakhulukazi i-benzothiazole]. I- DL-limonene ikhiqizeka ngokwemvelo futhi inani layo oketshezini olukhiqizwa emakhasini ezithelo ze-citrus iba ngobuningi ngaphezu kwengxenye engama-80 %. Inani lentengiso le-DL-limonene liphakathi kuka-2.5 no-30 US$/kg kuncike

ekucwengekeni kwayo. I-DL-limonene iyisici esibalulekile ezimbonini ezikhiqiza uketshezi lokuhlamba, elokwenza amafutha amakha, kanye nezinamathiseli. Ekubeni i-benzothiazole iyingxenye esemqoka ezithathiseleni ezilekelela ukukhiqizwa kwamathayi.

Indlela okwenziwe ngayo lolu cwaningo kubandakanya: i) izindlela ezahlukahlukene zokwandisa isivuno se-DL-limonene esitsheni sokushisa amathayi ngokuvalelekile, ii) ukuthuthukisa isivuno se-DL-limonene ngesikhathi isuswa esimweni somusi siya oketshezini, futhi iii) nokwehla ngamandla kokukhiqizwa kwemisi enyama nambana (eyizingxube ne-nitrogen, -oksijini, kanye nesibabule) ukuze kukhiqizeke uketshezi oluqukethe inani eliphakeme le-DL-limonene. Lendlela yocwaningo ivumele ukuba kubonakaliseke umthelela i) wezinga lokushisa noma ukubanda, ii) isivinini sokwenyuswa kwezinga lokushisa, iii) isikhathi esichithwa uketshezi lisesimweni somusi ezingxenyeni zovuthondaba ezishisayo esitsheni sokushisa amathayi ngokuvalelekile, kanye iv) nendlela yokuguqula futhi kupholiswe umkhiqizo osaketshezi lusuka esimweni somusi. Lezizimo zokusebenza ziguquguqulwe ngokushintshanisa izimbiza zokushisa amathayi ekuvalelekeni ngesivinini esincane, kanye ngokushesha kanjalo kusetshenzisw izitsha ezivumela ukuthintana kanye nokungathintani koketshezi lokubandisa noketshezi lwethayi olusesimweni somusi ngesikhathi sokuphendulwa nokupholiswa kwalo.

Opsomming

Globaal is die toenemende afvalstofopwekking 'n groot ekonomiese en omgewingsuitdaging. Ekonomiese uitdagings sluit in die verswakking van natuurlike hulpbronne en stygende ruolie pryse waaruit sintetiese rubbers afgelei word. Afvalbande word gekenmerk deur weerstand teen afbreking onder tipiese omgewingsomstandighede, hoë besoedeling veroorsaak deur vure, grond- en waterbesoedelingslekkasie, teelareas vir giftige insekte, soos slange en spinnekoppe.

Onder die konvensionele metodes wat gebruik word om afvalstortingstowwe te verminder, sluit in: i) die bandkrummel met asfalt vir siviele werke soos padkonstruksie, ii) verbranding vir die opwekking van elektrisiteit en / of stoom, iii) en hergebruik in die vervaardiging van plastiek en rubber produkte, soos vulsel. Die verlagingskoers van afvalmateriaal oorskry egter die verbruikskapasiteit deur hierdie tegnieke. Daarbenewens word hierdie tegnieke nog nie gekommersialiseer nie, aangesien hulle vol ekonomiese en omgewingsuitdagings is. Hierdie uitdagings sluit in kapitaal- en bedryfskoste van die produksiefasiliteite en eliminasievereistes vir giftige verbinding. Een van die belowende verwerkingsmetodes vir valorisering van afvalbande is om waardevolle chemikalieë (hoofsaaklik dl-limoneen) te produseer deur hul inhoud in die bande afgeleide olie (TDO) te verhoog en gebruik dan die oorblywende TDO vir energieherwinning.

In die huidige studie aanpassing van die bestaande afvalpyrolyse prosesse, en die ontwikkeling van die nuwe metodes wat krities is om die dl-limonene opbrengs in die pirolise olie te vermeerder, is bereik. Daarbenewens is die verbetering van die totale TDO opbrengs en kwaliteit [hoë kwaliteit gekenmerk deur hoë dl-limonieninhoud, maar minder iseroatomverbindings (stikstof-, suurstof- en swaelverbindings, hoofsaaklik bensotiasool)] is waargeneem . DL-limonien is 'n natuurlike voorkomende verbinding en die samestelling daarvan is hoog in sitrusvrugte, afgeleide olie by meer as 80% weeg. Die markprys van die dl-limonene wissel tussen 2,5 en 30 US $ / kg afhangende van die suiwerheid. DL-limonene is 'n belangrike komponent in die industriële formulasies van oplosmiddels, harpuis en bindmiddels. Terwyl bensotiasool 'n hoofkomponent is in die verwerkingsadditiewe wat gebruik word in die vervaardiging van die bande.

Die benadering van die huidige studie behels die ondersoek van i) verskeie maniere om dl-limonene opbrengs in die pyrolysereaktor te vermeerder, ii) die dl-limonien opbrengs te verbeter deur kondensasie van die warm pyrolyse-vlugtige bestanddele, en iii) die produksie van die meeste van die heteroatomverbindings (stikstofagtige, suurstof- en swaelhoudende bevattende verbindings) om TDO bestaande hoë hoeveelhede dl-limone te verkry. Hierdie benaderde studie van die effek van i) temperatuur, ii) verhittingstempo, iii), verblyf tyd van die warm vlugtige stowwe in die warm reaksie sones, en iv) kondensasie tipe en koelsnelheid van die warm vlugtige stowwe. Hierdie parameters vir die bedryfstoestande is gevarieer deur die stadige, flits-pyrolyse-reaktor sowel as die buis-en-dop-kondensor en die sluiting van die kondensator te wissel.

Acknowledgements

This work is based on the research supported in part by REDISA (Recycling and Economic Development Initiative of South Africa). The author acknowledges that opinions, findings and conclusions or recommendations expressed are those of the author, and the sponsors accepts no liability whatsoever in this regard.

I am grateful to REDISA programme research group members who were present during development of the programme, for the chapters in the present dissertation consist of the ideas developed during group discussion sessions. The research group supervisors and experts led by my supervisor Prof. Gorgens played an essential role not only in this work, but also in all of the research and consulting that led to it. They are, Profs van der Gryp, Schwarz, de Villiers, and Woolard, Drs Danon, Godongwana and Tredoux as well Mr van Niekerk.

My supervisors Profs Gorgens, van der Gryp and Dr Danon, influenced my reasoning over the period as both my mentors and colleagues. Special mention must be given to the postgraduate colleagues for they have been a great source of both encouragement and support. Particularly, Sithandile, our collaborative work, under supervision of Prof. de Villiers and Dr. Tredoux, was outstanding and I shudder to think about what I would have done without him and the Department of Analytical Chemistry in general. Also, Cleopatra, whose support offered towards submission of the current work was tremendous.

I offer my gratitude and unending loyalty to Drs Lopez, Alvarez and Amutio and Profs Olazar and Aguado from the Department of Chemical Engineering, University of the Basque Country, Spain for the collaboration we had which was established during the course of the project.

Tremendous support of those from the Department of Processes Engineering is acknowledged, particularly workshop, analytical laboratories, and administration department personnel.

Lastly but not least my family, naturally, nothing in this dissertation could have been developed without their support, especially Nothando for helping with Iqoqa and critical reasoning. My elders and those now ancestors who occupied the space between us in all walk of life, maximum respect, all your greatness and unrecognised accomplishments emulated has been reflected in the present work. I am my ancestor and my ancestor is me.

Table of contents

Nomenclature

A	Pre-exponential factor
AC	Activated carbon
ANOVA	Analysis of variance
ArN	Nitrogenated aromatic
ArNS	Nitrosulphurated aromatics
ArO	Oxygenated aromatic
ASTM	American society for testing and materials
BFBR	Bubbling fluidised bed reactor
BR	Polybutadiene rubber
BTX	Benzene, Toluene and Xylene
BTXE	Benzene, Toluene, Xylene and Ethylbenzene
C	Carbon
CB	Carbon black
CCD	Central composite design
CSBR	Conical spouted bed reactor
DEA	Department of Environmental Affairs
DL-limonene	D- and L-isomers of limonene
DTA	Derivative thermal analysis
DTG	Derivative thermogravimetric
E_a	Activation energy
EU	European Union
FBR	Fixed bed reactor
g	Grams
GC	Gas chromatography
GC/MS	Gas chromatography/mass spectrometry
GR-S	Government rubber-styrene
H	Hydrogen (elemental)
HHV	High heating rate
IIWTMP	Integrated Industry Waste Tyre Management Plan
kg	Kilograms
L	Litres
L/min	Litres per minute
M_c	Molecular weight between cross-links
mL	Milli-litres

MLR_i	Mass loss reaction
MS	Mass spectrometry
MT	Motorcycle tyre
N	Nitrogen (elemental)
n	Reaction order
Na_2CO_3	Sodium carbonate
NaOH	Sodium hydroxide
NAr	Non-aromatic
NArO	Oxygenated non-aromatic
NO_x	Nitrogen oxides
NPT	National pie taper
NR	Natural rubber
NRF	National research foundation
O	Oxygen (elemental)
PAHs	Polycyclic aromatic hydrocarbons
PCT	Passenger car tyre
PM	Particulate matter
ppm	Parts per million
R	Molar gas constant
REDISA	Recycling and Economic Development Initiative South Africa
S	Sulphur
SBR	Styrene-butadiene rubber
$scCO_2$	Supercritical carbon dioxide
SEM	Secondary electron multiplier
SO_2	Sulphur dioxide
SS	Stainless steel
TDO	Tyre derived oil
T_f	Fusion temperature
TG	Thermo gravimetric
T_g	Glass transition temperature
TT	Truck tyre
US$	United States of America dollar
VOCs	Volatile organic compounds
WFL	Williams-Landel-Ferry equation
wt.%	Mass basis percent
ΔH_f	Heat of fusion

CHAPTER 1. INTRODUCTION

1.1 Contextual background

Increasing waste tyre generation is a major economic and environmental challenge globally. Economic challenges include both the depletion of natural resources and crude oil from which synthetic rubbers are derived [1-6]. Environmental problems are mainly associated with the large piles of stocked waste tyres, which are very resistance to degradation under ambient conditions, and include e.g. high pollution emissions fires, soil and water pollutant leakage, breeding grounds for the pests, such as, rats or mosquitoes [2-4,7-9].

Conventional methods used to reduce waste tyre stock-piles include: blending the crumb rubber with asphalt for e.g., road construction, combustion for generation of electricity and/or steam, reuse in manufacturing of plastic and rubber product as a filler. However, the rate of waste tyre generation surpasses the consumption capacity by these conventional techniques significantly [3,4]. Moreover, these techniques are yet to be technically or commercially matured as they are fraught with economic and environmental challenges. Economic and environmental challenges include high capital and operating costs of the production facilities and toxic compounds emissions, respectively. A promising alterative process is pyrolysis of waste tyres to recover both energy and valuable chemicals from the products [3,4].

Waste tyre pyrolysis entails the thermal devolatilisation of the organic compounds present in the waste tyre under inert conditions, to produce gaseous, liquid and solid products. Pyrolysis of waste tyres has been extensively researched at laboratory scale. In South Africa, there is even a handful of commercial tyre-pyrolysis plants, such as, Green Premium Fuel, Metsa, and Milvinetrix to mention but a few. However, commercialisation of the pyrolysis technology in many regions is still has some challenges due to regional policies that lack clear differentiation among waste tyre incineration, combustion and pyrolysis. Thus, pyrolysis is regarded as an environmental unfavourable process and its characteristics are mistakenly associated with severe environmental emissions that are associated with incineration or combustion. Moreover, research focused on the production of the fuels from waste tyres pyrolysis. This has led to pyrolysis being perceived as a capital-intensive process which converts a single solid fuel into multi-phase low-grade fuels [10,11].

The complex chemical composition and yet to be expounded kinetic mechanism of the reactions involved in waste tyre pyrolysis, have both impeded industrial acceptance of the technology. Moreover, the markets

for the liquid and solid pyrolysis products are yet to be established. Waste tyre pyrolysis liquid fraction products, also known as tyre derived oil (TDO) compete with crude oil derived fuels at its current relatively low prices. The waste tyre pyrolysis solid fraction (char) is characterised by high content of impurities (e.g. ash content) [5].

Nevertheless, high contents of carbon and hydrogen in waste tyres have given preference to pyrolysis as a potential source of energy, materials and chemicals [12]. A recent shift has been to produce valuable chemicals from waste tyre pyrolysis, while using the remaining TDO as a fuel [13-16]. This entails two approaches, viz. the maximisation of the formation of valuable chemicals during the pyrolysis of the waste tyres [53], and during condensation of the hot volatiles from the reactor [24]. Additionally, research interests have also been to recover carbon black from waste tyre pyrolysis char. Some of the pyrolysis process conditions, such as, reactor type, operating temperature, pressure, heating rate, etc. are mainly examined. The effect of these operating conditions is on the production, recovery and quality of the carbon black. The objective is to meet set char products specifications to be readily recycled in the tyre manufacturing process.

Other researchers focused on the maximisation of the pyrolysis liquid fraction. It is known that among the waste tyre pyrolysis products, i.e., (pyro) gas, tyre derived oil (TDO) and (pyro) char, the TDO is the most important fraction for energy recovery (engine fuels) and for the recovery of valuable chemical products (e.g. dipentene or DL-limonene) [17]. High TDO yields of up to 60 wt.% have been reported [7,18-20]. However, the chemical composition of the TDO is very complex and differs with various pyrolysis operating conditions as well with the pyrolysis reactor configuration. Moreover, separation of the valuable chemicals from the rest of the TDO is required. Consequently, there is not yet a universally optimal waste tyre pyrolysis process suitable for all requirements. Therefore, in the current study the main goal is to investigate optimal operating conditions of the pyrolysis process in order to maximise chemicals and energy recovery from waste tyres.

This study is divided into three sections. The first stage involves investigating the pyrolysis operating conditions, i.e., temperature and heating rate, to maximise the yield and concentration of the L- and D-isomers of limonene (DL-limonene) in the TDO. Secondly, kinetic mechanisms and thermal analysis studies of the rubbery materials to maximise DL-limonene formation from waste tyre pyrolysis. Finally, effect of the method of condensation and cooling of the hot volatiles from waste tyre pyrolysis is assessed by comparing tube-and-shell and quenching condensers.

1.2 Structure of the dissertation

The current dissertation consists of ten chapters:

In CHAPTER 2 (Literature review), a detailed background and literature review of conventional methods for waste tyre recycling and pyrolysis methods is presented. Scientific data on the typical composition of waste tyre and reaction conditions in the waste tyres pyrolysis is discussed. Trends in conventional waste tyre pyrolysis processes equipment, reaction conditions and product fractions are reviewed. Characteristics of the pyrolysis products, particularly their chemical composition, are also investigated. The chapter concludes by presenting evidence showing that there is insufficient literature data on the effect of heating rate during the pyrolysis process, and on the treatment of hot volatiles from waste tyre pyrolysis, so as to maximise DL-limonene production.

CHAPTER 3 (Research objectives) elaborates on the aims and objectives, rationale, scope and hypothesis of the dissertation. The approach entails pointing out clearly how the current study overcomes or responses to the current shortcomings in the literature as well as novel waste tyre pyrolysis methods.

CHAPTER 4 (Effect of temperature and heating rate on Limonene production from waste tyres pyrolysis) discusses the effect of process operating parameters that have a significant impact on waste tyre pyrolysis, i.e. temperature and heating rate. The effect of these operating parameters is evaluated based on the DL-limonene yield (yield in the hot volatiles from pyrolysis reactor). Optimal pyrolysis conditions for maximum DL-limonene production from waste tyres pyrolysis in a slow pyrolysis reactor are presented in this chapter.

The kinetic mechanisms behind the formation of DL-limonene (depending on temperature and heating rate) are elaborated in CHAPTER 5 (Kinetic study of the effect of the heating rate on the waste tyre pyrolysis to maximise limonene production). The objective is to expand on the two competing polyisoprene depolymerisation pathways, i.e., allylic polyisoprene radicals depropagation to produce isoprene and intramolecular cyclization - scission to produce DL-limonene.

The focus in CHAPTER 6 (Condensation of the hot volatiles from waste tyre pyrolysis by quenching) is on the treatment of the hot volatiles from the pyrolysis reactor. The techniques by which the hot volatiles are condensed to yield the tyre derived oil (TDO) are investigated. Their impact on the DL-limonene yield and concentration in the TDO is explored by comparing two types of condensation techniques, i.e., a

conventional indirect tube-and-shell condenser, and direct contact between cooling fluid and hot volatiles using a quenching condenser. Using the latter system to improve TDO chemical composition, in terms of reduction in the concentration of heteroatom compounds, e.g., benzothiazole, was achieved, which improves not only recovery of the of the DL-limonene but also its quality as a potential liquid fuel.

In CHAPTER 7 (Various means of waste tyre pyrolysis to maximise DL-limonene production) various reactor types and different condensation techniques are integrated into one complete pyrolysis process for maximum DL-limonene yield from waste tyres incorporating the results of chapters 4 – 7. The results in this chapter thus covers a variety of process options, such as, slow and flash pyrolysis, slow and fast cooling rate of the hot volatiles as well as direct and indirect contact between the cooling fluid and the hot volatiles.

The main research findings of the current study are outlined in CHAPTER 8 (Main research project findings), while the recommendations are discussed in CHAPTER 9 (Recommendations).

The Appendix presented in CHAPTER 10 (Appendix) focuses on the additional work such as Patent as well the two publication papers that resulted from collaborating with the University of the Basque Country, Spain.

References

[1] B.J. Putman, S.N. Amirkhanian, Crumb rubber modification of binders: interaction and particle effects, Road Materials and Pavement Design. (2006).

[2] S. Ucar, S. Karagoz, A.R. Ozkan, J. Yanik, Evaluation of two different scrap tires as hydrocarbon source by pyrolysis, Fuel. 84 (2005) 1884-1892.

[3] S. Seidelt, M. Müller-Hagedorn, H. Bockhorn, Description of tire pyrolysis by thermal degradation behaviour of main components, J. Anal. Appl. Pyrolysis. 75 (2006) 11-18.

[4] R. Murillo, E. Aylón, M.V. Navarro, M.S. Callén, A. Aranda, A.M. Mastral, The application of thermal processes to valorise waste tyre, Fuel Process Technol. 87 (2006) 143-147.

[5] J.D. Martínez, N. Puy, R. Murillo, T. García, M.V. Navarro, A.M. Mastral, Waste tyre pyrolysis – A review, Renewable and Sustainable Energy Reviews. 23 (2013) 179-213.

[6] D. De, D. De, Processing and material characteristics of a reclaimed ground rubber tire reinforced styrene butadiene rubber, Materials Sciences and Applications. 2 (2011) 486-496.

[7] H. Pakdel, D.M. Pantea, C. Roy, Production of dl- limonene by vacuum pyrolysis of used tires, J. Anal. Appl. Pyrolysis. 57 (2001) 91-107.

[8] A.P. Smith, H. Ade, C.C. Koch, R.J. Spontak, Cryogenic mechanical alloying as an alternative strategy for the recycling of tires, Polymer. 42 (2001) 4453-4457.

[9] J. Karger-Kocsis, L. Meszaros, T. Barany, Ground tyre rubber (GTR) in thermoplastics, thermosets, and rubbers, J. Mater. Sci. 48 (2013) 1+.

[10] C. İlkılıç, H. Aydın, Fuel production from waste vehicle tires by catalytic pyrolysis and its application in a diesel engine, Fuel Process Technol. 92 (2011) 1129-1135.

[11] T. Gray, D. Humphrey, Scrap tires- handbook on recycling application and management for the U.S. and Mexico, (2010).

[12] I. Hita, M. Arabiourrutia, M. Olazar, J. Bilbao, J.M. Arandes, P. Castaño, Opportunities and barriers for producing high quality fuels from the pyrolysis of scrap tires, Renewable and Sustainable Energy Reviews. 56 (2016) 745-759.

[13] J.D. Martínez, M. Lapuerta, R. García-Contreras, R. Murillo, T. García, Fuel properties of tire pyrolysis liquid and its blends with diesel fuel, Energy and Fuels. 27 (2013) 3296-3305.

[14] N. Antoniou, A. Zabaniotou, Features of an efficient and environmentally attractive used tyres pyrolysis with energy and material recovery, Renewable and Sustainable Energy Reviews. 20 (2013) 539-558.

[15] P.T. Williams, Pyrolysis of waste tyres: A review, Waste Manage. 33 (2013) 1714-1728.

[16] A. Quek, R. Balasubramanian, Liquefaction of waste tires by pyrolysis for oil and chemicals—A review, J. Anal. Appl. Pyrolysis. 101 (2013) 1-16.

[17] B. Danon, P. Van Der Gryp, C.E. Schwarz, J.F. Görgens, A review of dipentene (dl-limonene) production from waste tire pyrolysis, J. Anal. Appl. Pyrolysis. 112 (2015) 1-13.

[18] H. PAKDEL, C. ROY, H. AUBIN, G. JEAN, S. COULOMBE, FORMATION OF DL-LIMONENE IN USED TIRE VACUUM PYROLYSIS OILS, Environ. Sci. Technol. 25 (1991) 1646-1648.

[19] G. Lopez, M. Olazar, M. Amutio, R. Aguado, J. Bilbao, Influence of tire formulation on the products of continuous pyrolysis in a conical spouted bed reactor, Energy and Fuels. 23 (2009) 5423-5431.

[20] M. Kyari, A. Cunliffe, P.T. Williams, Characterization of oils, gases, and char in relation to the pyrolysis of different brands of scrap automotive tires, Energy Fuels. 19 (2005) 1165-1173.

CHAPTER 2. LITERATURE REVIEW

2.1 Introduction

Burrueco et al. (2005) reported that production of the waste tyres in developed countries equals to approximately one waste tyre per capita per year [1]. Waste tyres are mainly disposed in landfills, particularly in countries that lack waste management strategies. Land filling as a waste tyres disposal method is fraught with challenges, such as, space inadequacy and accidental fires that result in high emissions of hazardous gases [2-4]. It is estimated that waste tyres in landfills can survive between 80 and 100 years without any noticeable degradation [3]. This is due to the tyre properties that are designed to withstand harsh mechanical and weather conditions, such as, ozone (the most damaging factor on the rubbers), light and bacteria. Thus, it is difficult to recycle and/or to further process waste tyres [1,3,5,6]. It is reported that waste tyres disposal is both an economic and environmental challenge [5].

In the developed countries, legislation that abolishes waste tyre landfilling has already been implemented [2]. For example, all European Union (EU) member states have been mandated to recover 65% of their waste tyres [7]. Moreover, in developing countries, establishment of waste tyre management plans are slowly being initiated. EU's waste tyre management plans includes, approval of the Integrated Industry Waste Tyre Management Plan (IIWTMP) by the Department of Environmental Affairs (DEA) of South Africa in 2009, which mandates all tyre manufactures in terms of the Waste Tyre Regulation to subscribe to it. The waste tyre management plan is a single-plan approach and it has avoided complications and shortcomings associated with conventional multiple-plan approaches. The DEA has appointed Recycling and Economic Development Initiative of South Africa (REDISA) to be the sole implementer of this plan, from 2012 to 2017.

The following is a summary of the EU Directives and Regulations related to the waste tyres and which may be beneficial to South Africa's IIWTMP [7]:

- Directive 75/442/EEC classifies waste tyres as non-hazardous waste.
- Directive 1999/31/EU prohibits land filling of whole and shredded waste tyres since July 2003 and July 2006, respectively.
- Directive 2000/532/EU, in addition to the classification of the waste tyres as a non-hazardous waste, it requires sorting of the waste tyres with code "16 01 03."
- Directive 2000/53/EU obliges removal of waste tyres from end-of-life vehicles.

- Directive 2000/76/EU sets maximum acceptable emission standards (as from 2002) for industries using waste tyres as an alternative energy source, such as, cement industries. It also sets new provisions applicable to cement kilns that co-incinerate waste tyres in their waste incineration feed.

2.2 Waste tyre composition

General waste tyre composition, including the functions of the different components, is depicted in Figure 2.1. However, waste tyre composition varies widely depending on the manufacturer, tyre type, and from country to country.

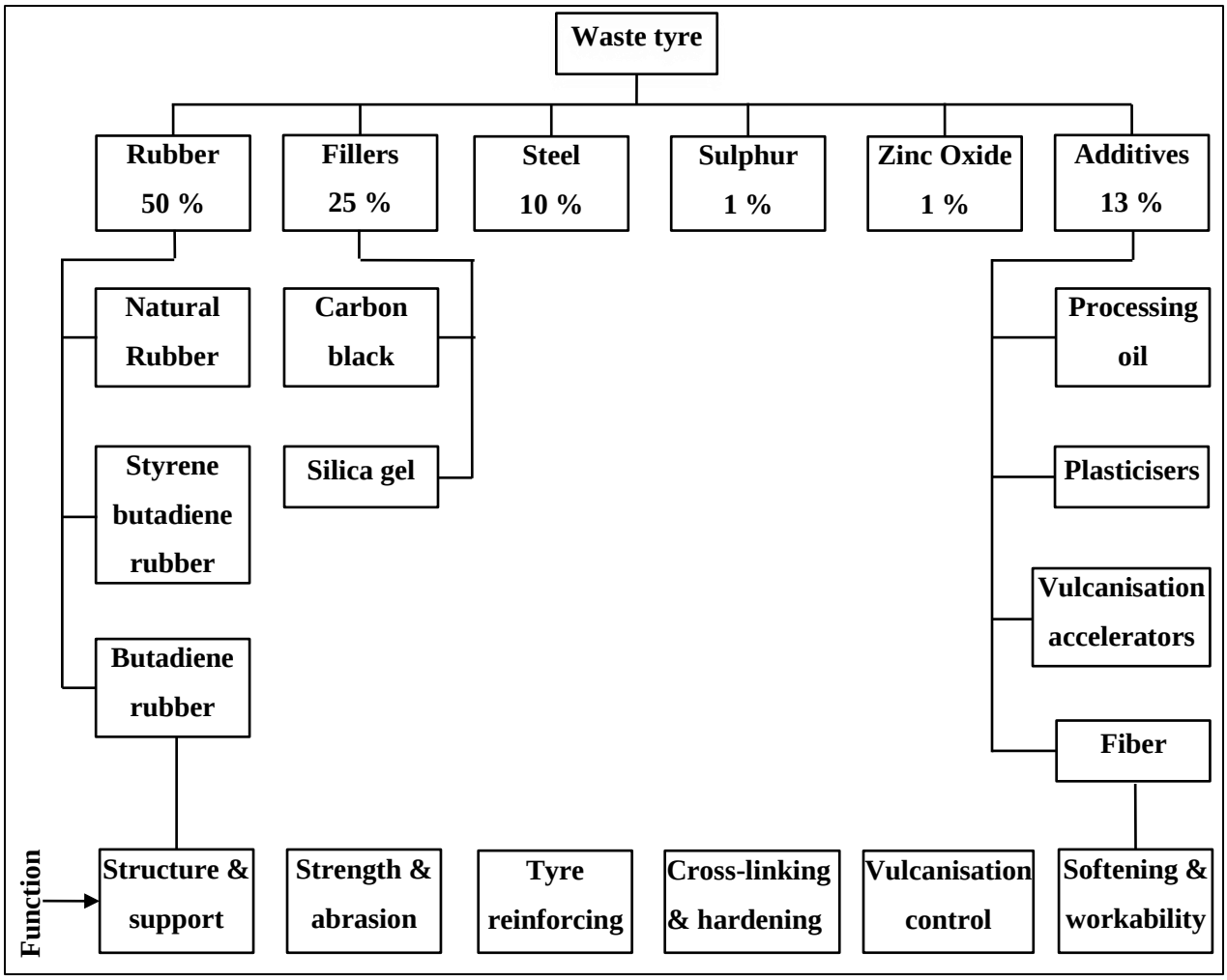

Figure 2.1: Main components of a waste tyre
Source: adapted from Evans and Evans (2006) [8], Kyari et al. (2005) [9], Seidelt et al. (2006) [2]

2.2.1 Rubber composition of waste tyres

The rubber or volatile matter of the waste tyre mainly consists of polyisoprene (natural rubber) (NR), butadiene rubber (BR) and styrene-butadiene rubber (SBR) [2,10,11]. NR is an elastic hydrocarbon polymer derived from latex, a milky colloid material extracted from plants. It is also referred to as Indian Rubber or caoutchouc [12]. SBR is a copolymer typically containing 75 wt.% butadiene and 25 wt.% styrene. BR consists of only repeating units of butadiene [12,13]. Different types of tyres, such as, truck tyres (TT), passenger car tyres (PCT) or motorbike tyres (MT) generally differ in NR, SBR and BR contents. TT is characterised by high amounts of NR compared to PCT. Typical ratios of NR to synthetic rubber (SBR and BR) are 2:1 and 4:3 for TT and PCT, respectively [3].

Lopez et al. (2009) reported that the composition of a waste tyre was 60 wt.% rubber, of which NR and SBR were 29.95 and 29.95 wt.%, respectively [14]. Waste tyre crumb used in their investigation was steel and fabric free PCT. However, the rubber ratio was not reported. Another study conducted by the same group used TT waste tyre consisting of 58.89 wt.% NR representing entire rubber content of the waste tyre [15]. Rubber composition of the waste tyre reported by Danon and Görgens was 64 wt.% NR and 36 wt.% synthetic rubber (SBR and BR) [16].

Each rubber fraction of the tyre has different functions in the tyre. For example, NR is an essential element of a tyre due to its unique elastic properties. BR is characterised by excellent mechanical properties. It is generally used in both tread and sidewalls of the tyres [17]. When cured, some properties of BR include abrasion resistance and low rolling resistance due to its low glass transition temperature (T_g). SBR is characterised by resistance to bending and wear. Moreover, SBR is the most consumed rubber after NR. NR, BR, and SBR are all classified as diene rubber polymers. They originate from the structure of the monomer diene, see Figure 2.2. The chain bonds are formed at one of the double bonds and the other goes to the central position when the monomers are polymerised.

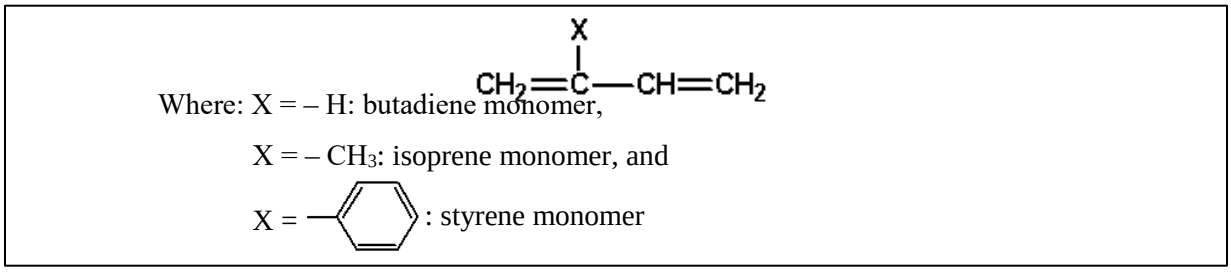

Figure 2.2: Representative structure of the general diene monomer

The kinetic mechanisms of polymers synthesis follow either the chain or step polymerisation paths [18]. As shown in Figure 2.3, chain polymerisation is a method by which free radical polymerisation mechanisms, such as, initiation, propagation and termination is followed. The initiation step usually includes addition of the first monomer molecule. In this reaction, the free radical attacks the monomer and is added to it. The double bond is broken open, and the free radical reappears at the far end.

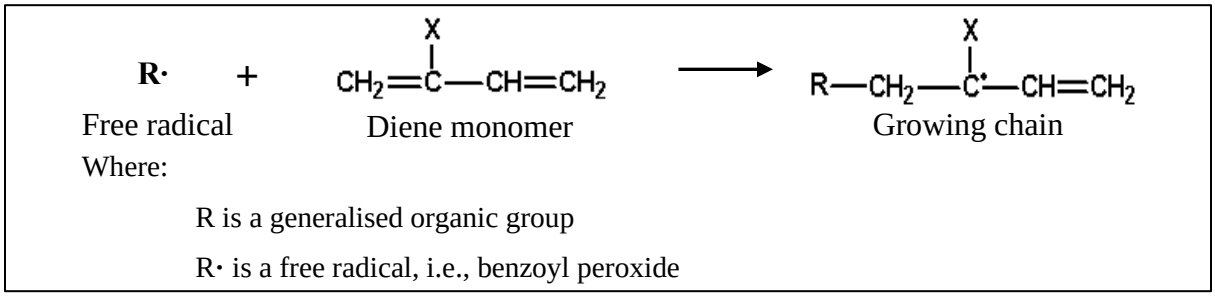

Figure 2.3: Illustration of the initiation step in the chain polymerisation

Propagation step involves rapid addition of many monomers, see Figure 2.4. On addition of each monomer, free radical moves to the end of the chain.

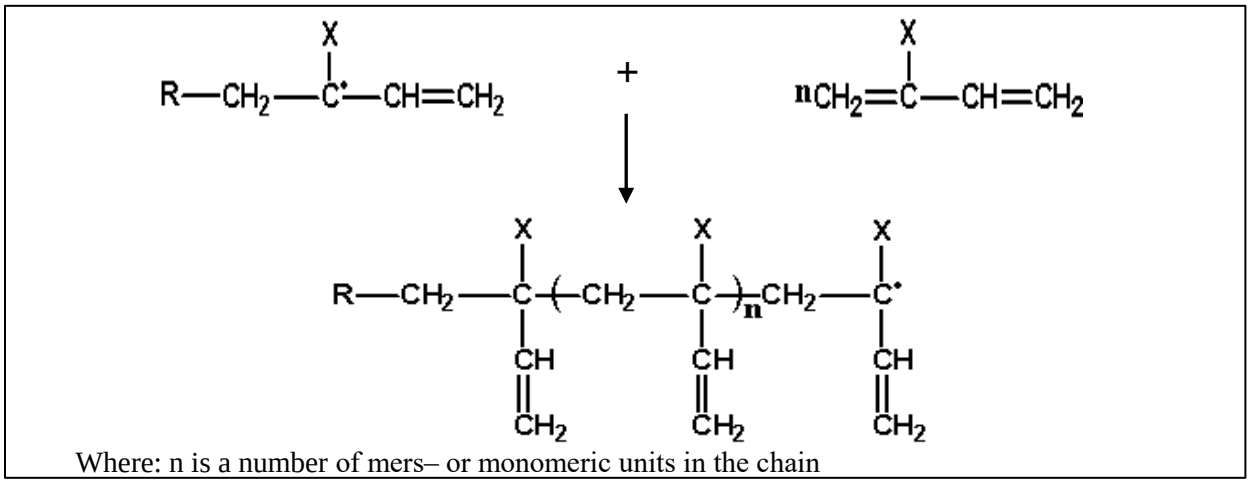

Figure 2.4: Illustration of the propagation step in the chain polymerisation

In the termination step, two free radicals react with each other. Termination is either by, 1) combination where hydrogen is transferred from one chain to the other, or 2) two long chains are combined; see Figure 2.5. The latter method results into two chains. While the normal mode of addition is a head-to-tail reaction, this termination step is normally head-to-head.

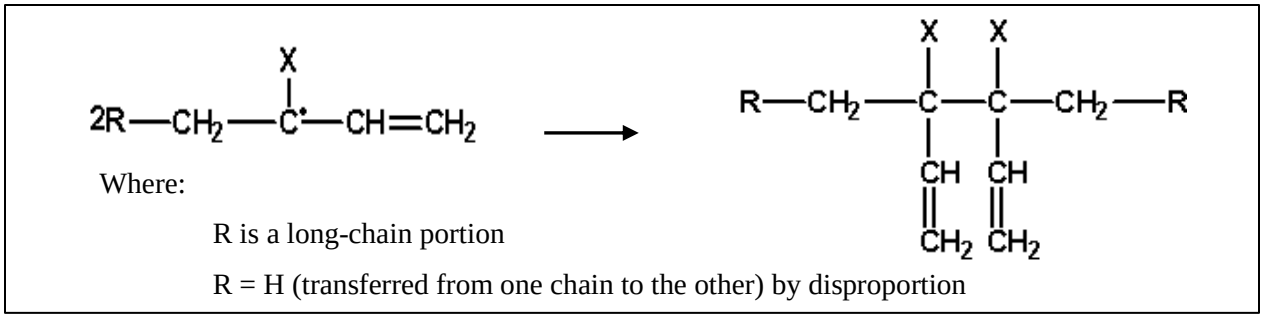

Figure 2.5: Illustration of the termination step in the chain polymerisation

The mers or monomer groups, Figure 2.6, n is allowed to increase up to several thousand.

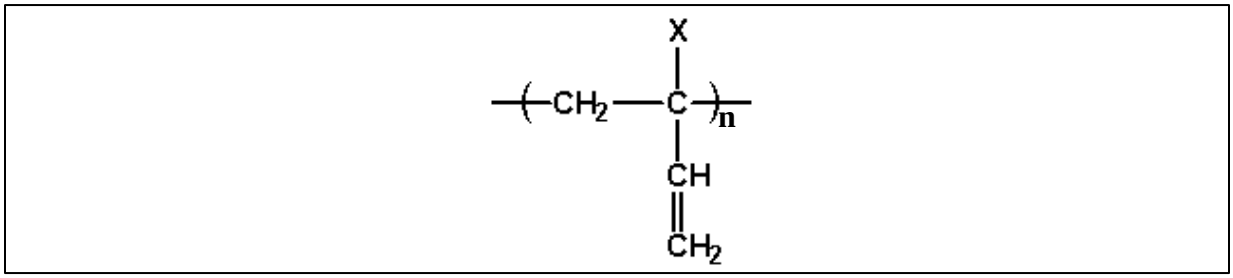

Figure 2.6: Mers or monomer groups

General molecular structures of the diene and corresponding rubber polymers are illustrated in Figure 2.7. The melting point or fusion temperatures, T_f, glass transition temperatures, T_g, and heats of fusion, ΔH_f, of each diene with a chain length of thousands of carbons is slightly molecular-weight-dependent. Cis-polyisoprene, 1,4-polybutadiene, and it-polystyrene have typical properties of: (T_f = 28 °C, T_g = -70 °C, ΔH_f = 4.40 kJ/mol), (T_f = -1 °C, T_g = – 85 °C, ΔH_f = 6.41 kJ/mol), (T_f = 240 °C, T_g = 100, ΔH_f = 8.37 kJ/mol), respectively [18]. A minimum molecular weight required for a substance to be called a polymer is approximately 25 000 g/mol. It is required for good physical and mechanical properties for many important polymers and is also near the onset of entanglement.

SBR is a copolymer consisting of polybutadiene and polystyrene, see Figure 2.8. It is formed by randomly copolymerisation of butadiene and styrene polymers [18]. Combining these two polymeric chains of constitutionally and configurationally different features linked in a linear fashion is governed by polymer mechanisms called a block.

a) Diene rubber polymer

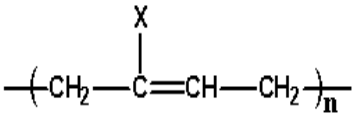

b) Polybutadiene rubber polymer

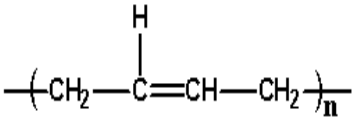

c) Polyisoprene rubber polymer

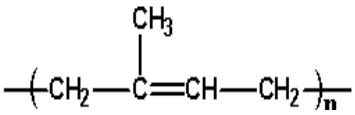

d) Polystyrene rubber polymer

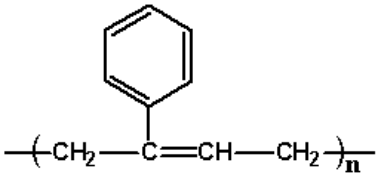

Where:

(a), (b), (c) and (d) are general polydiene, polybutadiene, polyisoprene and polystyrene mers– or monomeric units respectively

Figure 2.7: Illustration of the polydienes rubber polymers

$\cdots$–*A*–*A*–*A*–*A*–*A*–*A*–*B*–*B*–*B*–*B*–*B*–*B*–*B*–*B*–*B*–*B*–$\cdots$

Where:

–A–: polymer – A (polybutadiene)

–B–: polymer – B (polystyrene)

Figure 2.8: Illustration of the copolymerisation of polybutadiene and polystyrene polymers

Typical SBR copolymers are (1) Buna-S (32 %, styrene monomer), and (2) government rubber-styrene (GR-S) material (25 % styrene monomer) [18]. This difference in the composition is important for lowering the glass transition temperature. Using the Fox equation with a T_g of polystyrene of 100 °C and that of polybutadiene of – 85 °C. For Buna-S the T_g value is – 47 °C while for GR-S the T_g value is – 58 °C [18].

2.2.2 Polymer networks

Discussed so far were the linear, carbon-rich polymers formed by covalent linking of monomeric units (chain, i.e., polyisoprene, polybutadiene and polystyrene), and polymers that are derived from more than one species of monomer (copolymer, i.e., SBR). The tyre rubber, however, consists of the intimate combination of two or more polymer chains of constitutionally or configurationally different features [18].

When these chains are not bonded to each other, they are called a polymer blend. This blend of linear polymers can flow on heating and it is referred to as thermoplastic. To prevent flow, polymers are sometimes cross-linked [18]. The cross-linking of rubber with sulphur is called vulcanisation. Cross-linking binds together two or more chains to form a network, see Figure 2.9. The resulting product is called a thermoset, because it does not flow on heating [18].

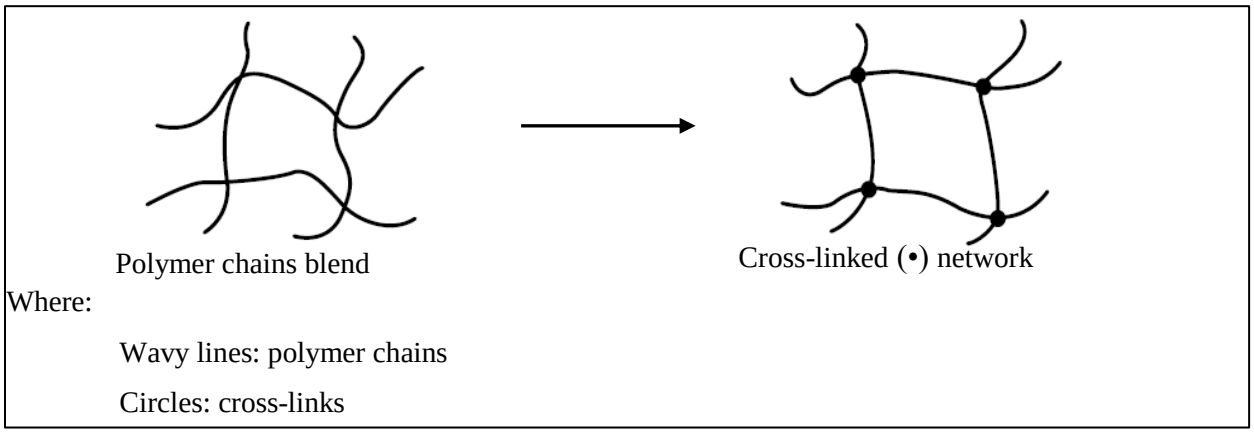

Figure 2.9: Illustration of polymer chains cross-linked network

During reaction, polymers may be cross-linked to several distinguishable levels [18]. At the lowest level, branched polymers are formed At this stage the polymers remain soluble, typically known as the sol stage. As the cross-links are added, clusters are formed, and cluster size increases [18]. Eventually the structure becomes infinite in size; that is, the composition gels. At this stage, a Maxwellian demon could, in principle, traverse the entire macroscopic system stepping on one covalent bond after another [18]. Continued cross-linking produces compositions where, eventually, all the polymer chains are linked to other chains at multiple points, producing, in principle, one giant covalently bonded molecule. This is commonly called a polymer network. Figure 2.10 shows sulphur cross-linked diene polymer, such as polyisoprene, polybutadiene and polystyrene. The resulting polymer network is characterised by non-reversible sulphur crosslinking [18].

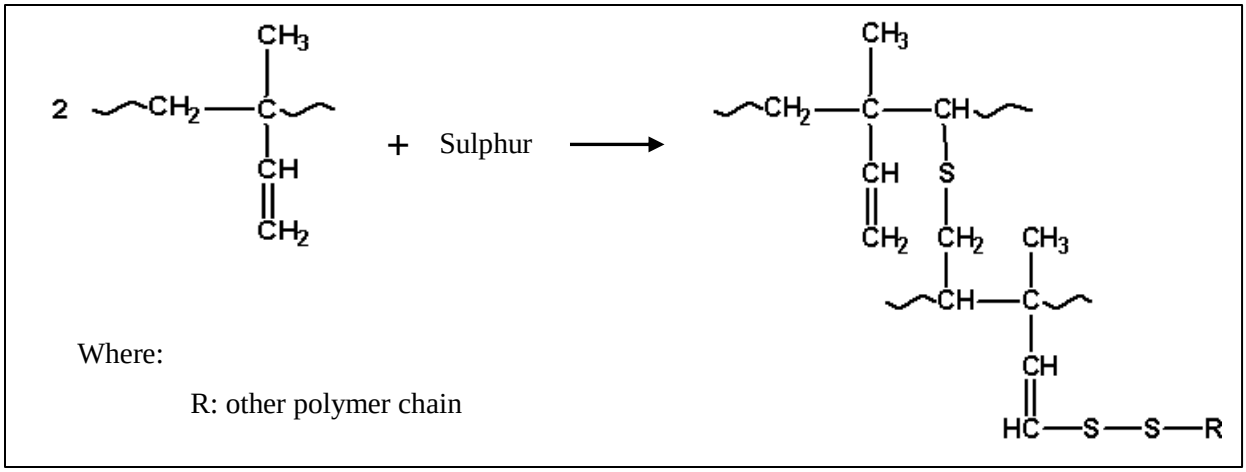

Figure 2.10: Cross-linking of the diene polymer in the present of sulphur

In an idealised structure of a cross-linked polymer, the primary chains are cross-linked at many points along their length. For materials such as rubber bands, tyres and gaskets, the primary chains may have molecular weights of the order of 1 x 10^5 g/mol and be cross-linked (randomly) every 5 to 10 x 10^3 g/mol along the chain, producing 10 to 20 cross-links per primary molecule [18]. It is convenient to define the average molecular weight between cross-links as M_c and to call chain portions bound at both ends by cross-link junctions active network chain segments.

Natural rubber has a certain degree of self-reinforcing, since it crystallizes on elongation [18]. The thermoplastic elastomers also gain strength by the presence of hard blocks. However, as illustrated in Figure 2.1, nearly all elastomeric materials have some type of reinforcing filler, usually finely divided carbon black or silica [18]. These reinforcing fillers, with dimensions of the order of 100 to 200 Å, form a variety of physical and chemical bonds with the polymer chains. Tensile and tear strength are increased, and the modulus is raised. The reinforcement can be understood through chain slippage mechanisms. The filler permits local chain segment motion but restricts actual flow [18].

From a viscoelastic point of view, a high-performance tyre should have a low tan δ value at 50 to 80 °C to reduce rolling resistance and save energy. The ideal material should also possess high hysteresis from –20 to 0 °C, for high skid resistance and wet grip [18].

The success in achieving the waste tyre properties, such as, glass transition temperature, modulus, elongation break, etc., has been overwhelming and there is no question about it. In tyre manufacturing, production of a melt processable from an infusible, insoluble, three-dimensional cross-linked structure (100 % gel content) [18]. However, due to non-reversible nature of the covalently bonded cross-linked polymer

network it is impossible to recycle waste tyre, the permanent gels consist of solvent-logged covalently bonded polymer networks. A pure polymer dissolves in two stages. First, solvent molecules diffuse into the polymer, swelling it to a gel state. Then the gel gradually disintegrates, the molecules diffusing into the solvent-rich regions. Cross-linked polymers may reach the gel state, but they do not dissolve [18].

Thus, simple disolving of cross-linked network in waste tyres is not possible. It is for this reason a study that investigates methods to recover the valuable polymeric from waste tyres is highly of interest. In addition, waste tyre consist of steel, fibers and processing oil as shown in Figure 2.1. Each waste tyre component can be recovered from the waste tyres separately from the other components [8]. For example steel and fiber can be recovered by shredding the tyres to small particles called crumb [8]. In this study the term waste trye(s), means shredded waste tyre crumbs (particle size between 0.5 to 5 mm).

2.3 Recovery of the polymeric components from waste tyre rubbers

If the cross-linked polymeric network can completely dissolve in a common organic solvent, such as, toluene, benzene or hexane, it will be simple to recover the polymeric materials from the waste tyres and the recycling of waste tyres would not be a challenge. However, since the gelation in the tyres is less than 100 %, i.e., not all its component can dissolve in the presence of a solvent, the solvent can dissolve only the chains that are not cross-linked in the polymer network. Shown also in Figure 2.1 is the presence of the processing additives in the waste tyres composition. Unlike the polymeric cross-linked network, tyre processing additives can be readily recovered by solvent extraction. Therefore, investigation of other waste tyre reclaiming techniques, such as, devulcanisation and thermal treatment processes is required for waste tyres recycling. In the following subsections devulcanisation, supercritical fluids treatment, solvent extraction, and thermal treatment (incineration and pyrolysis) techniques for waste tyre recycling are discussed.

2.3.1 Devulcanisation

Devulcanisation of waste tyres can result in rubber compounds that can be recompounded and re-vulcanised, similar to the fresh gum [19]. Devulcanisation is conducted by treating the crumb rubber over heat, pressure, or by addition of softening agents to alter the chemical composition of the materials [20].

Devulcanisation targets the sulphur crosslinks in the vulcanized rubber. Therefore, C–S and S–S bonds are selectively cleaved, see Figure 2.10. However, reclaiming is usually accompanied by considerable scission along the polymeric chains (i.e., C–C bonds cleavage), which results in lower molecular mass fractions and consequently poor tyre mechanical properties. Typical processes by which vulcanised rubber undergoes devulcanisation and reclamation are, 1) thermomechano-chemical, 2) thermochemical, 3) ultrasonic, and 4) microwave.

2.3.2 Supercritical fluids treatment

In the supercritical fluid pre-treatment systems, simultaneous devulcanisation and tyre processing additives removal from the waste tyres can be achieved. For example, supercritical CO_2 treatment of the waste tyres includes 1) rapid decompression of the supercritical fluid, or 2) in the presence of the devulcanising agents [21,22].

Hough and Hough (2009) investigated supercritical carbon dioxide ($scCO_2$) as the solvent in the decompression devulcanisation of waste tyres [21]. They postulated that the cross links became fully extended under strain to hold the internal pressures caused by the solvent swelling effect of the supercritical gas. When equilibrium swell has been achieved, the pressure within the processing vessel is rapidly dropped to a predetermined level causing a degassing and expansion of the supercritical fluid that has been absorbed within the vulcanized rubber [21]. Thus, the strain breaks sulphur-sulphur bonds.

Mangili et al. (2014) investigated devulcanisation of the waste truck tyres with $scCO_2$ in the presence of devulcanising agent, such as, diphenyl disulphide (DD) [22]. Carbon dioxide as a supercritical fluid has advantages in that supercritical conditions can be achieved at relatively low temperature and pressure. Thus, $scCO_2$ has the advantages as a suitable supercritical fluid. They concluded that crosslink scission occurred during devulcanisation. In addition, they reported that the mechanical properties of the blends of the devulcanised rubber and virgin rubber were poor compared to pure vulcanised rubber. However, acquiring and operating high pressure is typically comes at relatively expensive and with challenges.

2.3.3 Solvent extraction

Studies focusing on characterisation and determining of the extractable fraction of the waste tyres has been conducted. A train of Soxhlet extractions is generally used in the presence of organic solvents, such as, 1) toluene, 2) acetone, 3) chloroform, or 4) methanol [22,23]. Also, a reflux condenser can be used to extract

additives fraction from the waste tyres [23]. During such pretreatment of waste tyres, extraction of the tyre processing additives is targeted with no or minimum extraction of the polymer fraction.

Extraction of the tyre processing additives in the Soxhlet extration and reflux condenser either for characterisation or cleaning of rubber prior to devulcanisation has been reported in the literature. Soxhlet extraction was used by Mangili et al. (2014) in their study to investigate the amount of extractable fraction [22]. The solvents used were acetone and chloroform. When analysed, solvent extracts matched with plasticizers, accelerators and antioxidants, such as, N,N-dicyclohexyl and benzothiazolone. Dubkov et al (2012) carried out pre-cleaning of the crumb using chloroform-acetone mixture in the reflux condenser before the main reclaiming process [23]. The pre-cleaning was repeated three times at 70 °C for 1 hour each. The extracted fraction amounted to 10 wt.%, which corresponded to the processing additives content in waste tyres. However, total volatile matter in the waste tyres estimated at 60 wt.%.

The aim of the present study is to recycle the entire waste tyres and maximise recovery of the materials and chemicals production. It is known that at least 10 wt.% of the volatiles (processing additives) can be readily recovered using less severe processes such as solvent extraction. However, more severe processes are required to complete the extraction/recovery of market valuable materials from the waste tyres. Therefore, in the following subsections more severe processes, such as the thermal treatment of waste tyres (pyrolysis), are discussed.

2.3.4 Thermal devolatilisation processes of waste tyres

Conventional waste tyre treatment processes, such as re-treading or the use of the waste tyre crumb in sports fields, playgrounds, pavements and roads, cannot consume high enough volumes of discarded tyres [24,25]. Therefore, thermal treatments of waste tyres, such as, incineration, combustion and pyrolysis have been considered [26]. These processes have both advantages and disadvantages, as illustrated in Table 2.1.

Incineration is defined as the combustion of the feedstock with the objective of the complete burning of the material without entirely recovery of value, such as, energy or valuable chemicals [27]. It is relatively a simple process and the main disadvantage is enormous emission of toxic and mutagenic compounds, such as, dioxins, polycyclic aromatic hydrocarbons (PAHs), volatile organic compounds (VOCs) and particulate matter (PM) [27]. Incineration of waste tyres is not a favoured process, since the energy, materials and chemical products recovery is comparably efficient. This is not an adequate solution in times when depletion of fossil fuels and environmental emissions are of critical concerns.

Table 2.1: Thermal treatment of waste tyre processes comparison

Properties	Incineration	Combustion	Pyrolysis
Hazardous gases emission	High amount of PAHs, VOCs and PM	High amounts of PAHs, VOCs and PM	Low emission and smokeless depolymerisation of polymeric matter [28].
Complexity	Simple compared to combustion.	Simple compare to pyrolysis.	Complex and characterised by multiple parallel reactions and chemical products.
Energy recovery	No energy recovery.	Energy recovery.	Energy recovery and the liquid fraction can be transported to the location of use.
Materials and chemical products recovery	No materials or chemical recovery.	Some materials such as steel but not polymeric matter.	Effective in recovery of materials and chemical products.

PAHs: polycyclic aromatic hydrocarbons, PM: particulate matter, VOCs: volatile organic compounds
Source: adapted from Aylon *et al*. (2010) and Fullana *et al*. (2000) [27,29].

Waste tyre combustion differs from incineration in that the atmosphere under which it is conducted, i.e. the amount of oxygen, is controlled to maximise energy recovery. Its application includes power plants, tyre manufacturing facilities, cement kilns and pulp and paper industry boilers. However, the costs of cleaning the hazardous flue gases are relatively high. In addition, waste tyre combustion ignores recovery of materials and valuable chemicals. However, the steel can be recovered after combustion, but the polymeric matter is not recovered.

A pyrolysis process is defined as the thermal decomposition of organic volatile matter, in the absence of oxygen, to yield lower molecular chemical products, (solid, liquids and gasses) [28,30,31]. Some of the pyrolysis products, such as, the liquid fraction, has the advantage that it is easy to handle, store and transport [31]. The solid product (char) can be used as an energy source (solid fuel), or upgraded to carbon black (CB) or activated carbon (AC) [30,32]. Pyrolysis gas as a fuel can supply sufficient energy for the pyrolysis process due to its high calorific value [30,33]. In addition, Rombaldo et al. (2008) reported that pyrolysis

of waste tyres is one of the most reasonable alternatives in terms of environmental protection, due to relatively low greenhouse gases emissions [34].

2.3.5 Waste tyre pyrolysis

The earliest study of the pyrolysis of rubber dates back to 1920 and was conducted by Midgley and Henne [35]. Recently, Martínez et al. (2013) prepared a literature review of waste pyrolysis focussing on main product yields and distribution (gas, liquid and solid fractions) [3]. Process conditions such as heating rate, temperature, pressure, carrier gas type and flow rate, volatiles residence time and pyrolysis time, and their effects on the physicochemical properties and distributions of the waste tyre pyrolysis fractions, were evaluated. In their conclusion, contradictions on the operating conditions as well as reactor configurations were highlighted. Williams (2013) review on waste tyre pyrolysis has been purported mainly at investigating the effect of the configurations of the pyrolysis reactors on the pyrolysis products [36]. The pyrolysis reactors included fixed-bed (batch), screw kiln, rotary kiln, vacuum and fixed-bed reactors. Upgrading of the waste tyre pyrolysis products, such as 1) pyrolysis liquid or tyre derived oil (TDO) to energy fuels, and 2) pyrolysis solid (char) to higher quality carbon black or to activated carbon, were highlighted as possible options.

In their review of the waste tyre pyrolysis process, Antoniou and Zabaniotou (2013) carried out a study on the features and environmental benefits of the waste tyre pyrolysis processes [12]. Their study concluded that energy and material recovery from waste tyres is possible. The study covered mainly waste tyre pyrolysis studies conducted in the past 10 – 15 years (2002 – 2012). Another recent review of waste tyre pyrolysis processes was carried out by Quek and Balasubramanian (2013) [37]. The objective of the study was to provide a critical review on the work that has been carried out in the last four decades.

The effect of the pyrolysis conditions was similarly investigated to determine the trends of these parameters on the pyrolysis yields and liquid fraction composition. The summary of the pyrolysis conditions and effects is tabulated in Table 2.2. Table 2.2, is not exhaustive but lists significant and most reported pyrolysis reactor parameters, products and liquid fraction compositions.

Types of waste tyre pyrolysis

Martínez et al. (2013) mainly classified pyrolysis processes according to their operating conditions, such as, 1) heating rate, 2) volatiles residence time, and 3) temperature [3]. Consequently, pyrolysis processes

were classified as either slow or fast pyrolysis. Fast pyrolysis is characterised by very high (flash) heating rates and shorter volatiles residence times compared to slow pyrolysis. Another basis by which pyrolysis processes were classified by Martínez and co-workers was according to the environment under which the pyrolysis was carried out [3]. This class includes oxidative pyrolysis, hydro-pyrolysis, steam-pyrolysis, catalytic-pyrolysis and vacuum pyrolysis. Moreover, pyrolysis processes can be classified according to the heating system, such as, microwave or plasma pyrolysis. In the following subsections, the different types of pyrolysis will be discussed.

In Table 2.2, the pyrolysis processes were mainly categorised as either continuously fed or fixed-bed. Mainly all fluidised bed, screw kiln, and rotary kiln are fed continuously. To distinguish between the laboratory and industrial scale of the pyrolysis units, reactor size is included in the table. The pyrolysis parameters reported are temperature, heating rate, operating pressure, particle size, feed amount and catalysis. The output variables are pyrolysis main fractions yield (gas, TDO, and solid) and TDO chemical composition. TDO chemical composition was selected based on its high concentration of valuable chemicals, such as, DL-limonene, benzene, toluene, xylene and ethylbenze (BTXE), styrene, indane, indene and propylbenzene.

Temperature was the most significant parameter, since its effects on the overall yields of the main pyrolysis fractions and TDO chemical compositions, are relatively high [3]. Total TDO yield is generally high at low pyrolysis temperatures compared to high pyrolysis temperatures. Moreover, DL-limonene yield is higher at low temperatures when considering that at high temperatures most compounds undergo thermal cracking. High temperatures, however, favour the yield of a TDO with high BTXE content. BTXE (aromatic) is the second important group of compounds after terpenes (i.e., DL-limonene and terpinolene) in terms of industrial application and market value.

Moreover, another important parameter in waste tyre pyrolysis is catalysts. While most of the zeolite derived catalysts decrease the yield of DL-limonene, Na_2CO_3 and NaOH may improve the yield of DL-limonene in the TDO [3]. The effect of other parameters is not obvious. However, it can be noted that heating rate and pyrolysis pressure are important parameters. The significance of temperature is further discussed in the subsequent subsection where the kinetic mechanism of waste tyres devolatilisation is investigated.

Table 2.2: Summary of typical pyrolysis conditions and fraction yields and oil composition

Reference	Reactor type	Reactor size (cm^3 or ml)	Particle size (mm)	Sample amount (g)	Catalyst Type	Temperature (°C)	Heating rate (°C/min)	Pressure (kPa)	Global yield (wt%) Gas	Liquid	Solid	Component yield (wt. % of the liquid) Limonene	Benzene	Toluene	Xylene	Styrene	Indane	Indene	Ethylbenzene	Propylbenzene
Berrueco et al., 2005.	Fixed bed	950	20	300	None	400			2.40	30.00	64.00									
Berrueco et al., 2005.	Fixed bed	950	20	300	None	500			3.60	39.90	52.70									
Berrueco et al., 2005.	Fixed bed	950	20	300	None	550			3.60	39.10	52.50									
Berrueco et al., 2005.	Fixed bed	950	20	300	None	700			4.40	42.80	51.30									
Murillo et al., 2006.	Fixed bed	4		1	None	400	300	101		36.50										
Murillo et al., 2006.	Fixed bed	4		1	None	500	300	101		43.00										
Murillo et al., 2006.	Fixed bed	4		1	None	600	300	101		44.00										
Murillo et al., 2006.	Fixed bed	4		1	None	500	**25**	101		49.00										
Murillo et al., 2006.	Fixed bed	4		1	None	500	**100**	101		44.50										
Murillo et al., 2006.	Fixed bed	4		1	None	500	**300**	101		44.50										
Ucar et al., 2005.	Fixed bed	594	2	130	None	550	7		7.40	47.40	42.00									
Ucar et al., 2005.	Fixed bed	594	2	130	None	650	7		7.60	48.40	41.70		1.10	10.55	1.36	8.94			12.16	2.07
Ucar et al., 2005.	Fixed bed	594	2	130	None	800	7		7.80	47.20	41.50									
Ucar et al., 2005.	Fixed bed	594	2	130	None	550	7		7.60	55.60	33.80									
Ucar et al., 2005.	Fixed bed	594	2	130	None	650	7		7.60	56.00	33.80	*28.78	2.29	7.53	4.30				2.70	4.73
Ucar et al., 2005.	Fixed bed	594	2	130	None	800	7		8.80	55.10	33.20									
Williams and Brindle, 2002.	Fixed bed	1178		200	None	500	10		6.10	55.80	38.10		0.20	1.10	1.50		0.20		0.15	
Williams and Brindle, 2002.	Fixed bed	1178		200	Y-zeolite	430	10		16.30	38.70	38.00		1.75	3.36			0.87		1.91	
Williams and Brindle, 2002.	Fixed bed	1178		200	Y-zeolite	600	10		21.80	32.20	38.00		0.56	1.17			0.42		1.44	
Williams and Brindle, 2002.	Fixed bed	1178		200	ZSM-5	500	10			42.90			0.45	0.34			0.52		0.72	
Williams and Brindle, 2002.	Fixed bed	1178		200	ZSM-5	600	10		20.00	34.60	7.60		0.40	0.32			0.46		0.71	
Kar, 2011.	Fixed bed	317	2	10	None	375	10		2.99	46.24	50.67									
Kar, 2011.	Fixed bed	317	2	10	None	425	10			60.02		1.81			0.37	3.29			1.81	1.25
Kar, 2011.	Fixed bed	317	2	10	None	500	10		20.22	54.12										
Kar, 2011.	Fixed bed	317	2	10	Perlite	425	10			65.11		1.70		0.72	0.46	3.50			2.11	1.36
Kar, 2011.	Fixed bed	317	2	10	Perlite	425	10			55.89										
Zhang et al. 2008.	Fixed bed	97	1	100	None	450	20	4	15.40	32.90	51.70	11.97		1.30	1.48	0.53			0.86	
Zhang et al. 2008.	Fixed bed	97	1	100	None	500	20	4	21.80	42.10	36.10	11.73		0.18	0.49				0.21	
Zhang et al. 2008.	Fixed bed	97	1	100	None	550	20	4	16.00	47.10	36.90	4.72		0.85	1.27	0.46			0.42	
Zhang et al. 2008.	Fixed bed	97	1	100	None	600	20	4	16.30	48.80	34.80									
Zhang et al. 2008.	Fixed bed	97	1	100	Na_2CO_3	450	20	4	14.80	36.50	48.70									
Zhang et al. 2008.	Fixed bed	97	1	100	Na_2CO_3	500	20	4	15.30	42.00	42.70	11.95		0.52	1.15	0.32				
Zhang et al. 2008.	Fixed bed	97	1	100	Na_2CO_3	550	20	4	14.60	47.80	37.60									
Zhang et al. 2008.	Fixed bed	97	1	100	Na_2CO_3	600	20	4	16.20	48.50	35.20									
Zhang et al. 2008.	Fixed bed	97	1	100	NaOH	450	20	4	14.20	38.50	47.00									
Zhang et al. 2008.	Fixed bed	97	1	100	NaOH	480	20	4	13.70	49.70	36.70									
Zhang et al. 2008.	Fixed bed	97	1	100	NaOH	500	20	4	13.30	48.10	38.60	12.39		0.22	0.91	0.29				
Zhang et al. 2008.	Fixed bed	97	1	100	NaOH	520	20	4	16.80	46.90	36.40									
Zhang et al. 2008.	Fixed bed	97	1	100	NaOH	600	20	4	20.80	39.00	40.20									
Lopez et al., 2011	Continuous fed	25977	6	12000	None	550		101	13.90	46.10	40.00	12.20	16.60	12.20	5.20		1.70	7.70		
Islam et al., 2008.	Continuous fed	1951	2	750	None	375	167	101	8.00	42.00	50.00									
Islam et al., 2008.	Continuous fed	1951	2	750	None	475	167	101		49.00	41.00	*21.76	0.13	6.03	3.14					
Islam et al., 2008.	Continuous fed	1951	2	750	None	575	167	101	18.00	42.00	41.00									
Roy et al., 1999.	Fixed bed	848230	120	158000	None	520	10	7	6.00	45.00	36.00									
Roy et al., 1999.	Fixed bed	848230	1000	80000	None	500	10	7	5.00	47.00	37.00									
Roy et al., 1999.	Fixed bed	848230	120	180000	None	485	10	6	5.00	43.00	39.00									
Roy et al., 1999.	Continuous fed		30		None	550		10	10.00	56.00	33.00									
Boxiong et al., 2007.	Fixed bed	113	10	20	None	450	10		13.06	50.47	36.47									
Boxiong et al., 2007.	Fixed bed	113	10	20	None	500	10		11.92	51.98	36.09	*29.32	0.15	3.04	3.60	6.33			2.84	
Boxiong et al., 2007.	Fixed bed	113	10	20	None	550	10		11.70	52.61	35.69									
Boxiong et al., 2007.	Fixed bed	113	10	20	None	600	10		9.61	54.10	36.30									
Aydin and Ilkilic, 2012.	Fixed bed	1150			None	400		101	7.42	31.04	61.54									
Aydin and Ilkilic, 2012.	Fixed bed	1150			None	450		101	10.39	37.68	51.93									
Aydin and Ilkilic, 2012.	Fixed bed	1150			None	500		101	11.86	40.26	47.88									
Aydin and Ilkilic, 2012.	Fixed bed	1150			None	550		101	13.70	39.18	47.12									

***** Compositions in percent (%) peak area

Table 2.2 (continue)

Reference	Reactor type	Reactor size (cm^3 or ml)	Particle size (mm)	Sample amount (g)	Catalyst Type	Temperature (°C)	Heating rate (°C/min)	Pressure (kPa)	Global yield (wt%)			Component yield (wt. % of the liquid)								
									Gas	Liquid	Solid	Limonene	Benzene	Toluene	Xylene	Styrene	Indane	Indene	Ethylbenzene	Propylbenzene
Aydin and Ilkilic, 2012.	Fixed bed	1150			None	600		101	15.90	38.74	45.36									
Aydin and Ilkilic, 2012.	Fixed bed	1150			None	650		101	17.85	38.55	43.60									
Aydin and Ilkilic, 2012.	Fixed bed	1150			None	700		101	18.68	39.74	41.58									
Aydin and Ilkilic, 2012.	Fixed bed	1150			None	500		101	12.03	39.85	48.12									
Banar et al., 2012.	Fixed bed	240		10	None	400	5		27.20	38.80	34.00	1.71								
Banar et al., 2012.	Fixed bed	240		10	None	600	5			29.50										
Banar et al., 2012.	Fixed bed	240		10	None	400	35		33.80	31.10	35.10	0.02								
Murugan et al., 2008.	Fixed bed	2851		2090	None	500			40.00	50.00	10.00									
Raj et al., 2013.	Continuous fed		1	2000	None	350			28.05	40.54	31.41									
Raj et al., 2013.	Continuous fed		0	2000	None	400			27.00	40.50	32.50									
Raj et al., 2013.	Continuous fed		1	2000	None	400			29.00	44.50	26.50									
Raj et al., 2013.	Continuous fed		0	2000	None	400			22.50	44.00	33.50									
Raj et al., 2013.	Continuous fed		1	2000	None	400			16.18	44.95	37.87									
Raj et al., 2013.	Continuous fed		0	2000	None	475			18.38	36.12	45.50									
Raj et al., 2013.	Continuous fed		1	2000	None	475			34.00	41.50	24.50									
Raj et al., 2013.	Continuous fed		1	2000	None	475			24.90	40.60	34.50									
Raj et al., 2013.	Continuous fed		1	2000	None	475			34.00	41.50	24.50									
Raj et al., 2013.	Continuous fed		1	2000	None	475			34.00	41.50	24.50									
Raj et al., 2013.	Continuous fed		1	2000	None	475			24.90	40.60	34.50									
Raj et al., 2013.	Continuous fed		1	2000	None	475			34.00	41.50	24.50									
Raj et al., 2013.	Continuous fed		1	2000	None	475			34.00	40.00	26.00									
Raj et al., 2013.	Continuous fed		1	2000	None	475			27.75	42.40	29.85									
Raj et al., 2013.	Continuous fed		1	2000	None	475			30.50	39.25	30.25									
Raj et al., 2013.	Continuous fed		0	2000	None	550			30.16	29.30	40.54									
Raj et al., 2013.	Continuous fed		0	2000	None	550			45.50	28.25	26.25									
Raj et al., 2013.	Continuous fed		1	2000	None	550			37.58	32.00	30.45									
Raj et al., 2013.	Continuous fed		1	2000	None	550			34.00	35.20	30.80									
Raj et al., 2013.	Continuous fed		1	2000	None	600			46.00	25.30	28.70									
Martines et al., 2013.	Continuous fed		4	5000	None	550		101	16.90	42.60	40.50									
Pakdel et al., 1991.	Continuous fed	769690			None	404			6.98	63.95	29.07		2.30	8.54	4.36					
Pakdel et al., 2001.	Fixed bed	848230	38	200	None	480			3.60	60.00	36.40	3.30								
Pakdel et al., 2001.	Fixed bed	848230	38	200	None	440			3.20	43.40	53.40	3.30								
Pakdel et al., 2001.	Fixed bed	848230	38	1000	None	500			5.30	90.30	3.80	9.80								
Pakdel et al., 2001.	Continuous fed	848230	27		None	500			11.90	57.50	30.60	2.60								
Pakdel et al., 2001.	Continuous fed	848230	38		None	570			10.10	56.50	33.40	1.60								
Pakdel et al., 2001.	Continuous fed	848230	38		None	534			11.70	40.90	38.40	0.80								
Pakdel et al., 2001.	Continuous fed	848230	2		None	471			7.00	53.70	39.30	3.60								
Cunliffe and Williams, 1998.	Fixed bed	16286	30	3000	None	450	5		4.50	58.10	37.40	3.13	0.00	0.23		0.12		0.22	0.03	
Cunliffe and Williams, 1998.	Fixed bed	16286	30	3000	None	475	5		4.50	58.20	37.30	3.03	0.01	0.32		0.17		0.26	0.02	
Cunliffe and Williams, 1998.	Fixed bed	16286	30	3000	None	500	5		5.50	56.20	38.30	2.01	0.08	0.61		0.20		0.32	0.01	
Cunliffe and Williams, 1998.	Fixed bed	16286	30	3000	None	525	5		5.20	56.90	37.80	2.90	0.30	1.77		0.35		0.31	0.04	
Cunliffe and Williams, 1998.	Fixed bed	16286	30	3000	None	560	5		6.50	55.40	38.10	2.46	0.01	0.78		0.36		0.31	0.04	
Cunliffe and Williams, 1998.	Fixed bed	16286	30	3000	None	600	5		8.90	53.10	38.00	2.51	0.06	0.51		0.19		0.16	0.02	
Li et al., 2004.	Continuous fed	212058	15		None	450		86	13.10	43.00	43.90	5.44	0.40	2.27	1.54	1.21		0.83		
Li et al., 2004.	Continuous fed	212058	15		None	500		86	13.60	45.10	41.30	1.88	1.34	2.79	1.86	1.30		0.38		
Li et al., 2004.	Continuous fed	212058	15		None	550		86	15.50	44.60	39.90	0.42	1.49	5.16	2.05	1.42		0.90		
Li et al., 2004.	Continuous fed	212058	15		None	600		86	18.00	42.70	39.30	0.12	2.11	7.24	2.13	1.44		0.45		
Li et al., 2004.	Continuous fed	212058	15		None	650		86	18.30	42.90	38.30	0.07	2.09	7.06	2.02	2.64		0.38		
Dai et al., 2001.	Continuous fed	22777			None	450				50.00										
Kyari et al., 2005.	Fixed bed	200	30	45	None	500	10		2.50	60.10	37.10	4.76							1.51	
Laresgoiti et al., 2004.	Fixed bed	3500	30	175	None	300	15		7.60	4.80	87.60	*21.07	0.00					0.77	2.49	1.17
Laresgoiti et al., 2004.	Fixed bed	3500	30	175	None	400	15		19.30	24.80	55.90	*8.22	0.47					0.43	2.55	0.76
Laresgoiti et al., 2004.	Fixed bed	3500	30	175	None	500	15		17.20	38.00	44.80	*5.12	0.98					0.90	2.79	0.61
Laresgoiti et al., 2004.	Fixed bed	3500	30	175	None	600	15		17.60	38.20	44.20	*3.19	0.52					0.64	1.88	0.35
Laresgoiti et al., 2004.	Continuous fed	3500	30	175	None	700	15		17.80	38.50	43.70	*3.29	0.29					0.60	1.43	0.33

To distinguish between primary and secondary reactions in the pyrolysis of the tyre crumb (1 – 3 mm diameter), Senneca et al. (1999) carried out non-isothermal thermogravimetric analyses at various heating rates, up to 900 °C/min [38]. They concluded that at low heating rates the pyrolysis process involves primary and secondary stages as two distinguishable processes. Primary pyrolysis was associated with the scission of the main chains and depolymerisation reactions. They observed that these two pyrolysis stages were separated by repolymerisation reactions of the unstable polymer radicals (obtained from chain scission reactions) and cyclisation reactions of the primary products as the pyrolysis temperature was increased. Secondary pyrolysis was attributed to the degradation of the repolymerized and cyclised products. Senneca et al. (1999) also concluded that at a very high heating rate there was no distinction between primary and secondary pyrolysis [38]. This was attributed to the elimination of the cyclisation and re-polymerisation reactions due to the relatively rapid temperature increase as a result of the higher heating rate.

Investigations of the pyrolysis of the materials with known rubber compositions (NR, SBR and BR) using various heating rates in a thermogravimetric analyser (TGA) have also been conducted by Seidelt et al. (2006), Williams and Besler (1995), Brazier and Schwartz (1978), and Arockiasamy et al. (2013) [2,39-41]. They concluded that the polymers devolatilisation rate peaks at two distinctive temperatures (lower and higher). Peak mass loss rate at lower temperatures was attributed to NR and BR devolatilisation. Peak mass rate loss at higher temperatures was attributed to BR and SBR devolatilisation. For example, the first devolatilisation began at 180 °C, and finished at 360 °C. The second significant peak devolatilisation was reported between 330 and 458 °C, respectively.

To incorporate their understanding of the devolatilisation behaviour of waste tyres, Lam et al. (2010) modelled experimental results from thermogravimetric analysis (TGA) and differential thermal analysis (DTA) [42]. The model simulated pyrolysis as a stepwise process that employed a constant heating rate and non-heating stages. They have concluded that, compared to conventional pyrolysis, stepwise pyrolysis process consumed less energy. However, the pyrolysis time was doubled.

Cheung et al. (2011) further elaborated the stepwise pyrolysis idea by pointing out that initially the heat is applied to the organic matters (waste tyre) to initiate cracking of the long chains [43]. This is followed by non-heating conditions where the released exothermic heat is utilised for continuous cracking and devolatilisation. As soon as the exothermic heat is exhausted a second stage of heating is employed to finish the pyrolysis. They concluded that a low heating rate requires less energy but longer pyrolysis times. Both Lam et al. (2010) and Cheung et al. (2011) included the effect of the sample particle size on the energy

transfer from the surroundings to the centre of the particle [42,43]. However, this is beyond the scope of the current study.

Tremendous work was done by Oyedun el al. (2013) to shorten the pyrolysis time and energy consumption using stepwise pyrolysis [44]. The increase in pyrolysis times was limited to 37 – 50 % and simultaneous pyrolysis energy reductions of 24.7 – 37.9 % were achieved. They pointed out that optimisation of stepwise pyrolysis is based on the first non-heating stage initial temperature, first non-heating stage pyrolysis time and second a non-heating stage initial temperature.

Bridgwater and Peacocke (2000) and Mastral et al. (2002) independently reported short volatiles residence times were between 0.64 and 2.6 s at a pyrolysis temperatures as high as 850 °C in a fluidised bed reactor [45,46]. Bridgwater and Peacocke (2000) in their review study defined quenching as contact between the hot vapours and cooled liquid. According to their review, the rate of cracking of the vapours is slower at lower temperatures [45]. The normal cut-off temperature value for secondary reactions was 350 °C. However, due to unstable nature of some liquids, such as, bio-oils, secondary reactions can occur even at ambient temperature. At elevated temperatures, short volatiles residence times and high heating rates, large samples of approximately 500 g can be investigated using fast pyrolysis [28,46,47].

Moreover, lower pyrolysis temperatures between 350 and 600 °C have been investigated by Banar et al. (2012) [31], Barbooti et al. (2004) and Cunliffe and Williams (1998) in a fixed-bed batch reactor, to investigate the effect of the pyrolysis temperature [48,49]. The temperatures investigated were lower compared to those investigated in fast pyrolysis units. De Marco Rodriguez et al. (2001) and Laresgoiti et al. (2004) used similar fixed-bed pyrolysis reactor setups to investigate whole waste tyres (including steel and fibre), representing samples to study pyrolysis main fractions (gas, TDO and solid) and TDO properties [32,50]. In both studies pyrolysis temperatures were varied between 300 and 700 °C, while the other operating parameters, such as, particle size and nitrogen flow rate were constant at 2 – 3 cm and 0.06 m^3/h, respectively. In general, fixed-bed batch pyrolysis reactor configurations can be associated with slow pyrolysis. Sample sizes for slow pyrolysis are varied from tens of grams to few hundreds of grams. However, typical sample amounts for slow pyrolysis are closer to the tens of grams i.e. at the bottom of the range [31,32,48-50].

Relatively low pyrolysis temperatures and shorter volatiles residence times were applied by Roy et al. (1999) using pressures as low as 10 kPa [51]. In addition, Pakdel et al. (1991) carried out a study in a continuously fed vacuum reactor to investigate DL-limonene content in the pyrolysis TDO [52].

They concluded that the vacuum reduces volatiles residence time (in the pyrolysis reactor hot zones) and it was comparable to the fast pyrolysis process. Moreover, relatively low temperatures were used. Undesirable reactions, such as, formation of carbonaceous deposits on the pyrolysis carbon solid and secondary reactions, were eliminated. Similar work was carried out by Pakdel et al. (2001) to study the effect of pyrolysis temperature, pyrolysis pressure and feed flow rate on the content of the DL-limonene in the TDO [53]. Temperature was varied between 440 and 570 °C. Maximum pressure investigated was 12 kPa and the feed flow rate of the waste tyres was varied between 21 and 42 kg/h. They concluded that, at temperatures higher than 500 °C, DL-limonene was converted into secondary products. However, as the pressure was decreased the DL-limonene yield was increased.

2.3.6 Waste tyre devolatilisation mechanism

Lam et al. (2010) have pointed out that the economic viability of waste tyre pyrolysis is dependent mainly on the feedstock compositions and operating pyrolysis conditions, both of which affect the process performance, product yields and qualities. Waste tyre heating rate, β_{tyre}, is one of the major pyrolysis process parameters, due to its significant effect on the, 1) heat flow of the pyrolysis process, 2) kinetic mechanisms, and 3) total mass loss during waste tyre pyrolysis process [54]. Thus, Lam et al. (2010) proposed a novel description of the multi-stage pyrolysis process of a single piece of a tyre based on the, 1) temperature profile, 2) kinetics, and 3) heat flow results. These parameters were investigated from various amounts of initially feed (10, 20 and 30 mg) and heating rates (2, 5, 10 and 20 °C/min) in the TGA. The following different mass loss reactions (MLR) were assumed: 1) MLR_1, for the pyrolysis of tyre additives; 2) MLR_2, for the pyrolysis of depolymerized rubbers; and 3) MLR_3 for the pyrolysis of crosslinked/cyclised rubbers, see **Table 2.3**. They also assumed that the amount of the mass loss through MLR_1 is independent of heating rate, whereas mass loss due to MLR_2 and MLR_3 depended on the heating rate [54].

Since there was insignificant differences on the DTG profiles of the crumb with a particle size of more than 2 mm, Lam et al. (2010) concluded that pyrolysis of the tyre was complete before a temperature of 500 °C was reached [54]. They also observed that energy consumption in the pyrolyser increase as particle size increases. However, the shredding of tyre is energy intensive. Lower heating rates require lower energy in the pyrolysis of tyres, but longer reaction time and higher heat loss are the impediments.

Cheung *et al*. (2011) investigated the effect of the heating rate (2, 5, 10 and 20 °C/min) on the combined mass loss and exothermic kinetics with the heat flow in the pyrolysis of the large particle size of waste tyres [55]. They have integrated the kinetics and heat flow results to determine a suitable, energy saving strategy

for pyrolysis operations. The proposed pyrolysis kinetics entailed various reaction mechanisms, i.e. 1) organic tyre additives (TA) pyrolysis reaction (R1) to volatiles (V) and char (C); 2) main chain scission (R2) of the rubbers to intermediate (A) [IA]; 3) possible further depolymerisation of IA (R3a) to V and C; 4) or IA cracking to shorter chains of organic fractions, intermediate (B) [IB] (R3a); and 5) IB devolatilisation to form V and C (R3c). They have pointed out that TA are readily devolatilised, while the mass loss contributions of reactions R3a and R3c, ω_{3a} and ω_{3c}, were varied as the heating rate was varied, see Table 2.3. As the heating rate was increased, ω_{3a} increased while ω_{3c} decreased. This was attributed to the earlier attainment of the devolatilisation peak temperature. Therefore, earlier attainment of the devolatilisation peak temperature indicates that there was enough energy to devolatilise the tyre to various fractions, i.e. gas, volatiles and char.

Senneca *et al*. (1999) investigated the kinetic mechanisms of the pyrolysis of waste tyres to yield tyre derived oil (TDO) [38]. Waste tyre crumb samples with particle sizes of 1 and 3 mm were pyrolysed in thermogravimetric analysis (TGA) equipment capable of attaining heating rates 5, 20, 100 and 900 °C/min. Moreover, Arrhenius plots were applied at varies heating rates. Four temperature ranges were noted: 1) Region 1, at low temperature almost straight profiles of the reaction rate, increases as heating rate increases and was associated with main chain scission; 2) Region 2, at higher temperature characterised by common pre-exponential factor and activation energy, associated with depolymerisation and Arrhenius plots merge into a straight line; 3) Region 3, Arrhenius plots depart from the straight line associated with cyclisation and depends on heating rate; and 4) Region 4, once again linear portion of Arrhenius plots, associated with degradation of cycled products, see Figure 2.3.

Seidelt *et al*. (2006) characterised various pure rubbers (NR, three SBR with different styrene and oil contents and BR) using thermogravimetric/mass spectrometry (TG/MS) analysis technique [2]. At a heating rate of 10 °C/min NR had one significant devolatilisation peak temperature at 378 °C and a shoulder at higher temperature. SBR showed two-step mass loss. The first peak between 180 and 360 °C was attributed to the devolatilisation of processing additives (mainly oils and plasticisers). Devolatilisation of rubber at the temperature of 458°C was attributed to the second devolatilisation peak temperature. The DTG curve of the BR depicted two-step mass loss; one at 385 °C and the other at 468 °C and both steps were attributed to polymer devolatilisation, see Table 2.3.

The spectrum of volatiles released from SBR exhibited a characteristic series of several aromatic compounds, such as, ethylbenzene, styrene and cumene, which are mainly produced by the devolatilisation of the styrene fraction in the rubber. The butadiene (monomer) and 4-vinylclohexene (dimer) evolved at

earlier retention times. Also, investigated was a tyre and three peaks were observed: 1) between 150 and 320 °C which was attributed to the devolatilisation of the processing additives, 2) at 378 °C which was attributed to the NR devolatilisation and 3) at 458 °C which was attributed to the SBR devolatilisation, see Table 2.3.

Leung and Wang (1998) carried out kinetic study of waste tyre pyrolysis and combustion [56]. They pointed out that process and kinetic parameters vary with the heating rate but are less dependent on the particle size. They presented both the pyrolysis and combustion reactions by solid devolatilisation equation,

$$\frac{d\alpha_T}{dt} = \sum_{i=1}^{n} \frac{d\alpha_i}{dt} = \sum_{i=1}^{n} k_i(1-\alpha_i) \quad (1)$$

Where, α is the reaction progress (-), t is the time (s), and k is the reaction rate constant (1/s).

Arrehenius' Law was applied to estimate rate constant, k_i and was represented by,

$$k_i = A_i \exp(-E_i/RT). \quad (2)$$

Where, A is a pre-exponential constant (1/s), E is the activation energy (J/mole), R is the universal gas constant (J/mole/K) and T is the absolute temperature (K).

This was possible since the devolatilisation can be activated at a temperature lower than 800 °C, which is within the temperature range of the kinetic reaction. The thermogravimetric analysis (TGA) and derivative thermogravimetry (DTG) curves, obtained experimentally, were used to estimate parameters from equations (1) and (2) above. The curves were characterised by varying the heating rate to determine the effect of the heating rate as a function of reaction progress. It was deduced that the moisture inside the tyre powder evaporated before a temperature of 150 °C was reached. Whereas, oil, plasticizer and additives; and NR, SBR as well as BR are devolatilised at the temperature range of 150 – 350 and 340 – 550 °C, respectively, see Table 2.3.

Quek and Balasubramanian (2009) study of waste tyres pyrolysis exhibited different kinetic behaviours when pyrolysed under different heating rates [57]. An algorithm that included heat and mass transfer equations was developed, to account for different extents of thermal lag as the tyre was heated at different heating rates. An iterative approach was used to fit the model equations to experimental data to obtain

quantitative values of kinetic parameters. Frequency factors increased and time constants decreased with increasing heating rates.

Quek and Balasubramanian (2009) described the pyrolysis process by considering two equations, 1) to account for heat conduction from the exterior to the interior of the tyre particle, and 2) for mass transfer from within the tyre particle to the surface [57]. To decouple each decomposing fraction as an independent parallel reaction from each other, both reaction rates and heat transfer limitations were accounted for at low and high heating rates. They used three brands of tyres at the heating rates ranging from 10 – 50 °C/min. The corresponding activation energies, pre-exponential factors and characteristic parameters were determined and reported, see Table 2.3.

The kinetic equation,

$$\frac{dm}{dT} = \sum_{i=1}^{N} m_i k_i \tag{3}$$

Where:

$\frac{dm}{dT}$: is the rate of change of the total mass of the tyre (g/°C),

N: is the total number of components evolving independently (-),

$m_i k_i$: is reaction rate of the ith component (g/°C), and

k_i: is Arrhenius-type kinetic reaction coefficient of component i. (1/s)

$$k_i = \frac{dt}{dT} A_i e^{-E_a/RT} \tag{4}$$

Where:

$\frac{dt}{dT}$: is the inverse of the heating rate set at the beginning of each run (s/°C),

A: is the pre-exponential factor (frequency factor) (1/s),

E_a: is the activation energy of the particular reaction (J/mole),

R: is the molar gas constant, 8.314 (J/molK), and

T: the temperature of the particular data point (K).

Therefore, the Arrhenius equation $\left(A_i e^{-E_i/RT}\right)$ was multiplied by the inverse of the heating rate (dt/dT) because the rate of the mass change with respect to temperature was used (dm/dT).

It was found that the heating rate had a significant impact on the kinetics of pyrolysis [57]. At higher heating rates (≈ 50 °C/min or higher), the heat transfer to the interior of the particle severely limited the rate of reaction. At a molecular level, the polymer molecules within the tyre have not attained sufficient energy to break off from the main polymer chain, until sufficient heat has been conducted through it. This causes the sudden massive spike at around 427 °C as significant number of molecules at this point has obtained sufficient energy for reaction [57].

It was pointed out that at a heating rate of 50 °C/min the temperature gradient was so high that another smaller peak was observed at 627 °C, requiring the modelling of two distinct peaks due to thermal lag [57]. The thermal lag can also be observed usually in the external temperatures measured at the initiation and completion of tyre pyrolysis. At a low heating rate, the pyrolysis starts at 177 °C and ends at 507 °C. At a higher heating rate, the pyrolysis starts at 277 °C and ends at 727°C, see Table 2.3.

Mui *et al*. (2010) used a three component stages model to describe kinetic mechanisms of waste tyre devolatilisation [58]. Arrhenius equation was used to relate the dependency in the reaction rate and to estimate the pre-exponential factor and activation energy. Linear variation was assumed.

Table 2.3: Summary of the waste tyres devolatilisation kinetics and mechanism

Reference	Parameter	Processing oil	Polymer depolymerisation	Polymer degradation	Comment
Senneca *et al.* (1999) [38]	Heating rate (°C/min)	T_{max1}	T_{max2}	T_{max}	(1) $DTG: -\frac{1}{w_0}\frac{d\alpha}{dt}$; (2) $Arrhenius\ plots: In\left(-\frac{1}{w-w_f}\frac{dw}{dt}\right)$ $PLOT: In\left(-\frac{1}{w-w_f}\frac{dw}{dt}\ vs.\frac{1}{T}\right)$ $Kinetic\ expressions: \frac{dw}{dt} = -k_0 exp\left(\frac{-E}{RT}\right)(w-w_f)$ $\left[1)\ A \xrightarrow{1} V_1 + R_1 \quad main\ chani\ scission;\ \left\{2a)\ R_1 \xrightarrow{2a} V_2;\ 2b)\ R_1 \xrightarrow{2b} R_2;\ 2c)\ R_1 \xrightarrow{2c} V_3\right\} \quad deplolymerisation\right]$ primary pyrolysis $3)\ R_2 \xrightarrow{3} R_3 \quad cyclisation$ $4)\ R_3 \xrightarrow{4} V_4 + R_4\ degradation\ of\ cyclisation\ products$ $-\ secondary\ pyrolysis$ $r_1 = k_1 exp\left(-\frac{E_1}{RT}\right)C_A; r_2 = k_2 exp\left(-\frac{E_2}{RT}\right)C_A;\ r_3 = k_3 exp\left(-\frac{E_3}{RT}\right)C_R;$
	5	360 (360)	420 (400)	–	
	20	390 (390)	460 (470	–	
	100	–	–	420 (420)	
	900	–	–	500 (540)	

	Heating rate (°C/min)	Size (mesh)	Start Temp	Peak 1 T(°C)	Peak 2 T(°C)	Final (°C)	React time (min)	
Leung and Wang (1998) [56]	10	8 – 16	185	383	450	500	29.9	$ln\frac{d\alpha_T}{dt} = ln\sum_{i=1}^{3}\frac{d\alpha_i}{dt} = ln\left[\sum A_i exp\left(-\frac{E_j}{RT}\right)(1-\alpha_i)\right]$ $ln\frac{d\alpha_T}{dt} = ln\left(\frac{d\alpha_1}{dt}+\frac{d\alpha_2}{dt}\right) = ln\left[A_1 exp\left(-\frac{E_1}{RT}\right)(1-\alpha_1) + A_2 exp\left(-\frac{E_2}{RT}\right)(1-\alpha_2)\right]$ $\int_0^\alpha \frac{d\alpha}{(1-\alpha)} = \frac{A}{\beta}\int_0^T exp\left(-\frac{E}{RT}\right)dT$ $\frac{A}{\beta}\int_0^T exp\left(-\frac{E}{RT}\right)\mathrm{dT} = -\frac{A}{\beta}\frac{RT^2}{E}exp\left(-\frac{E}{RT}\right)\sum_{k=0}^{\infty}\frac{(-2)^k}{(E/RT)^k}$ $\alpha = 1 - \exp\left[-\frac{A}{\beta}\frac{RT^2}{E}exp\left(-\frac{E}{RT}\right)\sum_{k=0}^{\infty}\frac{(-2)^k}{(E/RT)^k}\right]$
		16	185	380	458	500	29.9	
		30	185	379	458	500	29.9	
		40	185	381	450	500	29.9	
	30	8 – 16	250	400	480	520	8.5	
		16	250	404	479	520	8.5	
		30	250	401	478	520	8.5	
		40	250	404	471	520	8.5	
	45	8 – 16	260	410		545	5.5	
		16	260	411	491	545	5.5	
		30	260	409	485	545	5.5	
		40	260	414	484	525	5.5	
	60	8 – 16	260	410	492	545	4.2	
		16	260	410	485	545	4.2	
		30	260	416	490	545	4.2	
		40	260	413	484	545	4.2	

Table 2.3 (continue)

Reference	Parameter		Processing oil	Polymer depolymerisation			Processing oil		Polymer depolymerisation		Comment
		Initial, peak and final temperature					Weight lost				
	Heating rate (°C/min)	Size (mesh)	Start Temp	Peak 1 T(°C)	Peak 2 T(°C)	Final (°C)	React t (min)	NWLR_1 (min^{-1})	WL @ Peak_1	NWLR_2 (min^{-1})	WL @ Peak_2	Total WL
Leung and Wang (1998) continue	10	8 – 16	185	383	450	500	29.9	0.1076	28.15	0.0621	**56.91**	**68.71**
		16	185	380	458	500	29.9	0.0932	22.84	0.0742	**55.39**	**65.84**
		30	185	379	458	500	29.9	0.1020	23.36	0.0668	56.69	65.26
		40	185	381	450	500	29.9	0.1078	25.78	0.0606	53.34	63.74
	30	8 – 16	250	400	480	520	8.5	0.3045	20.51	0.1949	53.92	64.40
		16	250	404	479	520	8.5	0.3141	24016	0.1853	56.39	66.73
		30	250	401	478	520	8.5	0.3107	21.86	0.1819	53.92	63.71
		40	250	404	471	520	8.5	0.3299	22.92	0.1700	50.17	61.41
	45	8 – 16	260	410		545	5.5	0.5873	25.21			66.45
		16	260	411	491	545	5.5	0.4882	20.12	0.2968	54.63	65.22
		30	260	409	485	545	5.5	0.4942	19.42	0.2736	52.23	63.62
		40	260	414	484	525	5.5	0.5216	23.10	0.2487	51.58	61.73
	60	8 – 16	260	410	492	545	4.2	0.8185	17.20	0.4125	52.41	64.15
		16	260	410	485	545	4.2	0.7300	19.49	0.3744	51.57	63.13
		30	260	416	490	545	4.2	0.7729	22.25	0.3485	53.32	63.42
		40	260	413	484	545	4.2	0.7804	20.68	0.3313	50.16	60.52

Table 2.3 (continue)

Reference	Parameter	Processing oil	Polymer devolatilisation					Comment
Quek and Balasubramanian (2009) [57]	Heating rate (°C/min)	**Reaction rate constant, k, (s^{-1})**						$\frac{dM}{dT} = \sum_{i=1}^{N} m_i k_i$
	E_a ($kJmol^{-1}$)	**Oil**	**NR**	**SBR**	**BR**			$k_i = \frac{dt}{dT} A_i e^{-E_{a,i}/RT}$
		43	**207**	**152**	**215**			$T(t) = T_f + [T(0) - T_f]e^{-rt}$
	10	13.7±2.3	7.68 ± 8.5 x 10^{13} s^{-1}	6.90 ± 7.6 x 10^{8} s^{-1}	2.94 ± 3.1 x 10^{12} s^{-1}			$m_i = m_{i,0} 4(x_i)[-In(x_i)]^{3/4}$
	20	17.1±2.5	1.20 ± 0.2 x 10^{14} s^{-1}	1.47 ± 0.3 x 10^{9} s^{-1}	7.46 ± 0.8 x 10^{12} s^{-1}			$m_i = m_{i,0} + \frac{dm_i}{dT} \Delta T$
	30	39.3±4.0	1.79± 0.2 x 10^{14} s^{-1}	1.27± 0.2 x 10^{9} s^{-1}	6.38 ± 0.7 x 10^{12} s^{-1}			
	40	58.5±6.0	2.15 ± 0.3 x 10^{14} s^{-1}	3.26 ± 0.4 x 10^{9} s^{-1}	1.52 ± 0.3 x 10^{13} s^{-1}			
	50	71.5±6.1	1.97 ± 0.3 x 10^{13} s^{-1}	1.00 ± 0.2 x 10^{7} s^{-1}	4.47 ± 0.5 x 10^{9} s^{-1}			
	30	149±15.5	8.41 ± 0.8 x 10^{13} s^{-1}	3.26 ± 0.3 x 10^{8} s^{-1}	1.93 ± 0.2 x 10^{11} s^{-1}			
	30	12.8±1.3	2.90 ± 0.3 x 10^{14} s^{-1}	6.90 ± 0.5 x 10^{8} s^{-1}	5.68 ± 0.6 x 10^{13} s^{-1}			
		Weight fraction, ω, (wt. %)						
		Oil	**NR**	**SBR**	**BR**	**Peak-1**	**Peak-2**	
	10	15.5 ± 1.6	11.6 ± 1.5	21.6 ± 1.9	51.3 ± 3.5	–	–	
	20	15.6 ± 2.5	11.1 ± 1.5	22.6 ± 2.1	50.7 ± 4.4	–	–	
	30	7.9 ± 0.6	16.9 ± 1.7	18.4 ± 2.1	46.4 ± 4.5	10.4 ± 1.0	–	
	40	5.0 ± 0.7	18.5 ± 1.8	41.9 ± 3.2	32.9 ± 3.3	1.7 ± 0.2	–	
	50	8.0 ± 0.8	26.6 ± 2.5	19.5 ± 2.5	24.7 ± 2.7	15.1 ± 0.2	6.1 ± 0.3	
	30	16.7 ± 0.2	28.4 ± 2.3	22.5 ± 2.4	7.6 ± 0.9	14.7 ± 0.2	–	
	30	16.3 ± 0.2	9.3 ± 1.0	34.3 ± 2.9	29.7 ± 3.0	10.4 ± 0.2	–	
		Late peaks						
	$T_i(s^{-1})$	**Brand**	**Peak-1**		**Peak-2**			
			E_a (kJ/mol	A (s^{-1})	E_a (kJ/mol	A (s^{-1})		
30	9.88±1.0 10^{-4}	1	583±62	6.30±0.7x10^{49}				
40	9.84±1.1x10^{-4}	1	536±73	6.60±0.7x10^{39}				
50	9.74±1.2x10^{-4}	1	418±68	7.22±1.0x10^{33}	275±29	1.89±1.0x10^{12}		
30	5.99±6.2x10^{-4}	2	129±13	3.28±0.4x10^{7}				
30	6.28±6.5x10^{-4}	3	77.7±8.4	2.56±0.4x10^{3}				

$$correl = \frac{\Sigma\left(\frac{dM}{dT_{exp\,t}} - \frac{\overline{dM}}{dT_{exp\,t}}\right)\left(\frac{dM}{dT_{model}} - \frac{\overline{dM}}{dT_{model}}\right)}{\sqrt{\Sigma\left(\frac{dM}{dT_{exp\,t}} - \frac{\overline{dM}}{dT_{exp\,t}}\right)^2 \Sigma\left(\frac{dM}{dT_{model}} - \frac{\overline{dM}}{dT_{mod}}\right)}}$$

Table 2.3 (continue)

Reference	Parameter	Processing oil			Polymer devolatilisation					
	Component	**Component 1 (additives)**			**Component 2 (NR)**			**Component 3 (SBR)**		
	Heating rate (°C/min)	**T (°C)**	**E_1 (kJ/mol)**	**A_1 (min^{-1})**	**T (°C)**	**E_2 (kJ/mol)**	**A_2 (min^{-1})**	**T (°C)**	**E_3 (kJ/mol)**	**A_3 (min^{-1})**
	10	150–350	74.42	4.1×10^6	270–405	115.87	1.08×10^8	320–470	97.89	3.25×10^9
	60	150–350	78.19	6.4×10^7	310–430	135.49	1.05×10^9	350–485	95.45	6.72×10^9
Islam *et al*. (2009) [59]		**Initial, peak and final temperature**						**Weight lost**		
		Tyre type	Start, T (°C)	Peak 1 (°C)	Peak 2 (°C)	Finish, T (°C)	Reaction, t (min)	NWLR at peak1		NWLR at peak2		Total loss (wt. %)
								µg/min	wt.%	µg/min	wt. %	
	10	Truck tire	200	365	405–450	470	27.00	495.50	3.39	245	64.04	68.60
	60		135	395	420–460	500	6.08	2824.53	34.85	1447.05	60.60	67.80
	$\frac{dX}{dt} = k_i(1-X_i)^{n_i}; where: k_i = A_i e^{-\frac{E_i}{RT}}$ and $n_i(assumed) = 1; \Rightarrow \frac{dX}{dt} = A_i e^{-E_i/RT}(1-X_i)$; linear heating rate, $\beta = \frac{dT}{dt}, \Rightarrow \frac{dX}{dT} = \frac{A_i}{\beta} e^{-\frac{E_i}{RT}}(1-X_i)$; $In\frac{dX_i}{dT} = In\left[\frac{A_i}{\beta}(1-X_i)\right] - \frac{E_i}{RT}$ $Straight\ line, y = a_0 + ma : In\left(\frac{dX_i}{dT} vs \frac{1}{T}\right)$; (***provided that the values of β and X_i are fixed***): Kinetic parameters are estimated from: $ma_0 + a\sum_{i=1}^{m} X_i = \sum_{i=1}^{m} y_i;\ \ a_0 \sum_{i=1}^{m} X_i + a\sum_{i=1}^{m} X_i^2 = \sum X_i y_i$											
Chen *et al*. (2001) [60]	**Heating rate ($°C.min^{-1}$)**	**Tyre type**	**Start, T (°C)**	**Peak 1 (°C)**	**Peak 2 (°C)**	**Finish, T (°C)**	**Reaction, t (min)**	**NWLR at peak1**		**NWLR at peak2**		**Total loss (wt. %)**
								µg/min	wt.%	µg/min	wt. %	
	5	Truck tyre	238	392	–	493	51.00	–	35	–	–	62
	20		205	414	–	533	16.40	–	30	–	–	61.1
	30		185	429	–	553	12.20	–	28	–	–	62.4

Table 2.3 (continue)

Reference	Parameter		Processing oil	Polymer depolymerisation	Polymer degradation	Comment
Lam *et al.* (2010) [42]	**E_a (kJ.mol^{-1})**		69.73	118.04	128.92	$\frac{d\alpha}{dt} = \sum_{i=1}^{3} w_i Z_i exp\left(\frac{-E_i}{RT}\right)$ $exothermic\ heat: q_{exo} = \sum h_{d,j} \frac{dN_{j,t}}{dt}(1-\alpha_i)^{n_i}$ $\Rightarrow \frac{d\alpha}{dT} = \frac{1}{\beta_{tyre}} \sum_{i=1}^{3} w_i Z_i exp\left(\frac{-E_i}{RT}\right)(1-\alpha_i)^{n_i}$ $sensible\ heat: q_s = \sum \frac{dm_t C_{p,t} T}{dt}$; $endothermic\ heat: q_{end} = \sum h_{g,i} \frac{dm_{i,t}}{dt}$
	A (min^{-1})		4.62 x 10^6	5.03 x 10^8	1.24 x 10^9	
	n_i (reaction order)		2.26	0.93	0.90	
	ω_i (mass loss fraction	2 °C/min	4.81	20.65	31.54	
		5 °C/min	4.81	22.16	27.01	
		10 °C/min	4.81	24.22	26.50	
		20 °C/min	4.81	50.98	0.00	
Cheung *et al.* (2011) [43]	**Heating rate (°C/min)**		10	10	10	$\frac{d\alpha}{dt} = \sum_{i=1}^{3} w_i Z_i exp\left(\frac{-E_i}{RT}\right)(1-\alpha_i)^{n_i}$ $\Rightarrow \frac{d\alpha}{dT} = \frac{1}{\beta_{tyre}} \sum_{i=1}^{3} w_i Z_i exp\left(\frac{-E_i}{RT}\right)(1-\alpha_i)^{n_i}$ $sensible\ heat: q_s = \sum \frac{dm_t C_{p,t} T}{dt}$; $endothermic\ heat: q_{end} = \sum h_{g,i} \frac{dm_{i,t}}{dt}$ $exothermic\ heat: q_{exo} = \sum h_{d,j} \frac{dN_{j,t}}{dt}$ $(R_1): TA \xrightarrow{1} V + C;\ (R_2): R \xrightarrow{2} IA$ $(R_3): IA \xrightarrow{3a} V + C;\ IA \xrightarrow{3b} IB;\quad IA \xrightarrow{3c} V + C$
	E_a (kJ.mol^{-1})		69.73	118.04	128.92	
	A (min^{-1})		4.62 x 10^6	5.03 x 10^8	1.24 x 10^9	
	n_i (reaction order)		2.26	0.93	0.90	
	ω_i (mass loss fraction	2 °C/min	4.81	20.65	31.54	
		5 °C/min	4.81	22.16	27.01	
		10 °C/min	4.81	24.22	26.50	
		20 °C/min	4.81	50.98	0.00	

Table 2.3 (continue)

Reference	Parameter		Processing oil	Polymer depolymerisation	Polymer degradation	Comment
Mui *et al*. (2010) [61]	**Heating rate (°C/min)**	**Final Temperature (°C)**	**Component 1**	**Component 2**	**Component 3**	*Kinetic equation:* $\frac{dw_i}{dt} = -k_i(w_i - w_f)^{n_i}$; *Arrhenius equation:* $k_i = A_i e^{-E/RT}$ $\therefore \frac{dw_i}{dt} = -A_i e^{-E/RT}(w_i - w_f)^{n_i}$; *Where:* $\frac{dw_i}{dt}$: *reaction rate;* w_i: *componet i mass at time, t;* k_i: *rste contant;* w_i: *final mass;* n_i: *reaction order* A_i: *pre − exponential factor;* E_a: *activation energy;* R: *universal gas constant;* T: *temperature* (K) *Assuming that thereaction order,* n_i, *is 1 for all components, therefore* (1) *DTG:* $-\frac{1}{w_0}\frac{d\alpha}{dt}$; (2) *Arrhenius plots:* $In\left(-\frac{1}{w - w_f}\frac{dw}{dt}\right)$ *PLOT:* $In\left(-\frac{1}{w - w_f}\frac{dw}{dt}\right)$ *vs.* $\frac{1}{T}$ $\left[\begin{array}{ll} 1)\ A \xrightarrow{1} V_1 & \text{component 1} \approx \text{processing oils} \\ 2)\ A \xrightarrow{2} V_2 & \text{component 2} \approx \text{natural rubber} \\ 3)\ A \xrightarrow{3} V_3 & \text{component 3} \approx \text{synthetic rubber} \end{array}\right]$ *volatiles* 4) $A \xrightarrow{4}$ *solid* *carbon black ≈ char* $r_1 = k_1 e^{-E/RT} C_A$; $r_2 = k_2 e^{-E/RT} C_A$; $r_3 = k_3 e^{-E/RT} C_A$; $r_4 = k_4 e^{-E/RT} C_A$;
			Pre-exponential factor, A (1/min)			
	1	550	27	1.13×10^9	5.26×10^{10}	
	5	550	426	1.45×10^8	1.21×10^{11}	
	10	550	501	1.90×10^7	1.13×10^{17}	
	20	550	114	2.98×10^5	3.16×10^{12}	
			Activation energy, E (kJ/mol)			
	1	550	42.8	127.0	152.2	
	5	550	51.3	116.3	158.0	
	10	550	50.3	102.8	237.1	
	20	550	40.5	77.2	171.4	

Mui *et al*. (2008) [58]	**Heating rate (°C/min)**	**Component 1 (natural rubber)**		**Component 2 (butadiene rubber)**		**Component 3 (styrene butadiene rubber)**	
		A (min^{-1})	E (kJ/mol)	A (min^{-1})	E (kJ/mol)	A (min^{-1})	E (kJ/mol)
	1	$3.69x10^5$	71.2	$1.96x10^{14}$	179.4	$1.95x10^8$	122.2
	5	$2.88x10^5$	67.4	$2.02x10^{14}$	180.0	$3.98x10^7$	111.0
	10	$1.26x10^5$	67.6	$2.03x10^{14}$	180.9	$1.64x10^8$	117.9
	20	$1.18x10^4$	49.3	$3.43x10^{13}$	167.2	$3.55x10^7$	105.4
		Component 1		**Component 2a**		**Component 2b**		**Component 3**	
		A (min^{-1})	E (kJ/mol)	A (min^{-1})	E (kJ/mol)	A (min^{-1})	E (kJ/mol)	A (min^{-1})	E (kJ/mol)
	1	$8.13x10^5$	74.0	$1.01x10^{13}$	165.3	$2.80x10^{11}$	159.7	$2.35x10^7$	111.1
	5	$1.27x10^7$	83.9	$2.21x10^{13}$	170.6	$1.29x10^{14}$	175.1	$3.17x10^9$	136.1
	10	$1.74x10^6$	93.0	$2.80x10^{13}$	190.6	$8.21x10^{13}$	176.1	$2.82x10^6$	89.2
	20	$7.10x10^5$	67.0	$1.58x10^{14}$	174.9	$1.09x10^{16}$	204.8	$6.58x10^8$	122.9

Table 2.3 (continue)

Reference	Parameter	Processing oil		Polymer depolymerisation				Polymer degradation			
	Heating rate (°C.min^{-1})	Component 1		Component 2a		Component 2b		Component 3a		Component 3b	
		A (min^{-1})	E (kJ/mol)	A (min^{-1})	E (kJ/mol)	A (min^{-1})	E (kJ/mol)	A (min^{-1})	E (kJ/mol)	A (min^{-1})	E (kJ/mol)
Mui *et al*. (2008) continue.	1	$4.99\text{x}10^{5}$	72.0	$1.21\text{x}10^{14}$	177.8	$9.19\text{x}10^{11}$	152.8	$5.23\text{x}10^{9}$	139.0	$1.20\text{x}10^{7}$	108.1
	5	$3.41\text{x}10^{6}$	78.0	$5.69\text{x}10^{15}$	196.6	$5.71\text{x}10^{12}$	178.2	$1.21\text{x}10^{11}$	144.3	$6.50\text{x}10^{9}$	140.7
	10	$2.91\text{x}10^{5}$	65.6	$9.06\text{x}10^{13}$	176.3	$8.80\text{x}10^{12}$	163.7	$4.79\text{x}10^{12}$	180.1	$3.56\text{x}10^{9}$	130.0
	20	$1.22\text{x}10^{5}$	58.9	$1.67\text{x}10^{15}$	185.9	$1.41\text{x}10^{10}$	136.7	$1.05\text{x}10^{11}$	153.8	$1.80\text{x}10^{11}$	142.7
	$Kinetic\ equation: \frac{dw_i}{dt} = -k_i(w_i - w_f)^{n_i};\ Arrhenius\ equation:\ k_i = A_i e^{-E/RT}$ $\therefore \frac{dw_i}{dt} = -A_i e^{-E/RT}(w_i - w_f)^{n_i};\ Where: \frac{dw_i}{dt}: reaction\ rate;\ w_i: componet\ i\ mass\ at\ time, t;\ k_i: rste\ contant;$ $\left[\begin{array}{ll} 1)\ A \xrightarrow{1} V_1 & component\ 1 \approx natural\ rubber \\ 2)\ A \xrightarrow{2} V_2 & component\ 2 < \frac{component\ 2a}{component\ 2b} \approx butadiene\ rubber \\ 3)\ A \xrightarrow{3} V_3 & component\ 3 < \frac{component\ 3a}{component\ 3b} \approx styrene\ butadiene\ rubber \end{array}\right] volatiles$ $4)\ A \xrightarrow{4} solid \qquad carbon\ black \approx char$										

2.4 Waste tyre pyrolysis fractions

The main products from waste tyre pyrolysis are: 1) pyro-gas (gas), 2) TDO, and 3) pyro-solid (char) [3,12,36]. Alternatively, waste tyre pyrolysis progress can be based on the proximate analysis to determine tyre crumb moisture, volatile matter (processing oils and rubbery materials) and non-volatiles (fixed carbon and ash) [27,30,48,62,63]. De Marco Rodríguez et al. (2001) pointed out that for complete waste tyre pyrolysis, i.e. pyrolysis at temperatures from 500 °C and above, all volatile matter was devolatilised to the TDO and gas fractions as well degraded into char through secondary reactions cracking [32]. They also reported that the char should be closely correspond to the sum of the fixed carbon and ash. Therefore, an increase in pyrolysis temperature from 500 to 700 °C and longer pyrolysis times do not decrease the char yield. Also, Antoniou and Zabaniotou (2013) pointed out that the gas and TDO comprises about half of the pyrolysis products by weight [12].

In the following subsection studies that have specifically investigated TDO, the most [/interesting main pyrolysis fraction, will be discussed.

2.5 Tyre derived oil (TDO)

Williams (2013) described TDO as a dark/black coloured, medium viscosity oil with sulphurous/aromatic odour [36]. TDO contains hundreds of compounds. Quek and Balasubramanian (2013) reviewed liquefaction of waste tyres by pyrolysis for TDO and chemicals production at various pyrolysis conditions [37]. Pyrolysis parameters that affect process performance include temperature, heating rate, tyre particle size, gas flow rate and pressure. They concluded that the effect of increasing or decreasing the pyrolysis operating parameters, particularly temperature and pressure, was not clear. This was attributed to the pyrolysis operating parameters associated with pyrolysis reactor configuration, such as, the size of the reactor, hot volatiles residence time in the hot reaction zones of the reactor and the efficiency of heat transfer from the reactor to and within the tyre mass.

Antonniou and Zabaniotou (2013) reported a temperature of 500 °C as the optimal value for high TDO yield [12]. They also reported that the volume of the lighter products in the TDO increase as the temperature increase. Lighter products include benzene and kerosenes. Burrueco et al. (2004) also carried out experiments in a fixed-bed batch reactor to investigate the effect of increasing temperature from 400 to 500 °C on the TDO yield [1]. At temperatures above 500 °C the TDO yield did not change significantly. It was also concluded that the yields of the TDO and gas were interrelated, e.g. the TDO yield decreases as the

gas yield was increased by increasing temperature. However, at a very high temperatures the TDO-gas yield relation cease to be related as a results of secondary reactions which promotes cracking of the primary products, i.e., cracking of gases to char or TDO to gases.

TDO is the most valuable waste tyre pyrolysis product fraction [5]. This claim by Murillo et al. (2006) has led to their intensive study of the pyrolysis operating conditions effects on the TDO [5]. They concluded that at a temperature of 500 °C maximum TDO yield was obtained. This was confirmed by observing that neither the total conversion nor the TDO yield increased as the pyrolysis temperature was increased from 500 °C to 600 °C. They also concluded that the effect of the pyrolysis time and heating rate was insignificant, as there were no significant differences in the chemical compositions of the TDOs. This insignificance of the pyrolysis time was attributed to the short residence times of the hot volatiles, which in turn was due to their rapid sweeping by the purging gas.

A study on the production of pyrolysis liquid fuels and chemicals from motorcycle waste tyres was conducted by Islam et al. (2008) [63]. A TDO yield of 49 wt.% was reported as the maximum yield at a pyrolysis temperature of 475 °C. They carried out experiments in a fixed-bed fire-tube heated reactor with typical volatiles residence times of 5 s and feed size of 4 cm^3. They also concluded that the TDO obtained was suitable for usage as a liquid fuel and as a chemical production feedstock

TDO yields reported by Roy et al. (1999) from waste tyre pyrolysis experiments conducted in a continuous vacuum pyrolysis reactor were between 43 and 47 wt.% (steel and moisture included) [51]. The feedstock was either passenger car tyres or truck tyres. The pressure investigated was between 6 and 10 kPa and the pyrolysis temperature was between 485 and 550 °C. At a pyrolysis temperature of 500 °C, residence times of the hydrocarbons formed from the cracked rubber were considerably shorter in the vacuum process. Moreover, undesirable secondary degradation reactions of the valuable chemicals can be reduced. Therefore, the highest TDO yields could be obtained at pyrolysis temperatures around 500 °C. In vacuum pyrolysis, lower pressure closer to 0 kPa favours higher TDO yields.

2.6 Waste tyre pretreatment prior to pyrolysis

Kebritchi et al. (2013) compared the pyrolysis of vulcanised and devulcanised waste tyre feedstocks [64]. De-vulcanisation was conducted in an autoclave reactor using chemical treatment methods to soften or plasticise the crumb rubber at a temperature between 140 and 200 °C. They used a vacuum pyrolysis reactor to investigate the effect of the temperature ranging between 400 and 600 °C and at a pressure of 2.2 kPa.

They concluded that the pyrolysis time of the de-vulcanised waste tyre was shorter compared to vulcanised waste tyre pyrolysis [64]. They also pointed out that the TDO yield from de-vulcanised waste tyre was higher than that from vulcanised waste tyre. The pyrolysis char yield was, however, lower from de-vulcanised waste tyres than from vulcanised waste tyres. Shorter pyrolysis times from de-vulcanised waste tyre were attributed to the ease in the cracking of bonds of the previously cracked chains in the devulcanised waste tyres [64]. The higher TDO yield was attributed to the readily devolatilisation of the de-vulcanised waste tyres during pyrolysis.

It is only in the Kebritchi et al. (2013) study that the effect of pre-treatment of the waste tyres was studied on the waste tyre pyrolysis [64]. However, it was not intended for production of valuable chemicals and recovery of the materials. Most work that involved pre-treatment of waste tyre which was intended for the reclaiming of the waste tyres has been done by various researchers [65-67]. None of these researchers investigated the effects of waste tyre pre-treatment on materials recovery and chemicals production.

In addition to the production of the chemicals, separation and recovery is important [61]. Therefore, extraction of the processing additives can simplify the composition of the TDO as well as TDO processing post-pyrolysis processes. A portion of extractives (≈ 10 wt.%) is readily extractable by solvent. Also, stepwise temperature pyrolysis (from less server to server conditions) as well as stepwise production and recovery of the chemicals is possible.

2.7 Cooling and condensation of hot volatiles

There is limited literature on selective temperature condensation of waste tyre volatiles from the pyrolysis reactor to produce TDO, in particular to concentrate particular chemicals of interest in specific fractions. Williams and Brindle (2003) investigated step-wise condensation of the hot volatiles evolved from waste tyre pyrolysis in a fixed-bed reactor [24]. They investigated the effect of maintaining the entire condensation unit at different temperatures (100, 150, 200 and 250 °C) on the yield of single ring aromatic compounds and the molecular weight distribution in the TDO fractions [24]. These temperatures were maintained on each of the first three condensers, while two subsequent impingers were maintained at a temperature of – 70 °C using dry ice-acetone mixtures. In addition, the effect of the mesh and pall ring both made of stainless steel was investigated. With the pyrolysis temperature, similar for all experiments at 570 °C they pointed out that the TDO yield was the same at 57.1 wt.%, while its fractional distribution yield in the condensers varied [24].

The amount of TDO collected in the first three condensers decreases from 70 to 50 wt.% (of the total TDO), when the temperature was increased from 100 to 250 °C. The TDO collected in the first condenser was 42 wt.% at a condenser temperature of 100 °C and decreased to 25 wt.% as the condenser temperature was increased to 250 °C. This was attributed to the longer time the volatiles remained in the gaseous phase at the high condenser temperatures. Also, an increase in the condenser temperature reduced the residence time of the gases in the condenser, due to the increase in gas flow rate. Thus, equilibrium state was not achieved due to shorter vapours residence times. This resulted in less mass transfer from vapour phase to liquid phase at higher condensation temperatures compared to lower condensation temperatures. Total DL-limonene yield in the first three stainless steel condensers maintained at 100 °C was 1.5 wt.%, while at a temperature of 250 °C it was reduced to 0.5 wt.%. In the impingers, DL-limonene decreased from 6.8 to 5.6 wt.% as the temperature was increased from 100 to 250 °C. Toluene and m/p-xylene yield in the three stainless steel condensers decreased from 0.3 wt.% to null from 100 °C to 250 °C operated system. This was attributed to the carry through of the TDO to the final glass impingers as temperature was increased [24].

They have pointed out that when a pall ring packing was used and the temperature of the condensers was 100 °C, 45 wt.% of the TDO was collected compared to 32 wt.% for unpacked condensers [24]. Moreover, 70 wt.% of the total TDO was collected in the pall ring packed condensers compared to 60 wt.% in the unpacked condensers. This was attributed to the high contact area between the hot vapours and the surfaces of the pall rings. Thus, mass transfer from gaseous phase to liquid phase was increased. They have also concluded that average molecular weight distribution between the first condenser and the last impinger was wider for pall ring packing condensers while for unpacked was narrower [24].

There are also various publications on the processing of pyrolysis products into several pyrolysis fractions using distillation techniques. For example, Aylon et al. (2010), Laresgoiti et al. (2004), Li et al. (2004), and Aylon et al. (2008) [29,50,68,69]. Benallal et al. (1995), Roy et al. (1997), reported DL-limonene as one of the major compounds at 7 wt.% [70,71].

2.8 Valuables chemicals production and recovery

TDO has been reported as the major waste tyre pyrolysis fraction by most researchers [9,25,47,49,69]. TDO can be used as an energy source as well as the source of materials and chemical products [12,25,36,37]. The main objective of this study is production of the market-valuable DL-limonene from waste tyre pyrolysis, which is one of the primary chemical components in TDO.

Table 2.4 a list of the valuable chemicals from waste tyre pyrolysis identified from the literature is presented. Table 2.4 only lists the most significant valuable chemicals that are of interest in general. However, only maximisation of the DL-limonene will be studied here. This list is not a complete list of all the chemical products from waste tyre pyrolysis, which includes many those compounds, such as, hetero-atoms (polyaromatic nitrogen and polyaromatic sulphur hydrocarbons), polycyclic aromatic hydrocarbons, aliphatic as well as single-ring aromatics. Table 2.5 lists typical concentrations of these chemical products reported from the literature thus far.

TDO mainly contains organic compounds of C_5 to C_{20} [25]. It has been classified in various product fractions by different authors. Williams et al. (2013) reported aliphatic, aromatic, hetero-atom and polar fractions the main constituents of the TDO [36]. Cunliffe and Williams (1998) classified TDO according to the fractional solvent extraction, such as pentane (aliphatics), benzene (aromatics), ethyl acetate (hetero-atoms) and methanol (polar) fractions [49]. Williams et al. (1990) further divided the pentane fraction into two subfractions in addition to these three main fractions of the TDO [4]. Therefore, this resulted in five fractions of the TDO, i.e., pentane-1, pentane-2, benzene, ethyl acetate and methanol fractions. Another classification of the TDO was employed by Dai et al. (2001), viz., alkanes (aliphatics), aromatics, non-hydrocarbons (hetero-atom) and asphalt (polar) fractions [47]. Laresgoiti et al. (2004) classified the TDO fractions as either aromatic (Ar), non-aromatic (NAr), oxygenated aromatic (ArO), oxygenated non-aromatic (NArO), nitrogenated aromatic (ArN) or nitrosulphurated aromatics (ArNS) [50]. Kar (2011) reported TDO fractions as paraffin (alkanes), olefins (alkenes) and aromatics [72]. Other researchers have reported TDO fractions as non-aromatics (C_5 – C_{10} hydrocarbons), aromatic (single-ring C_{10}^- aromatic hydrocarbons) and tar (C_{11}^+ hydrocarbons, not of the aromatic or non-aromatics nature) [15,73-75]. However, the most common TDO fractions classification includes aliphatic, aromatic, hetero-atom and polar fractions.

Table 2.4: Significant chemical products from waste tyre pyrolysis liquid fraction.

Chemical product	Source	Type	Industrial applications	References
Isoprene	NR	Monomer		[7,52,53,69,76]
Butadiene	SBR and BR	Monomer		[7,52,53,69,76]
Styrene	SBR	Monomer, single-ring aromatic	Plastics and polymer industry feedstocks [65],	[52,53,69,76]
DL-limonene	NR, isoprene	Dimer	Feedstock in the industrial formulations of solvents, resins, and adhesives [7,52,53,66]	[52,53,69,76]
4-vinyl-1-cyclohexene	SBR, butadiene	Dimer	Sold as-is or converted to 4-vinylcyclohexene diepoxide.	[52,53,69,76]
[α]Indane				[52,53,69,76]
[α]*m*-cymene				[52,53,69]
[α]Trimethylbenzene			Plastics and polymer industry feedstocks [66].	[52,53,69,76]
Dimethylbenzene (1,2- and 1,3-)	NR, DL-limonene	Single-ring aromatic		[52,53,69]
Indene			Used to produce indene-coumarone resins [49,68].	[52,53,69,76]
Benzene			Plastics and	[7,52,53,69,76]
Toluene			polymer industry	[7,52,53,69,76]
Xylenes (*m*-, *o*- and *p*-)	SBR, styrene, DL-limonene, butadiene	Single-ring aromatic	feedstocks [7,49,69]. *o*-Xylenes uses to produce phthalic anhydride	[7,52,53,69,76]

Table 2.5: Typical valuable chemicals yields from waste tyre pyrolysis (wt.% steel and synthetic fiber free basis).

Reference	Temperature (°C)	Residence time (s)	Liquid yield (wt.%)	DL-limonene	trimethyl-benzene	styrene	indene	Dimethyl-benzene	benzene	toluene	xylenes
Li et al. (2004)	450	n.a.	43.00	5.440	1.989	0.519	0.357	1.263	0.172	0.976	0.661
	500	n.a.	45.10	1.883	3.304	0.587	0.172	2.437	0.605	1.258	0.841
	550	n.a.	44.60	0.419	2.794	0.635	0.401	3.151	0.664	2.302	0.915
	600	n.a.	42.70	0.122	2.703	0.613	0.191	3.556	0.900	3.093	0.908
	650	n.a.	42.90	0.070	2.616	1.133	0.164	3.243	0.898	3.027	0.864
Pakdel et al. (1991)	226 - 510	n.a.	31.53	4.704					0.801	2.191	1.930
Pakdel et al. (2001)	431 - 471	n.a.		3.600							
Leresgoiti et al. (2004)	400	n.a.	24.80	2.040							
Williams and Brindle (2003)	500	30	55.80	2.009					0.112	0.614	0.837

Table 2.5 (continue)

Reference	Temperature (°C)	Residence time (s)	Liquid yield (wt.%)	DL-limonene	trimethyl-benzene	styrene	indene	Dimethyl-benzene	benzene	toluene	xylenes
Williams and Brindle (2003)	450	n.a.	55.5	2.750					0.110	0.110	0.330
	600	n.a.	43.5	0.000					0.870	2.175	3.480
Boxiong et al. (2007)	500	n.a.	45.9	4.00	0.682	1.264	0.026		0.210	1.092	0.936

Note: The list includes only pyrolysis liquid derived valuable chemicals. Pyrolysis gas derived valuable products such as butadiene, isoprene, etc are not included.

The most of valuable chemicals from waste tyre devolatilisation are in the form of monomers, dimers and single ring aromatics. These chemical products include isoprene, butadiene, styrene, DL-limonene, 4-vinyl-cyclohexene, 1,2,4-methylbenzene, m-cumene, indane, 1,4-cyclohexadiene, benzene, toluene, xylene and ethylbenzene (BTXE) [11]. Most of these compounds end up in the TDO. Illustrated in Figure 2.11 are typical chemical products categorised in monomers, dimers and aromatics, as well as their source of volatile organic matter. Also, the most predominant valuable chemicals identified from the literature are listed in Table 2.5.

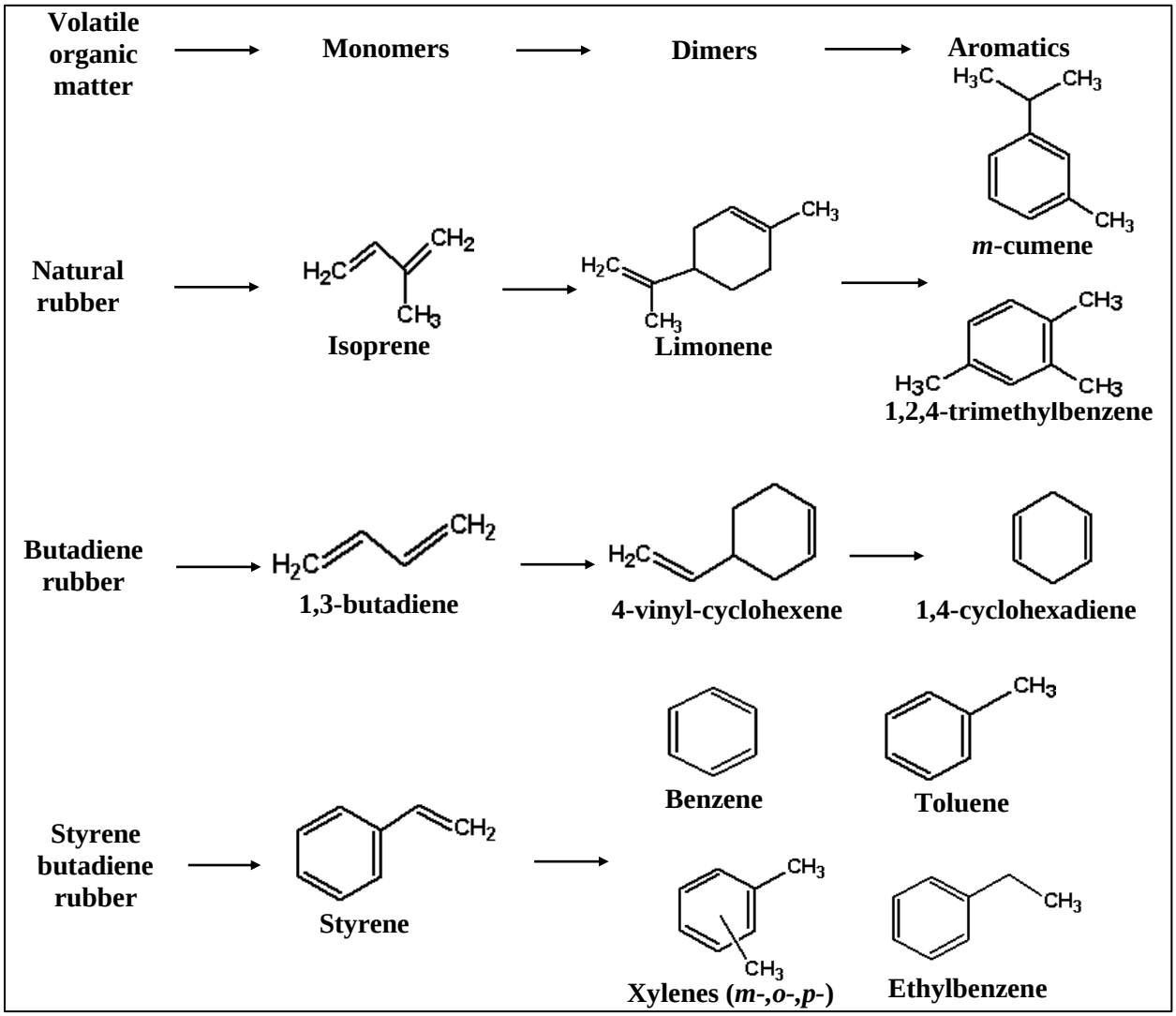

Figure 2.11: Typical monomers, dimers and single ring aromatics from different rubber polymers.

DL-limonene is a naturally occurring compound and its composition is high in citrus oil at more than 80 %. It is an important component in the industrial formulations of solvents, resins, and adhesives [29,51,72]. It

formation mechanisms from waste tyres is shown in Figure 2.12. DL-limonene formation involves an initial step of thermal devolatilisation of polyisoprene rubber by β-scission to form isoprene intermediate radicals. This is immediately followed by the formation of the intermediate radicals. The next step is the dimerisation of the isoprene in the gas phase to DL-limonene (dipentene).

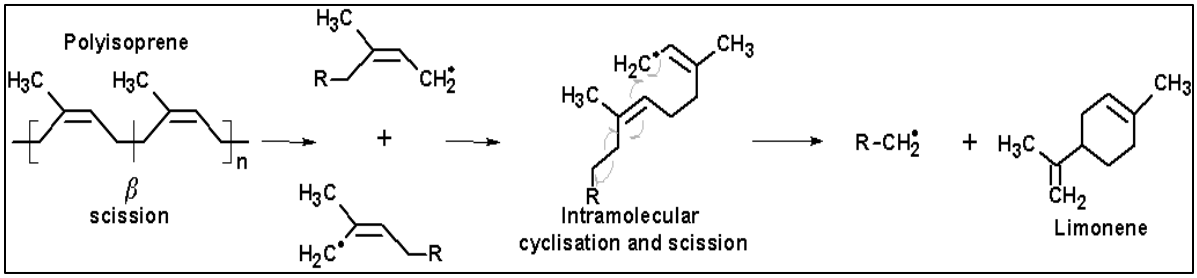

Figure 2.12: Typical mechanisms of the formation of DL-limonene from waste tyre pyrolysis
Source: Pakdel et al. (1991) [52].

The first reaction depends on high energy and results into higher C:H ratios, while the latter two reactions depend on lower energy and are characterised by lower C:H ratios. Pakdel et al. (2001) pointed out that these mechanisms are not easy to control in waste tyre pyrolysis processes [53]. They are dependent on the temperature, the residence time and location of the volatiles within the reactor.

Constituent 4-vinyl-1-cyclohexene is an organic compound formed by dimerisation of 1,3-butadiene by Diels-Alder reaction, as shown in Figure 2.13. It is found in the industrial processes involving 1,3-butadiene, including the manufacturing of lauric acid. It may be sold as it is or it can be converted to 4-vinylcyclohexene diepoxide.

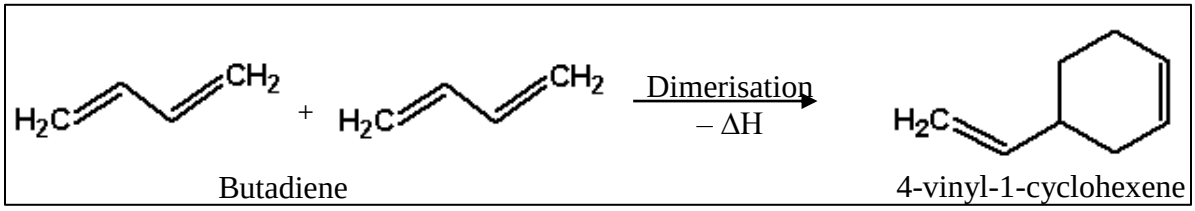

Figure 2.13: Illustration of cyclisation/dimerization of butadiene to form 4-vinyl-1-cyclohexene

Moreover, it has been concluded that the pyrolysis temperature significantly affects rubber materials devolatilisation mechanism. As shown from Figure 2.12 to Figure 2.17, temperature affects the rate of the two main devolatilisation mechanisms, viz., high energy and low energy mechanism. The high-energy

mechanism favours decomposition of a large molecule to the small molecules and formation of higher C:H ratio products. This phenomenon is illustrated in Figure 2.14, Figure 2.16 and Figure 2.17 and it is associated with high pyrolysis temperature *β*-scission mechanism, aromatisation, Diels-Alder reactions and formation of the PAHs, respectively. Low energy mechanism can be associated with low pyrolysis temperature and short volatiles residence times. Figure 2.12, Figure 2.13 and Figure 2.15 shows Diels-Alder cyclisation, dimerisation and cyclisation reactions, respectively.

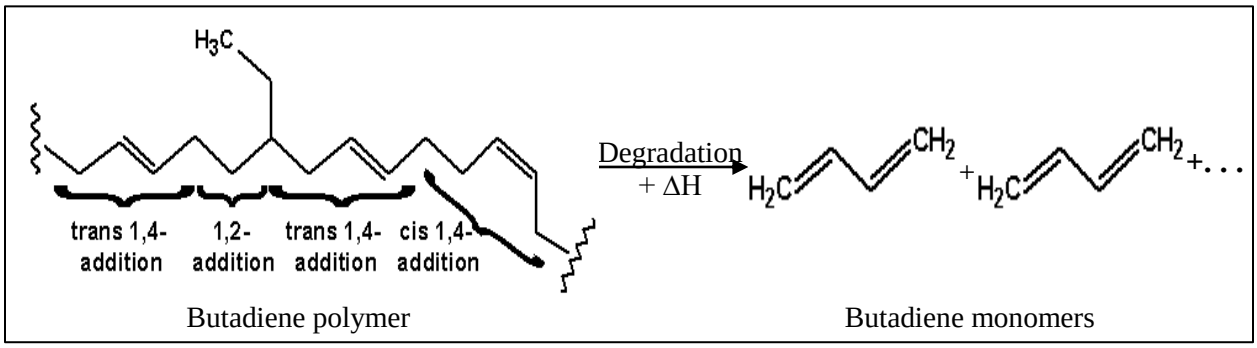

Figure 2.14: Illustration of β-scission degradation of the butadiene polymer

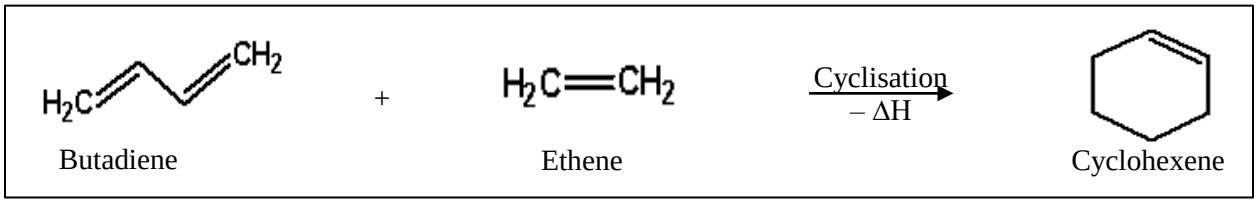

Figure 2.15: Illustration of the formation of cyclohexene by Diels-Alder cyclisation

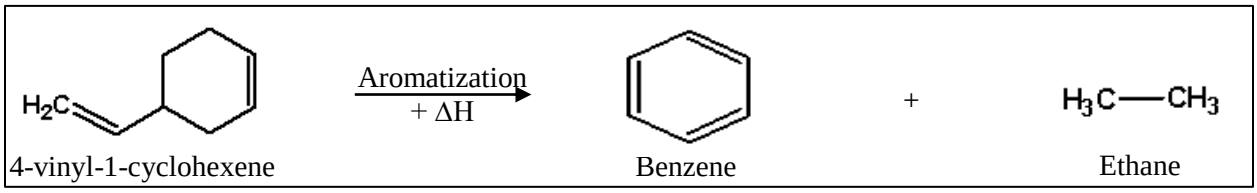

Figure 2.16: Illustration of aromatisation reaction of 4-vinyl-1-cyclohene to benzene

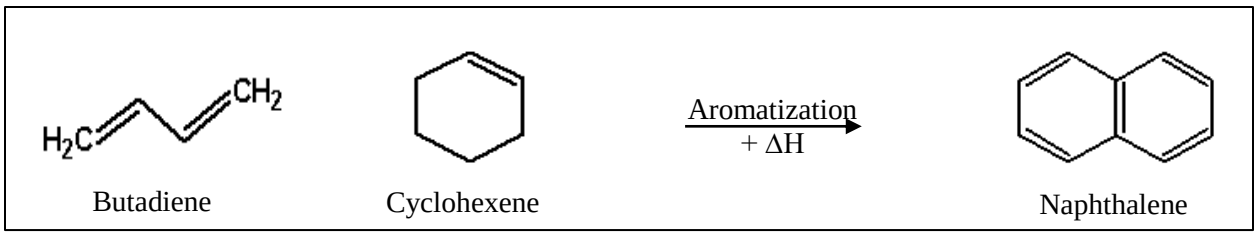

Figure 2.17: Illustration of the formation of naphthalene by a Diels-Alder type aromatisation reaction

Concentrations of most compounds in the TDO are mainly dependent on the pyrolysis operating conditions. The main operating parameters are temperature, pressure, heating rate and residence time of the hot volatiles in the hot reaction zones. Thus, maximising valuable chemicals production depends primarily on the pyrolysis operating conditions.

Pakdel et al. (1991) studied formation of DL-limonene from waste tyres using a vacuum pyrolysis unit consisting of multiple hearths (six in total) [52]. The hearths corresponded to temperatures at 226, 295, 366, 404, 450, and 510 °C, from the top to the bottom of the hearths. They reported temperatures between 295 and 450 °C as most favourable for the formation of DL-limonene. Moreover, 4-vinyl-1-cyclohexene was reported as a major compound in this temperature range. Other compounds in high amounts in the light naphtha fraction reported were: benzene, toluene and xylenes (*p*-, *m*- and *o*-) BTX, methylpentane, dimethylpentane, 2,4,4-trimethyl-1-pentane, dimethylcyclopentadiene, trimethylpentadiene, ethypentadiene 3-methyl-1,4-hexadiene and isopropylbenzene. They concluded that 95 % pure DL-limonene could be achieved when a pentane and subsequently dichloromethane solvent elution was carried out. Later a vacuum pilot-plant was used by Pakdel et al. (2001) to investigate DL-limonene purification under vacuum conditions [53].

Pyrolysis of the waste tyres was conducted over a temperature range between 440 and 570 °C and at a pressure ranging between 1.3 – 28 kPa followed by distillation to recover light naphtha concentrated with DL-limonene by Roy et al. (1999) [51]. They concluded that at pyrolysis temperatures higher than 500 °C DL-limonene reacted to form compounds with boiling points similar to it. These compounds were trimethylbenzene, m-cymene and indane. An increase was also observed in the DL-limonene yield as the pressure was decreased. Maximum DL-limonene yield reported was at 3.6 wt.% of the waste tyre feed, see Table 2.5.

Li et al. (2004) reported high volatile compounds, such as, benzene, toluene, and xylene (BTX), (1,2 and 1,3)-dimethyl benzenes, styrene, trimethylbenzene, C^{10}-based aromatics, indene and DL-limonene as the most significant compound in the TDO [69]. Single-ring aromatics can be used as a feedstock in formulation processes in the plastics and polymer industry [49]. By increasing the temperature from 450 to 600 °C, higher yields of aromatics and lower DL-limonene yields were obtained. A further increase in the temperature from 600 to 650 °C also decreased the BTX concentration in the TDO. This was attributed to the occurrence of the Diels-Alder type aromatisation of the single-ring aromatics to polycyclic aromatic hydrocarbons (PAHs), see Table 2.5. Maximum DL-limonene yield of 5.44 wt.% was obtained at lower pyrolysis temperature of 450 °C, see also Table 2.5.

Similar compounds were reported by Cunliffe and Williams (1998) when analysing the TDO from a batch pyrolysis reactor [49]. They reported DL-limonene, methylstyrene, dimethylbenzene, toluene, indene, styrene and trimethylbenzene, as the most significant compounds at lower temperatures (450 °C). At a higher pyrolysis temperature (600 °C), DL-limonene was still the most abundant compound though its content in the TDO was lower than at lower temperature. The content of benzene and toluene in the TDO significantly increased at the higher temperature.

Kyari et al. (2005) observed significant amounts of DL-limonene, styrene, indene, toluene, ethylbenzene, indene biphenyl and traces of benzene and polycyclic aromatic hydrocarbons in seven different types of automotive tyres [9]. They also reported the presence of the non-aromatic compounds, alkanes, sulphur-containing compounds, nitrogen-containing compounds in the TDO.

DL-limonene was reported as the most abundant chemical by Laresgoiti et al. (2004) at 2.04 wt.% of the tyre [50]. A maximum DL-limonene yield was obtained at a pyrolysis temperature of 400 °C. They noted that DL-limonene yield increased as the temperature increased from 300 to 400 °C and decreased as the temperature further increased from 400 to 700 °C. However, the highest DL-limonene yield was obtained at a very low TDO yield, see Table 2.5. Moreover, they reported that the TDO contained mainly aromatic compounds. This was attributed to the aromatic nature of the source of the polymeric material, i.e. styrene-butadiene rubber, as well as the cyclisation of the olefin structures followed by dehydrogenation reactions during pyrolysis.

The DL-limonene yield was also high in the TDO obtained by Williams and Brindle (2003) from waste tyre pyrolysis at a temperature and residence time of 500 °C and 30 s, respectively [77]. Other compounds detected were benzene, toluene and xylenes. They also investigated the effect of the two zeolite catalysts

on the aromatics yield, which resulted in null DL-limonene yield and an increase in the BTX yield, see Table 2.5. These experiments were carried out in a fixed-bed batch reactor. They noted, however, that the TDO yield decreased from 55.8 to 32 wt.% due to the secondary reactions over the catalysts which promoted permanent gases formation. Williams and Brindle (2003) also used a fluidised-bed reactor to investigate two different catalysts [7]. TDO yields decreased from 55.0 to 43.5 wt.% as the temperature increased from 450 to 600 °C. At similar pyrolysis conditions, single-ring aromatics yields increased from 0.11 to 0.8 wt.%, 0.11 to 2.175 wt.% and 0.33 to 3.48 wt.% for benzene, toluene and xylenes, respectively. The DL-limonene yield was reported to decrease from 2.75 to 0.00 wt.% as the temperature was increased.

Boxiong et al. (2007) examined chemical composition of the light naphtha fraction distilled from TDO that was obtained from a fixed-bed batch reactor at a temperature of 500 °C [76]. They reported TDO yield of 45.9 wt.% of which 34.4 wt.% was recovered as light naphtha. The most significant compound detected in the light naphtha was DL-limonene. Other compounds detected from this fraction were trimethylbenzene, styrene, indene, benzene, toluene, xylene and ethylbenzene (BTXE) in high concentrations. They also fed the volatiles into a fixed-catalytic bed at 400 °C to allow secondary reactions. It was concluded that the secondary reaction of the volatiles over the catalytic bed resulted in lower TDO yields as well as lower DL-limonene yields. The yield of the other compounds in the naphtha fraction increased after the catalytic bed treatment and with increasing catalyst to feed ratio.

Lopez et al. (2010) used a conical spouted bed reactor using continuous tyre feeding system to investigate the effect of the temperature (425 and 500 °C) and pressure (25, 50 and 101 kPa) on the chemical product distribution and properties of TDO [78]. They reported maximum isoprene yields at the lower temperatures and pressures. The DL-limonene yield increased as the temperature was decreased. However, as the vacuum pressure was reduced at a temperature of 425 and 500 °C, the DL-limonene yield decreased. This was attributed to isoprene inhibition from dimerisation to yield DL-limonene in a vacuum. The effect of the temperature and pressure on the styrene yield was similar to that of the DL-limonene yield. Also, they reported that the BTXE yield increase with increasing temperature while the vacuum had no effect. This was attributed to the aromatisation reaction mechanism as shown in Figure 2.16.

2.9 Rationale for the study

While the optimal waste tyre pyrolysis technology is yet to be established and commercialised, production of waste tyres is constantly increasing and with an estimated rate of one waste tyre per year per person in the developed countries [79]. There is yet to be a solution that can entirely accommodate the increasing

amount of waste tyres and it must meet both technical and legislative requirements. Thus, there is a need for novel methods to deal with these high amounts of waste tyres. Conventional waste tyre recycling methods, such as, landfilling and dumping in the rural areas are prohibited due to environmentally unfriendliness [79]. Despite recent development of environmental friendly waste tyre recycling methods, such as, tyre re-treading, co-combustion of the waste tyres in the cement kiln and pulp industry for energy and civil engineering applications, the waste tyres problem remains unresolved [6].

To minimise usage of the depleting natural resources and environmental emissions, material recovery and valuable chemicals production from waste tyres is required. Most valuable chemicals include rubber derived monomers and dimers. These are butadiene, isoprene and DL-limonene, 4-vinyl-1-cyclohexene and styrene. They are the derivatives of polybutadiene rubber (BR), natural rubber (NR) and styrene-butadiene rubber (SBR). Consequently, study of the waste tyre pyrolysis process to maximise DL-limonene production and using the remaining tyre derived oil as a fuel is investigated.

Pyrolysis is the most promising technology for the recycling of waste tyres. However, the complexity of the technology, due to the numerous reactions involved in this process, is a major impediment. In addition, conventional trend towards waste tyre pyrolysis for merely energy recovery (liquid fuels production) has limited implementation of waste pyrolysis due to competition with petroleum-derived fuels. This approach ignores the production and recovery of the valuable chemicals from the waste tyres.

The yields of the main fractions of waste tyre pyrolysis (gas, TDO and char) reported in the literature are scattered. Thus, there is no single set of optimal pyrolysis reactor operating conditions that can achieve a predetermined pyrolysis main fractions yield and quality for a specific waste tyre pyrolysis process. This is firstly attributed to various tyre formulations depending on the tyre manufacturer. Secondly, there are numerous waste tyre pyrolysis reactors and configurations that affect waste tyre pyrolysis main fractions yield and quality. Thirdly, operating conditions at which pyrolysis processes are conducted are different from one study to another. Lastly, studies on the production and recovery of the valuable chemicals have not been extensively conducted.

2.10 Conclusions

Valuable chemicals (particularly DL-limonene) production from waste tyres depends primarily on the pyrolysis conditions and type of the waste tyre being pyrolysed, such as, TT and PCT [15,59,72,80].

Although in general researchers employ different pyrolysis conditions based on the envisioned application of the final products, there are however four important conclusions that can be drawn.

Firstly, pyrolysis temperature and hot volatiles residence time in the hot zones of the pyrolysis reactor are potentially the main pyrolysis parameters that significantly affect the yields of the main pyrolysis fractions and their chemical composition. Proper application and monitoring of these parameters may result in the production of a TDO at the desired yield and chemical composition. However, micro-gram scale (TGA) studies have showed that heating rate has significant effect on the waste tyre components devolatilisation (processing additives and polymeric matter). The main shortcoming from the literature regarding heating rate studies is to associate it effect on the TDO yield and chemical composition. This is not surprising since conventional waste tyre pyrolysis research work has been purported to the maximisation of the TDO yield for merely energy recovery (liquid fuels). However, Banar et al. (2012) indicated that, at a final pyrolysis temperature of 400 °C, DL-limonene content in the TDO decreased from 17,062 to 219 ppm, as the heating rate was increased from 5 to 35 °C/min [31]. Their study entailed investigating of the heating rate effect on the characteristics of the TDO as a replacement of the petroleum derived oil rather than for valuable chemicals production [31]. In the current study the effect of the heating rate and temperature on the TDO chemical composition is investigated. This entails studying pyrolysis parameters, i.e., optimal temperature and heating rate in the pyrolysis reactor to maximise TDO and DL-limonene yield from waste tyre pyrolysis.

Secondly, it is known that there is substantial literature that investigate the kinetic mechanisms of the componential depolymerisation of the waste tyres, see Table 2.3. In the literature, it is observed that heating rate is a common pyrolysis parameter in most studies tabulated in Table 2.3. The main focus is on the devolatilisation of components with, however, less focus on the product compounds that are formed during devolatilisation of the waste tyre components. Studies on the devolatilisation kinetic mechanisms for waste tyres pyrolysis have indicated that mass loss reactions of the waste tyres during pyrolysis occur stepwise, depending on temperature and heating rate. In addition, kinetic mechanisms of the depolymerisation of the polymeric matter can guide the selection of the various optimal pyrolysis techniques. Non-isothermal operated pyrolysis processes are the most favourable method since the kinetic mechanisms depend on the temperature and heating rate. The study of the kinetic mechanism on the formation of valuable chemicals (DL-limonene) will be carried out in the current study.

The first and second observations discussed above are both associated with the pyrolysis reactor during devolatilisation of the waste tyre to produce hot volatiles. Varies techniques of cooling and condensing the hot volatiles from the pyrolysis reactor have not been widely explored in the literature to improve TDO

yield or it chemical composition. Therefore, a third shortcoming in the literature is the study of the cooling and condensation of the hot volatiles from the pyrolysis reactor. This shortcoming can be attributed to, 1) less consideration of the cooling and condensation of the hot volatiles from pyrolysis reactor as part of the pyrolysis process, and 2) conventionally, waste tyre pyrolysis is intended for production of fuels. With the latter point, however, a shift to the production of the valuable chemicals from waste pyrolysis has been observed. Few techniques to improve the pyrolysis process has been investigated. In the conventional pyrolysis processes, the hot volatiles from pyrolysis reactor are condensed in the conventional tube-and-shell condensers with the objective of condensing and recovery nearly all the hot volatiles. This technique results in a single liquid fraction that consists a plethora of compounds. It is subsequently very difficult to separate all the valuable chemicals from this mixture. Thus, expensive and costly separation processes, such as, distillation, are required. Part of the study of the cooling and condensation of the hot volatiles will focus on the effect of the contact between the cooling fluid and the hot volatiles while being cooled and condensed to the TDO.

Therefore, there is limited literature available that focuses on developing novel methods for treating the hot volatiles from the pyrolysis reactor to improve the TDO yield and its content of valuable chemicals. The exception, however, is the work carried out by Williams and Brindle (2003) where condensation of the hot volatiles from waste tyre pyrolysis in a fixed-bed reactor was investigated [24].

Finally, since conventional waste tyre pyrolysis processes has not been intended for the maximisation of the valuable chemicals production, there has been no thorough study on the various pyrolysis reactors, types, configuration and sizes and their effect on the TDO chemical composition. These parameters also influence on how the optimal pyrolysis conditions are achieved and maintained. It is difficult to achieve and maintain them in some pyrolysis reactors. This was reported by Roy et al. (1999) when a pilot-scale-plant was used to investigate the influence of the temperature and pressure on the chemical composition of the waste tyre pyrolysis main fractions [51]. Therefore, the effect of various pyrolysis reactors and condensation techniques of the hot volatiles from pyrolysis reactors on the DL-limonene production will be integrated to propose a most efficient pyrolysis process.

References

[1] C. Berrueco, E. Esperanza, F.J. Mastral, J. Ceamanos, P. García-Bacaicoa, Pyrolysis of waste tyres in an atmospheric static-bed batch reactor: Analysis of the gases obtained, J. Anal. Appl. Pyrolysis. 74 (2005) 245-253.

[2] S. Seidelt, M. Müller-Hagedorn, H. Bockhorn, Description of tire pyrolysis by thermal degradation behaviour of main components, J. Anal. Appl. Pyrolysis. 75 (2006) 11-18.

[3] J.D. Martínez, N. Puy, R. Murillo, T. García, M.V. Navarro, A.M. Mastral, Waste tyre pyrolysis – A review, Renewable and Sustainable Energy Reviews. 23 (2013) 179-213.

[4] P.T. Williams, S. Besler, D.T. Taylor, The pyrolysis of scrap automotive tyres: The influence of temperature and heating rate on product composition, Fuel. 69 (1990) 1474-1482.

[5] R. Murillo, E. Aylón, M.V. Navarro, M.S. Callén, A. Aranda, A.M. Mastral, The application of thermal processes to valorise waste tyre, Fuel Process Technol. 87 (2006) 143-147.

[6] D. De, D. De, Processing and material characteristics of a reclaimed ground rubber tire reinforced styrene butadiene rubber, Materials Sciences and Applications. 2 (2011) 486-496.

[7] P.T. Williams, A.J. Brindle, Fluidised bed pyrolysis and catalytic prolysis of scrap tyres, Environmental Technology. 24 (2003) 921-929.

[8] A. Evans, R. Evans, The composition of a tyre: typical components, (2006) 1.

[9] M. Kyari, A. Cunliffe, P.T. Williams, Characterization of oils, gases, and char in relation to the pyrolysis of different brands of scrap automotive tires, Energy Fuels. 19 (2005) 1165-1173.

[10] I.S. Amosova, E.I. Andreikov, Thermal degradation of butadiene and isoprene rubbers in organic solvents, International Polymer Science and Technology. 36 (2009) T/5+.

[11] J.A. Conesa, I. Martin-Gullón, R. Font, Rubber tire thermal decomposition in a used oil environment, J. Anal. Appl. Pyrolysis. 74 (2005) 265-269.

[12] N. Antoniou, A. Zabaniotou, Features of an efficient and environmentally attractive used tyres pyrolysis with energy and material recovery, Renewable and Sustainable Energy Reviews. 20 (2013) 539-558.

[13] A. Macsiniuc, A. Rochette, D. Rodrigue, Effect of SBR rubber particle size distribution on its thermo-mechano-chemical regeneration, Progress in Rubber, Plastics and Recycling Technology. 29 (2013) 217+.

[14] G. Lopez, R. Aguado, M. Olazar, M. Arabiourrutia, J. Bilbao, Kinetics of scrap tyre pyrolysis under vacuum conditions, Waste Manage. 29 (2009) 2649-2655.

[15] G. Lopez, M. Olazar, M. Amutio, R. Aguado, J. Bilbao, Influence of tire formulation on the products of continuous pyrolysis in a conical spouted bed reactor, Energy and Fuels. 23 (2009) 5423-5431.

[16] B. Danon, J. Görgens, Determining rubber composition of waste tyres using devolatilisation kinetics, Thermochimica Acta. 621 (2015) 56-60.

[17] A.J. Marzocca, A.L. Rodriguez Garraza, P. Sorichetti, H.O. Mosca, Cure kinetics and swelling behaviour in polybutadiene rubber, Polym. Test. 29 (2010) 477-482.

[18] L.H. Sperling, Introduction to Physical Polymer Science, 4th ed., John Wiley & Sons, Inc, 2006.

[19] J. Karger-Kocsis, L. Meszaros, T. Barany, Ground tyre rubber (GTR) in thermoplastics, thermosets, and rubbers, J. Mater. Sci. 48 (2013) 1+.

[20] D.E. Newcomb, M. Stroup-Gardiner, J.R. Kim, B. Allen, J. Wattenhoffer-Spry, Polymerized crumb rubber mixtures in Minnesota, (1994).

[21] P.J. Hough, A.N. Hough, Rubber de-vulcanisation using rapid decompression of supercritical fluid, (2009) 1.

[22] I. Mangili, E. Collina, M. Anzano, D. Pitea, M. Lasagni, Characterization and supercritical CO2 devulcanization of cryo-ground tire rubber: Influence of devulcanization process on reclaimed material, Polym. Degrad. Stab. 102 (2014) 15-24.

[23] K.A. Dubkov, S.V. Semikolenov, D.P. Ivanov, D.E. Babushkin, G.I. Panov, V.N. Parmon, Reclamation of waste tyre rubber with nitrous oxide, Polym. Degrad. Stab. 97 (2012) 1123-1130.

[24] P.T. Williams, A.J. Brindle, Temperature selective condensation of tyre pyrolysis oils to maximise the recovery of single ring aromatic compounds☆, Fuel. 82 (2003) 1023-1031.

[25] J.D. Martínez, M. Lapuerta, R. García-Contreras, R. Murillo, T. García, Fuel properties of tire pyrolysis liquid and its blends with diesel fuel, Energy and Fuels. 27 (2013) 3296-3305.

[26] S. Galvagno, S. Casu, T. Casabianca, A. Calabrese, G. Cornacchia, Pyrolysis process for the treatment of scrap tyres: preliminary experimental results, Waste Manage. 22 (2002) 917-923.

[27] A. Fullana, R. Font, J.A. Conesa, P. Blasco, Evolution of products in the combustion of scrap tires in a horizontal, laboratory scale reactor, Environmental Science and Technology. 34 (2000) 2092-2099.

[28] S. Murugan, M.C. Ramaswamy, G. Nagarajan, The use of tyre pyrolysis oil in diesel engines, Waste Manage. 28 (2008) 2743-2749.

[29] E. Aylón, A. Fernández-Colino, R. Murillo, M.V. Navarro, T. García, A.M. Mastral, Valorisation of waste tyre by pyrolysis in a moving bed reactor, Waste Manage. 30 (2010) 1220-1224.

[30] M. Betancur, J.D. Martínez, R. Murillo, Production of activated carbon by waste tire thermochemical degradation with CO2, J. Hazard. Mater. 168 (2009) 882-887.

[31] M. Banar, V. Akyildiz, A. Özkan, Z. Çokaygil, Ö Onay, Characterization of pyrolytic oil obtained from pyrolysis of TDF (Tire Derived Fuel), Energy Conversion and Management. 62 (2012) 22-30.

[32] I. de Marco Rodriguez, M.F. Laresgoiti, M.A. Cabrero, A. Torres, M.J. Chomón, B. Caballero, Pyrolysis of scrap tyres, Fuel Process Technol. 72 (2001) 9-22.

[33] D.M. Money, G. Harrison, Liquefaction of scrap automobile tyres in different solvents and solvent mixes, Fuel. 78 (1999) 1729-1736.

[34] C.F.S. Rombaldo, A.C.L. Lisboa, M.O.A. Mendez, A. dos Reis Coutinho, Effect of operating conditions on scrap tire pyrolysis, Materials Research. 11 (2008) 359-363.

[35] T.J. Midgley, A.I. Henne, Natural and synthetic rubber I. Products of the destructive distillation of natural rubber, Journal of the American Chemical Society. 51 (1929) 1215-1226.

[36] P.T. Williams, Pyrolysis of waste tyres: A review, Waste Manage. 33 (2013) 1714-1728.

[37] A. Quek, R. Balasubramanian, Liquefaction of waste tires by pyrolysis for oil and chemicals—A review, J. Anal. Appl. Pyrolysis. 101 (2013) 1-16.

[38] O. Senneca, P. Salatino, R. Chirone, A fast heating-rate thermogravimetric study of the pyrolysis of scrap tyres, Fuel. 78 (1999) 1575-1581.

[39] P.T. Williams, S. Besler, Pyrolysis-thermogravimetric analysis of tyres and tyre components, Fuel. 74 (1995) 1277-1283.

[40] D.W. Brazier, N.V. Schwartz, The effect of heating rate on the thermal degradation of polybutadiene, Journal of Applied Polymer Science. 22 (1978) 113-124.

[41] A. Arockiasamy, H. Toghiani, D. Oglesby, M.F. Horstemeyer, J.L. Bouvard, R.L. King, TG-DSC-FTIR-MS study of gaseous compounds evolved during thermal decomposition of styrene-butadiene rubber, Journal of Thermal Analysis and Calorimetry. 111 (2013) 535+.

[42] K.-. Lam, C.-. Lee, C.-. Hui, Multi-stage waste tyre pyrolysis: An optimisation approach, Chemical Engineering Transactions. 21 (2010) 853-858.

[43] K. Cheung, K. Lee, K. Lam, T. Chan, C. Lee, C. Hui, Operation strategy for multi-stage pyrolysis, J. Anal. Appl. Pyrolysis. 91 (2011) 165-182.

[44] A.O. Oyedun, K.L. Lam, T. Gebreegziabher, C.W. Hui, Optimization of multi-stage pyrolysis, Appl. Therm. Eng. 61 (2013) 123-127.

[45] A.V. Bridgwater, G.V.C. Peacocke, Fast pyrolysis processes for biomass, Renewable and Sustainable Energy Reviews. 4 (2000) 1-73.

[46] F.J. Mastral, E. Esperanza, P. García, M. Juste, Pyrolysis of high-density polyethylene in a fluidised bed reactor. Influence of the temperature and residence time, J. Anal. Appl. Pyrolysis. 63 (2002) 1-15.

[47] X. Dai, X. Yin, C. Wu, W. Zhang, Y. Chen, Pyrolysis of waste tires in a circulating fluidized-bed reactor, Energy. 26 (2001) 385-399.

[48] M.M. Barbooti, T.J. Mohamed, A.A. Hussain, F.O. Abas, Optimization of pyrolysis conditions of scrap tires under inert gas atmosphere, J. Anal. Appl. Pyrolysis. 72 (2004) 165-170.

[49] A.M. Cunliffe, P.T. Williams, Composition of oils derived from the batch pyrolysis of tyres, J. Anal. Appl. Pyrolysis. 44 (1998) 131-152.

[50] M.F. Laresgoiti, B.M. Caballero, I. de Marco, A. Torres, M.A. Cabrero, M.J. Chomón, Characterization of the liquid products obtained in tyre pyrolysis, J. Anal. Appl. Pyrolysis. 71 (2004) 917-934.

[51] C. Roy, A. Chaala, H. Darmstadt, The vacuum pyrolysis of used tires: End-uses for oil and carbon black products, J. Anal. Appl. Pyrolysis. 51 (1999) 201-221.

[52] H. PAKDEL, C. ROY, H. AUBIN, G. JEAN, S. COULOMBE, FORMATION OF DL- LIMONENE IN USED TIRE VACUUM PYROLYSIS OILS, Environ. Sci. Technol. 25 (1991) 1646-1648.

[53] H. Pakdel, D.M. Pantea, C. Roy, Production of dl- limonene by vacuum pyrolysis of used tires, J. Anal. Appl. Pyrolysis. 57 (2001) 91-107.

[54] K. Lee, K. Cheung, K.L. Lam, C.W. Hui, Optimization of multi-stage waste tyre pyrolysis process, 1 (2010).

[55] K. Cheung, K. Lee, K. Lam, C. Lee, C. Hui, Integrated kinetics and heat flow modelling to optimise waste tyre pyrolysis at different heating rates, Fuel Process Technol. 92 (2011) 856-863.

[56] D.Y.C. Leung, C.L. Wang, Kinetic study of scrap tyre pyrolysis and combustion, J. Anal. Appl. Pyrolysis. 45 (1998) 153-169.

[57] A. Quek, R. Balasubramanian, An algorithm for the kinetics of tire pyrolysis under different heating rates, J. Hazard. Mater. 166 (2009) 126-132.

[58] E.L.K. Mui, W.H. Cheung, V.K.C. Lee,G. McKay, Compensation effect during the pyrolysis of tyres and bamboo, Waste Maanage. 30 (2010) 821-830

[59] M.R. Islam, H. Haniu, J. Fardoushi, Pyrolysis kinetics behaviour of solid tire wastes available in Bangadesh, Waste Manage. 29 (2009) 668-677.

[60] J.H. Chen, K.S. Chen, L.Y. Tong, On the pyrolysis kinetics of scrap automative tires, J. Hazard. Mater. B84 (2001) 43-55.

[61] E.L.K. Mui, V.K.C. Lee, W.H. Cheung, G. McKay, Kinetic modeling of waste tire carbonization, Energy and Fuels. 22 (2008) 1650-1657.

[62] S. Ucar, S. Karagoz, A.R. Ozkan, J. Yanik, Evaluation of two different scrap tires as hydrocarbon source by pyrolysis, Fuel. 84 (2005) 1884-1892.

[63] M. Rofiqul Islam, H. Haniu, M. Rafiqul Alam Beg, Liquid fuels and chemicals from pyrolysis of motorcycle tire waste: Product yields, compositions and related properties, Fuel. 87 (2008) 3112-3122.

[64] A. Kebritchi, H. Firoozifar, K. Shams, A. Jalali-Arani, Effect of pre-devulcanization and temperature on physical and chemical properties of waste tire pyrolytic oil residue, Fuel. 112 (2013) 319-325.

[65] M.I.A. De Silva, D.G. Edirisinghe, J.K. Premachandra, A novel reclaiming agent for ground rubber tyre (GRT). Part 1: property evaluation of virgin natural rubber (NR)/novel reclaimed GRT blend compounds, Progress in Rubber, Plastics and Recycling Technology. 27 (2011) 31+.

[66] B. Adhikari, D. De, S. Maiti, Reclamation and recycling of waste rubber, Progress in Polymer Science. 25 (2000) 909-948.

[67] S. Rooj, G.C. Basak, P.K. Maji, A.K. Bhowmick, New route for devulcanisation of natural rubber and the properties of devulcanised rubber, Journal of Polymer and Environment. 19 (2011) 382-390.

[68] E. Aylon, A. Fernandez-Colino, M.V. Navarro, A. Murillo, T. Garcia, A.M. Mastral, Waste tire pyrolysis: comparison between fixed bed reactor and moving bed reactor, Industrial and Engineering Chemistry Research. 47 (2008) 4029-4033.

[69] S.-. Li, Q. Yao, Y. Chi, J.-. Yan, K.-. Cen, Pilot-scale pyrolysis of scrap tires in a continuous rotary kiln reactor, Industrial and Engineering Chemistry Research. 43 (2004) 5133-5145.

[70] B. Benallal, C. Roy, H. Pakdel, S. Chabot, M.A. Poirier, Characterization of pyrolytic light naphtha from vacuum pyrolysis of used tyres comparison with petroleum naphtha, Fuel. 74 (1995) 1589-1594.

[71] C. Roy, H. Darmstadt, B. Benallal, C. Amen-Chen, Characterization of naphtha and carbon black obtained by vacuum pyrolysis of polyisoprene rubber, Fuel Process Technol. 50 (1997) 87-103.

[72] Y. Kar, Catalytic pyrolysis of car tire waste using expanded perlite, Waste Manage. 31 (2011) 1772-1782.

[73] M. Arabiourrutia, G. Lopez, G. Elordi, M. Olazar, R. Aguado, J. Bilbao, Product distribution obtained in the pyrolysis of tyres in a conical spouted bed reactor, Chemical Engineering Science. 62 (2007) 5271-5275.

[74] M. Arabiourrutia, M. Olazar, R. Aguado, G. Lopez, A. Barona, J. Bilbao, HZSM-5 and HY Zeolite catalyst perfomance in the pyrolysis of tires in a conical spouted bed reactor, Industrial and Engineering Chemistry Research. 47 (2008) 7600-7609.

[75] M. Olazar, R. Aguado, M. Arabiourrutia, G. Lopez, A. Barona, J. Bilbao, Catalyst effect on the composition of tire pyrolysis products, Energy Fuels. 22 (2008) 2909-2916.

[76] S. Boxiong, W. Chunfei, L. Cai, G. Binbin, W. Rui, Pyrolysis of waste tyres: The influence of USY catalyst/tyre ratio on products, J. Anal. Appl. Pyrolysis. 78 (2007) 243-249.

[77] P.T. Williams, A.J. Brindle, Aromatic chemicals from the catalytic pyrolysis of scrap tyres, J. Anal. Appl. Pyrolysis. 67 (2003) 143-164.

[78] G. Lopez, M. Olazar, R. Aguado, G. Elorrdi, M. Amutio, M. Artetxe, Vacuum pyrolysis of waste tires by continuous feeding into a conical spouted bed reactor. Industrial and Engineering Chemistry Research. 49 (2010) 8990-8997.

[79] Y.S. Lee, W. Lee, S. Cho, I. Kim, C. Ha, Quantitative analysis of unknown compositions in ternary polymer blends: A model study on NR/SBR/BR system, J. Anal. Appl. Pyrolysis. 78 (2007) 85-94.

[80] C. Roy, B. Labrecque, B. de Caumia, Recycling of scrap tires to oil and carbon black by vacuum pyrolysis, Resour. Conserv. Recycling. 4 (1990) 203-213.

CHAPTER 3. RESEARCH OJECTIVES

3.1 Aims and objectives

3.1.1 Aims

The aim of the current study is to develop and modify existing waste tyre pyrolysis processes in order to maximise DL-limonene (a market valuable chemical) production and content in the tyre derived oil (TDO). The approach entails maximising the DL-limonene yield and content in the TDO by 1) optimising various conditions in the pyrolysis reactor, 2) cooling and condensing hot volatiles from pyrolysis reactor in different way, and 3) improving the TDO quality by eliminating most of the heteroatom compounds (oxygenic, nitrogenous and sulphurous) other than DL-limonene from the TDO. These aims have been formulated to address specific shortcomings in published literature with regards to preferred pyrolysis processes for DL-limonene production from waste tyres, as described in section 2.9.

3.1.2 Objectives

The research aims will be achieved by the following specific objectives:

i) To determine the optimal operating conditions in the pyrolysis reactor, such as, pyrolysis temperature and heating rate in order to maximise DL-limonene yield. The effect of temperature and particularly heating rate on the production of DL-limonene has not been significantly investigated. The study of the temperature and heating rate at both milligram- and gram-scale will be published as a paper in the international journal, CHAPTER 4.

ii) Establish the kinetic mechanism of DL-limonene production using various heating rates up to 100 °C to establish the selectivity of DL-limonene production over competing reaction pathways during devolatilisation of the waste tyre polymeric matter (polyisoprene). Ion current signals were used to track during pyrolysis the evolution of the predominant ions of isoprene and DL-limonene, by using a thermogravimetric analyser coupled with a mass spectrometry (TGA/MS). In addition to the contribution to the understanding of the kinetic mechanism of DL-limonene production from waste tyres, using DL-limonene formation profiles in the hot volatiles, rather devolatilisation profiles of the tyre components is highly novel. The manuscript submitted for publication is presented in CHAPTER 5.

iii) To investigate the effect of the condensing type and cooling rate of the hot volatiles on DL-limonene production using either a conventional tube-and-shell condenser or direct contact between the hot volatile and quenching fluid in a quenching condenser. The application of the scrubbing of gases in the pyrolysis of waste tyres is novel. Using quenching condensation presents an opportunity to consider new insights on the DL-limonene production. Moreover, the technology contributes significantly on the elimination of the heteroatom compounds from DL-limonene rich TDO to improve it recovery. Quenching condensation work has been published in the international journal, CHAPTER 6.

iv) To integrate objectives i), ii), and iii) into a single complete waste tyre pyrolysis process which examines various types of pyrolysis reactors and means of cooling and condensing of hot volatiles from pyrolysis reactor to maximise DL-limonene production and high quality TDO. The main novelty with this objective is comparing of the three types of pyrolysis reactors at the same temperature to maximise DL-limonene production. The manuscript presented in CHAPTER 7.

3.2 Hypothesis

Maximum DL-limonene production (and other monomers and dimers) from waste tyre pyrolysis can be achieved by establishing optimal pyrolysis operating conditions. It is envisaged that these optimal operating conditions affect the pyrolysis main fractions chemical composition and total yield. Additionally, novel method of treating the hot volatiles from the pyrolysis reactor can further improve the DL-limonene production and the quality of the TDO.

Direct contact between the hot volatiles from the pyrolysis reactor and a cooling fluid to cool and condense these hot volatiles to TDO using a quenching condenser is more effective than using a conventional tube-and-shell condenser. Some of the potential benefits of using a quenching condenser, compared to a heat exchanger condenser, are i) complete condensation of the hot volatiles leading to high overall TDO yields; ii) rapid condensation of the hot volatiles and thus elimination of the potential secondary reactions (degradation of monomers or dimers); iii) improved DL-limonene content in the TDO while elimination of nitrogenous and sulphurous compounds and other solids residues (soot, sand, wires) from the TDO, and iv) scrubbing and cleaning of the permanent gases.

For a complete optimal pyrolysis process, both the pyrolysis reactor (the pyrolysis operating conditions therein) and the condensation technique (either slow or rapid cooling and/or condensation of the hot volatiles) require to be integrated to a single process.

CHAPTER 4. EFFECT OF TEMPERATURE AND HEATING RATE ON LIMONENE PRODUCTION FROM WASTE TYRES PYROLYSIS

Published research paper

Title: Effect of temperature and heating rate on limonene production from waste tyre pyrolysis

Journal: Journal of analytical and applied pyrolysis

Issue: 120

Pages: 314 – 320

Short summary

Objective 1, entailing investigation of the optimal operating conditions of the waste tyre pyrolysis in the pyrolysis reactor to maximise DL-limonene production is presented in the current chapter (CHAPTER 4). A fixed bed reactor (FBR) is used to determine the effect of the temperature and heating rate on the DL-limonene production from waste tyre pyrolysis. FBR is characterised by low heating rate (up to 30 °C/min) and long hot volatiles residence time in the hot reaction zones (at least 41 s). Since the interest in this chapter is to determine optimal temperature and heating rate to improve DL-limonene yield, other operating parameters, such as, hot volatiles residence time, and condensation type and cooling rate of the hot volatiles were held constant. It is postulated that the quality of the hot volatiles, evolving during waste tyre devolatilisation (in the pyrolyser), is adequately high for their further treatment during cooling and condensation to produce TDO. High quality hot volatiles refer to the hot volatiles that consist high amount of the DL-limonene in the vapour form that results in to a reasonable high TDO yield and DL-limonene content in the TDO and when they are cooled and condensed. Some desirability comparisons are required to ensure that there is a balance between the total TDO yield and DL-limonene content in the TDO with respect to economic feasibility for further processing of the TDO to recover DL-limonene. Only the effect of the pyrolysis temperature was significant on the tyre derived oil (TDO) yield, while the effects of both pyrolysis temperature and heating rate were significant on the chemical composition of the TDO, i.e., DL-limonene yield. Therefore, indicating the significance of the heating rate as factor for improving TDO composition. It was showed that DL-limonene formation occurred at slightly higher temperatures compared

to isoprene formation, indicating differences in the reaction pathways. With regard to objective 1 there is indeed an optimal point for temperature and heating rate. Future work will entail the investigation of even higher heating rates (in order to further improve the DL-limonene yield) and modelling of the kinetic parameters of the isoprene and DL-limonene reactions.

Declaration by the candidate:

With regard to CHAPTER 4, pages 61 – 77, the nature and scope of my contribution were as follows:

Nature of contribution	**Extent of contribution (%)**
Planning of the experiments	70
Execution of the experiments	80
Interpretation of the results	70
Compilation of the chapter	100

The following co-authors have contributed to CHAPTER 4, pages 61 – 77:

Name	**e-mail address**	**Nature of contribution**	**Extent of contribution (%)**
Bart Danon	bdanon@sun.ac.za	Planning of the experiments	20
		Execution of the experiments	20
		Interpretation of the results	30
		Revision of the chapter	80
Percy van der Gryp	pvdg@sun.ac.za	Planning of the experiments	5
		Revision of the chapter	10
Johann Gorgens	jgorgens@sun.ac.za	Planning of the experiments	5
		Revision of the chapter	10

Signature of candidate…….

Date…….

Declaration by the co-authors:

The undersigned hereby confirm that

1. the declaration above accurately reflects the nature and extent of the contributions of the candidate and the co-authors to CHAPTER 4, pages 61 – 77,
2. no other authors contributed to CHAPTER 4, pages 61 – 77 besides those specified above, and
3. potential conflicts of interest have been revealed to all interested parties and that the necessary arrangements have been made to use the material in CHAPTER 4, pages 61 – 77 of this dissertation.

Signature	**Institutional affiliation**	**Date**
	Stellenbosch University	
	Stellenbosch University	
	Stellenbosch University	

Effect of temperature and heating rate on limonene production from waste tyre pyrolysis

N. M. Mkhize, P. van der Gryp, B. Danon, J. F. Görgens*

Department of Process Engineering, Stellenbosch University, Private Bag X1, Matieland, 7602, Stellenbosch, South Africa

* Corresponding author: jgorgens@sun.ac.za

Abstract

The effect of pyrolysis temperature and heating rate on DL-limonene production during waste tyre pyrolysis was investigated using gram-scale (fixed-bed) and microgram-scale (TGA) pyrolysis reactors. The investigation was carried out with final pyrolysis temperatures between 350 and 550 °C and heating rates in the range of 5 – 25 °C/min. Only the effect of the pyrolysis temperature was significant on the tyre derived oil (TDO) yield, while the effects of both pyrolysis temperature and heating rate were significant on the chemical composition of the TDO, i.e., DL-limonene yield. In the gram-scale reactor, a maximum DL-limonene yield was obtained at a pyrolysis temperature of 475 °C and a heating rate of 20 °C/min, with a value of 7.62 wt.% (based on the steel- and fabric-free tyre) or 22 wt.% (based on the polyisoprene content of the tyre). DTG curves showed that increasing the heating rate led to (1) a decrease in secondary degradation reactions, and (2) an increased temperature at the maximum depolymerisation rate. At the same heating rate, MS ion current signals showed that DL-limonene formation occurred at slightly higher temperatures compared to isoprene formation, indicating a slight higher activation energy for the former reaction. Since a higher activation energy indicates a stronger temperature dependency for a reaction, it implies, in combination with the observation of higher temperatures at maximum DL-limonene production rate in the MS ion current signal, an improvement of the selectivity of polyisoprene depolymerisation towards DL-limonene.

4.1 Introduction

The development of waste tyres recycling using pyrolysis has encountered various legislative barriers due to its classification as incineration in most regions [1]. Moreover, the markets for both the liquid (tyre derived oil or TDO) and solid (char) pyrolysis products are not yet fully established. The TDO cannot, at the current relatively low oil prices, compete with fossil fuels, while the char is characterised by relatively high levels of impurities (e.g. ash and sulphur contents) [1]. To improve the economic feasibility of waste tyre pyrolysis, recovery of valuable chemicals from the TDO, while using the remainder as a fuel, has been proposed [2-5]. These valuable chemicals include rubber monomers (isoprene, butadiene, styrene), some

of their dimers (DL-limonene, 4-vinyl-cyclohexene), as well as a variety of aromatics [6-8]. The present study focusses on the production of DL-limonene ($C_{10}H_{16}$) from waste tyre pyrolysis. DL-limonene is derived from the polyisoprene (natural rubber or NR) fraction of a tyre and is typically the most abundant compound in the TDO [9,10]. DL-limonene e is an important starting material in several industrial formulations for e.g. solvents, resins, or adhesives, with an estimated price of 2 USD/kg [11-13].

In previous studies [7,9] the influence of the pyrolysis temperature (i.e. the final/highest temperature of the heating programme) on the chemical composition of the TDO was predominantly investigated. It has been reported that DL-limonene yields are highest for temperatures between 400 and 500 °C [10]. The maximum DL-limonene concentration in the TDO reported by Cunliffe and Williams was at a temperature of 450 °C [14]. Islam et al. obtained highest DL-limonene concentration in the TDO at a temperature of 475 °C [15]. The influence of the heating rate on DL-limonene yields has received considerably less attention. It is nevertheless known that the heating rate has a significant effect on rubber devolatilisation during waste tyre pyrolysis [16-21]. A study by Banar et al. indicated that, at a final pyrolysis temperature of 400 °C, DL-limonene concentration in the TDO decreases from 17,062 to 219 ppm, as the heating rate was increased from 5 to 35 °C/min [20]. However, a study carried out by Brazier and Schwartz reported a higher combined butadiene and vinylcyclohexene yield (95 %) at a higher heating rate (100 °C/min) compared to 66 % at a heating rate of 5 °C/min, for polybutadiene depolymerisation [21]. They also indicated that the depolymerisation of polybutadiene is analogous to that of polyisoprene. Therefore, it remains unclear how the heating rate affects the production of DL-limonene.

Some studies [16,19,22] investigated the effect of heating rate on the pyrolysis of the different components of waste tyre, such as, processing additives and rubbers. Cheung et al. pointed out that, when the heating rate was increased, the processing additives in the tyre were more readily devolatilised, while the fraction of the tyre that devolatilises via depolymerisation was increased at the expense of the fraction devolatilising via degradation [16]. A similar observation was reported by Leung and Wang (1998) [22]. Lam et al. observed that lower heating rates required a lower energy input for the pyrolysis of tyres, while reaction times and heat losses were increased [19].

The main objective of this study is to investigate the effect of the pyrolysis temperature and the heating rate on the DL-limonene yield from waste tyres pyrolysis. A central composite design of gram-scale experiments (in a fixed-bed reactor) was used to investigate the influences of these two variables. Additionally, experiments on microgram-scale, using a thermogravimetric analyser (TGA), which could be combined with a mass spectrometer (TGA-MS) were performed to farther elucidate the effect of the heating rate.

4.2 Materials and methods

A bulk sample of approximately 500 kg crumbed (steel- and fabric-free) waste truck tyres, consisting of particle sizes up to 5 mm, was supplied by a local waste tyre recycler. Subsampling was carried out to ensure feedstock homogeneity. Subsequently, the sample was sieved to obtain two samples with particle size ranges of 0.6 to 0.8 mm and 2.8 to 3.4 mm. All experiments in the gram-scale reactor were performed with the larger particle size sample, while for the microgram-scale experiments both particle sizes were employed. Preliminary experiments indicated that the effect of particle size between 0.6 and 3.4 mm on pyrolysis oil yield and its chemical composition was insignificant, which is also supported by previous studies [16,19,23]. Proximate analysis on the larger particles was conducted using a slightly adjusted version of ASTM E1131 – 08 (with X = 275 °C). Additionally, kinetics experiments were carried out (using the smaller particle size) to determine the rubber composition of the crumb using a procedure described by Danon and Görgens [24]. The results of the proximate analysis and rubber composition are shown in Table 4.1.

Table 4.1: Proximate analysis and rubber composition of the crumb.

Proximate analysis (wt.%)	Moisture	Oils	Volatile matter	Fixed carbon	Ash
	0.6	5.6	56.0	30.0	7.8
Rubber composition/volatile matter (wt.%)	Polyisoprene (natural rubber)		Synthetic rubber (SBR and BR)[α]		
	64		36		

[α]By difference

For the gram-scale experiments a fixed-bed slow pyrolysis reactor was used, see Figure 4.1. The sample size used in these experiments was 40 g. The hot volatiles were purged with nitrogen gas (99.5% purity, Afrox, South Africa) at a constant flow rate of 1 L/min. A two-level full factorial design with two replicates and augmented with 3 centre points, i.e. a central composite design (CCD) was employed. All the design and response factors are overviewed in Table 4.2. The pyrolysis temperature range, heating rate range and centre points were selected based on the operability range of the existing setup and typical values reported in the literature [3,25,26]. Moreover, statistical analysis of variance (ANOVA) was employed to study the effects of the individual factors and their interactions. Additionally, a response surface model was fitted to determine optimal operating conditions and to show the effects of the pyrolysis temperature and heating rate on the liquid and DL-limonene yield.

The obtained TDO was qualitatively and quantitatively analysed using a Hewlett Packard 5890 Series II model gas chromatography (GC) coupled with a Hewlett Packard 5973 mass spectrometry (MS). GC oven

temperature program was set to maximise elution of major chemicals from the TDO. A volume of 1µl mixture consisting of TDO and dichloromethane solvent (99.9% purity, Sigma Aldrich, South Africa) was then introduced in a 60 m x 0.18 mm ID x 0.10 µm film thickness, non-polar Rxi-5% Sil-MS capillary column using helium gas (99.999 % purity, Air Products, South Africa) as a carrier gas at a constant flow of 1.20 ml/min (linear velocity of 27.9 cm/s) at 348 kPa. The measured DL-limonene concentration ($C_{limonene}$) was converted to a DL-limonene yield ($Y_{limonene}$) based on the mass of the steel- and fabric-free tyre using Equation (1),

$$Y_{limonene} = C_{limonene} \times Y_{liquid}/100 \quad (1)$$

Where: $Y_{limonene}$ = DL-limonene e yield (wt.%, steel/fabric free tyre), $C_{limonene}$ = DL-limonene concentration in the TDO (wt.%) and Y_{liquid} = liquid yield (wt.%, steel/fabric free tyre).

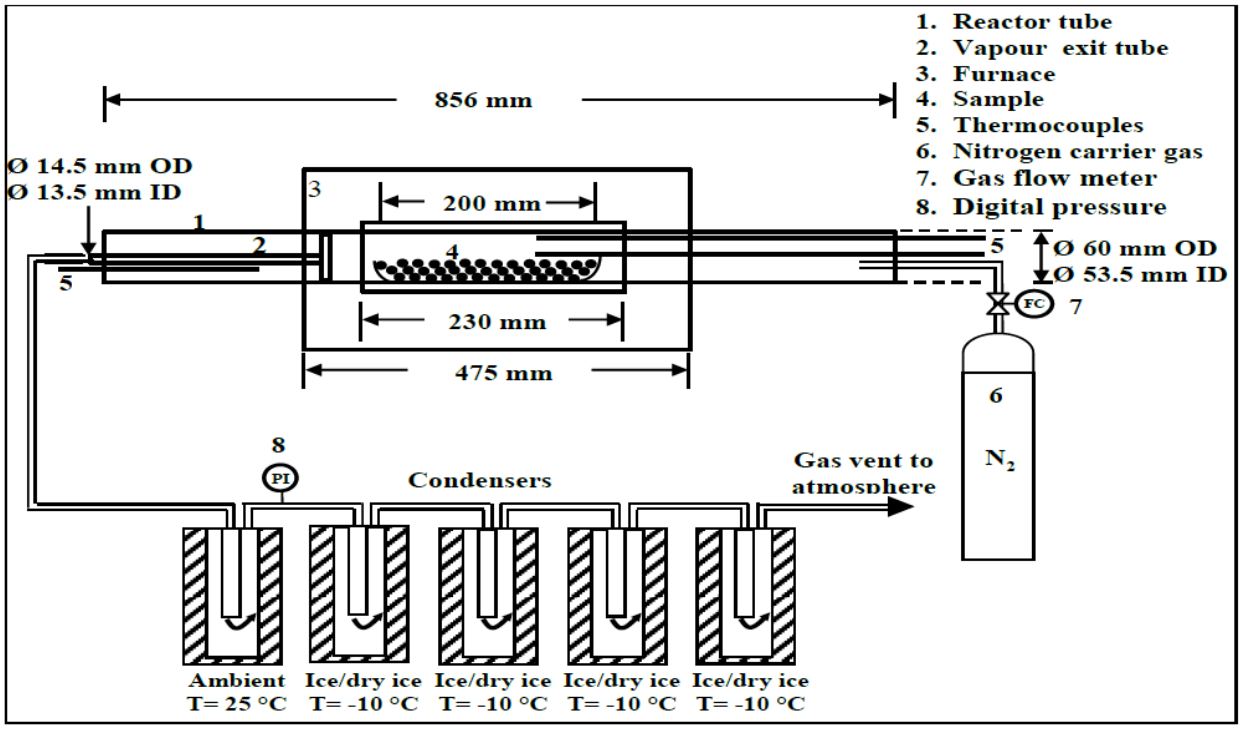

Figure 4.1: Fixed-bed slow pyrolysis reactor.

Table 4.2: Central composite design (CCD) factors.

Factor	Unit	Factor type	Lower level (–)	Centre point (0)	Upper level(+)	Lower axial (–δ)	Higher axial (+δ)
Temperature	°C	Variable	350	450	550	309	591
Heating rate	°C/min	Variable	5	15	25	0.86	29.14
Particle size	mm	Constant	2.8 - 3.4	2.8 - 3.4	2.8 - 3.4	2.8 - 3.4	2.8 - 3.4
Sample amount	g	Constant	40	40	40	40	40
Holding time	min	Variable	120	60	30	120	30
Liquid yield	wt.%	Response					
Solid yield	wt.%	Response					
DL-limonene yield	wt.%	Response					

A Mettler Toledo TGA/DCS 1 thermogravimetric analyser (TGA) was used for the microgram-scale experiments. The CCD experiments (using the larger particle size) have been repeated in the TGA to confirm the solid yields. For this purpose, a heating program was employed in the TGA which included the cooling down of the reactor at gram-scale. Sample size in these experiments was 250 mg and the nitrogen flow rate was 100 ml/min.

Finally, the TGA was also connected to a ThermoStar GSD 320 T3 (Pfeiffer Vacuum, Germany) mass spectrometer (MS) for further investigation of the effect of the heating rate on DL-limonene production. The ionisation energy was set to 70 eV, using a Secondary Electron Multiplier (SEM) to amplify the MS signal. Argon gas (99.999% purity, Afrox, South Africa) was used as a carrier gas in these experiments. The mass over charge ratios of the two most predominant fragments of isoprene and DL-limonene (67 and 93 amu, respectively, as well as 68 amu which represents both) were monitored [27]. Using the smaller particle size and sample sizes of 10 mg, experiments up to 600 °C at three different heating rates (5, 15 and 25 °C/min) were performed. Shown in Table 4.3 is a summary of the pyrolysis operating conditions for gram- and microgram scale experiments.

Table 4.3: Gram-scale and microgram-scale pyrolysis operating conditions

	Gram-scale	Microgram-scale	
		TGA	TGA-MS
Particle size (mm)	2.8 – 3.4	2.8 – 3.4	0.6 – 0.8
Pyrolysis temperature (°C)	350 – 550	350 – 550	600
Heating rate (°C/min)	5 – 25	5 – 25	5 – 25
Sample size	40 g	250 mg	10 mg
Purge gas (ml/min)	1 000 (N_2, 99.5 %)	100 (N_2, 99.5 %)	100 (Ar, 99.999 %)

4.3 Results and discussion

The effect of the pyrolysis temperature and heating rate on the three main pyrolysis products (solid, liquid and gas) and DL-limonene yield were investigated by CCD experiments at gram-scale as given in Table 4.2. The results obtained are summarised in Table 4.4. Furthermore, the interpolated results of the statistical model used on the CCD results are given in Table 4.4. It is clear from the results that heating rate has an insignificant effect on the pyrolysis product yields at a probability of 95% (p-values above 0.6). However, the effect of pyrolysis temperature on the pyrolysis product yields was substantial (p-values below 0.07). It was observed that at low temperatures (350 °C and lower) the liquid yield was relatively low and the solid yield higher. The relative low liquid yields in combination with the high solid yields indicated incomplete pyrolysis [4].

Table 4.4: Tyre pyrolysis product yields and limonene yield of CCD experiments.

Pyrolysis parameters		Tyre pyrolysis products			DL-limonene yield
Temperature (°C)	Heating rate (°C/min)	Gas yield[α] (wt.%)	Solid yield (wt.%)	Liquid yield (wt.%)	GC/MS (wt.%)
350	5	11.54	61.26	27.20	7.17
550	5	19.86	36.64	43.50	6.88
350	25	17.15	60.26	22.59	4.67
550	25	20.37	36.20	43.43	6.70
450	15	19.66	36.64	43.70	7.14
309	15	4.36	83.67	11.97	2.10
591	15	17.79	36.37	45.84	6.49
450	0.86	23.04	37.35	39.60	4.14
450	29.14	18.44	36.66	44.90	7.62

[α] By difference

As the pyrolysis temperature was increased to 450 °C and above, the solid yield decreased to a constant value of approximately 36.5 wt.%, a value which corresponds roughly to the fixed carbon and ash contents of a tyre sample, see Table 4.1 and [4].

A different picture was, however, observed when the effect of pyrolysis temperature and heating rate on the DL-limonene yield was considered. The p-values (probability of 95%) of both pyrolysis temperature ($p = 0.03$) and heating rate ($p = 0.05$), as well as the temperature-heating rate interaction ($p = 0.04$), were well close to zero, indicating that their effect on the DL-limonene yield was significant. The surface plot of the DL-limonene yield versus temperature and heating rate illustrates these effects (see Figure 4.2 b). These results indicated that with higher heating rates (especially at higher pyrolysis temperatures) the DL-limonene yield is increased.

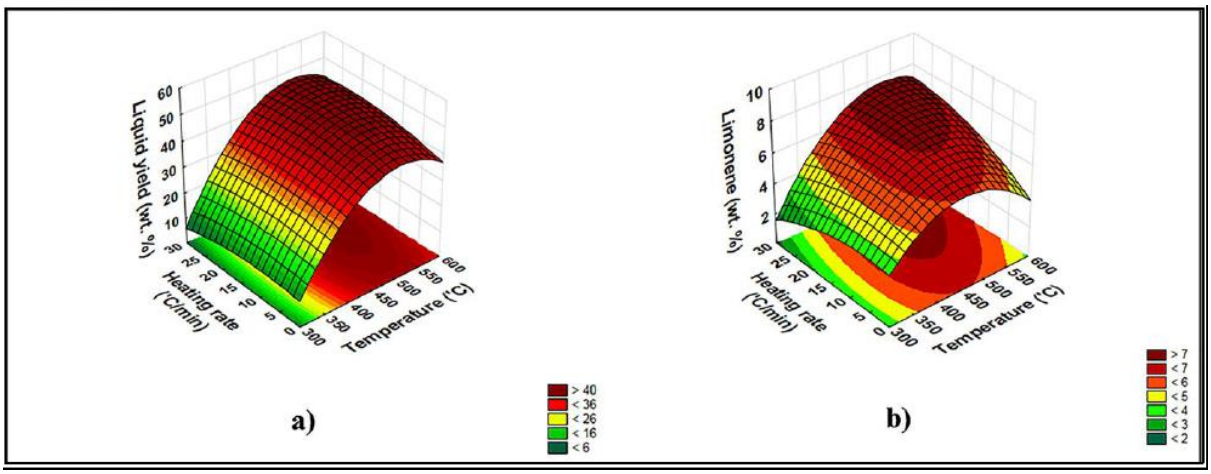

Figure 4.2: Effect of both temperature and heating rate on a) liquid yield and b) DL-limonene yield.

From the statistical model, it was predicted that the theoretical optimal DL-limonene yield is at a temperature of 475 °C and heating rate of 20 °C/min. A confirmative experiment at gram-scale was performed at these conditions. The experimental liquid yield was 45 wt.%, with a DL-limonene yield of 7.6 wt.% based on the steel- and fabric-free tyre, which are indeed the highest values obtained within the range of conditions of the CCD. It was, however, observed that comparable yields were obtained at one of the extreme points of the CCD, i.e. at a lower temperature but with a higher heating rate, i.e. 450 °C and 29 °C/min, see Table 4.4. This observation stresses the importance of the heating rate for limonene production. It is known that DL-limonene is derived from NR [10]. Therefore, considering that the current crumb consists of 56.0 wt.% volatile matter, assuming that this constitutes the total rubber content, of which 64 wt.% is NR (see Table 4.1) the 'effective DL-limonene yield' obtained was 22 wt.%.

Table 4.5: Solid yields for CCD experiments at the two difference scales.

Natural variables		Solid yield	
Temperature (°C)	**Heating rate (°C/min)**	**Fixed-bed pyrolyser (wt.%)**	**TGA (wt.%)**
350	5	61.26	61.20
550	5	36.64	37.23
350	25	60.26	59.24
550	25	36.20	36.53
450	15	36.64	34.53

In order to verify the comparability of the reactors operating at the two different scales (gram- and microgram-scale), the CCD experiments were repeated on microgram-scale. The resulting solid yields are presented in Table 4.5. It can be seen that these solid yields were very similar for the two setups. This indicates that the mass and heat transfer within the two setups was comparable and therefore comparative

analyses between the results at the two different scales were possible. A study investigating the effect on process and kinetic parameters (maximum devolatilisation rate temperature, nominal weight loss rate and weight loss fractions) of the particle size (0.42 – 2.38 mm) and heating rate was carried out by Leung and Wang [22]. They observed that process and kinetic parameters vary with heating rate but were less depended on the particle size.

Further investigation of the effect of heating rate was performed using TGA-MS. The derivative thermogravimetric (DTG) curve and ion current signal of 68 amu as a function of temperature at heating rates of 5, 15 and 25 °C/min are presented in Figure 4.3. Firstly, the DTG curves illustrated that tyre devolatilisation was completed before the final pyrolysis temperature (at 600 °C for all the TGA-MS experiments) was reached. Thus, the effect of final temperature on the devolatilisation was eliminated in these experiments.

Secondly, in the DTG curves, it was observed that at a lower heating rate (5 °C/min) the temperature at maximum devolatilisation was the lowest (366 °C), while increasing to 386 °C at 15 °C/min and to 396 °C at 25 °C/min. Senneca et al. reported the same trend when the heating rate was increased temperatures at maximum devolatilisation of 360 and 390 °C for heating rates of 5 and 20 °C/min, respectively [28].. Also, Leung and Wang, Islam et al. and Chen et al. observed the same trend [22,29,30]. Quek and Balasubramaniam attributed the difference in the peak devolatilisation temperature to thermal lagging, i.e. the temperature increase on the surface of the tyre particle was relatively faster compared to the temperature increase at the centre of the particle [31].

Thirdly, the effect of the heating rate was also evident from the two DTG curves peak intensities (i.e. the main peak and the shoulder at higher temperatures), as observed in Figure 4.3. These DTG curves indicated that the intensity of the shoulders decreases, relative to the main peak, at higher heating rates. Lee et al. reported that, as the heating rate was increased from 2 to 20 °C/min, the mass fraction of the first peak was increased, while the mass fraction of the second peak was reduced and finally disappeared [32]. Cheung et al. later agreed with Lee et al. and attributed this behaviour to the earlier attainment of high temperatures in the sample at higher heating rates [16]. It has been reported that the first peak is due to depolymerisation and the second peak due to degradation [10,21]. DL-limonene is formed during depolymerisation. Therefore, when the first peak increases with increasing heating rates, this implies more depolymerisation and potentially more DL-limonene.

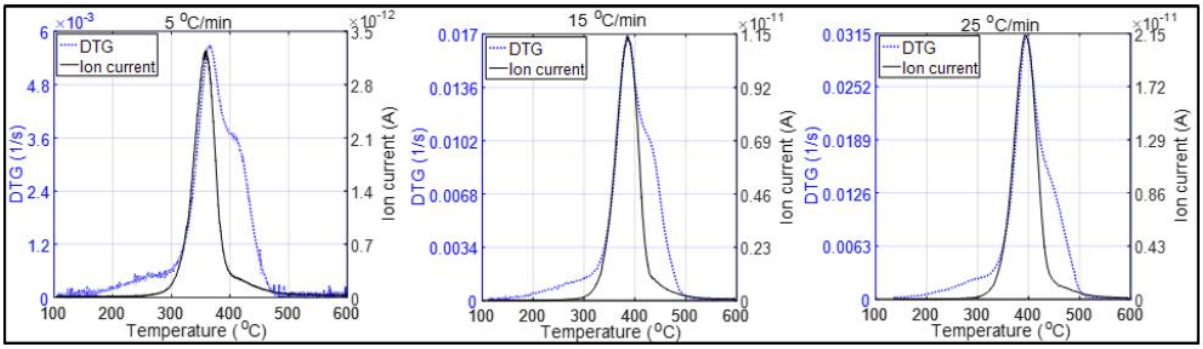

Figure 4.3: Derivative thermogravimetric (DTG) data and ion current signal at 68 amu as a function of temperature at a) 5 °C/min, b) 15 °C/min and c) 25 °C/min.

Finally, the effect of the heating rate was elucidated using the MS ion current signals of the main fragment of isoprene (67 amu) and DL-limonene (93 amu). MS ion current signals are primarily used to detect shifting of the ion current signal peaks of isoprene and DL-limonene with regards to temperature. In Figure 4.4 these ion current signals are presented. The temperatures at maximum ion current signal showed a similar trend as the DTG curves (compare with Figure 4.3); as the heating rate was increased from 5 to 25 °C/min these temperatures also increased. This indicates that both isoprene and DL-limonene were produced at higher temperatures when the heating rate was increased.

Isoprene and DL-limonene are the products of two competitive depolymerisation reactions of the allylic polyisoprene radicals during pyrolysis, i.e. from depropagation and intramolecular cyclization - scission reactions, respectively. A possible reaction pathway is given in Figure 4.5. In Figure 4.6 the ion current signal peaks for isoprene and DL-limonene production are shown for the experiment at 15 °C/min. It was observed that for the same heating rate the DL-limonene ion current signal peak was at slightly higher temperatures than the isoprene ion current signal peak (ΔT = 12 °C at 15 °C/min). Moreover, this difference increases for increasing heating rates, with ΔT of 4 and 16 °C for 5 and 25 °C/min, respectively (not depicted) and it implies that the DL-limonene reaction has a slightly higher activation energy than the isoprene reaction. A higher activation energy for the DL-limonene reaction seems reasonable, since this reaction includes both the formation of a bond (during cyclisation) and the breakage of a bond (scission), while the depropagation reaction only entails the latter, see also Figure 4.5.

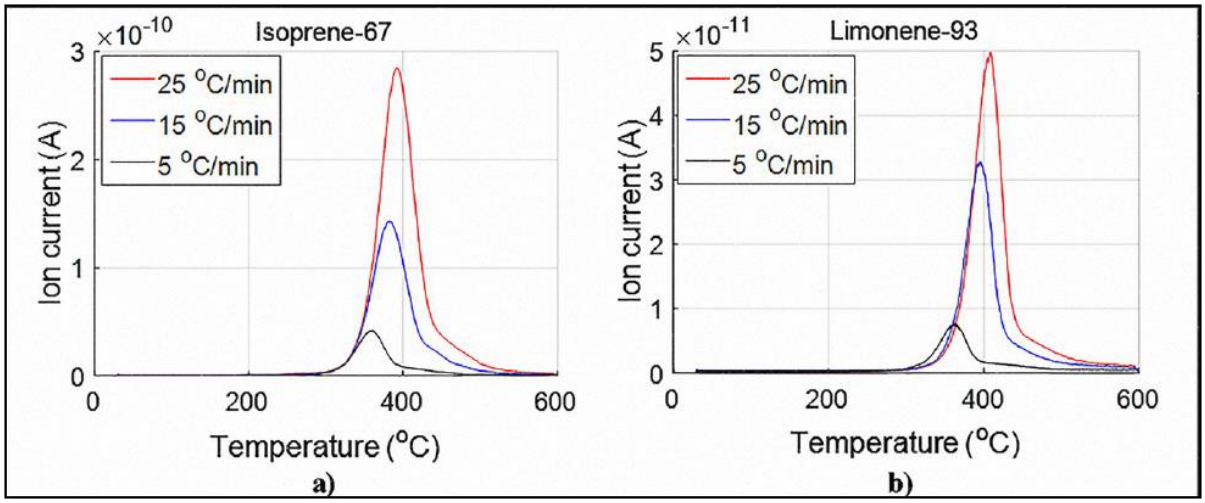

Figure 4.4: Ion current signals of a) isoprene (67 amu) and b) DL-limonene (93 amu) at 5, 15 and 25 °C/min.

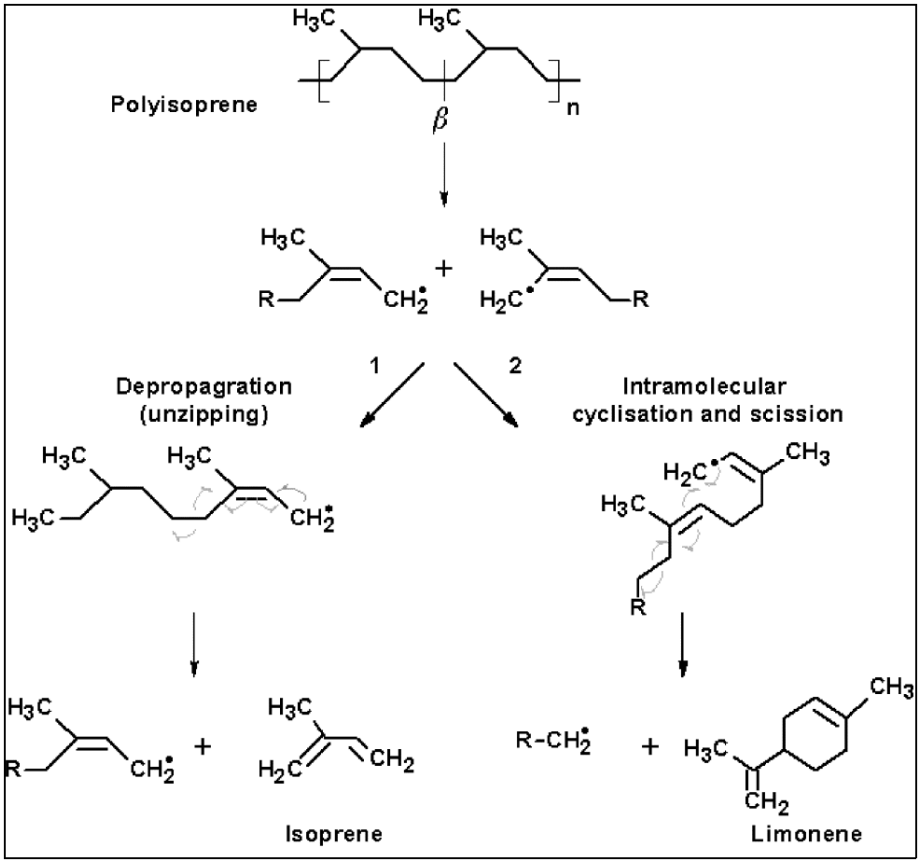

Figure 4.5: Polyisoprene depolymerisation by 1) depropagation to isoprene and 2) intramolecular cyclisation and scission to DL-limonene [10].

Because a higher activation energy also represents a higher temperature dependency of the reaction rate (following Arrhenius law), it follows that higher depolymerisation temperatures favour the production of DL-limonene over isoprene. Therefore, the observations that higher heating rates resulted in (1) relatively more depolymerisation reactions and (2) these depolymerisation reactions to occur at higher temperatures (specifically the reaction towards DL-limonene), could explain the higher DL-limonene yields at higher heating rates.

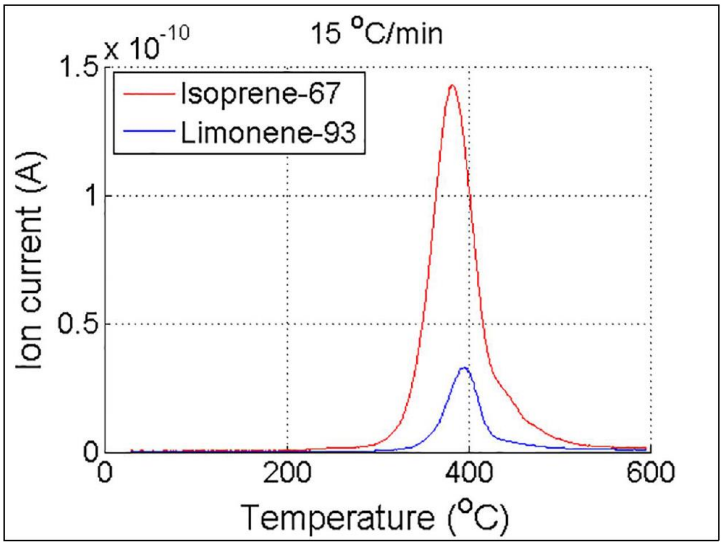

Figure 4.6: Ion current signals of isoprene (67 amu) and DL-limonene (93 amu) at 15 °C/min.

4.4 Conclusions

In this study, the effect of pyrolysis temperature and heating rate was evaluated for the pyrolysis of waste tyre to TDOs, specifically focusing on the production of DL-limonene. Two reactors, at gram- and microgram-scale, were used in the investigation. The experiments conducted in the gram-scale reactor showed that the effect of pyrolysis temperature on the TDO yield was significant, whereas the effect of the heating rate was insignificant. However, the effect of both the pyrolysis temperature and the heating rate was significant for DL-limonene production. Additionally, microgram-scale experiments analysis using DTG curves showed that increasing the heating rate led to (1) a decrease in secondary degradation reactions, and (2) an increased temperature at the maximum depolymerisation rate. Moreover, MS ion current signals showed that, at the same heating rate, DL-limonene formation occurred at slightly higher temperatures (compared to isoprene formation), indicating a slight higher activation energy for this reaction. Since a higher activation energy indicates a stronger temperature dependency for a reaction, it implies, in combination with the observation of higher temperatures at maximum DL-limonene production rate in the

MS ion current signal, an improvement of the selectivity of polyisoprene depolymerisation towards DL-limonene. Future work will entail the investigation of even higher heating rates (in order to further improve the DL-limonene yield) and modelling of the kinetic parameters of the isoprene and DL-limonene reactions.

Acknowledgements

This research was supported by the Recycling and Economic Development Initiative of South Africa (REDISA) and the National Research Foundation (NRF). The authors acknowledge that opinions, findings and conclusions or recommendations expressed are those of the authors only, and the sponsors accept no liability whatsoever in this regard.

References

[1] J.D. Martínez, N. Puy, R. Murillo, T. García, M.V. Navarro, A.M. Mastral, Waste tyre pyrolysis – A review, Renewable and Sustainable Energy Reviews. 23 (2013) 179-213.

[2] J.D. Martínez, M. Lapuerta, R. García-Contreras, R. Murillo, T. García, Fuel properties of tire pyrolysis liquid and its blends with diesel fuel, Energy and Fuels. 27 (2013) 3296-3305.

[3] N. Antoniou, A. Zabaniotou, Features of an efficient and environmentally attractive used tyres pyrolysis with energy and material recovery, Renewable and Sustainable Energy Reviews. 20 (2013) 539-558.

[4] P.T. Williams, Pyrolysis of waste tyres: A review, Waste Manage. 33 (2013) 1714-1728.

[5] A. Quek, R. Balasubramanian, Liquefaction of waste tires by pyrolysis for oil and chemicals—A review, J. Anal. Appl. Pyrolysis. 101 (2013) 1-16.

[6] P.T. Williams, S. Besler, D.T. Taylor, The pyrolysis of scrap automotive tyres: The influence of temperature and heating rate on product composition, Fuel. 69 (1990) 1474-1482.

[7] G. Lopez, M. Olazar, M. Amutio, R. Aguado, J. Bilbao, Influence of tire formulation on the products of continuous pyrolysis in a conical spouted bed reactor, Energy and Fuels. 23 (2009) 5423-5431.

[8] H. pakdel, C. ROY, H. AUBIN, G. JEAN, S. COULOMBE, FORMATION OF DL- LIMONENE IN USED TIRE VACUUM PYROLYSIS OILS, Environ. Sci. Technol. 25 (1991) 1646-1648.

[9] M.F. Laresgoiti, B.M. Caballero, I. de Marco, A. Torres, M.A. Cabrero, M.J. Chomón, Characterization of the liquid products obtained in tyre pyrolysis, J. Anal. Appl. Pyrolysis. 71 (2004) 917-934.

[10] B. Danon, P. Van Der Gryp, C.E. Schwarz, J.F. Görgens, A review of dipentene (dl-limonene) production from waste tire pyrolysis, J. Anal. Appl. Pyrolysis. 112 (2015) 1-13.

[11] E. Aylón, A. Fernández-Colino, R. Murillo, M.V. Navarro, T. García, A.M. Mastral, Valorisation of waste tyre by pyrolysis in a moving bed reactor, Waste Manage. 30 (2010) 1220-1224.

[12] Y. Kar, Catalytic pyrolysis of car tire waste using expanded perlite, Waste Manage. 31 (2011) 1772-1782.

[13] C. Roy, A. Chaala, H. Darmstadt, The vacuum pyrolysis of used tires: End-uses for oil and carbon black products, J. Anal. Appl. Pyrolysis. 51 (1999) 201-221.

[14] A.M. Cunliffe, P.T. Williams, Composition of oils derived from the batch pyrolysis of tyres, J. Anal. Appl. Pyrolysis. 44 (1998) 131-152.

[15] M.R. Islam, H. Hiroyuki, B.M.R. Alam, Limonene-rich liquid from pyrolysis of heavy automotive tire waste, Journal of Environment and Engineering. 2 (2007) 981-695.

[16] K. Cheung, K. Lee, K. Lam, C. Lee, C. Hui, Integrated kinetics and heat flow modelling to optimise waste tyre pyrolysis at different heating rates, Fuel Process Technol. 92 (2011) 856-863.

[17] S. Seidelt, M. Müller-Hagedorn, H. Bockhorn, Description of tire pyrolysis by thermal degradation behaviour of main components, J. Anal. Appl. Pyrolysis. 75 (2006) 11-18.

[18] S. Charpenay, M.A. Wójtowitcz, M.A. Serio, E. Arenas, A. Hill, J.C. Rojas, Pyrolysis kinetics of the waste-tire constituents: Extender oil, natural rubber, and styrene-butadiene rubber, ACS Division of fuel Chemistry, Preprints. 43 (1998) 185-191.

[19] K.-. Lam, C.-. Lee, C.-. Hui, Multi-stage waste tyre pyrolysis: An optimisation approach, Chemical Engineering Transactions. 21 (2010) 853-858.

[20] M. Banar, V. Akyildiz, A. Özkan, Z. Çokaygil, Ö Onay, Characterization of pyrolytic oil obtained from pyrolysis of TDF (Tire Derived Fuel), Energy Conversion and Management. 62 (2012) 22-30.

[21] D.W. Brazier, N.V. Schwartz, The effect of heating rate on the thermal degradation of polybutadiene, Journal of Applied Polymer Science. 22 (1978) 113-124.

[22] D.Y.C. Leung, C.L. Wang, Kinetic study of scrap tyre pyrolysis and combustion, J. Anal. Appl. Pyrolysis. 45 (1998) 153-169.

[23] K. Cheung, K. Lee, K. Lam, T. Chan, C. Lee, C. Hui, Operation strategy for multi-stage pyrolysis, J. Anal. Appl. Pyrolysis. 91 (2011) 165-182.

[24] B. Danon, J. Görgens, Determining rubber composition of waste tyres using devolatilisation kinetics, Thermochimica Acta. 621 (2015) 56-60.

[25] R. Murillo, E. Aylón, M.V. Navarro, M.S. Callén, A. Aranda, A.M. Mastral, The application of thermal processes to valorise waste tyre, Fuel Process Technol. 87 (2006) 143-147.

[26] C. Berrueco, E. Esperanza, F.J. Mastral, J. Ceamanos, P. García-Bacaicoa, Pyrolysis of waste tyres in an atmospheric static-bed batch reactor: Analysis of the gases obtained, J. Anal. Appl. Pyrolysis. 74 (2005) 245-253.

[27] S. Stein, NIST Chemistry WebBook, No 69, NIST Standard Reference Database, 2015 (2015).

[28] O. Senneca, P. Salatino, R. Chirone, A fast heating-rate thermogravimetric study of the pyrolysis of scrap tyres, Fuel. 78 (1999) 1575-1581.

[29] M.R. Islam, H. Haniu, J. Fardoushi, Pyrolysis kinetics behavior of solid tire wastes available in Bangladesh, Waste Manage. 29 (2009) 668-677.

[30] J.H. Chen, K.S. Chen, L.Y. Tong, On the pyrolysis kinetics of scrap automotive tires, J. Hazard. Mater. 84 (2001) 43-55.

[31] A. Quek, R. Balasubramanian, An algorithm for the kinetics of tire pyrolysis under different heating rates, J. Hazard. Mater. 166 (2009) 126-132.

[32] K. Lee, K. Cheung, K.L. Lam, C.W. Hui, Optimization of multi-stage waste tyre pyrolysis process, 1 (2010).

CHAPTER 5. KINETIC STUDY OF THE EFFECT OF THE HEATING RATE ON THE WASTE TYRE PYROLYSIS TO MAXIMISE LIMONENE PRODUCTION

Manuscript

Title: Kinetic study of the effect of the heating rate on the waste tyre pyrolysis to maximise limonene production

Targeted journal: Thermochimica Acta

Issue: xxx

Pages: xxx - xxx

Short summary

Kinetic mechanisms for DL-limonene formation in relation to the established optimal waste tyre pyrolysis operating conditions (475 °C and 20 °C) from objective 1 (CHAPTER 4) is elaborated in objective 2 in the current chapter (CHAPTER 5). The objective of the current chapter is to expand on the findings regarding the effect of the heating rate on the two-competing polyisoprene depolymerisation pathways, i.e., i) allylic polyisoprene radicals depropagation to produce isoprene, and ii) intramolecular cyclization - scission to produce DL-limonene. Since the heating rate investigated in CHAPTER 4 was limited to 29 °C/min, it has been significantly increased up to 100 °C/min to improve and confirm the findings in this chapter. A high precision milligram-scale reactor, thermogravimetric analyser (TGA) connected to an online mass spectrometer (MS) is used, to investigate conditions for maximum production of DL-limonene. The findings from the current chapter contribute significantly on the subsequent.

Declaration by the candidate:

With regard to CHAPTER 5, pages 78 – 100, the nature and scope of my contribution were as follows:

Nature of contribution	**Extent of contribution (%)**
Planning of the experiments	70
Execution of the experiments	80
Interpretation of the results	70
Compilation of the chapter	100

The following co-authors have contributed to CHAPTER 5, pages 78 – 100:

Name	**e-mail address**	**Nature of contribution**	**Extent of contribution (%)**
Bart Danon	bdanon@sun.ac.za	Planning of the experiments	20
		Execution of the experiments	20
		Interpretation of the results	30
		Revision of the chapter	80
Percy van der Gryp	pvdg@sun.ac.za	Planning of the experiments	5
		Revision of the chapter	10
Johann Gorgens	jgorgens@sun.ac.za	Planning of the experiments	5
		Revision of the chapter	10

Signature of candidate…….

Date…….

Declaration by the co-authors:

The undersigned hereby confirm that

1. the declaration above accurately reflects the nature and extent of the contributions of the candidate and the co-authors to CHAPTER 5, pages 78 – 100,
2. no other authors contributed to CHAPTER 5, pages 78 – 100 besides those specified above, and
3. potential conflicts of interest have been revealed to all interested parties and that the necessary arrangements have been made to use the material in CHAPTER 5, pages 78 – 100 of this dissertation.

Signature	**Institutional affiliation**	**Date**
	Stellenbosch University	
	Stellenbosch University	
	Stellenbosch University	

Kinetic study of the effect of the heating rate on the waste tyre pyrolysis to maximise limonene production

N. M. Mkhize, B. Danon, P. van der Gryp, J. F. Görgens*

Department of Process Engineering, Stellenbosch University, Private Bag X1, Matieland, 7602, Stellenbosch, South Africa

* Corresponding author: jgorgens@sun.ac.za

Abstract

The formation of isoprene and DL-limonene during waste tyre pyrolysis was investigated in terms of the effect of the heating rate (up to 100 °C/min). Ion current signals were used to track during pyrolysis the evolution of the predominant ions of isoprene and DL-limonene, by using a thermogravimetric analyser coupled with a mass spectrometry (TGA/MS). Using both model-free and model-based kinetics were applied, to estimate the activation energy (E_a) for isoprene and DL-limonene formation at 131 and 115 kJ/mole, respectively, based on the Kissinger method. The n values were estimated at 1.2 and 1.1 for isoprene and DL-limonene, respectively. Better model fit (R^2 closer to the unity) of the experimental data to the Arrhenius equation for isoprene and DL-limonene, respectively, was observed when the Kissinger method was used compare to Friedman method. Although the E_a values for isoprene and DL-limonene were not significantly different, the combined three kinetic parameters (E_a, A, and n) may be significantly different. Therefore, for DL-limonene formation selectivity over isoprene, the effect of the combined three kinetic parameters and heating rate on the reaction progress was significant. The reaction progress at peak isoprene and DL-limonene formation rate increased from 0.42 to 0.45 and more significantly from 0.35 to 0.44, respectively as heating rate increased, confirming that the preferred strategy to maximise DL-limonene production is rapid heating to moderate final pyrolysis temperature.

5.1 Introduction

Waste tyre piles are increasing at a high rate compared to the rate of their elimination as provided by various recycling techniques. Among the techniques of waste tyre processing [1-3], pyrolysis is one of the most promising, since it results in products that have a variety of industrial and domestic applications [4,5]. Pyrolysis is defined as the thermal treatment of waste tyres under inert conditions to yield pyro-gas, tyre derived oil (TDO) and pyro-char [6,7]. The pyro-gas can be used as fuel for the endothermic pyrolysis process [5] or various other applications, e.g. when further processed to recover valuable chemicals, such

as, butadiene or isoprene. TDO's significantly high hydrogen and carbon element content and high concentration of valuable chemicals, e.g., DL-limonene, terpinolene and p-cymene characterises it as a potential alternative for liquid fuel, or as a feedstock for the production of valuable chemicals [4,8]. The pyro-char mainly contains carbon and can be upgraded into the carbon black or activated carbon [9]. However, to achieve these beneficial applications for the waste tyre pyrolysis products, intensive processing to improve products, such as, product refining, upgrading, and purification, are required.

TDO is the main pyrolysis product fraction (in weight), is relatively easy to handle, which make it the most interesting pyrolysis product [8]. TDO is a potential source for the recovery of valuable chemicals, while the resulting residues can be upgraded to liquid fuels, comparable to the conventional petroleum derived products and fuels [5,8]. There is substantial literature on the upgrading of the TDO to liquid fuels, however, the employed techniques are mainly focusing on the post-treatment of the TDO after pyrolysis. These processes include moisture removal, desuphurisation, hydrotreatment, thermal treatment, catalytic treatment and biological processes [10-13], but they are relatively complex, expensive and can generate environmental unfriendly waste streams requiring further treatment.

An alternative to post-pyrolysis TDO upgrading, is the modification of the pyrolysis process to improve the TDO quality in terms of chemical composition [4,14]. For successful process optimisation kinetic mechanisms of the waste tyre devolatilisation needs to be understood [15-18]. Activation energies (E_a) and pre-exponential rate constants (A) in relation to the pyrolysis temperature and heating rate have been reported [19-22]. These studies mainly concluded that devolatilisation kinetics consist of various parallel and serial devolatilisation reaction pathways, such as, devolatilisation of the tyre processing oils followed by devolatilisation of the natural rubber and finally synthetic rubbers (styrene butadiene rubber and butadiene rubber). Additionally, waste tyre pyrolysis has been kinetically presented according to products volatilisation, such as, gaseous products, variety of TDO sub-fractions (aromatics, aliphatics, poly aromatic hydrocarbons and heteroatom compounds) and char [23]. Some effort has been done to study waste tyre pyrolysis kinetics based on the formation of chemical compounds [24]. In most of the studies, heating rate has been an important parameter in the waste tyre pyrolysis kinetic mechanism study [25].

For example, Lam *et al*. (2010) proposed a multi-stage pyrolysis process with 1) pyrolysis of tyre additives, 2) pyrolysis of polymerised rubbers, and 3) pyrolysis of the cross-linked and/or cyclised rubbers [19]. Cheung *et al*. (2011) propounded the following pyrolysis stages: 1) pyrolysis of the volatiles, 2) main chain scission (depolymerisation) to intermediates, 3) further depolymerisation of the intermediates (pyrolysis of cross-linked rubbers), and 4) cracking of the intermediates to shorter chain compounds (degradation) [20].

Danon *et al*. (2015) in the study of devolatilisation kinetics of tyre rubbers defined tyre devolatilisation as a three-stage process: 1) devolatilisation of additives, 2) crosslinking and depolymerisation of the rubbers into intermediates and volatiles, respectively, and 3) finally degradation of the intermediates to volatiles [21]. There has been therefore substantial literature data mainly focusing on tyre components devolatilisation mechanism kinetics and there seems to be agreements on the observations, however little is known about product formation kinetics.

The present work focuses on the kinetic mechanism of waste tyre pyrolysis based on the products formed in the hot volatiles, rather than considering the devolatilisation of the tyre components. Polyisoprene (natural rubber) devolatilisation forms two compounds (isoprene or DL-limonene) via two supposedly competing reaction pathways. Kinetic parameters are evaluated for the formation of isoprene and DL-limonene to elucidate these mechanisms, through the application of thermogravimetric analysis (TGA), with various constant heating rates up to 100 °C/min. Isoprene and DL-limonene formation are monitored using a mass spectrometry (MS) (67 and 93 amu, respectively).

5.2 Theoretical background

The kinetic model used in the current study entails description of the formation of the isoprene and DL-limonene from waste tyre or polyisoprene (tyre rubbery component) pyrolysis. In the literature, it has been pointed out that devolatilisation of the polyisoprene results into two competing product formation reaction pathways, i.e. the formation of allylic radicals that will either i) depropagate (unzip) to form isoprene or, ii) undergo intramolecular cyclisation followed by chain scission to form DL-limonene [26], see Figure 5.1.

Kinetic analysis requires tracking of the formation of isoprene and DL-limonene. This is achieved by MS, where the ion current signals are obtained through ion extraction method using predominant mass-over-charge-ratios of 67 and 93 amu, from fragmentation of the isoprene and DL-limonene, respectively. It is assumed that tracking of isoprene and DL-limonene formation ions for ion current signals is independent from one another, i.e., do not influence one another or influenced by other ions that are present due to fragmentation of various molecules from other tyre components.

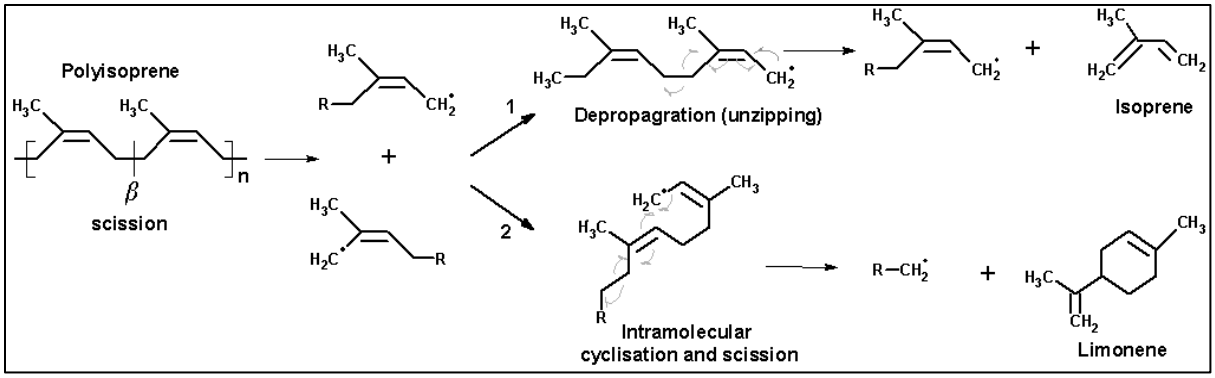

Figure 5.1: Polyisoprene depolymerisation by 1) depropagation to isoprene and 2) intramolecular cyclisation and scission to DL-limonene.

The proposed model is therefore based on the devolatilisation of the polyisoprene component of the tyre rubber as well as formation of the isoprene and DL-limonene. The conversion rate of polyisoprene or natural rubber (NR) is given by the mass fraction devolatilisation equation, Equation 1.

Equation 1

$$\frac{dm}{dt} = k(T)f(m)$$

where: *m* is mass fraction, *t* is time, *k*(*T*) is reaction rate constant at temperature, *T* (*K*), and *f(m)* is the reaction model.

Subsequent to devolatilisation of the polyisoprene, is the formation of isoprene and DL-limonene and can be represented by the Equation 2.

Equation 2

$$\frac{dS_i}{dt} = k(T)f(S)$$

where: S_i is MS ion current fraction of either the isoprene or DL-limonene, and *f*(*S*) is the reaction model for isoprene or DL-limonene formation reaction.

The reaction progress, α_i, of the formation reaction rate of either isoprene and DL-limonene is represented by Equation 3.

Equation 3

$$\alpha_i = \frac{S_{i,cumsum}}{S_{sum}}$$

where: α_i is the reaction progress for the formation of either isoprene or DL-limonene, $S_{i,cumsum}$is the cumulative sum of the ion current at time t, and $S_{i,sum}$ is the sum of ion current up to final time for either isoprene or DL-limonene formation.

Therefore, Equation 2 can be presented by Equation 4.

Equation 4

$$\frac{d\alpha_i}{dt} = k(T)f(S_i)$$

The time, t, and heating rate, β, can be related by Equation 5.

Equation 5

$$\beta = \frac{dT}{dt}$$

where: $\beta$is the heating rate, and $T$is the absolute temperature.

The reaction rate constant, *k*, can be presented by Equation 6.

Equation 6

$$k(t) = Aexp(\frac{-E_a}{RT})$$

where: *k* is the reaction rate constant, *A* is a pre-reaction rate constant, E_a is the activation energy, and *R* is the universal gas constant.

Therefore, by substituting Equation 4 and Equation 5 in Equation 2:

Equation 7

$$\frac{d\alpha}{dT} = \frac{1}{\beta} A exp(-\frac{E_a}{RT}) f(S)$$

5.2.1 Determination of kinetic parameters

Kinetic parameters (E_a, A, and n) can be determined using various techniques classified according to i) pyrolysis conditions, i.e., isothermal or non-isothermal, or ii) mathematical analysis of the experimental results, i.e., linear or nonlinear. In the current study, non-isothermal pyrolysis conditions were used since the experiments were carried out at various heating rates (15, 25, 50, 75 and 100 °C/min). The linear mathematical analysis methods for experimental results analysis were selected due to their conventional application in the analysis of thermal devolatilisation of the solids. These methods allow determination of a linear relationship between the kinetic parameters using MS ion current data generated at various reaction rates. Linear regression methods using experimental results are applied to determine coefficients of the linear relation. Typical non-isothermal and linear methods were considered in the present study, in particular the iso-conversional methods of Friedman (differential approach) and Kissinger (integration approach) [16,17]. Matlab 2015a was used in the analysis of the experimental results.

5.2.2 Friedman method

Taking a natural logarithm of Equation 7, the linear relationship is employed in the equation and resulted into Equation 8.

Equation 8

$$ln\left(\beta \frac{d\alpha}{dT}\right) = lnA + lnf(\alpha) - \frac{E_a}{RT}$$

Plotting $ln\left(\beta \frac{d\alpha}{dT}\right)$ versus $\frac{1}{T}$ at a given reaction progress, α, for various heating rates yields a straight line with slope $\frac{-E_a}{R}$. Activation energy can be obtained from this slope without knowing the reaction function $f(\alpha)$. The pre-exponential reaction rate constant, *A*, is the y-intercept of a straight line. Friedman method is one of the model-free iso-conversional method [16].

5.2.3 Kissinger method

The Kissinger method is based on the determination of the temperature at the maximum devolatilisation rate of the polyisoprene, or the temperature associated with the maximum formation rate of isoprene or DL-limonene temperatures, both at various heating rates [17]. In the Kissinger method, Equation 7 is modified to Equation 9.

Equation 9

$$ln\left(\frac{\beta}{T^2}\right) = ln\left(\frac{AR}{f(\alpha)}\right) - \frac{E_a}{RT}$$

A plot of $ln\left(\frac{\beta}{T_{max}^2}\right)$ versus $\frac{1}{T_{max}}$ at various heating rates yields a straight line that allows determination of the activation energy, E_a, from the gradient of the straight line, $\frac{-E_a}{R}$. The y-intercept can be used to estimate pre-exponential reaction rate factor. Similar to the Friedman method, Kissinger method is another example of a model-free iso-conversional method.

5.2.4 Master plots

Introduction of the explicit value of the heating rate reduces the applicability of Equation 6 to processes in which the sample temperature does not deviate significantly from the reference temperature. Therefore, integration of Equation 7 results into Equation 10:

Equation 10

$$g(\alpha) = \int \frac{d\alpha}{f(\alpha)} = \frac{A}{\beta}\int exp\left(-\frac{E_a}{RT}\right)dT = \left(\frac{AE_a}{R\beta}\right)\int exp\frac{(-x)dx}{x^2} = \left(\frac{AE_a}{R\beta}\right)p(x)$$

where: $x = E_a/RT$, and p(x) is the temperature integral.

By using a reference value at midpoint of the reaction progress, α = ref., Equation 11 is obtained.

Equation 11

$$g(ref.) = \left(\frac{AE_a}{R\beta}\right) p(ref.)$$

Typical theoretical kinetic models summary for solids devolatilisation are represented in Table 5.1 [27,28].

Table 5.1: Typical solids decomposition models.

Model	$f(\alpha)$	$g(\alpha)$	Symbol
Half order	$\alpha^{0.5}$	$2\alpha^{0.5}$	P3
First order	α^{1}	$ln\alpha$	F1
Second order	α^{2}	$-1/\alpha$	F2
Phase boundary	$3\alpha^{2/3}$	$3\alpha^{1/3}$	R3
Two-dimensional diffusion	$1/(ln\alpha + 2)$	$\alpha ln\alpha + \alpha$	D2

At a given reaction progress, experimental and theoretical progress are represented by Equation 12.

Equation 12

Experimental: $\left(\frac{T}{T_{ref}}\right)^2 \left[\left(\frac{d\alpha}{dt}\right) / \left(\frac{d\alpha}{dt}\right)_{ref}\right]$

Theoretical: $g(\alpha) \cdot f(\alpha) / [g(\alpha) \cdot f(\alpha)]_{ref}$

5.3 Equipment and method

Truck tyre sample with particle size range of 0.6 to 0.8 mm was sieved from a bulk of approximately 500 kg crumbed (steel- and fabric-free) waste tyres, consisting of particle sizes up to 5 mm. The crumb was supplied by a local waste tyre recycler. A slightly adjusted version of ASTM E1131 – 08 (with X = 275 °C) was used to determine proximate analysis. Additionally, rubber composition of the crumb was determined using a procedure described by Danon and Görgens [29]. The results of the proximate analysis and rubber composition are shown in Table 5.2.

Table 5.2: Proximate analysis and rubber composition of the crumb.

Proximate	Moisture	Oils	Volatile matter	Fixed carbon	Ash
analysis (wt.%)	0.6	5.6	56.0	30.0	7.8

Rubber composition/volatile matter (wt.%)	Polyisoprene (natural rubber)	Synthetic rubber (SBR and BR)[α]
	64	36

[α]By difference

A Mettler Toledo TGA/DCS 1 thermogravimetric analyser (TGA) connected to a ThermoStar GSD 320 T3 (Pfeiffer Vacuum, Germany) mass spectrometer (MS) was used for all experiments. The ionisation energy was set to 70 eV, using a Secondary Electron Multiplier (SEM) to amplify the MS signal. Argon gas (99.999% purity, Afrox, South Africa) was used as a carrier gas. Sample size of 10 mg in these experiments was pyrolysed up to 800 ° C at five different constant heating rates (15, 25, 50, 75, and 100 °C/min). The mass-over-charge-ratios of the two most predominant fragments of isoprene and DL-limonene (67 and 93 amu, respectively) were monitored [30].

5.4 Results and discussion

5.4.1 Thermogravimetric analysis

Thermogravimetry (TG) and its derivative (DTG) profiles on the pyrolysis temperature basis at various heating rates up to 100 °C/min are illustrated in Figure 5.2 a) and b), respectively. From the TG profiles in Figure 5.2 a) it can be observed that, regardless of the heating rate, the profiles converge at the same value of solid residual at the end of pyrolysis. In Figure 5.2 b), the shape of the curves at a lower heating rate show two peaks, i.e. the main devolatilisation peak at low temperature and a small peak (shoulder) at the high temperature. As the heating rate increases the main peak become higher, while the shoulder disappears, as has been observed by other researchers [21]. This can be attributed to the elimination of the secondary reactions (primary products cracking) at higher heating rates, while promoting devolatilisation of the rubbers. The effect of the heating rate on the devolatilisation peak temperature is characterised by an increase in the temperature associated with the maximum devolatilisation rate, as the heating rate increases.

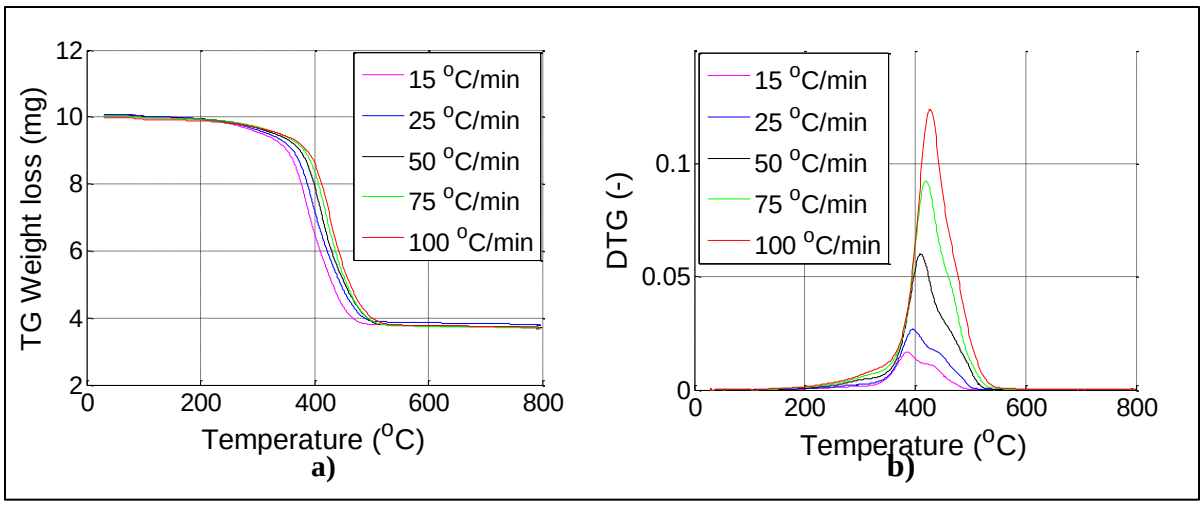

Figure 5.2: Profiles of the a) thermogravimetric (TG) and b) derivative thermogravimetric (DTG) of waste tyre devolatilisation.

5.4.2 Mass spectrometric analysis

Illustrated in Figure 5.3 a) and b) are the MS ion current profiles of the isoprene and DL-limonene, respectively. These profiles resemble the DTG curves of the devolatilisation of the tyre rubber component (Figure 5.2 b)), in that the shape of the curves at a lower heating rate show two peaks, i.e., main devolatilisation peak at low temperature and a small peak (shoulder) at the high temperature. However, zooming in on both the peaks of the tyre devolatilisation temperature (DTG) and the peaks of the products volatilisation temperature (MS) as shown in Table 5.3, a slight difference in profiles peak temperatures was observed. For example, the DTG curves showed that increasing the heating rate resulted in i) a decrease in the secondary degradation reactions, and ii) an increase in the temperature at which the maximum depolymerisation rate occured. At the same heating rate, MS ion current signals showed that maximum DL-limonene formation occurred at slightly higher temperatures compared to the maximum isoprene formation rate temperature. An increase in the heating rate from 15 to 100 °C/min increased the isoprene formation peak temperature from 380 to 432 °C, while that for DL-limonene was increased from 380 to 438 °C. This indicated that isoprene and DL-limonene formation pathways were not identical and the effect of the heating rate on the DL-limonene formation was more significant compared to the isoprene formation.

Moreover, the increases in the peak temperatures for DL-limonene formation reaction were less severe at higher heating rates. Devolatilisation of the polyisoprene (rubbery component in the tyre) is characterised by volatilisation of unstable allylic radicals. These allylic radicals further react by i) depropagation (unzipping) to form isoprene or, ii) intramolecular cyclisation followed by chain scission to form DL-

limonene. Therefore, suggesting that as the heating rate increases, its effect on the DL-limonene formation is becoming less significant, see Table 5.3.

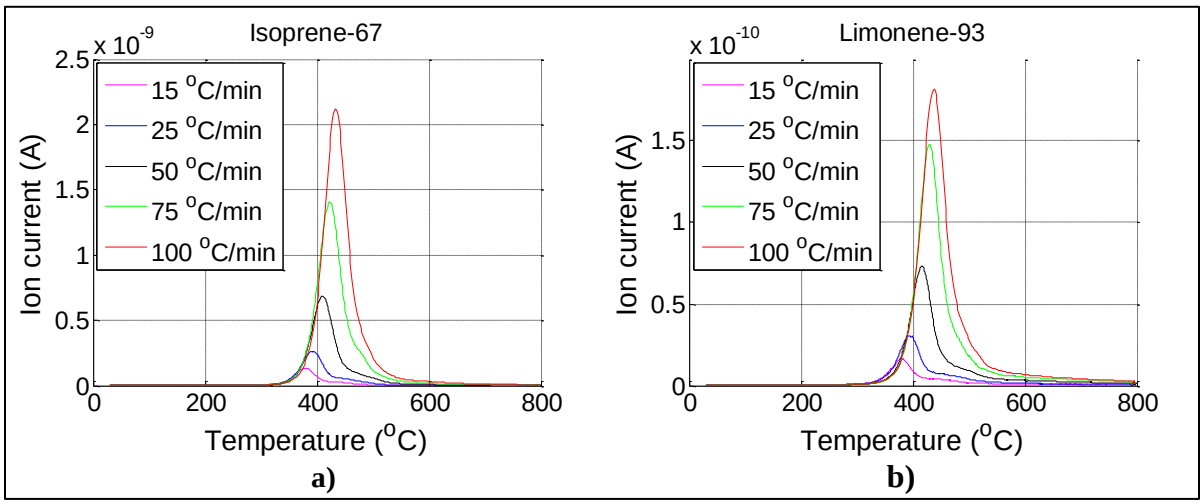

Figure 5.3: MS Ion current signals of a) isoprene (67 amu) and b) DL-limonene (93 amu) at 15, 25, 50, 75 and 100 °C/min.

Table 5.3: Tyre devolatilisation DTG and products formation MS ion current peak temperatures at 15, 25, 50, 75 and 100 °C/min.

Heating rate (°C/min)	DTG peak temperature (°C)	Ion	MS ion current peak temperature (°C)
15	385.50	Isoprene-67	380.48
		Limonene-93	380.23
25	396.67	Isoprene-67	392.07
		Limonene-93	393.74
50	410.38	Isoprene-67	409.53
		Limonene-93	415.45
75	418.71	Isoprene-67	422.54
		Limonene-93	430.18
100	425.88	Isoprene-67	432.70
		Limonene-93	437.80

5.4.3 Reaction progress

Figure 5.4 presents isoprene and DL-limonene formation or reaction progress as a function of temperature. The effect of the heating rate on the progress of the DL-limonene formation reaction was more significant than on isoprene formation, as per Figure 5.4 a) and b). The curves are relatively more vertical and parallel for isoprene (Figure 5.4 a), while being less vertical and cease to be parallel towards the end of the reaction for DL-limonene (Figure 5.4 b). Maximum DL-limonene formation rate at peak reaction progress which corresponds to the peak temperature increased from 0.35 to 0.44, while that of isoprene merely increased from 0.42 to 0.45 as the heating rate was increased from 15 to 100 °C/min, see Figure 5.4 c). The relation between the heating rate and reaction progress at the maximum formation rate indicated a more rapid conversion of the tyre rubber to DL-limonene than to isoprene, at similar temperature increases. Therefore, lower activation energy (E_a) at higher heating rates favoured DL-limonene formation compared to isoprene formation.

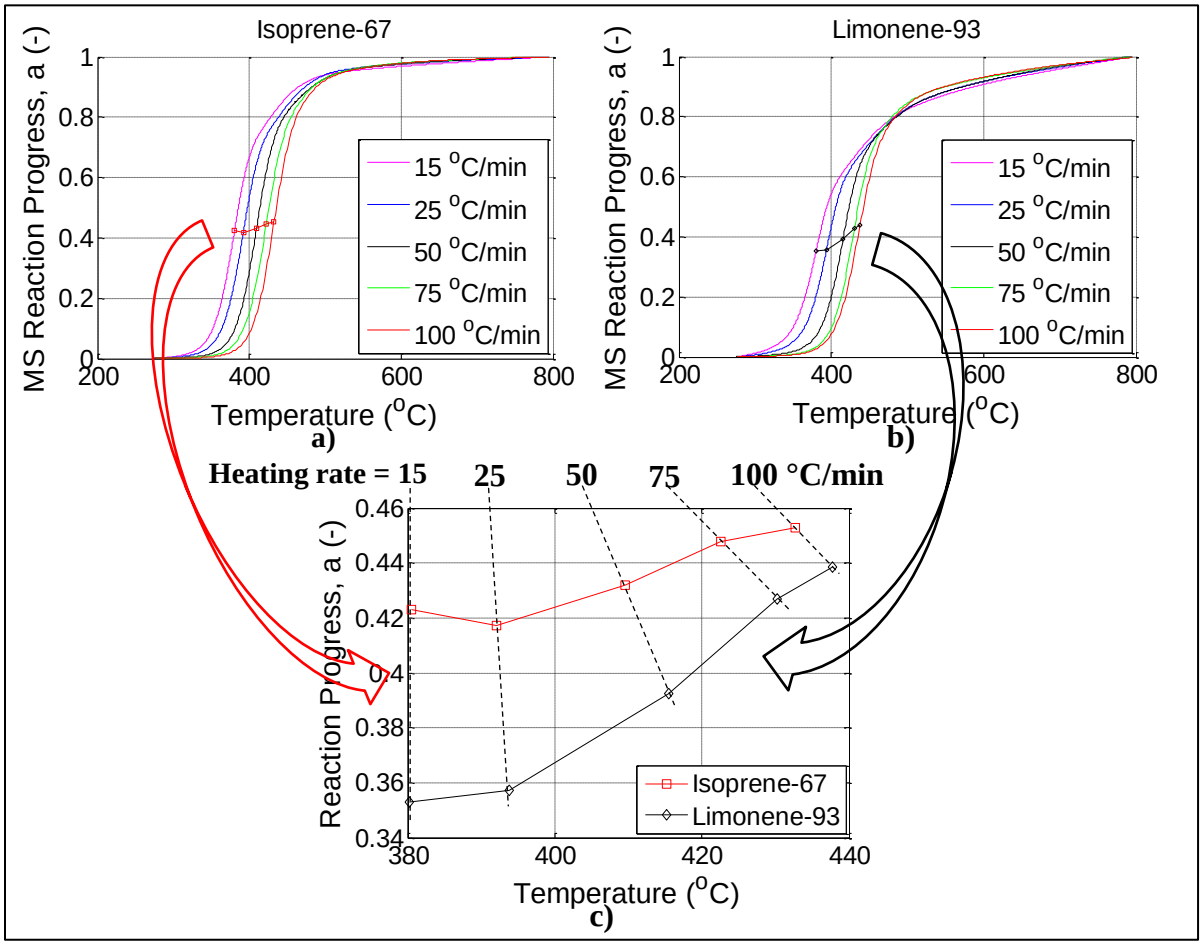

Figure 5.4: Reaction progress of a) isoprene (67 amu) and b) DL-limonene (93 amu) at 15, 25, 50, 75 and 100 °C/min.

5.4.4 Friedman method

Estimation of the apparent activation energy, E_a, as a function of reaction conversion with the differential-based, iso-conversional Friedman method are presented in Figure 5.5 a) and b), for isoprene and DL-limonene formation, respectively. In Figure 5.5 a) the E_a of isoprene formation remained relatively constant at approximately 141 kJ/mole for a reaction progress up to $\alpha = 0.5$. For the DL-limonene formation reaction, an E_a of approximately 145 kJ/mole was observed at a reaction progress between 0.1 and 0.5.

For the substantial increases in the E_a for both isoprene and DL-limonene above $\alpha = 0.5$, the Friedman method ceases to be reliable as indicated by large relative standard deviation. Capart et al. (2004), also observed a large standard error at α above 0.7 as well a sudden change in the slopes of the curves [31]. The changes in the apparent E_a for DL-limonene formation, for α above 0.5, was more severe than for isoprene formation. In Figure 5.5 b), the E_a not only ceases to be constant above $\alpha = 0.5$, but became negative towards the completion of the DL-limonene formation.

The observations in Figure 5.5 a) and b) are in agreement with the trends as illustrated in Figure 5.4 above, i.e. more uniformity in isoprene formation compared to DL-limonene formation. Base on merely Figure 5.4 which is within reliable extent of reaction progress, this distinction can be attributed to the different reaction pathways by which isoprene and DL-limonene are formed. Moreover, isoprene at ambient temperature is a gas, while limonene is normally a liquid. Therefore, the requirement in dealing with the DL-limonene at a gaseous phase may be relatively more complicated compared to isoprene. This indicates that isoprene formation may be comparably less sensitive than DL-limonene formation at the ranges of the parameters (temperature of 475 °C and heating rate up to 100 °C/min).

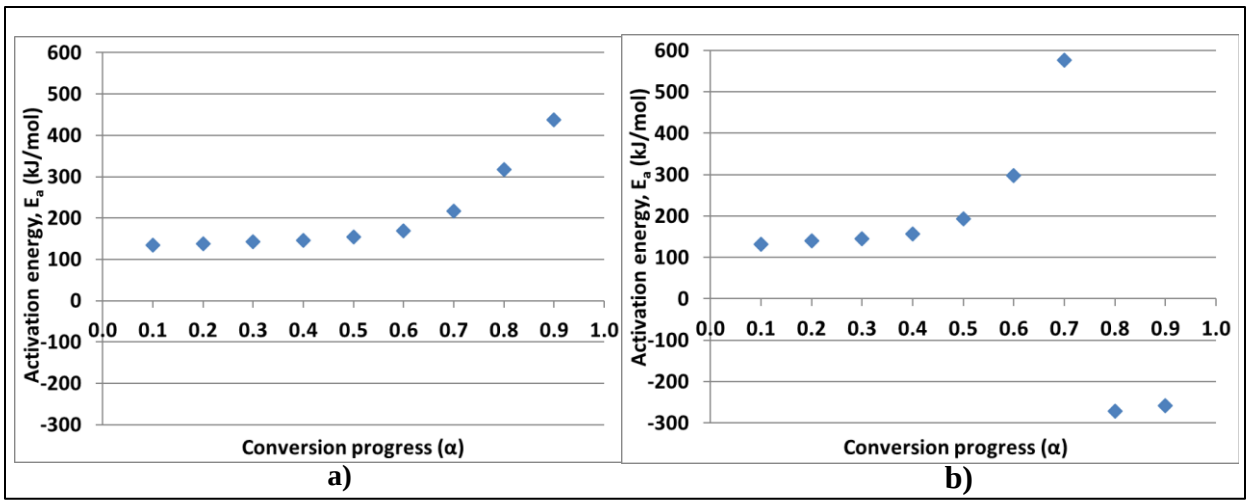

Figure 5.5: Iso-conversional Friedman method plot for a) isoprene and b) DL-limonene as various reaction progress.

5.4.5 Kissinger method

Alternative to Friedman method, the Kissinger method is an iso-conversional method based on an integration approach, which was also applied to estimate E_a for both isoprene and DL-limonene formation. Figure 5.6 a) and b) show the Kissinger plots for isoprene and DL-limonene, respectively. The Kissinger method plots seem to be uniform and constitute adequately straight-line fits for both isoprene and DL-limonene. This can be attributed to the use of the peak temperatures when constructing the Kissinger plots, which are below a nominal reaction progress of 0.5. A nominal reaction progress is a reaction progress by which the kinetic mechanism can be mathematically analysed using linear methods. The estimated E_as from Kissinger method were 129 and 113 kJ/mole for isoprene and DL-limonene, respectively.

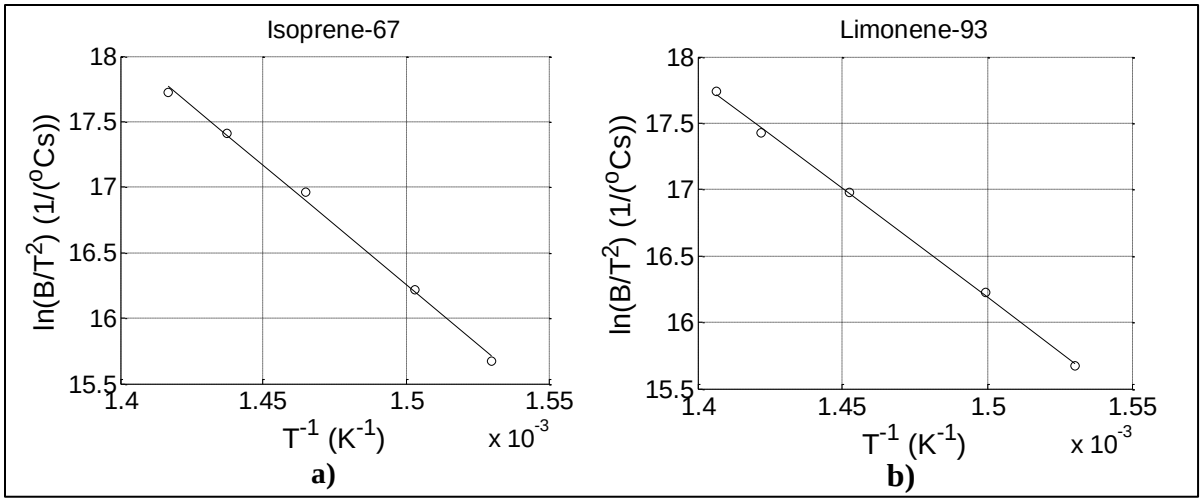

Figure 5.6: Iso-conversional Kissinger method plot for a) isoprene and b) DL-limonene at various reaction progress.

Using Friedman method, the E_a for isoprene (141 kJ/mole) and DL-limonene (145 kJ/mole) formation were not significantly different, which may indicate the limitations of the Friedman method in estimating the E_a values. Similar E_a values would suggest similar kinetic mechanisms for isoprene and DL-limonene formation, which is unlikely since isoprene formation entails depropagation (unzipping) of the polyisoprene allylic radicals, while DL-limonene is formed through intramolecular cyclisation of the allylic radicals followed by chain scission, see Figure 5.1 [26].

However, using the Kissinger method the estimated E_as for isoprene (129 kJ/mole) and DL-limonene (113 kJ/mole) formation were significantly different, see Table 5.4. Aguado et al (2005) also observed higher E_a in the isoprene (108 kJ/mole) formation compared to DL-limonene (97 kJ/mole), although the actual values were lower than those observed in the present study, see Table 5.4. This is not surprising since the rate of the increase in the peak temperature for DL-limonene formation is higher than for the isoprene formation at the same heating rate.

Table 5.4: Kinetic parameter estimated using iso-conversional methods for isoprene and l DL-limonene.

Ion	E_a (kJ/mol)	
	Current work: Kissinger method	**Literature [Aguado et al. (2005)]**
Isoprene-67	129	108
Limonene-93	113	97

5.4.6 Master plots

Estimation of the kinetic parameters (E_a, A, and n) for isoprene and DL-limonene formation model, reaction order (n) was also performed graphically using model based plots, called master plots. Various established models based on the solids devolatilisation were examined using master plots, i.e. half order (P3), first order (F1), second order (F2), phase boundary (R3) and two-dimensional diffusion (D2); see Table 5.1. The comparisons of the various models and experimental data are presented in Figure 5.7. Both isoprene (Figure 5.7 a)) and DL-limonene (Figure 5.7 b)) experimental data profiles were between P3 and F1. Figure 5.7 c) and d) illustrate a more detailed comparison of the P3 and F1 models to the experimental data for isoprene and DL-limonene formation, respectively. These results imply that n (reaction order) for both isoprene and DL-limonene formation is between 0.5 and 1.

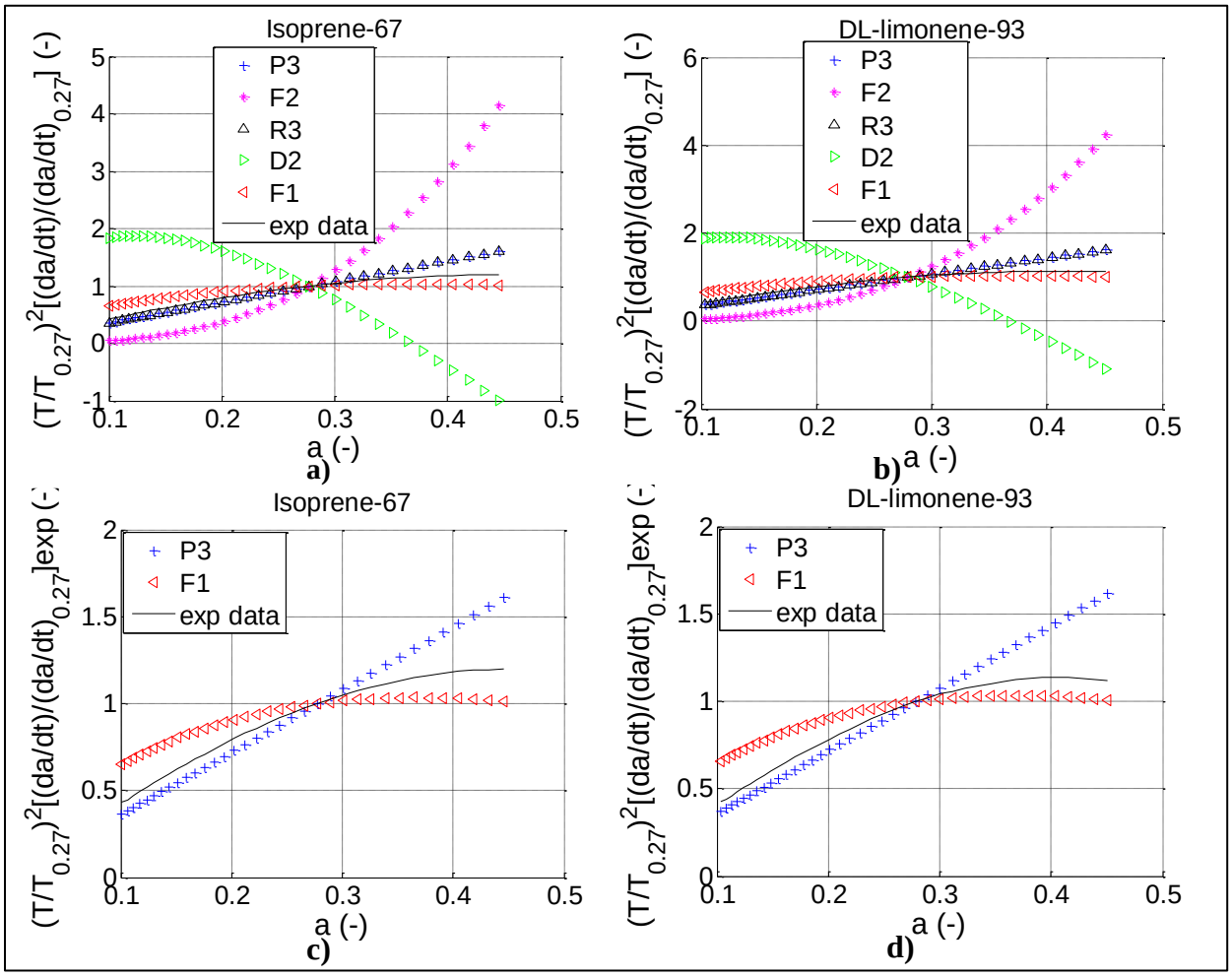

Figure 5.7: Master plots of various models for isoprene a) and DL-limonene e b) and zoomed in of the half and first order for isoprene c) and DL-limonene d).

5.4.7 Reaction model

The sum of least square difference between the model and experimental data was applied to optimise the reaction models for isoprene and DL-limonene formation, using Matlab 2015a© programming software. As a first-guess, the E_a and A values obtained from the iso-conversional methods using Kissinger method were substituted in Equation 12, together with a value of n = 0.7, between 0.5 and 1; results are shown in Figure 5.8. The subsequent regression further improved the model so that the model fit to the experimental data had the R^2 value closer to a unity. As shown in Figure 5.8, the best-fit models were able to follow the trends of the main peak at all heating rates. The second peak (shoulder) on the high temperature side was poorly modelled, particularly for low heating rate experimental data. This was attributed to the fact that at lower heating rate the shoulder is relatively more significant, while at high heating rate the shoulder is insignificant.

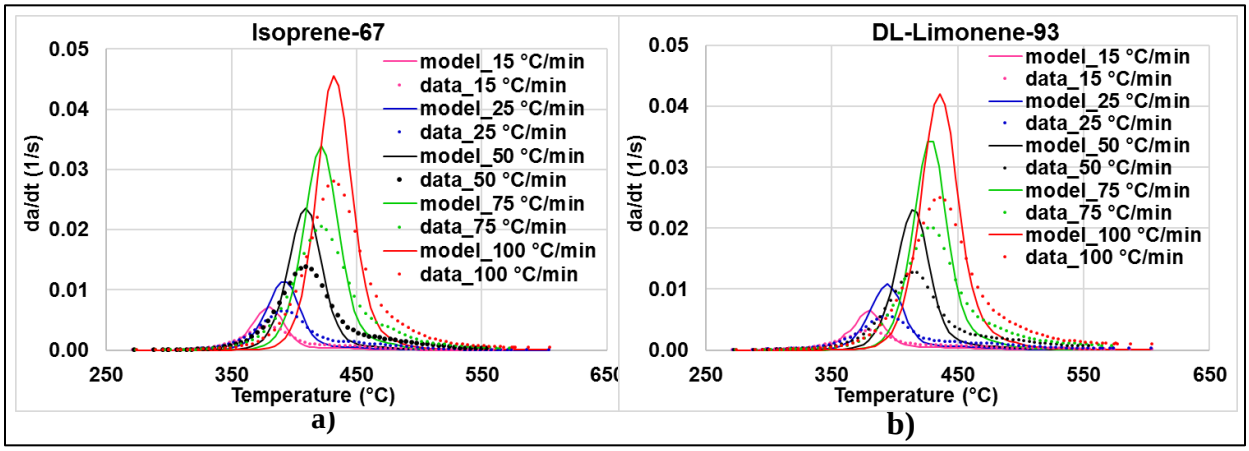

Figure 5.8: Model fitting on the experimental data for isoprene a) and DL-limonene b).

The values of E_a for isoprene and DL-limonene formation in the best-fit models were estimated at 132 and 115 kJ/mole, respectively, while the corresponding n values were estimated at 1, for both isoprene and DL-limonene. The E_a and A kinetic parameters did not change significantly during model-optimisation, indicating that the model-free estimations of these values were effective. The n-value of 2 for both isoprene and DL-limonene suggested first order formation reactions.

The comparison of the experimental data to the model for both isoprene and DL-limonene was satisfactory and resulted in an R^2 closer to 1, i.e., 0.998 and 0.997, respectively. The difference in the E_a values for between the for isoprene and DL-limonene indicate that their formation pathways differ. Therefore, it is possible to optimise the formation of DL-limonene over isoprene through setting the operating parameters.

Although temperature and heating rate were the only parameters investigated, they are some other reactor operating parameters that their effect is probably significant on the DL-limonene high yield and formation selectivity e.g., residence time of the hot volatiles on the reaction zones and the rate of cooling and condensing of the hot volatiles from the reactor [32].

5.5 Conclusions

The increase in the heating rate up to 100 °C/min increased the peak temperature of both the isoprene and DL-limonene formation reactions, during waste tyre pyrolysis. Peak temperature increase was more significant in the DL-limonene compared to the isoprene with increasing heating rate. In addition, maximum DL-limonene formation rate was relatively higher compared to maximum isoprene formation rate as the heating rate increased. This suggested that rapid heating resulted in the less energy was being allocated to the formation of products, therefore the increase in the heating rate favoured formation of the low E_a (i.e., DL-limonene). The model first-guess provided master plots was able to precisely predict the model for both for isoprene and DL-limonene. Model parameter estimations through the Kissinger method provided activation energies of approx. 133 and 115 kJ/mol for isoprene and DL-limonene formation reactions, respectively. Above $\alpha = 0.5$, the E_a strongly increased for both isoprene and DL-limonene and the Friedman method ceased to be accurate as indicated by large relative standard deviation. However, other factors, such as, hot volatiles residence time in the hot reaction zones and the rate of cooling of the hot volatiles also affect DL-limonene formation from waste tyre pyrolysis. Therefore, to maximise DL-limonene yield and recovery, heating rate, hot volatiles residence time in the hot reaction zones and the rate of cooling the hot volatiles should be considered.

Acknowledgements

This research was supported by the Recycling and Economic Development Initiative of South Africa (REDISA) and the National Research Foundation (NRF). The authors acknowledge that opinions, findings and conclusions or recommendations expressed are those of the authors only, and the sponsors accept no liability whatsoever in this regard.

References

[1] M. Sienkiewicz, J. Kucinska-Lipka, H. Janik, A. Balas, Progress in used tyres management in the European Union: A review, Waste Manage. 32 (2012) 1742-1751.

[2] M.A. Barlaz, W.E. Eleazer II, D.J. Whittle, Potential To Use Waste Tires As Supplemental Fuel In Pulp And Paper Mill Boilers, Cement Kilns And In Road Pavement, Waste Manage. Res. 11 (1993) 463-480.

[3] M. Giugliano, S. Cernuschi, U. Ghezzi, M. Grosso, Experimental evaluation of waste tires utilisation in cement kilns. Journal of the Air & Waste Management Association. 49 (1999) 1405-1414.

[4] A. Quek, R. Balasubramanian, Liquefaction of waste tires by pyrolysis for oil and chemicals—A review, J. Anal. Appl. Pyrolysis. 101 (2013) 1-16.

[5] P.T. Williams, Pyrolysis of waste tyres: A review, Waste Manage. 33 (2013) 1714-1728.

[6] E.L.K. Mui, D.C.K. Ko, G. McKay, Production of active carbons from waste tyres—a review, Carbon. 42 (2004) 2789-2805.

[7] N. Antoniou, A. Zabaniotou, Features of an efficient and environmentally attractive used tyres pyrolysis with energy and material recovery, Renewable and Sustainable Energy Reviews. 20 (2013) 539-558.

[8] M. Banar, V. Akyildiz, A. Özkan, Z. Çokaygil, Ö Onay, Characterization of pyrolytic oil obtained from pyrolysis of TDF (Tire Derived Fuel), Energy Conversion and Management. 62 (2012) 22-30.

[9] A. Zabaniotou, P. Madau, P.D. Oudenne, C.G. Jung, M.-. Delplancke, A. Fontana, Active carbon production from used tire in two-stage procedure: industrial pyrolysis and bench scale activation with H2O–CO2 mixture, J. Anal. Appl. Pyrolysis. 72 (2004) 289-297.

[10] H. Aydın, C. İlkılıç, Optimization of fuel production from waste vehicle tires by pyrolysis and resembling to diesel fuel by various desulfurization methods, Fuel. 102 (2012) 605-612.

[11] C. İlkılıç, H. Aydın, Fuel production from waste vehicle tires by catalytic pyrolysis and its application in a diesel engine, Fuel Process Technol. 92 (2011) 1129-1135.

[12] M. Rofiqul Islam, H. Haniu, M. Rafiqul Alam Beg, Liquid fuels and chemicals from pyrolysis of motorcycle tire waste: Product yields, compositions and related properties, Fuel. 87 (2008) 3112-3122.

[13] S. Murugan, M.C. Ramaswamy, G. Nagarajan, Performance, emission and combustion studies of a DI diesel engine using Distilled Tyre pyrolysis oil-diesel blends, Fuel Process Technol. 89 (2008) 152-159.

[14] N.M. Mkhize, P. van der Gryp, B. Danon, J.F. Görgens, Effect of temperature and heating rate on limonene production from waste tyre pyrolysis, J. Anal. Appl. Pyrolysis. 120 (2016) 314-320.

[15] J.H. Chen, K.S. Chen, L.Y. Tong, On the pyrolysis kinetics of scrap automotive tires, J. Hazard. Mater. 84 (2001) 43-55.

[16] H.L. Friedman, Kinetics of thermal degradation of char-forming plastics from thermogravimetry. Application to a phenolic plastic, Journal of polymer science part C: Symposia. 6 (1964) 183-195.

[17] H.E. Kissinger, Reaction kinetics in differential thermal analysis, Analytical Chemistry. 27 (1957) 1702-1706.

[18] O. Senneca, P. Salatino, R. Chirone, A fast heating-rate thermogravimetric study of the pyrolysis of scrap tyres, Fuel. 78 (1999) 1575-1581.

[19] K.-. Lam, C.-. Lee, C.-. Hui, Multi-stage waste tyre pyrolysis: An optimisation approach, Chemical Engineering Transactions. 21 (2010) 853-858.

[20] K. Cheung, K. Lee, K. Lam, T. Chan, C. Lee, C. Hui, Operation strategy for multi-stage pyrolysis, J. Anal. Appl. Pyrolysis. 91 (2011) 165-182.

[21] B. Danon, N.M. Mkhize, P. Van Der Gryp, J.F. Görgens, Combined model-free and model-based devolatilisation kinetics of tyre rubbers, Thermochimica Acta. 601 (2015) 45-53.

[22] S. Seidelt, M. Müller-Hagedorn, H. Bockhorn, Description of tire pyrolysis by thermal degradation behaviour of main components, J. Anal. Appl. Pyrolysis. 75 (2006) 11-18.

[23] M. Olazar, G. Lopez, M. Arabiourrutia, G. Elordi, R. Aguado, J. Bilbao, Kinetic modelling of tyre pyrolysis in a conical spouted bed reactor, J. Anal. Appl. Pyrolysis. 81 (2008) 127-132.

[24] R. Aguado, M. Olazar, D. Vélez, M. Arabiourrutia, J. Bilbao, Kinetics of scrap tyre pyrolysis under fast heating conditions, J. Anal. Appl. Pyrolysis. 73 (2005) 290-298.

[25] D.Y.C. Leung, C.L. Wang, Kinetic study of scrap tyre pyrolysis and combustion, J. Anal. Appl. Pyrolysis. 45 (1998) 153-169.

[26] B. Danon, P. Van Der Gryp, C.E. Schwarz, J.F. Görgens, A review of dipentene (dl-limonene) production from waste tire pyrolysis, J. Anal. Appl. Pyrolysis. 112 (2015) 1-13.

[27] J.M. Criado, Kinetic analysis of DTG data from master curves, Thermochimica Acta. 24 (1978) 186-189.

[28] L.A. Pérez-Maqueda, A. Ortega, J.M. Criado, The use of master plots for discriminating the kinetic model of solid state reactions from a single constant-rate thermal analysis (CRTA) experiment, Thermochimica Acta. 277 (1996) 165-173.

[29] B. Danon, J. Görgens, Determining rubber composition of waste tyres using devolatilisation kinetics, Thermochimica Acta. 621 (2015) 56-60.

[30] S. Stein, NIST Chemistry WebBook, No 69, NIST Standard Reference Database, 2015 (2015).

[31] R. Capart, L. Khezami, A.K. Burnham, Assessment of various kinetic models for the pyrolysis of a microgranular cellulose, Thermochimica Acta. 417 (2004) 79-89.

[32] N.M. Mkhize, B. Danon, P. van der Gryp, J.F. Görgens, Condensation of the hot volatiles from waste tyre pyrolysis by quenching, J. Anal. Appl. Pyrolysis. 124 (2017) 180-185.

CHAPTER 6. CONDENSATION OF THE HOT VOLATILES FROM WASTE TYRE PYROLYSIS BY QUENCHING

Published research paper

Title: Condensation of the hot volatiles from waste tyre pyrolysis by quenching

Journal: Journal of analytical and applied pyrolysis

Issue: 124

Pages: 180 – 185

Short summary

Objective 3 which aims at devising novel methods of cooling and condensing hot volatiles in order to maximise DL-limonene production from waste tyres pyrolysis is presented in this chapter. In the current chapter objectives 1 and 2 which are to establish the optimum operating conditions in the reactor and kinetic mechanism to maximise DL-limonene production are expanded through condensation of the direct contact between the hot volatiles and cooling fluid, i.e., quenching condensation. The effect of exchanging the tube-and-shell condenser with the quenching condenser on the total TDO yield and DL-limonene yield and content in TDO was significant. Quenching condenser improved both TDO and DL-limonene yield. Due to relatively high performance of the quenching condenser, additional benefits, such as, reduction of heteroatom compounds (mainly benzothiazole) content in the was also significant. The current chapter allowed treatment of the hot volatiles from pyrolysis reactor as they are cooled and condensed to TDO, which has not been significantly considered in the most waste tyre pyrolysis studies.

Declaration by the candidate:

With regard to CHAPTER 6, pages 101 – 116, the nature and scope of my contribution were as follows:

Nature of contribution	**Extent of contribution (%)**
Planning of the experiments	70
Execution of the experiments	80
Interpretation of the results	70
Compilation of the chapter	100

The following co-authors have contributed to CHAPTER 6, pages 101 – 116:

Name	**e-mail address**	**Nature of contribution**	**Extent of contribution (%)**
Bart Danon	bdanon@sun.ac.za	Planning of the experiments	20
		Execution of the experiments	20
		Interpretation of the results	30
		Revision of the chapter	80
Percy van der Gryp	pvdg@sun.ac.za	Planning of the experiments	5
		Revision of the chapter	10
Johann Gorgens	jgorgens@sun.ac.za	Planning of the experiments	5
		Revision of the chapter	10

Signature of candidate…….

Date…….

Declaration by the co-authors:

The undersigned hereby confirm that

1. the declaration above accurately reflects the nature and extent of the contributions of the candidate and the co-authors to CHAPTER 6, pages 101 – 116,
2. no other authors contributed to CHAPTER 6, pages 101 – 116 besides those specified above, and
3. potential conflicts of interest have been revealed to all interested parties and that the necessary arrangements have been made to use the material in CHAPTER 6, pages 101 – 116.

Signature	**Institutional affiliation**	**Date**
	Stellenbosch University	
	Stellenbosch University	
	Stellenbosch University	

Condensation of the hot volatiles from waste tyre pyrolysis by quenching

N. M. Mkhize, B. Danon, P. van der Gryp, J. F. Görgens*

Department of Process Engineering, Stellenbosch University, Private Bag X1, Matieland, 7602, Stellenbosch, South Africa

* Corresponding author: jgorgens@sun.ac.za

Abstract

Two techniques for cooling and condensing of the hot volatiles to produce tyre derived oil (TDO) from a waste tyre pyrolysis reactor were compared, i.e., conventional tube-and-shell heat exchanger type condensation, and quenching condensation by direct contact between the hot volatiles and quenching water. Exchanging the tube-and-shell condenser with direct quenching condensation increased the total TDO yield. Additionally, application of the quenching condenser increased the L- and D-isomers of limonene (DL-limonene) yield from 7.6 to 7.9 wt.%, while the benzothiazole concentration (a sulphurous and nitrogenous compound) in the TDO was decreased by 60 %. The optimal operating conditions for quenching condensation were a quenching water volume of 2.1 L (a 50:1 weight of water to weight of tyre crumb ratio) and a spraying flow rate of 0.96 L/min. Additionally, the quenching condenser unit worked as a gas cleaner by wetting and trapping soot and fine solids from the permanent gases.

6.1 Introduction

High content of carbon and hydrogen elements in waste tyre results in its pyrolysis being a potential means to produce energy, materials and chemicals [1]. Waste tyre pyrolysis is the thermal devolatilisation of the organic compounds present in the waste tyre under inert conditions to produce gaseous, liquid and solid products. Among the three products from waste tyre pyrolysis, i.e., (pyro) gas, tyre derived oil (TDO) and (pyro) char, TDO is potentially the most valuable fraction, since it can be used for both energy recovery and for the recovery of valuable chemical products (e.g. dipentene or DL-limonene) [2]. In order to maximise economic potential of the TDO, the valuable chemicals concentration should be maximised, while the concentration of the heteroatom compounds (nitrogen, oxygen and sulphur containing) should be as low as possible to use the TDO as a fuel.

The quality of the TDO, which is generally low compared to diesel fuels, is typically influenced by the techniques used to cool and condense the hot volatiles from the pyrolysis reactor. The conventional technique for condensation consists of a tube-and-shell type heat exchangers connected in series

(condensation train) as the primary unit for gas cooling and condensing [3-6]. Using a tube-and-shell heat exchanger to cool and condense the hot volatiles from the pyrolysis reactor results in a TDO that has high amounts of nitrogenous (1.35 wt.%) and sulphurous (0.89 wt.%) compounds [7,8]. These compounds are products of the thermal devolatilisation of processing additives (mostly benzothiazole) and sulphur-containing vulcanisation agents used in the tyre formulation/manufacturing [7,9]. In addition, TDO typically contains char, sand and alkali metals as well as tar and polymers in the form of gumming materials [10]. Therefore, TDO typically has a higher viscosity and sulphur content compared to conventional fuels [11]. Moreover, nitrogenous compounds in the TDO are undesirable because during refining to higher quality fuels, these compounds may poison catalysts and promote gum formation [7,12]. Viscosity and sulphur content of the TDO influences the combustion efficiency and emissions, respectively [13]. Finally, the presence of polymers, tars and solid particles in the TDO may cause formation of deposits in the liquid fuel injection system.

The quality of crude TDO can be improved through various modification methods, such as, i) removal of moisture, ii) desulphurisation, and iii) distillation [13-16]. Murugan et al. (2008) upgraded TDO by firstly evaporating moisture, followed by desulphurisation through addition of hydrosulphuric acid, and finally by distillation, resulting in an improved TDO with a higher calorific value [17]. Lopez et al. (2011) used distillation simulations to propose a method to reduce the sulphur content of the TDO [18]. Chen et al. (2010) reported that TDO contains heteroatom compounds, such as, alkyl benzothiaphene and a variety of sulphoxides and sulphones compounds [12]. They also observed sulphur removal from TDO with an efficiency of 80 % when using solvent extraction with acetonitrile as the polar solvent. Conversely, Murena (2000) observed that only about 1 % of the sulphur originally included in the tyre, was detected in the TDO [19]. They assumed that the remaining sulphur evolves as H_2S in the (pyro) gas phase. Some other techniques for TDO desulphurisation include i) catalytic pyrolysis, ii) hydrogenative pyrolysis, iii) ultrasound-assisted oxidative desulphurisation, and iv) solid adsorption [12,15,19]. However, the chemical composition of the TDO is typically complex, consisting of a plethora of compounds. For example, benzothiazole was reported as the main heteroatom compound (2.28 wt.%) in TDO by Frigo et al. (2014) [20]. Therefore, a TDO with lower concentration of heteroatom compounds is highly desirable.

Nevertheless, upgraded crude TDO cannot commercially compete with petroleum-derived fuels at current relatively low oil prices [21]. To improve the competitiveness of the TDO as a fuel, many researchers are investigating novel methods to maximising valuable chemicals (e.g. DL-limonene) recovery from TDO, and then use the remaining TDO as a fuel [22-25]. DL-limonene is a valuable chemical in the TDO, with an

estimated price of around 2 US$ /kg) [2]. Therefore, DL-limonene yield and concentration in the TDO should be maximised.

The objective of the present study is to investigate the effect of replacing a conventional tube-and-shell heat exchanger for condensation of hot volatiles from the pyrolysis reactor, with quenching condensation. The impact on total TDO yield, DL-limonene yield and concentration, and benzothiazole concentration in the TDO will be considered. The present study focuses on water as a quenching fluid, as it is a relatively cheap, readily available and good medium for energy transfer (cooling of hot volatiles). Moreover, the effect of the amount of quenching water used and the rate of spraying will be investigated.

6.2 Methodology

Waste tyre crumb (steel- and fabric-free) with particle size ranging between 2.8 and 3.4 mm were isolated by sieving from a bulk sample (500 kg), consisting of up to 5 mm particle size and supplied by a local waste tyre recycler. The waste tyre crumb was similar to feedstock used previously for pyrolysis process development [26]. Proximate analysis was conducted using a slightly adjusted version of ASTM E1131 – 08 (with X = 275 °C) [26]. The results of the proximate analysis are shown in Table 6.1.

Table 6.1: Proximate analysis of the crumb.

Proximate analysis (wt.%)	Moisture	Oils	Volatile matter	Fixed carbon	Ash
	0.6	5.6	56.0	30.0	7.8

A sample size of 40 g waste tyre crumb was fed in the pyrolysis reactor. The preferred operational conditions, suitable for a maximum DL-limonene e yield in the TDO, were similar to those established from previous work, i.e., a final pyrolysis temperature of 475 °C, a heating rate of 20 °C/min, and a pyrolysis time of 60 min [26]. The hot volatiles were purged out from the reactor with nitrogen gas (99.5 % purity, Afrox, South Africa) at a constant flow rate of 1 NL/min. The same operating conditions were applied to the two different condensation units, in order to determine the effect of those units.

Two types of condensation units, i.e., a tube-and-shell heat exchanger condensation train and a water quenching direct-contact condenser, were compared for cooling and condensation of the hot volatiles from the pyrolysis reactor. Each condensation unit was connected to the horizontal (850 mm long, 60 mm OD) quartz tube pyrolysis reactor. The source of heat in the pyrolysis reactor furnace consisted of six well-insulated heating elements. The pyrolysis reactor, as connected to the tube-and-shell heat exchanger type condensation train, is shown in Figure 6.1. The tube-and-shell condensation train consisted of five tube-

and-shell heat exchangers each maintained at a pre-determined temperature. The first condenser was maintained at ambient temperature. The subsequent condensers (two to five) were maintained at a temperature of – 10 °C using ice-dry ice slurries. Similar to the conventional tube-and-shell heat exchanger condenser, the hot volatiles were cooled and condensed to yield the TDO without physical contact with the cooling fluid.

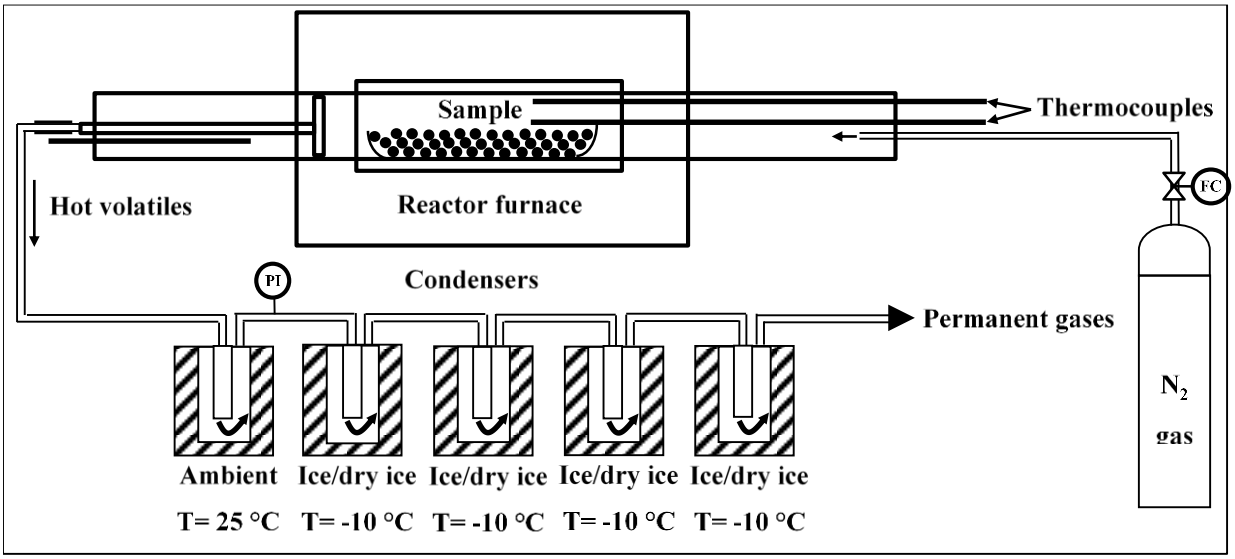

Figure 6.1: Schematic diagram of the experimental setup with tube-and-shell heat exchanger type condensation train.

The pyrolysis reactor connected to the quenching condenser is presented in Figure 6.2. The quenching condenser tower replaces the tube-and-shell heat exchangers. Quencher condensation entails direct contact of the hot volatiles from the pyrolysis reactor with the quenching liquid, which is injected through a spraying nozzle. The hot volatiles from the pyrolysis reactor are introduced at the lower half of the quenching tower through the inlet pipe connected to the pyrolysis reactor. This pipe is maintained at a temperature of 200 °C, to prevent condensation of the hot volatiles. The quenching liquid was demineralised water, introduced at the top of the quenching tower using a spraying nozzle. The nozzle is a standard type, 0.635 cm NPT removable cap male made from stainless steel (316SS) (Spraying Systems Company, South Africa). The nozzle is designed to form a full cone-spray profile covering the whole cross-sectional area of the quenching tower, to maximise contact between quenching water spray and the hot volatiles that rise in the quenching tower.

Condensable gases condensed to yield TDO when contacted with the quenching water spray. A mixture of the TDO and quenching water is collected in the TDO/quenching water collecting tank at the bottom of the

quenching tower. The two fluids are immiscible, complete separation was achieved by leaving the products for 12 hours and was then separated using a separation funnel. The permanent gases exit the quenching tower via the top exit point above the nozzle and were not analysed.

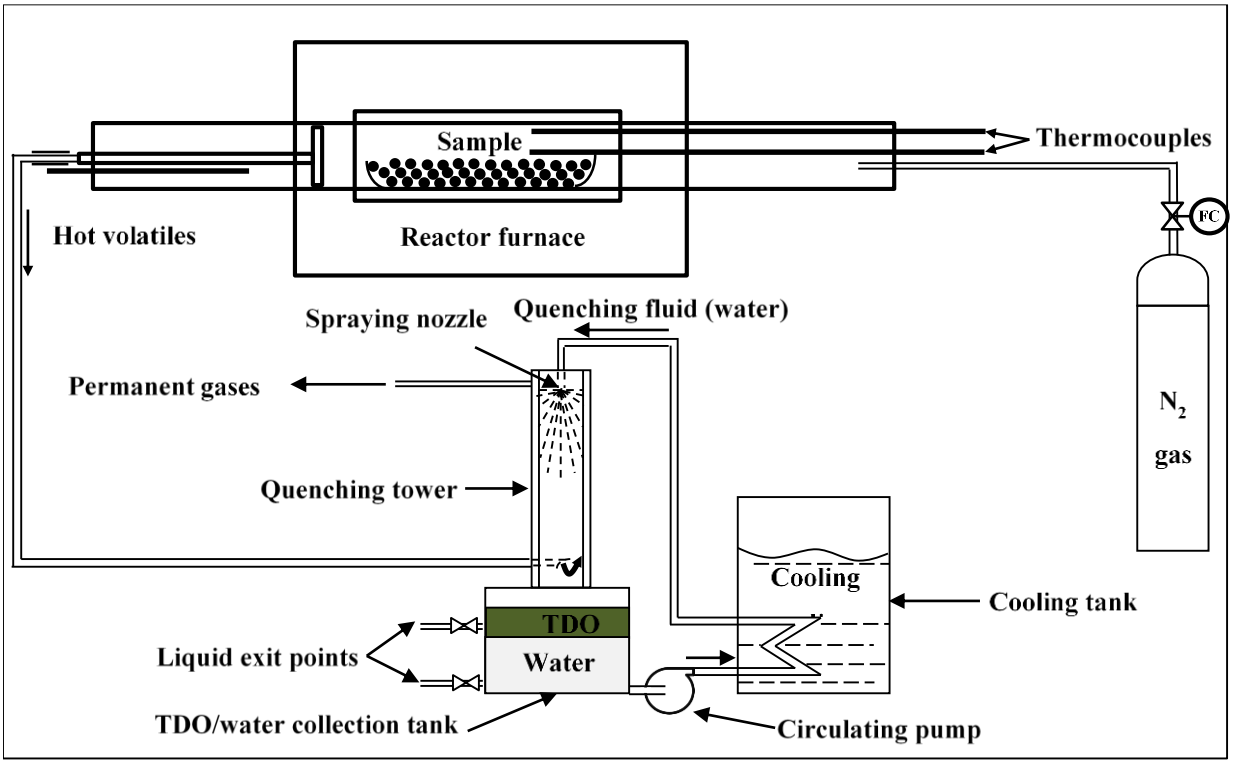

Figure 6.2: Schematic diagram of the experimental setup with water quenching condenser.

A known volume of quenching water was continuously circulated between the TDO/quenching water tank (TDO floats on the water) and the quenching tower, by withdrawing water from the bottom of the tank at a known flow rate using a pump. The pump continuously circulates quenching water through a heat removal unit (cooling tank) to lower the temperature of the quenching water before being fed back into the quenching tower. The cooling medium in the cooling tank was ice-water slurry. The cycle continues until pyrolysis is complete, with both the amount of water circulated and the flow rate of circulation being variables for optimisation. These factors were optimised for quenching prior to comparison of this technique to the conventional shell-and-tube condensation. The design and response factors used to determine the effect of total quenching water volume and quenching water spraying rate on the TDO chemical composition using a Central Composite Design (CCD) statistical method are summarised in Table 6.2. The selected ranges and centre points of the input variables were based on the operability range of the quencher unit (maximum volume capacity of 4 L and maximum nozzle spraying rate of 1 L/min). A response surface model was

fitted to determine optimal operating conditions to maximise DL-limonene yield and concentration in the TDO and minimise benzothiazole concentration in the TDO.

Table 6.2: Central composite design (CCD) factors.

Factor	Unit	Factor type	Lower level (–)	Centre point (0)	Upper level(+)	Lower axial(–δ)	Higher axial(+δ)
Temperature	°C	Constant	475	475	475	475	475
Heating rate	°C/min	Constant	20	20	20	20	20
Holding time	min	Constant	60	60	60	60	60
Particle size	mm	Constant	2.8 – 3.4	2.8 – 3.4	2.8 – 3.4	2.8 – 3.4	2.8 – 3.4
Sample amount	g	Constant	40	40	40	40	40
Water volume	l	Variable	1.2	2.1	3.0	0.83	3.37
Water flow rate	l/min	Variable	0.6	0.75	0.9	0.54	0.96
Liquid yield	wt.%	Response					
Solid yield	wt.%	Response					
Gas yield	wt.%	Response					
DL-limonene (TDO)	wt.%	Response					
DL-limonene (TDO)	ppm	Response					
Benzothiazole (TDO)	wt.%	Response					
Benzothiazole (TDO)	ppm	Response					
Water content (TDO)	wt.%	Response					

Triplicate experiments using a tube-and-shell condenser, were carried out using previously optimised pyrolysis operating conditions [26]. The char and TDO yields were determined gravimetrically, and DL-limonene and benzothiazole contents in the TDO were determined chromatographically. When the quenching condenser was used, two liquid phases, TDO (non-polar and less dense liquid containing majority of the DL-limonene) and quenching water (polar and denser liquid containing majority of the benzothiazole) were obtained from the storage tank and were separated using a separation funnel. The TDO was qualitatively and quantitatively analysed. A Hewlett Packard 5890 Series II model gas chromatography (GC) coupled with a Hewlett Packard 5973 mass spectrometry (MS) was used to analyse the TDO. A volume of 1µl mixture of the TDO, internal standards, and dichloromethane solvent (99.9% purity, Sigma Aldrich, South Africa) was injected in a 60 m x 0.18 mm ID x 0.10 µm film thickness, non-polar Rxi-5% Sil-MS capillary column. Helium gas (99.999 % purity, Air Products, South Africa) was used as a carrier gas at a constant flow rate of 1.20 ml/min (linear velocity of 27.9 cm/s) at 348 kPa. Additionally, water content was determined in all TDO samples using titration methods.

6.3 Results and discussion

The effects of the total volume of water being circulated through the quencher, as well as the spraying rate of water into the quencher, on the TDO yield, DL-limonene yield and concentration and benzothiazole concentration, are shown in Figure 3. The surface plots were obtained from statistical interpolation of the CCD experimental design, as presented in Table 6.2. Figure 6.3 a) illustrates that a slight increase in TDO yield was obtained by increasing the total volume of water circulated through the quencher, although the total increase was limited to 1 wt.%. This increase was attributed to the separability of the TDO and the quenching water. The water-to-TDO ratio was higher when a larger water volume was used. Moreover, too little quenching water resulted in insufficient cooling (a lower amount of water in the quenching tower heated up faster). A slight decrease in the gas yield, about 1 wt.%, which corresponds approximately to the TDO yield increase, was observed as the quenching water volume and quenching water spraying rate were increased. This supports the assumption that cooling of hot volatiles was insufficient when the volume of the quenching water was lower. Char yield remained unchanged at 36.4 wt.% with varying quenching water volume and quenching water spraying rate.

The highest DL-limonene yield of 7.9 wt.% was obtained by circulating 2.1 L of quenching water through the quencher at a spraying rate of 0.96 L/min (Figure 6.3 b). Operating the quenching unit at the quenching water volume of 3.37 L and quenching water spraying rate of 0.75 L/min resulted in the lowest DL-limonene yield at 6.9 wt.%. This observation can be attributed to excessive quenching water resulting to lower DL-limonene recovery. Too little quenching water resulted in insufficient cooling as well as poor separation of DL-limonene from the quenching water. Similar trends of the effect of quenching water volume and quenching water spraying rate on the concentration of the DL-limonene in the TDO were observed, Figure 6.3 c). Additionally, a higher TDO yield results in DL-limonene dilution, therefore, lower DL-limonene concentrations in the TDO.

The benzothiazole concentration in the TDO varied with quenching water volume and spraying rate, see Figure 6.3 d). TDO with low benzothiazole concentration was observed at a quenching volume of 2.1 L and spraying rate of 0.75 L/min. Higher benzothiazole content in the TDO at both lower quenching water volumes and spraying rates can be attributed to insufficient water to extract the benzothiazole from the hot volatiles into the quenching water. At higher quenching water volume and spraying rate, benzothiazole concentration in the TDO was surprisingly higher. This can be attributed to the negative effect of a lower temperature of the quenching water on the solubility (in terms of equilibrium) of benzothiazole.

Therefore, optimal operating conditions of the quenching condenser were selected at a quenching water volume of 2.1 L and quenching water spraying rate of 0.96 L/min. At these operating conditions, DL-limonene yield and benzothiazole concentration are at a maximum and a minimum, respectively. Since DL-limonene is a valuable chemical and benzothiazole is undesirable in the TDO, this support the choice of optimal operating conditions of the quencher.

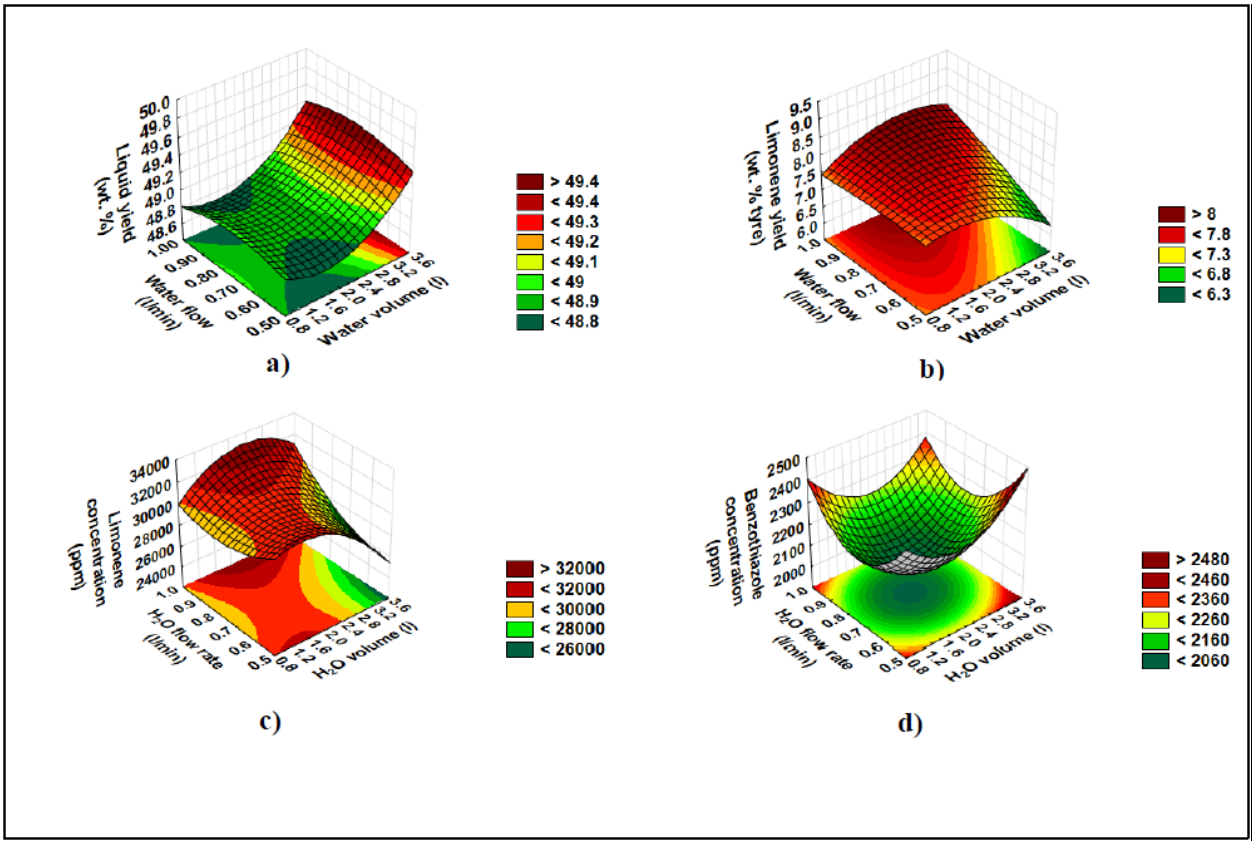

Figure 6.3: Effect of the quenching water volume and spraying flow rate on a) total liquid yield, b) DL-limonene yield, c) DL-limonene concentration and d) benzothiazole concentration in the TDO.

The results of the shell-and-tube condenser and the water quencher (with a quenching water volume of 2.1 L and spray flow of 9.96 L/min), both coupled to waste tyre crumb pyrolysis at a temperature of 475 °C and heating rate 20 °C/min, are presented in Table 6.3. Quenching condensation improved the total TDO yield from 46.6 wt.% (tube-and-shell heat exchanger) to 48.9 wt.%. The DL-limonene yield in the TDO from quenching condensation was higher at 7.9 wt.%, compared to 7.6 wt.% with the tube-and-shell heat exchanger. Benzothiazole concentration decreased by 60 % (from 5 382 to 2 168 ppm) when the shell-and-tube condensation train was replaced by quenching condensation. The effectiveness of the quencher to reduce benzothiazole, as a major sulphurous and nitrogenous compound in the TDO, was comparable to

conventional post-treatment desulphurisation techniques that are potentially complex and/or costly. Lopez et al. (2011) reduced sulphur content of the TDO to 0.58 wt.% from 1.4 wt.% when a filter system was used. Chen et al. (2010) observed a desulphurisation efficiency of 89 % with two ultrasound-assisted oxidative desulphurisation units connected in series combined with solid adsorption over Al_2O_3.

Table 6.3: Properties of the products from waste tyre pyrolysis with condensation train and quenching condenser.

Process	Parameters	Type of condensation	
		Condensation train	Quenching condenser
Waste tyre pyrolysis	Temperature (°C)	475	475
	Heating rate (°C/min)	20	20
Quenching condensation	Cooling water (l)	–	2.10
	Water spray flow (l/min)	–	0.96
Main products yield	Tyre derived oil TDO (wt.%)	46.6	48.9
	Solid residue or char (wt.%)	35.7	36.4
	Permanent gases (wt.%)	17.7	14.7
Organic phase (TDO)	DL-limonene concentration (wt.%)	7.6	7.9
	DL-limonene concentration (ppm)	28 178	31 990
	Benzothiazole (wt.%)	1.5	0.7
	Benzothiazole (ppm)	5 382	2 168
	Water content (wt. %)	0.7	0.3

The increase in total TDO yield due to quenching condensation was attributed to rapid and efficient cooling and condensation of the hot volatiles through direct contact with the quenching water. The increase in the rate of cooling and condensation due to quenching had a similar positive effect on the DL-limonene yield. Rapid cooling and condensation of DL-limonene reduced degradation of DL-limonene due to shorter residence times of the hot volatiles when the quenching condenser is used compared to longer residence time with the tube-and-shell condenser [27]. Highly volatile condensable compounds (with boiling points around room temperature and are therefore difficult to condense) were condensed when the more efficient quencher was used, which by direct contact and more efficient capture of these compounds contributed to the total TDO yield increase. Furthermore, a decrease in benzothiazole concentration is attributed to the fact that water and benzothiazole are highly polar compared to DL-limonene and all other major components of the TDO. The benzothiazole is thus effectively extracted from the hot volatiles (and TDO) into the quenching water during cooling and condensation. Separation of the majority of benzothiazole from the TDO resulted in a higher quality TDO for fuel applications, e.g., less nitrogenous, oxygenous or sulphurous compounds.

Moreover, benzothiazole devolatilises at lower temperatures than the polymeric matter [28]. During a batch pyrolysis process, as applied in the present study, the earlier devolatilisation of the benzothiazole results in a type of 'stepwise' devolatilisation process; the concentration of benzothiazole is relatively high in the hot volatiles from the reactor entering the quenching condenser at lower pyrolysis temperatures, resulting in more efficient extraction of the benzothiazole. Illustrated in Figure 6.4 is the effect of temperature and heating rate on the yield of benzothiazole in the TDO. Chromatographic comparison of the TDOs from the condensation train and the quenching condenser showed similar trends for other heteroatom compounds, i.e., thiophene isomers (3-methyl thiophene), phenols (3-methyl phenol), and quinoline isomers (2,4-dimethylquinoline). The concentrations of these compounds in the TDO decreased by 50 to 60 % by using quenching condensation.

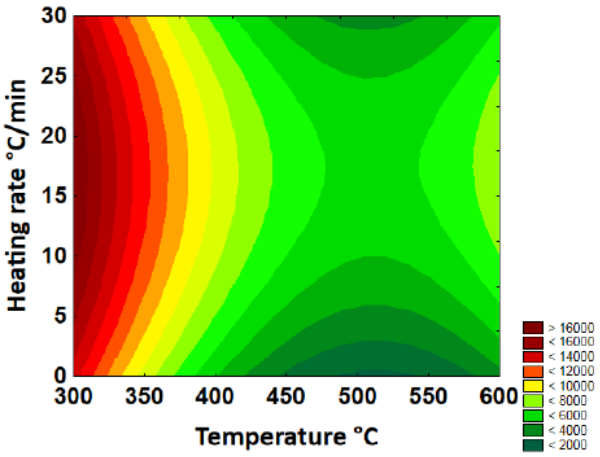

Figure 6.4: Effect of both temperature and heating rate on benzothiazole concentration in the TDO.

Finally, it is also evident that the two liquids (TDO and quenching water) separated well, which was observed from the low water content in the TDO from the quenching condenser (0.3 wt.%). This water content in the TDO from the quenching condenser is even lower than that of the TDO from the condensation train (the latter being 0.7 wt.%). Moreover, the quenching condenser unit can work as a gas cleaner and potentially eliminates solid residues from the TDO by wetting and trapping soot and fine solid particles from the hot volatiles.

6.4 Conclusions

Quenching condensation increased the total TDO yield due to direct contact between the hot volatiles from the pyrolysis reactor and the quenching water (resulting in efficient cooling and condensation), compared to a conventional tube-and-shell heat exchanger condensation train. Rapid condensation of hot volatiles

with the quenching condenser also improved the DL-limonene yield in the TDO. On the other hand, benzothiazole (a nitrogen- and sulphur-containing compound) concentration in the TDO was reduced when the quenching condenser was used. Since water and benzothiazole are highly polar compared to the DL-limonene and the majority of the compounds in the TDO, benzothiazole was separated from the TDO. Application of the quenching condenser on industrial-scale seems to be promising, but additional larger-scale experiments will be required to confirm this. Moreover, as benzothiazole is an important ingredient in the tyre manufacturing process, it can be potentially recovered from the used quenching water to improve the feasibility of quenching condensation for the pyrolysis of waste tyres.

Acknowledgements

This research was supported by the Recycling and Economic Development Initiative of South Africa (REDISA) and the National Research Foundation (NRF). The authors acknowledge that opinions, findings and conclusions or recommendations expressed are those of the authors only, and the sponsors accept no liability whatsoever in this regard.

References

[1] I. Hita, M. Arabiourrutia, M. Olazar, J. Bilbao, J.M. Arandes, P. Castaño, Opportunities and barriers for producing high quality fuels from the pyrolysis of scrap tires, Renewable and Sustainable Energy Reviews. 56 (2016) 745-759.

[2] B. Danon, P. Van Der Gryp, C.E. Schwarz, J.F. Görgens, A review of dipentene (dl-limonene) production from waste tire pyrolysis, J. Anal. Appl. Pyrolysis. 112 (2015) 1-13.

[3] P.T. Williams, A.J. Brindle, Fluidised bed pyrolysis and catalytic prolysis of scrap tyres, Environmental Technology. 24 (2003) 921-929.

[4] M. Kyari, A. Cunliffe, P.T. Williams, Characterization of oils, gases, and char in relation to the pyrolysis of different brands of scrap automotive tires, Energy Fuels. 19 (2005) 1165-1173.

[5] M.F. Laresgoiti, B.M. Caballero, I. de Marco, A. Torres, M.A. Cabrero, M.J. Chomón, Characterization of the liquid products obtained in tyre pyrolysis, J. Anal. Appl. Pyrolysis. 71 (2004) 917-934.

[6] Y. Kar, Catalytic pyrolysis of car tire waste using expanded perlite, Waste Manage. 31 (2011) 1772-1782.

[7] S. Mirmiran, H. Pakdel, C. Roy, Characterization of used tire vacuum pyrolysis oil: Nitrogenous compounds from the naphtha fraction, J. Anal. Appl. Pyrolysis. 22 (1992) 205-215.

[8] I. de Marco Rodriguez, M.F. Laresgoiti, M.A. Cabrero, A. Torres, M.J. Chomón, B. Caballero, Pyrolysis of scrap tyres, Fuel Process Technol. 72 (2001) 9-22.

[9] S. Murugan, M.C. Ramaswamy, G. Nagarajan, Assessment of pyrolysis oil as an energy source for diesel engines, Fuel Process Technol. 90 (2009) 67-74.

[10] A.A. Zabaniotou, G. Stavropoulos, Pyrolysis of used automobile tires and residual char utilization, J. Anal. Appl. Pyrolysis. 70 (2003) 711-722.

[11] S. Murugan, M.C. Ramaswamy, G. Nagarajan, The use of tyre pyrolysis oil in diesel engines, Waste Manage. 28 (2008) 2743-2749.

[12] X. Chen, G. Clet, K. Thomas, M. Houalla, Correlation between structure, acidity and catalytic performance of WOx/Al2O3 catalysts, Journal of Catalysis. 273 (2010) 236-244.

[13] S. Murugan, M.C. Ramaswamy, G. Nagarajan, Performance, emission and combustion studies of a DI diesel engine using Distilled Tyre pyrolysis oil-diesel blends, Fuel Process Technol. 89 (2008) 152-159.

[14] H. Aydın, C. İlkılıç, Optimization of fuel production from waste vehicle tires by pyrolysis and resembling to diesel fuel by various desulfurization methods, Fuel. 102 (2012) 605-612.

[15] C. İlkılıç, H. Aydın, Fuel production from waste vehicle tires by catalytic pyrolysis and its application in a diesel engine, Fuel Process Technol. 92 (2011) 1129-1135.

[16] M. Rofiqul Islam, H. Haniu, M. Rafiqul Alam Beg, Liquid fuels and chemicals from pyrolysis of motorcycle tire waste: Product yields, compositions and related properties, Fuel. 87 (2008) 3112-3122.

[17] S. Murugan, M.C. Ramaswamy, G. Nagarajan, A comparative study on the performance, emission and combustion studies of a DI diesel engine using distilled tyre pyrolysis oil–diesel blends, Fuel. 87 (2008) 2111-2121.

[18] F.A. López, T.A. Centeno, F.J. Alguacil, B. Lobato, Distillation of granulated scrap tires in a pilot plant, J. Hazard. Mater. 190 (2011) 285-292.

[19] F. Murena, Kinetics of sulphur compounds in waste tyres pyrolysis, J. Anal. Appl. Pyrolysis. 56 (2000) 195-205.

[20] S. Frigo, M. Seggiani, M. Puccini, S. Vitolo, Liquid fuel production from waste tyre pyrolysis and its utilisation in a Diesel engine, Fuel. 116 (2014) 399-408.

[21] J.D. Martínez, N. Puy, R. Murillo, T. García, M.V. Navarro, A.M. Mastral, Waste tyre pyrolysis – A review, Renewable and Sustainable Energy Reviews. 23 (2013) 179-213.

[22] J.D. Martínez, M. Lapuerta, R. García-Contreras, R. Murillo, T. García, Fuel properties of tire pyrolysis liquid and its blends with diesel fuel, Energy and Fuels. 27 (2013) 3296-3305.

[23] N. Antoniou, A. Zabaniotou, Features of an efficient and environmentally attractive used tyres pyrolysis with energy and material recovery, Renewable and Sustainable Energy Reviews. 20 (2013) 539-558.

[24] P.T. Williams, Pyrolysis of waste tyres: A review, Waste Manage. 33 (2013) 1714-1728.

[25] A. Quek, R. Balasubramanian, Liquefaction of waste tires by pyrolysis for oil and chemicals—A review, J. Anal. Appl. Pyrolysis. 101 (2013) 1-16.

[26] N.M. Mkhize, P. van der Gryp, B. Danon, J.F. Görgens, Effect of temperature and heating rate on limonene production from waste tyre pyrolysis, J. Anal. Appl. Pyrolysis. 120 (2016) 314-320.

[27] A.M. Cunliffe, P.T. Williams, Composition of oils derived from the batch pyrolysis of tyres, J. Anal. Appl. Pyrolysis. 44 (1998) 131-152.

[28] O. Senneca, P. Salatino, R. Chirone, A fast heating-rate thermogravimetric study of the pyrolysis of scrap tyres, Fuel. 78 (1999) 1575-1581.

CHAPTER 7. VARIOUS MEANS OF WASTE TYRE PYROLYSIS TO MAXIMISE DL-LIMONENE PRODUCTION

Manuscript

Title: Effect of direct contact between the hot volatiles and cooling water in the flash pyrolysis of the waste tyres

Targeted journal: Fuel processing technology

Issue: xxx

Pages: xxx - xxx

Short summary

So far, the findings reported are based on the work carried out in a fixed bed reactor (FBR). The quenching condenser is undoubtedly efficient in cooling and condensing the hot volatiles from waste tyre pyrolysis reactor. The question remains, however, how the quenching condenser will perform under operating conditions different from those in the FBR. A further investigation on the condensation type and cooling rate of the hot volatiles was carried out under conditions characterised by flash heating of the waste tyre crumb, and relative shorter hot volatiles residence times in the hot reaction zones. In order to achieve these pyrolysis operating conditions, a bubbling fluidised bed reactor (BFBR) was used. In addition, a handful of experiments were carried out in a conical spouted bed reactor (CSBR), Basque Country, Spain, using the same tyre crumb type and size as in the FBR and BFBR which resulted to two collaborative paper publications, i.e., sections 10.2 and 10.3. Therefore, TDO from CSBR was analysed using similar method to FBR and BFBR methods and the results were incorporated in present chapter.

In the current chapter (CHAPTER 7), objective 4 is elaborated and the findings from CHAPTER 6 and section 10.1 are further assessed. In section 10.1, in the patent it was observed that in addition to the novelty and innovative from the quenching condenser, applicability and simplicity of the quenching condenser are some of the additional favourable features. Scalability of the quenching condenser is partly examined through various adjustments, i.e., tyre crumb feed, quenching water volume, and quenching water flow rate

ratios are 1:5 (40 g in the FBR, 200 g in the BFBR), 1:6 (2.1 L in the FBR, 14 L in the BFBR), and 1:4 (0.96 L/min in the FBR, 4 L/min in the BFBR), respectively. Finally, the performance of the FBR, BFBR and CSBR each augmented with a tube-and-shell condenser as well as FBR and BFBR each augmented with a quenching condenser are compared.

Exchanging the tube-and-shell condenser with the quenching condenser in both the FBR and BFBR improved the TDO yield and quality (high DL-limonene concentration and low benzothiazole concentration) from waste tyre pyrolysis. Total TDO and DL-limonene yields increased when the FBR was exchanged with the BFBR in combination with both the tube-and-shell and quenching condenser, while benzothiazole concentration increased in the TDO from the BFBR in combination with the tube-and-shell condenser and decreased in combination with the quenching condenser. Some further increases in the TDO and DL-limonene yield, and a decrease in the benzothiazole concentration, was observed when a CSBR was used in combination with the tube-and-shell condenser. High DL-limonene concentration in the TDO indicated that the TDO has high potential of being used as a source of DL-limonene production and recovery when it is further processed. Moreover, low benzothiazole concentration in the TDO indicated that the TDO has a high potential to be further upgraded for fuels production since the TDO refining processes will be less intensive and expensive once the sulphur and nitrogen contents are reduced.

Declaration by the candidate:

With regard to CHAPTER 7, pages 117 – 137, the nature and scope of my contribution were as follows:

Nature of contribution	**Extent of contribution (%)**
Planning of the experiments	60
Execution of the experiments	70
Interpretation of the results	70
Compilation of the chapter	100

The following co-authors have contributed to CHAPTER 7, pages 117 – 137:

Name	**e-mail address**	**Nature of contribution**	**Extent of contribution (%)**
Bart Danon	bdanon@sun.ac.za	Planning of the experiments	15
		Interpretation of the results	30
		Execution of the experiments	5
		Revision of the chapter	55
Gartzen Lopez	gartzen.lopez@ehu.eus	Planning of the experiments	10
		Execution of the experiments	15
		Revision of the chapter	5
Jon Alvarez	jon.alvarezg@ehu.eus	Execution of the experiments	10
		Revision of the chapter	5
Maider Amutio	maider.amutio@ehu.es	Revision of the chapter	5
Javier Bilbao	javier.bilbaoe@ehu.es	Revision of the chapter	5
Martin Olazar	martin.olazar@ehu.es	Planning of the experiments	5
		Revision of the chapter	5
Percy van der Gryp	pvdg@sun.ac.za	Planning of the experiments	5
		Revision of the chapter	10
Johann Gorgens	jgorgens@sun.ac.za	Planning of the experiments	5
		Revision of the chapter	10

Signature of candidate……. **Date**…….

Declaration by the co-authors:

The undersigned hereby confirm that

1. the declaration above accurately reflects the nature and extent of the contributions of the candidate and the co-authors to CHAPTER 7, pages 117 – 137,
2. no other authors contributed to CHAPTER 7, pages 117 – 137 besides those specified above, and
3. potential conflicts of interest have been revealed to all interested parties and that the necessary arrangements have been made to use the material in CHAPTER 7, pages 117 – 137 of this dissertation.

Signature	**Institutional affiliation**	**Date**
	Stellenbosch University	
	University of the Basque Country	
	University of the Basque Country	
	University of the Basque Country	
	University of the Basque Country	
	University of the Basque Country	
	Stellenbosch University	
	Stellenbosch University	

Influence of reactor and condensation system design on tyre pyrolysis products yield

N. M. Mkhize[a], B. Danon[a], G. Lopez[b], J. Alvarez[b], M. Amutio[b], J. Bilbao[b], M. Olazar[b], P. van der Gryp[b], J. F. Görgens[a*]

[a]Department of Process Engineering, Stellenbosch University, Private Bag X1, Matieland, 7602, Stellenbosch, South Africa

[b]Department of Chemical Engineering, University of the Basque Country UPV/EHU, P.O. Box 644-E48080 Bilbao, Spain

* Corresponding author: jgorgens@sun.ac.za

Abstract

The current study investigates the effect of the type of pyrolysis reactor and condensing system on the total tyre derived oil (TDO) and DL-limonene yield as well as benzothiazole concentration in the TDO. The type of condensation (indirect or direct contact between the hot volatiles and cooling liquid) was achieved by exchanging between a tube-and-shell condenser and a quenching condenser. Three types of reactor have been investigated, a fixed bed reactor (FBR), a bubbling fluidised bed reactor (BFBR) and a conical spouted bed reactor (CSBR). The pyrolysis temperature in each experiment was maintained at 475 °C. The total TDO and DL-limonene yield from the BFBR was compared to the FBR. Further improvements in the TDO and DL-limonene yield were observed when the tube-and-shell condenser was exchanged with the quenching condenser for both reactors. Simultaneously, the benzothiazole concentration in the TDO decreased when the quenching condenser replaces the tube-and-shell condenser in both the FBR and BFBR. A further increase in the DL-limonene yield was observed from the CSBR compared to the BFBR when the tube-and-shell was used, while benzothiazole concentration in the TDO significantly increased. The type of condensation (exchanging the tube-and-shell condenser with a quenching condenser) mainly influences benzothiazole concentration in the TDO.

7.1 Introduction

Waste tyre pyrolysis, a thermal treatment of the waste tyres under inert conditions to yield pyro-gas, tyre derived oil (TDO) and pyro-char [1,2], is among the oldest thermal treatment methods to eliminate increasing waste tyre accumulation. Various means have been implemented to improve the pyrolysis process to be an effective elimination technique with reduced environmental emissions are reduced and improved waste tyre valorisation [3-6]. The rate by which waste tyre piles are increasing is higher than the

rate of their elimination, due to insufficient capacity of various techniques for waste tyre treatment and recycling [7-9]. This implies that waste tyre pyrolysis presents economic opportunities, in particular the TDO, which is a good source of valuable chemicals and liquid fuels, which are both possibly alternatives to petroleum-derived products. DL-Limonene, terpinolene and p-cymene are some of these valuable chemicals which can be recovered from the TDO, with the DL-limonene yield as high as 7.6 % and an estimated market price of 2 US$ /kg [10]. Upgrading the TDO into liquid fuels that have qualities comparable to the conventional petroleum-derived fuels, is also technically viable [5,6].

The yield and quality (based on the DL-limonene and heteroatomic compounds concentration) of the TDO from waste tyre pyrolysis is affected by various factors, such as the pyrolysis temperature, heating rate, residence time of the hot volatiles in the hot reaction zone, and the type of cooling and condensation of the hot volatiles. Mkhize et al. in their study of the effect of the temperature and heating rate on the DL-limonene yield from waste tyre pyrolysis, reported high DL-limonene yield (7.6 wt.%) at a temperature of 475 °C and heating rate of 20 °C/min [11] in a fixed bed reactor (FBR). A FBR is characterised by relatively lower heating rates, longer residence times of the hot volatiles in the hot reaction zone. In a subsequent study, Mkhize et al. presented the effect of a quenching condenser on the DL-limonene yield from the FBR [12]. Higher DL-limonene yield observed was probably due to the higher cooling rate when the quenching condenser was used [12].

Other pyrolysis reactors are characterised by relatively higher heating rates and shorter residence times of the hot volatiles, such as fluidised bed reactors, auger reactors as well as conical spouted bed reactors. Rapid removal of the hot volatiles was attained by Williams and Brindle in the fluidized bed reactor by employing high nitrogen gas flow rates [13]. The conical spouted bed reactor was proposed by Olazar et al., which could attain higher gas velocities, which promotes shorter residence time of the hot volatiles in the hot reaction zones [14]. Using similar tyre crumb and pyrolysis temperature (475 °C) [11,12], under high heating rate and short residence time of the hot volatiles in the hot reaction zones pyrolysis operating conditions, DL-limonene yield was 22.84 wt.% (based on GC/MS peak area) [15,16]. Moreover, in both the fluidised bed and conical spouted bed reactor the heating rates are relatively high.

Reduction of the heteroatomic compounds in the TDO, such as, benzothiazole or 2,4-dimethylquinoline, have been proposed using a combination of an auger and a fluidised bed reactors [17]. Choi et al. observed that when a two-stage pyrolysis (firstly pyrolysis in the auger reactor and then in the fluidised bed reactor) was compared to a one-stage auger reactor pyrolysis, the concentrations of heteroatomic compounds in the TDO were reduced [17]. Recently, reduction of the heteroatomic compounds concentration in the TDO was

reported by Mkhize et al. when a tube-and-shell condenser was exchanged with the quenching condenser [12].

Typical methods employed to improve the quality of the crude TDO to be suitable fuel application include, i) removal of the moisture, ii) desulphurisation, and iii) distillation [18-21]. However, these methods are mainly used during post-processing of the TDO after the pyrolysis has been completed and their combined effect is limited. Lopez et al. reduced sulphur content of the TDO to 0.58 wt.% from 1.4 wt.% when a filter system was used [22]. Chen et al. observed a desulphurisation efficiency of 89 % with two ultrasound-assisted oxidative desulphurisation units connected in series combined with solid adsorption over Al_2O_3 [23].

A waste tyre pyrolysis process aimed at improving TDO and DL-limonene yield and lower heteroatomic compounds concentration in the TDO is required. The approach in this study entails comparison of a fixed bed reactor (FBR), a bubbling fluidised bed reactor (BFBR), and a conical spouted bed reactor (CSBR), each augmented with either a tube-and-shell condenser (indirect contact between cooling liquid and hot volatiles) or a quenching condenser (direct contact between the cooling water and the hot volatiles), to investigate the effect of the reactor and condensation type on the total TDO yield, as well as the DL-limonene and benzothiazole concentrations in the TDO. The three different types of pyrolysis reactors were operated at the same temperature, fed with the same waste tyre crumb, and combined with alternative methods to condense the hot volatiles. The experimental results from the FBR have been previously published [11,12], while the experimental results from the CSBR were obtained from the TDO derived from the CSBR [15,16].

7.2 Equipment and methods

7.2.1 Waste tyre crumb

The same waste tyre crumb as used in the previous works [11,12] was used, i.e., waste truck tyre with particle size range between 2.80 to 3.30 mm sieved from a bulk of approximately 500 kg crumbed (steel- and fabric-free) waste tyre. The locally supplied waste tyre crumb was characterised by proximate analysis using a slightly adjusted version of ASTM E1131 – 08 (with X = 275 °C) [24]. Moreover, the rubber composition and thermograms of the crumb were estimated using Mettler Toledo TGA/DCS 1 thermogravimetric analyser (TGA). The results are shown in Table 7.1.

Table 7.1: Proximate analysis and rubber composition of the crumb.

Proximate analysis (wt.%)	Moisture	Oils	Volatile matter	Fixed carbon	Ash
	0.6	5.6	56.0	30.0	7.8

Rubber composition/volatile matter (wt.%)	Polyisoprene (natural rubber)	Synthetic rubber (SBR and BR)[α]
	64	36

[α]By difference, *Outstanding, still to be obtained.

7.2.2 Pyrolysis reactors and experiments

7.2.2.1 Fixed bed reactor

A sample size of 40 g waste tyre crumb was fed in a fixed bed pyrolysis reactor. The pyrolysis operating conditions are similar to those established from previous work using the same setup, see Figure 7.1 [11]. The FBR consists of a long horizontal quartz tube pyrolysis reactor (850 mm long, 60 mm OD), a heating furnace, and five tube-and-shell condensers connected in series. The pyrolysis reactor furnace is heated at a rate of 20 °C/min up to 475 °C by six well-insulated heating elements. The hot volatiles were purged out from the reactor with nitrogen gas (99.5% purity, Afrox, South Africa) at a constant flow rate of 1 NL/min resulting in a residence time of approximately 41 s.

Initially, the FBR was connected into five tube-and-shell condensers arranged in series to investigate an indirect contact between the cooling liquid and hot volatiles cooling system. The temperature in the first condenser was maintained at ambient temperature. While the temperature in the subsequent condensers (two to five) was maintained at – 10 °C using ice-dry ice slurry. The FBR connected to the tube-and-shell condensation system is shown in Figure 7.1.

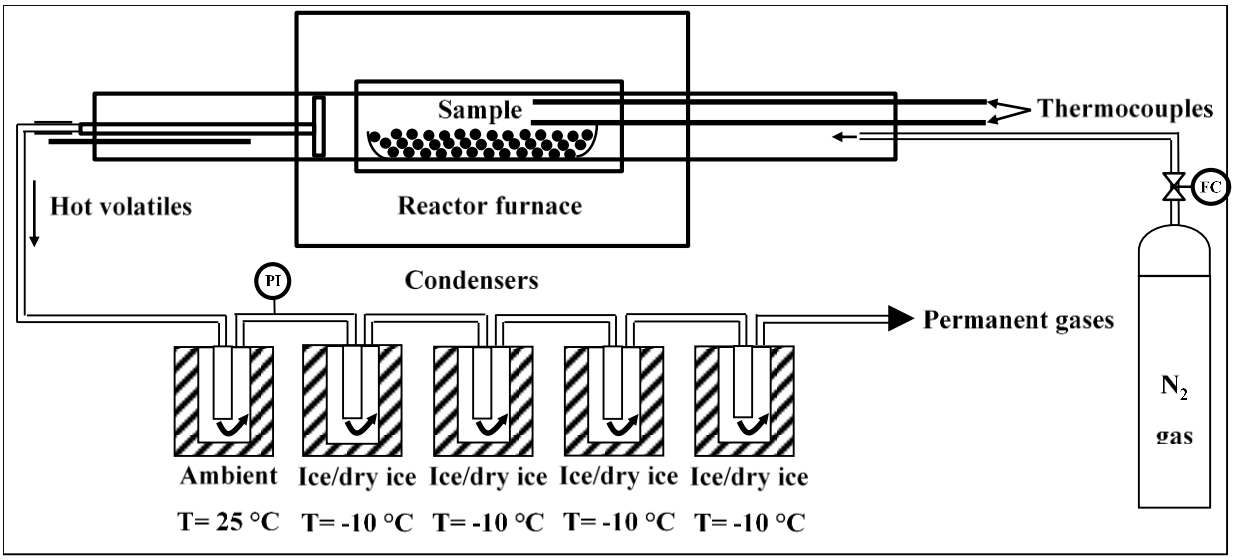

Figure 7.1: Schematic diagram of the FBR augmented with a tube-and-shell condensers experimental setup.

The same pyrolysis reactor setup illustrated in Figure 7.1 but with the tube-and-shell condensers exchanged for the quenching condenser, see Figure 7.2, was used to carry out FBR-quenching condenser experiments. The quenching liquid, is injected through a spraying nozzle. The hot volatiles from the pyrolysis reactor are introduced at the lower half of the quenching tower through the inlet pipe connected to the pyrolysis reactor. To prevent condensation of the hot volatiles before they are introduced into the quenching tower the inlet pipe is maintained at a temperature of 200 °C. Using a spraying nozzle, quenching liquid (demineralised water) was introduced at the top of the quenching tower. The nozzle, supplied by Spraying Systems Company, South Africa, is a standard type, 0.635 cm NPT removable cap male, made from stainless steel (316SS). Maximum contact between the quenching water spray and the hot volatiles that rise up ward in the quenching tower was achieved by forming a full cone-spray profile covering the whole cross-sectional area of the quenching tower. As the condensable gases are contacted with the quenching water spray, it results in the downward flow of both the condensed TDO and quenching water. A mixture of the TDO and quenching water is collected in the TDO/quenching water collecting tank at the bottom of the quenching tower. The permanent gases exit the quenching tower via the top exit point above the nozzle.

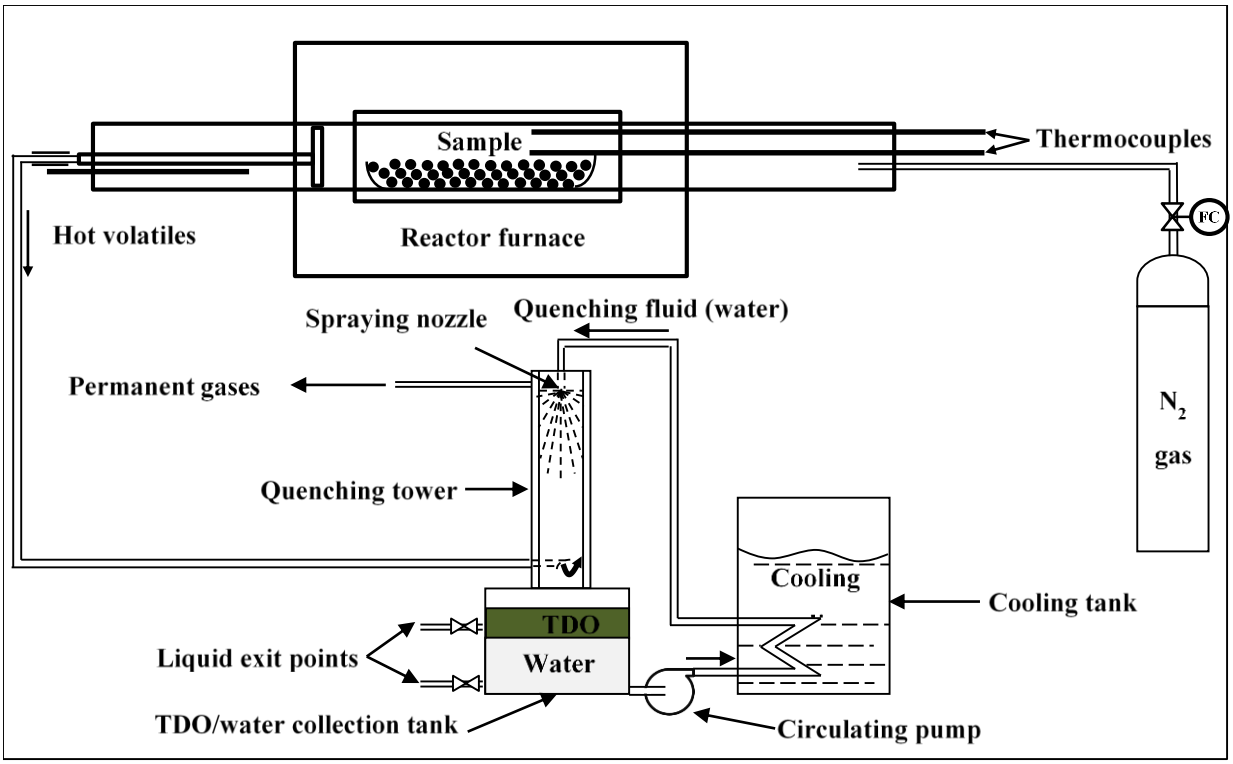

Figure 7.2: Schematic diagram of the FBR augmented with a quenching condenser experimental setup.

7.2.2.2 Bubbling fluidised bed reactor

A total sample size of 200 g waste tyre crumb was fed in the BFBR pyrolysis reactor at a feed rate of 6 g/min. The optimal pyrolysis temperature (475 °) was determined from previous work [11]. The BFBR consists of, i) the feeding system, ii) the reactor, and iii) the char separation system, see Figure 7.3. In the feeding system, the tyre crumb is initially loaded in the hopper, then fed in the reactor using a screw feeder. The hopper is slightly over pressurised with nitrogen gas (99.5% purity, Afrox, South Africa) to prevent hot volatiles pushing back from the reactor. The reactor is divided into two compartments, bottom and top reactor. The entire reactor is heated by a hot chamber consisting eight heating elements. To ensure rapid pyrolysis (high heating rate) of the tyre crumb, the reactor and fluidising nitrogen gas entering the reactor were preheated at 475 °C. A residence time of approximately 5 s was achieved by setting N_2 flow at 42 NL/min. This flow rate was also required to keep the fluidising material bubbling and suspended as well as to purge out char and hot volatiles from the reactor. The fluidising material was silica sand (0.4 – 0.6 mm sieved, AFS 45 fused silica sand, supplied by CONSOL (Pty) Ltd, South Africa) at an amount of 450 g per experiment. The char separation system is also maintained at 475 °C in the hot chamber to prevent condensation of the hot volatiles before they are introduced into the condenser. The hot volatiles from the

reactor are separated from the char by means of the two cyclones and char ports in the char separation system.

Finally, the hot volatiles are introduced in a water-cooled tube-and-shell condensation train (i.e., arranged in series). The condensation train consists of two stainless steel condensers. Cooling water temperature is maintained below 5 °C by circulation through a tank and using a chiller, see Figure 7.3. The TDO obtained is collected for further analysis.

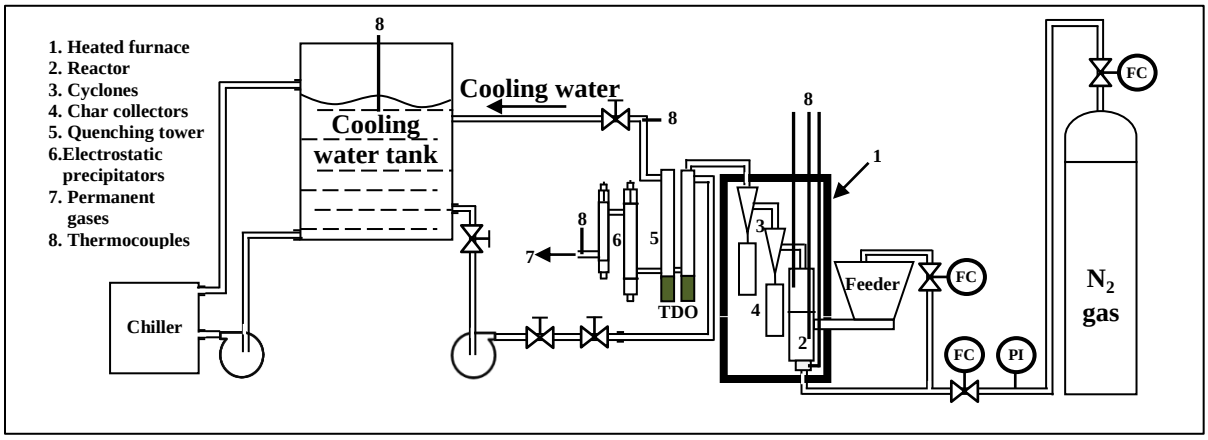

Figure 7.3: Schematic diagram of the BFBR experimental setup with tube-and-shell condenser.

The same pyrolysis reactor setup illustrated in Figure 7.3 but with a tube-and-shell condenser exchanged for a quenching condenser to investigate the type of condensation and cooling rate of the hot volatiles was used, see Figure 7.4. The hot volatiles from the pyrolysis reactor are introduced at the top half of the quenching tower through an inlet pipe connected to the pyrolysis reactor. To prevent condensation of the hot volatiles before they are introduced into the quenching tower the inlet pipe is maintained at a temperature of 350 °C. Using a spraying nozzle, quenching liquid (demineralised water) was introduced at the top of the quenching tower. The nozzle is a spiral type, supplied by Spraying Systems Company, South Africa, standard type, 0.9525 cm NPT removable cap male, made from stainless steel (316SS). Maximum contact between quenching water spray and the hot volatiles that are flowing upward in the quenching tower was achieved by nozzle spray pattern designed to form a spiral cone-spray profile covering the whole cross-sectional area of the quenching tower, see Figure 7.4.

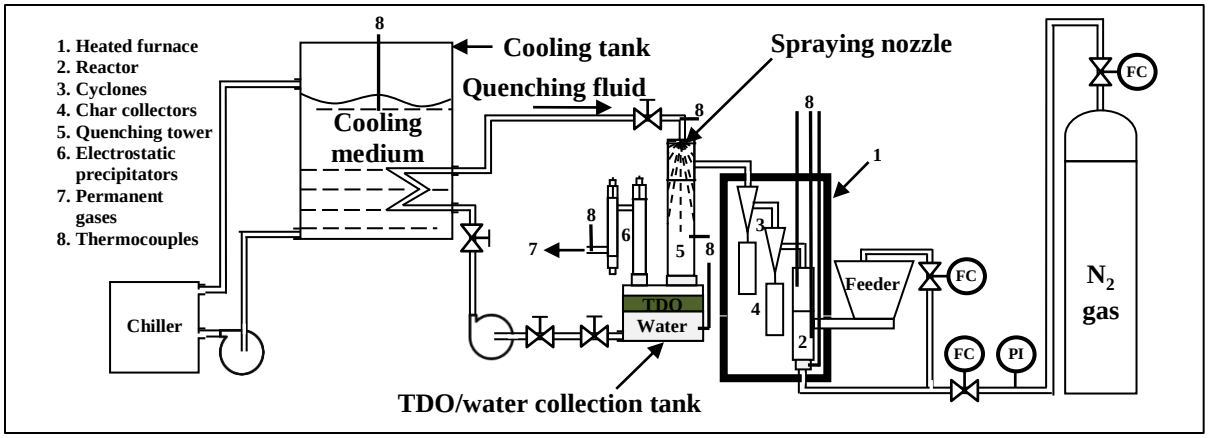

Figure 7.4: Schematic diagram of the BFBR experimental setup with a quenching condenser.

The TDO/quenching water tank was initially fed with a volume of 14 L demineralised water. Quenching water was continuously circulated from the bottom of the TDO/quenching water tank (while TDO floats on the water) and the top of the quenching tower. Water withdrawal flow rate from the bottom was maintained at a flow rate of 4 L/min, using a pump. The temperature of the quenching water at the quenching tower inlet was maintained below 5 °C by leading it through a cooper coil submerged in a cooling tank. The hot volatiles are introduced, contacted with the quenching water spray, and the TDO recovered similar to the FBR.

7.2.2.3 Conical spouted bed reactor augmented with a tube-and-shell condenser

The main components of the CSBR are illustrated in Figure 7.5 and include, i) solid and gas feeding devices, ii) a pyrolysis reactor, iii) fine particle retention system, and iv) hot volatiles condensation system. To feed the solids, the feeding system uses a vertical shaft connected to a piston placed below the solids. Waste tyre crumb feed rate was maintained at 1.3 g/min using a Brooks SLA5800 mass flow meter and the experiment duration was 30 min. The reactor design allows cyclic and vigorous movement of the solids which results in high heat and mass transfer. High heat transfer rates in the reactor are further enhanced by using 150 g silica sand (0.3 – 0.8 mm). The sand is fluidised with nitrogen gas at a flow of 8 NL/min, which also maintains inert conditions and spouting velocity in the reactor and results in a residence time of the hot volatiles in the hot zones between 30 and 500 ms, [14]. While the experiment is in progress, the char formed is separated from the hot volatiles using a cyclone and then a 5 µm sintered steel filter. The tubing, cyclone and filter were maintained at 300 °C to eliminate condensation of the hot volatiles before the condensation system. The hot volatiles are introduced in a water-cooled tube-and-shell condenser. The resulting TDO

and permanent gases are passed through a 5 µm steel filter to retain solid residues and the fine TDO droplets from the gas.

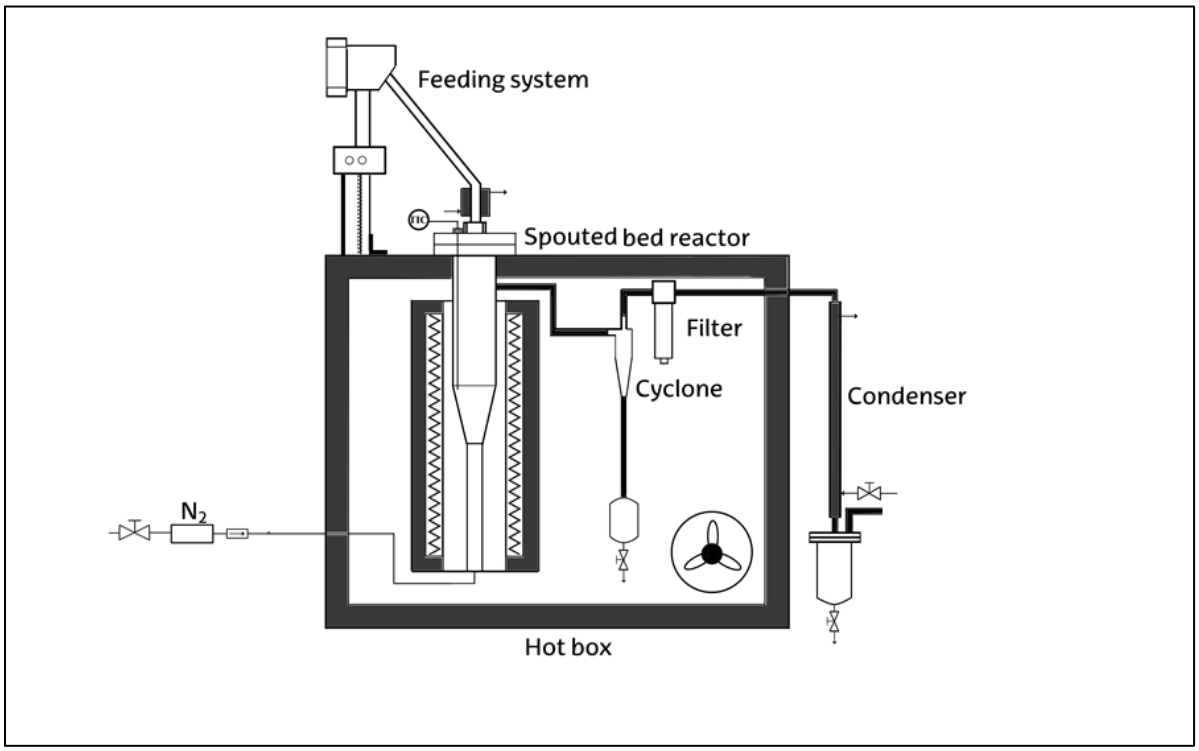

Figure 7.5: Schematic diagram of conical spouted bed reactor experimental setup with a tube-d-shell condensation.

7.2.3 TDO analysis

All experiments were conducted in duplicate and a representative TDO sample was taken for further analysis. Gravimetrical methods were used to determine the char and TDO yields, while chromatographical methods were employed for DL-limonene yield and benzothiazole concentration in the TDO. When the quenching condenser was used, two liquid phases, TDO (non-polar and less dense liquid containing majority of the DL-limonene) and quenching water (polar and denser liquid containing majority of the benzothiazole) were obtained from the storage tank and were separated using a separation funnel (12 h). The TDO was qualitatively and quantitatively analysed. A Hewlett Packard 5890 Series II model gas chromatography (GC) coupled with a Hewlett Packard 5973 mass spectrometry (MS) was used to analyse the TDO. A volume of 1µl mixture of the TDO, internal standards, and dichloromethane solvent (99.9% purity, Sigma Aldrich, South Africa) was injected in a 60 m x 0.18 mm ID x 0.10 µm film thickness, non-polar Rxi-5% Sil-MS capillary column. Helium gas (99.999 % purity, Air Products, South Africa) was

used as a carrier gas at a constant flow rate of 1.20 ml/min (linear velocity of 27.9 cm/s) at 348 kPa. Additionally, water content was determined in all TDO samples using titration methods.

7.3 Results and discussion

7.3.1 Effect of the type of condensation

The results from the FBR and BFBR each augmented with a tube-and-shell condenser and quenching condenser as well as the CSBR augmented with a tube-and-shell condenser are presented in Table 7.2. The experimental results from the FBR have been previously published [11,12], while the experimental results from the CSBR were obtained from the analysis of the TDO derived from the CSBR [15,16]. Exchanging the tube-and-shell condenser with a quenching condenser in the FBR improved the total TDO yield from 46.6 wt.% to 48.9 wt.% as was observed from previous work [11,12]. The effect of a quenching condenser was relatively insignificant on the char yield, 35.7 wt.% was obtained from the tube-and-shell condenser while 36.4 wt.% from a quenching condenser. The observed results were expected since the char remained in the pyrolysis reactor and was not in contact with either the tube-and-shell or quenching condenser. The gas yield decreases from 17.7 to 14.6 wt.% when the tube-and-shell condenser replaces the quenching condenser, see Table 7.2. The amount by which the gas yield decreases is comparable to the amount by which TDO increase. Therefore, indicating that the quenching condenser improved condensing of the volatiles that may have not condensed when the tube-and-shell condenser was used.

DL-limonene yield in the TDO from the quenching condenser augmented with the FBR was higher at 7.9 wt.%, compared to 7.6 wt.% from the tube-and-shell condenser, see Table 7.2. Benzothiazole concentration in the TDO decreases from 5382 to 2168 ppm when a tube-and-shell condenser replaces a quenching condenser. Exchanging the tube-and-shell condenser with the quenching condenser provided not only investigation of direct or indirect contact between the hot volatiles and quenching water, but also variation in the cooling rates of the hot volatiles [12]. The contact between the hot volatiles with the quenching water promotes dissolution of the heteroatom compounds, particularly benzothiazole [12].

Summary results in Table 7.2 were obtained from the BFBR either augmented with a tube-and-shell condenser or a quenching condenser. The results were derived from pyrolysis operating conditions characterised by relative higher heating rates (> 10 000 °C/min) [11,12] and shorter hot volatiles residence times in the hot reaction zone (~ 5 s, estimated). A total TDO yield of 50.0 wt.% was observed in the tube-and-shell condenser, while in the quenching condenser 55.9 wt.%. The increase in the total TDO yield is

similar to the results in the FBR, and can be attributed to the efficiency of the quenching condenser [12]. Similar to the FBR, char yield remained relatively constant at 35.4 wt.% in the tube-and-shell condenser and 34.1 wt.% in the quenching condenser while the gas yield decreased from 14.6 to 10.0 wt.%, see Table 7.2.

Table 7.2: Properties of the products from the FBR, BFBR and CSBR waste tyre pyrolysis augmented with the tube-and-shell and quenching condensers.

	Parameters	Type of condensation				
		Tube-and-shell condenser			Quenching condenser	
		*FBR	BFBR	αCSBR	*FBR	BFBR
Reactor operating conditions	Temperature (°C)	475	475	475	475	475
	Heating rate (°C/min)	20	>γ10000	>β10000	20	>γ10000
	γGas residence time (s)	~ 41	~ 5	~ β0.5	~ 41	~ 5
Quenching condensation	Cooling water (L)	–	–	–	2.10	14
	Water spray flow (L/min)	–	–	–	0.96	4
Main products yield	Tyre derived oil TDO (wt.%)	46.6	50.0	58.2	48.9	55.9
	Solid residue or char (wt.%)	35.7	35.4	35.9	36.4	34.1
	Permanent gases (wt.%)	17.7	14.6	5.9	14.7	10.0
Organic phase (TDO)	DL-limonene yield (wt.%)	7.62	8.04	8.39	7.90	8.13
	Benzothiazole concentration (ppm)	5382	6287	2354	2168	1862
	Water content (wt.%)	0.7	0.1	0.1	0.3	0.3

* Adapted from [11,12]

α Adapted from [15,16]

β Adapted from [15,16]

γ Estimated from reactor dimension and configuration

DL-limonene yield in the TDO from the quenching condenser connected to the BFBR was higher at 8.13 wt.%, compared to 8.04 wt.% from the tube-and-shell condenser. Also, a decrease in the benzothiazole concentration in the TDO from 6287 to 1862 ppm was observed when a quenching condenser was used

compared to a tube-and-shell condenser. Therefore, the effect of direct contact between the hot volatiles and quenching water was observed for both reactor types. The observed results can be attributed to the high cooling rate of the hot volatiles when contacted with the quenching water compared to the lower cooling rate during indirect contact between the cooling water and the hot volatiles. High polar quenching water additionally reduces polar benzothiazole concentration in the TDO through dissolution in the water phase as the two phases separates at the end of the pyrolysis process.

7.3.2 Effect of the reactor type

Compared in Table 7.2 are the total TDO yield, DL-limonene yield and benzothiazole concentration in the TDO the FBR, BFBR, and CSBR. In the BFBR total TDO yield improved by 3.4 wt.% from 46.6 in the FBR [11] to 50.0 wt.% in the tube-and-shell condenser. A further increase in the TDO yield by 8.2 wt.% to 58.2 wt.% was observed when the CSBR augmented with a tube-and-shell condenser was used [15,16]. TDO yield increases by 7.0 wt.% from 48.9 in the FBR to 55.9 wt.% in the BFBR augmented with a quenching condenser. The gas yield from the FBR decreased by 3.1 and 11.8 wt.%, similar amount as the TDO yield increases, when the BFBR and CSBR are used instead of the FBR, respectively. Therefore, implying significant effect of the BFBR and CSBR designs characterised by bubbling and cyclic vigorous movement of the solids on the TDO and gas yield. Compared to the FBR where the tyre crumb is static, in the BFBR and CSBR the tyre crumb is bubbling and cyclic vigorous moving and results to the improvement in the heating rate. The trade-off between TDO and gas yields was confirmed by comparable char yields at 36.4, 34.1 and 35.9 wt.% from the FBR, BFBR and CSBR, respectively.

DL-limonene yield, a high valuable chemical, increased when the FBR is exchanged with the BFBR and CSBR from 7.62 to 8.04 and 8.39 wt.%, in combination with the tube-and-shell condenser and from 7.90 wt.% (FBR) to 8.13 wt.% (BFBR) in combination with the quenching condenser (Table 7.2). The increase in the DL-limonene yield was also attributed to the rapid heating of the waste tyre crumb in the BFBR and CSBR as compared to the FBR. Similar trend was observed on the benzothiazole concentration in the TDO when a tube-and-shell condenser was used. The concentration of the benzothiazole in the TDO increased from 5382 to 6287 and 6354 ppm when the FBR was exchanged for BFBR and CSBR, respectively, see Table 7.2.

The results from the FBR, BFBR and CSBR, each augmented with the tube-and-shell condenser, are illustrated in Table 7.2 and Figure 7.6, are also representative of the effect of the hot volatiles residence time. Longer residence time (~ 41 s) of the hot volatiles in the hot reaction zones was attained in the FBR,

while it was shorter in the BFBR (~ 5 s) and CSBR (~ 0.5 s). Short residence time of the hot volatiles from FBR, BFBR, and then CSBR improved total TDO yield. A slight increase in the DL-limonene yield was also observed as the FBR was exchange with the BFBR and then the CSBR. In terms of the benzothiazole concentration in the TDO, a trend similar to that obtained in the heating rate was observed when the FBR was exchange with the BFBR and then with the CSBR, see Table 7.2 and Figure 7.6.

Regarding residence time of the hot volatiles in the hot reaction zones, improvements in the TDO and DL-Limonene yield and reduction in the benzothiazole concentration in the TDO can be attributed to the elimination of the secondary reactions. Longer hot volatiles residence times in the hot reaction zone of the FBR promotes cracking of the longer chain molecules to form permanent gases with shorter chain molecules. Therefore, gas yield from the FBR is higher than that from the BFBR, while from the BFBR is higher than from the CSBR, see Table 7.2. Figure 7.6 also shows clearly significant effect of the residence time on the DL-Limonene yield and benzothiazole concentration in the TDO from 8.13 wt.% in the BFBR to 8.39 wt.% in the CSBR as the hot residence time reduces from 5 to 0.5 s, respectively particularly even when a heating rate >10000 °C/min and the tube-and-shell condenser are used in both the BFBR and CSBR. DL-limonene yield at these operating conditions increases.

In the current study when waste tyre pyrolysis is conducted at higher heating rates, shorter residence times of the hot volatiles in the hot reaction zone, and using a quenching condenser, benzothiazole concentration in the TDO decreased to 1862 ppm from 5382 ppm, equivalent to the reduction of 70%. Therefore, implying that both the pyrolysis reactor operating conditions and a method of cooling/condensation of the hot volatiles have significant effect on the quality of the TDO, in terms of benzothiazole concentration. Moreover, other heteroatom compounds, i.e., thiophene isomers (3-methyl thiophene), phenols (3-methyl phenol), and quinoline isomers (2,4-dimethylquinoline), showed similar trends as benzothiazole. The concentrations of these compounds in the TDO decreased by 60 to 90 % when higher heating rates, shorter residence times of the hot volatiles in the hot reaction zones and a quenching condenser were employed.

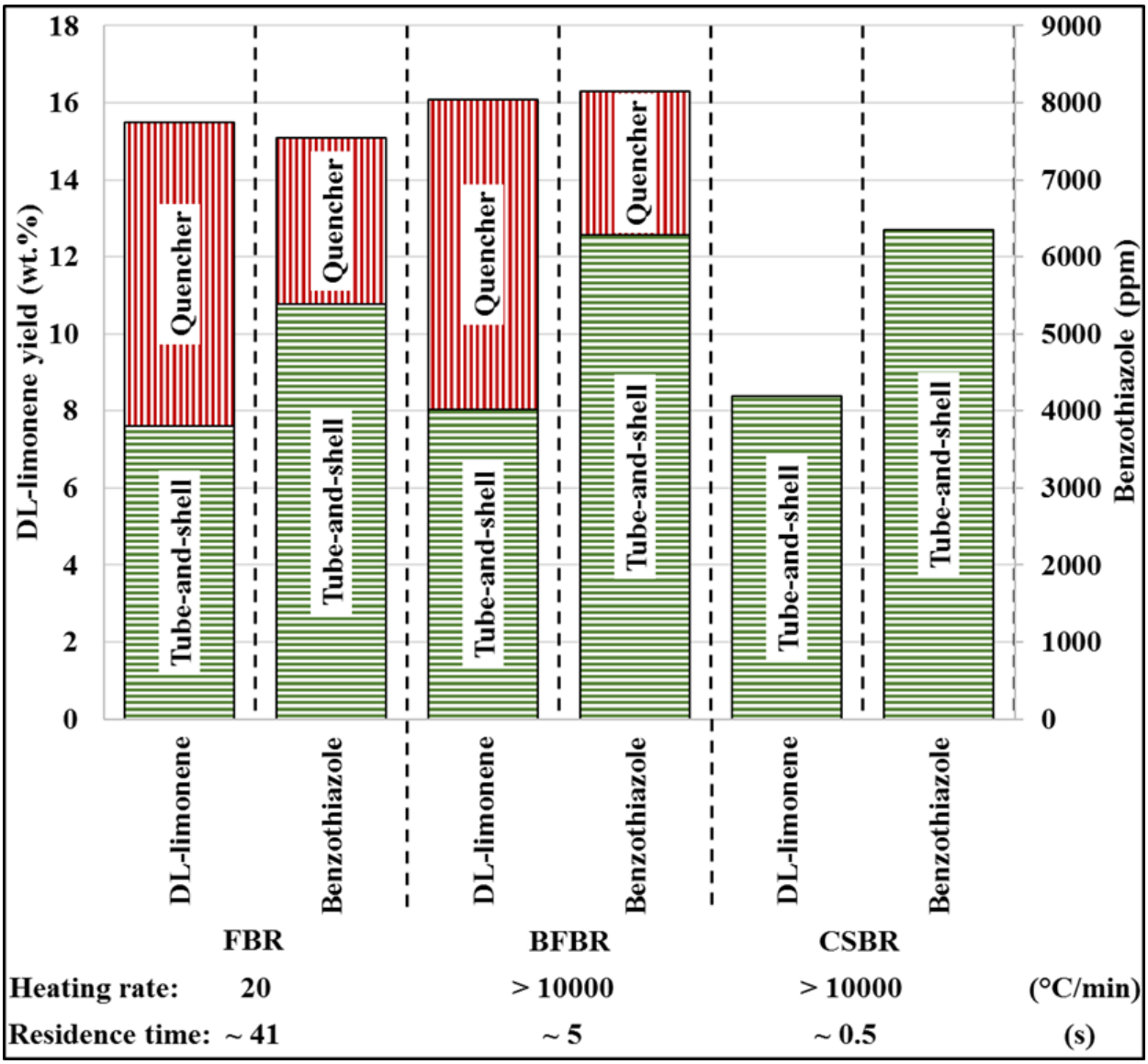

Figure 7.6: Effect of the condensation, heating rate and residence time of the hot volatiles on the DL-limonene yield and benzothiazole concentration in the TDO from the FBR, BFBR and CSBR.

Lower heteroatom compounds concentration in the TDO favours recovery of the valuable chemicals. The lower the concentration of these compounds in the TDO the more it is suitable as the starting material for DL-Limonene and fuel production [18]. There is a potential that by exchanging the tube-and-shell condenser with the quenching condenser, the majority of the heteroatom compounds are reduced or eliminated. For example, the observed effectiveness of the quencher to reduce benzothiazole concentration. This significant reduction of the benzothiazole (a major sulphurous and nitrogenous compound) in the TDO, was comparable to conventional post-treatment through desulphurisation techniques that are potentially complex and/or costly.

7.4 Conclusions

Exchanging the tube-and-shell condenser with the quenching condenser in both the FBR and BFBR improved the TDO yield and quality (high DL-limonene concentration and low benzothiazole concentration) from waste tyre pyrolysis. Total TDO and DL-limonene yields increased when the FBR was exchanged with the BFBR in combination with both the tube-and-shell and quenching condenser, while benzothiazole concentration increased in the TDO from the BFBR in combination with the tube-and-shell condenser and decreased in combination with the quenching condenser. A further increase in the TDO and DL-limonene yield, and a decrease in the benzothiazole concentration, was observed when a CSBR was used in combination with the tube-and-shell condenser. High DL-limonene concentration in the TDO indicated that the TDO has high potential of being used as a source of DL-limonene production and recovery when it is further processed. Moreover, low benzothiazole concentration in the TDO indicated that the TDO has a high potential to be further upgraded for fuels production since the TDO refining processes will be less intensive and expensive once the sulphur and nitrogen contents are reduced. Quenching condenser can be widely applied as a preferred technique for cooling and condensing of the hot volatiles particularly under high heating rates and short residence time of the hot volatiles from the hot reaction zone pyrolysis operating conditions. Moreover, high benzothiazole concentration in the used quenching water may result in the benzothiazole recovery and then used in the tyre manufacturing.

Acknowledgements

This research was supported by the Recycling and Economic Development Initiative of South Africa (REDISA) and the National Research Foundation (NRF). The authors acknowledge that opinions, findings and conclusions or recommendations expressed are those of the authors only, and the sponsors accept no liability whatsoever in this regard.

References

[1] E.L.K. Mui, D.C.K. Ko, G. McKay, Production of active carbons from waste tyres—a review, Carbon. 42 (2004) 2789-2805.
[2] N. Antoniou, A. Zabaniotou, Features of an efficient and environmentally attractive used tyres pyrolysis with energy and material recovery, Renewable and Sustainable Energy Reviews. 20 (2013) 539-558.

[3] A. Zabaniotou, P. Madau, P.D. Oudenne, C.G. Jung, M.-. Delplancke, A. Fontana, Active carbon production from used tire in two-stage procedure: industrial pyrolysis and bench scale activation with H2O–CO2 mixture, J. Anal. Appl. Pyrolysis. 72 (2004) 289-297.

[4] A. Quek, R. Balasubramanian, Liquefaction of waste tires by pyrolysis for oil and chemicals—A review, J. Anal. Appl. Pyrolysis. 101 (2013) 1-16.

[5] M. Banar, V. Akyildiz, A. Özkan, Z. Çokaygil, Ö Onay, Characterization of pyrolytic oil obtained from pyrolysis of TDF (Tire Derived Fuel), Energy Conversion and Management. 62 (2012) 22-30.

[6] P.T. Williams, Pyrolysis of waste tyres: A review, Waste Manage. 33 (2013) 1714-1728.

[7] M. Sienkiewicz, J. Kucinska-Lipka, H. Janik, A. Balas, Progress in used tyres management in the European Union: A review, Waste Manage. 32 (2012) 1742-1751.

[8] M.A. Barlaz, W.E. Eleazer II, D.J. Whittle, Potential To Use Waste Tires As Supplemental Fuel In Pulp And Paper Mill Boilers, Cement Kilns And In Road Pavement, Waste Manage. Res. 11 (1993) 463-480.

[9] M. Giugliano, S. Cernuschi, U. Ghezzi, M. Grosso, Experimental evaluation of waste tires utilisation in cement kilns. Journal of the Air & Waste Management Association. 49 (1999) 1405-1414.

[10] B. Danon, P. Van Der Gryp, C.E. Schwarz, J.F. Görgens, A review of dipentene (dl-limonene) production from waste tire pyrolysis, J. Anal. Appl. Pyrolysis. 112 (2015) 1-13.

[11] N.M. Mkhize, P. van der Gryp, B. Danon, J.F. Görgens, Effect of temperature and heating rate on limonene production from waste tyre pyrolysis, J. Anal. Appl. Pyrolysis. 120 (2016) 314-320.

[12] N.M. Mkhize, B. Danon, P. van der Gryp, J.F. Görgens, Condensation of the hot volatiles from waste tyre pyrolysis by quenching, J. Anal. Appl. Pyrolysis. 124 (2017) 180-185.

[13] P.T. Williams, A.J. Brindle, Fluidised bed pyrolysis and catalytic prolysis of scrap tyres, Environmental Technology. 24 (2003) 921-929.

[14] M. Olazar, R. Aguado, M.J. San José, S. Alvarez, J. Bilbao, Minimum spouting velocity for the pyrolysis of scrap tyres with sand in conical spouted beds, Powder Technol. 165 (2006) 128-132.

[15] J. Alvarez, G. Lopez, M. Amutio, N.M. Mkhize, B. Danon, P. van der Gryp, J.F. Görgens, J. Bilbao, M. Olazar, Evaluation of the properties of tyre pyrolysis oils obtained in a conical spouted bed reactor, Energy. 128 (2017) 463-474.

[16] G. Lopez, J. Alvarez, M. Amutio, N.M. Mkhize, B. Danon, D.G. van, J.F. Görgens, J. Bilbao, M. Olazar, Waste truck-tyre processing by flash pyrolysis in a conical spouted bed reactor, Energy Conversion and Management. 142 (2017) 523-532.

[17] G. Choi, S. Oh, J. Kim, Non-catalytic pyrolysis of scrap tires using a newly developed two-stage pyrolyzer for the production of a pyrolysis oil with a low sulfur content, Appl. Energy. 170 (2016) 140-147.

[18] H. Aydın, C. İlkılıç, Optimization of fuel production from waste vehicle tires by pyrolysis and resembling to diesel fuel by various desulfurization methods, Fuel. 102 (2012) 605-612.

[19] C. İlkılıç, H. Aydın, Fuel production from waste vehicle tires by catalytic pyrolysis and its application in a diesel engine, Fuel Process Technol. 92 (2011) 1129-1135.

[20] M. Rofiqul Islam, H. Haniu, M. Rafiqul Alam Beg, Liquid fuels and chemicals from pyrolysis of motorcycle tire waste: Product yields, compositions and related properties, Fuel. 87 (2008) 3112-3122.

[21] S. Murugan, M.C. Ramaswamy, G. Nagarajan, Performance, emission and combustion studies of a DI diesel engine using Distilled Tyre pyrolysis oil-diesel blends, Fuel Process Technol. 89 (2008) 152-159.

[22] F.A. López, T.A. Centeno, F.J. Alguacil, B. Lobato, Distillation of granulated scrap tires in a pilot plant, J. Hazard. Mater. 190 (2011) 285-292.

[23] X. Chen, G. Clet, K. Thomas, M. Houalla, Correlation between structure, acidity and catalytic performance of WOx/Al2O3 catalysts, Journal of Catalysis. 273 (2010) 236-244.

[24] B. Danon, J. Görgens, Determining rubber composition of waste tyres using devolatilisation kinetics, Thermochimica Acta. 621 (2015) 56-60.

CHAPTER 8. MAIN RESEARCH PROJECT FINDINGS

The current chapter presents the main findings from the studies on the effects of the i) temperature, ii) heating rate, iii), reactor type, and iv) type of condensation and cooling rate of the hot volatiles on the DL-limonene production from waste tyre pyrolysis.

8.1 Effect of temperature

The present study was initiated by investigating the effect of the pyrolysis temperature effect, the most common factor in waste tyre pyrolysis studies. Investigation of the temperature in pyrolysis reactors showed a significant effect on the pyro-char, tyre derived oil (TDO) and pyro gas. The TDO total yield and was dependent on the temperature and a desirability study was employed. The best improvement was observed for the pyrolysis main product fractions yield.

8.1.1 Effect of the temperature on the pyrolysis main product fractions yield

At low pyrolysis temperatures (350 °C and lower), the liquid yield was relatively low and the solid yield relatively high. Relative low liquid yields in combination with high solid yields indicated incomplete pyrolysis. Increasing the pyrolysis temperature to 450 °C and above, significantly increased the liquid yield. While the solid yield decreased to a constant value of approximately 36.5 wt.%, a value that corresponds roughly to the fixed carbon and ash content of a tyre crumb. The study was conducted in a FBR, which is a gram-scale slow pyrolysis reactor. Similar observations were obtained in a microgram-scale set-up to confirm the effect of the temperature on the waste tyre char yield. It was observed that the minimum temperature required for complete pyrolysis of the waste crumb is 425 °C.

The effect of the temperature was investigated on the most important product fraction, i.e., TDO. The TDO yields at temperatures of 309 °C to 590 °C indicated that there was an optimal point within this range. A temperature of 475 °C was found to be the optimal temperature for maximum total TDO yield. At a temperature above 475 °C the TDO yield decrease as it was being cracked to form gaseous products since, the char yield remained constant while the gas yield increase.

8.1.2 Effect of the temperature on the DL-limonene yield

The quality of the TDO at this stage was measured by determination of the DL-limonene yield. Having drawn conclusions on the optimal temperature based on both the minimum temperature required for complete pyrolysis of the waste tyres and maximum TDO yield, maximum DL-limonene yield surprisingly was not significantly affected by temperature. When the DL-limonene yield is considered, a pyrolysis temperature of 475 °C remained the optimal value since pyrolysis at this temperature resulted in the highest DL-limonene yield of 7.6 wt.%.

8.2 Effect of heating rate

The study of the effect of the heating rate on the waste tyre pyrolysis main product fractions and DL-limonene yield and content in the TDO was carried out parallel to the temperature. To isolate the effect of the heating rate from that of the temperature, the conclusion drawn were based on different levels of the pyrolysis temperature, i.e., exclusion of the interactive effect between the temperature and heating rate.

8.2.1 Effect of the heating rate on the pyrolysis main product fractions

The effect of the heating rate on the waste tyre pyrolysis main products yields (pyro-gas, TDO and pyro-char) was insignificant. The effect of both the temperature and heating rate on the pyrolysis main product fractions was not relatively significant. However, an increase in the TDO yield from 39.6 to 46.6 wt.% when the heating rate was increased from 1 to 20 °C/min at the same temperature was observed. A further increase in the heating rate to 29 °C/min resulted in a decrease in the TDO yield to 44.9 wt.%. It was observed that, at a heating rate of 20 °C/min TDO yield was at maximum (48.9 wt.%).

8.2.2 Effect of the heating rate on the DL-limonene yield

The effect of the heating rate on the DL-limonene yield was insignificant at low pyrolysis temperatures, while it was significant at higher pyrolysis temperatures. Maximum DL-limonene yield was obtained at a heating rate of 20 °C/min using the FBR. The optimal heating rate was observed at a temperature of 475 °C. The study of the temperature and heating rate effect on the DL-limonene yield from waste tyre pyrolysis in the FBR was concluded with temperature of 475 °C and heating rate of 20 °C/min as the optimal operating conditions.

8.2.3 Effect of the heating rate on the DL-limonene formation selectivity

The DL-limonene formation selectivity study was based on the products of the two competing reactions of the allylic polyisoprene radicals from depolymerisation of the natural rubber during pyrolysis. Natural rubber depolymerisation constitutes depropagation and intramolecular cyclization and scission of the allylic polyisoprene radicals to form isoprene and DL-limonene, respectively. Derivative thermogravimetric analysis (DTG) curves showed that increasing the heating rate led to 1) a decrease in the secondary degradation reactions, and 2) increase in the temperature at the maximum depolymerisation rate. At the same heating rate, mass spectrometry (MS) ion current signals showed that DL-limonene formation occurred at slightly higher temperatures compared to isoprene formation, indicating a slightly higher activation energy for the former reaction. The study of the effect of the heating rate on the DL-limonene selectivity was extended to a heating rate of up to 100 °C/min. DTG peak temperature increase was more significant on the DL-limonene compared to the isoprene with increasing heating rate. The rate of increase in the peak temperature for DL-limonene formation reaction decreases as the heating rate increases.

Kissinger method provided activation energy (E_a) around 133 and 115 kJ/mol for isoprene and DL-limonene formation reactions, respectively. Since the optimal pyrolysis conditions favouring high DL-limonene yield were a higher heating rate of at least 20 °C/min and a moderate temperature of 475 °C. At the higher heating rate, there is only a low total amount of energy supplied during pyrolysis as a result of the short reaction time. Additionally, shorter residence (at 0.5 s compared to 5 s) time at constant heating rate (> 10000 °C/min) and temperature (475 °C) increased DL-limonene yield (from 8.04 to 8.39 wt.%). Therefore, providing the evidence that lower E_a for DL-limonene compared to isoprene is the resulted in selective the DL-limonene production. Above α = 0.5, the E_a strongly increases for both isoprene and DL-limonene and the Friedman method ceases to be satisfactory. Direct use of the MS ion current signals to develop a model for products formation reaction from waste tyre pyrolysis seems to be a reliable approach as it resulted in a good model fitting of the experimental data.

As the heating rate significantly increases by different reactors, DL-limonene yield increases from 7.62 wt.% (FBR) to 8.13 wt.% (BFBR). Similarly, an increase in the DL-limonene yield was attributed to the rapid mass transfer and heat transfer resistance to further cracking of the dimer DL-limonene.

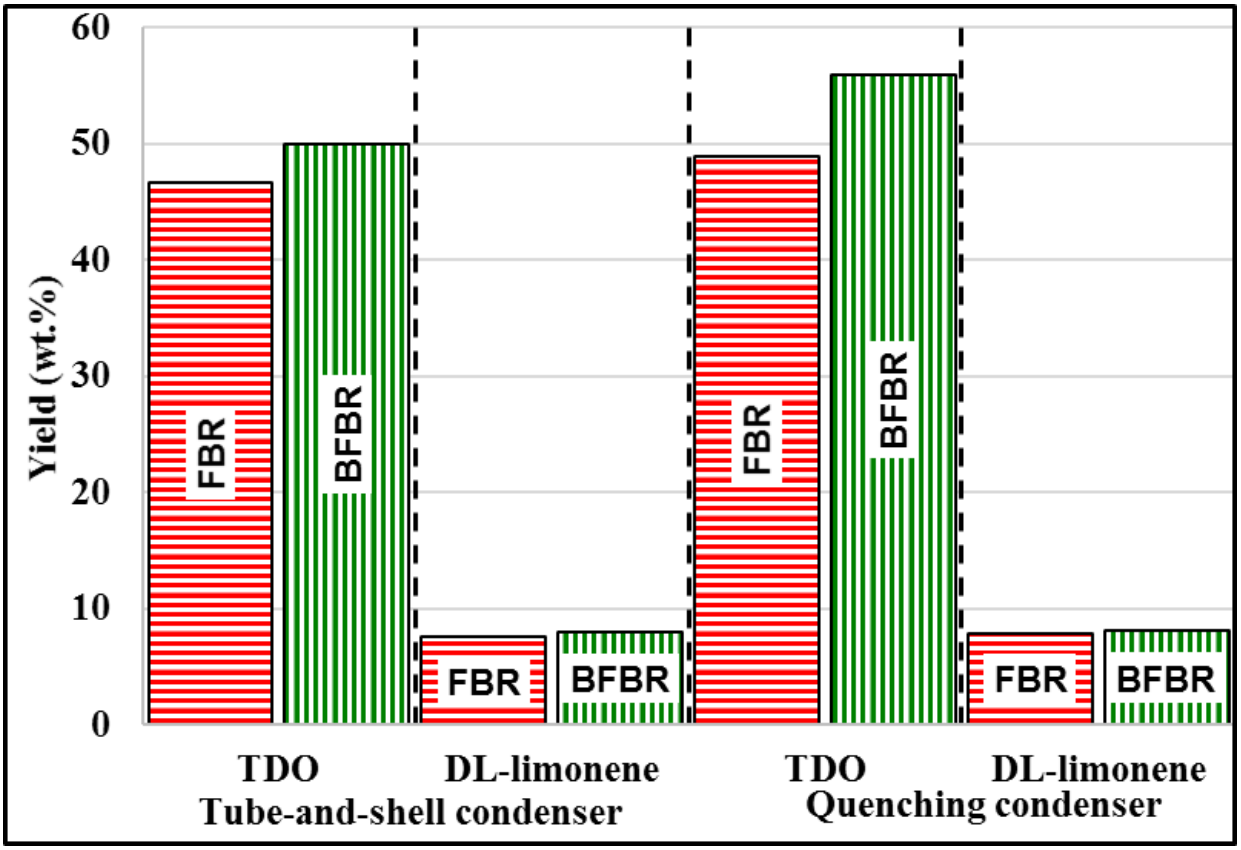

Figure 8.1: Illustration of the total TDO and DL-limonene yield

8.3 Reactor type

Various operating conditions were attained by interchanging a fixed bed reactor (FBR) and a bubbling fluidised bed reactor (BFBR). In the FBR a temperature up to 600 °C and relatively low heating rates of up to 29 °C/min were attained. While the heating rate in the BFBR is a thousand times higher as that in the FBR, estimated at > 10000 °C/min. The temperature range in the BFBR was similar to the FBR range. The residence time of the volatiles in the hot reaction zones was relatively long in the FBR at 41 s, while in the BFBR was relatively short at 5 s.

In the FBR the heating rate range was limited to 1 – 29 °C/min, while merely a heating rate up to 100 °C/min was attained in the microgram-scale (TGA), DL-limonene increase with increasing heating rate and waste tyre pyrolysis temperature. It was necessary to explore other reactors. The BFBR is characterised by rapid pyrolysis (high heating rate). The estimated heating rate in the BFBR was > 10000 °C/min. Solid (pyro-char) yield remained constant in the two investigated pyrolysis reactors at an average of 36 wt.%. The observed pyro-char yield and its stability at various heating rate as provided in the pyrolysis reactors

corresponds roughly to the fixed carbon and ash contents of a tyre sample as pointed out in subsection 8.1. In the BFBR total TDO yield improved by 3.4 wt.% from 46.6 in the FBR to 50.0 wt.% in the tube-and-shell condenser. TDO yield increases by 7.0 wt.% from 48.9 in the FBR to 55.9 wt.% in the BFBR augmented with a quenching condenser, see Figure 8.1.

The increase in the DL-limonene yield (from 7.62 to 8.04 wt.%) was not significant compared to further increases in the heating rate (from 20 to > 10000 °C/min). Therefore, it should be considered if it is economical justifiable to extensively increase the heating rate to increase DL-limonene yield by 1 wt.%. Two main factors should be considered, i) there is limited fraction of polyisoprene in the tyre which can be converted to DL-limonene, and ii) the reaction pathway to DL-limonene compete with other formation pathways, mainly isoprene.

8.4 Effect of condensation type and cooling rate of the hot volatiles

A tube-and-shell condenser is characterised by indirect contact between the hot volatiles and the cooling medium during cooling and condensation of the hot volatiles as well as lower cooling rate of the hot volatiles. Direct contact between the hot volatiles and rapid cooling of the hot volatiles was achieved using a quenching condenser.

The type of condensation was varied between a tube-and-shell condenser and a quenching condenser to study the effect of indirect or direct contact between the hot volatiles and the cooling medium on the TDO and DL-limonene yield and the benzothiazole content in the TDO. Exchanging the tube-and-shell condenser with a quenching condenser also achieves a variation in the cooling rate of the hot volatiles. Detailed descriptions of the tube-and-shell condenser and the quenching condenser connected to either the FBR and BFBR are presented in CHAPTER 6 and CHAPTER 7, respectively.

8.4.1 Effect of condensation type on the total TDO yield

Products were obtained from the FBR and BFBR pyrolysis systems at a temperature of 475 °C. Total TDO yield increase when the tube-and-shell condenser was replaced with the quenching condenser, particularly for the BFBR, see Figure 8.1. In the FBR, exchanging the tube-and-shell condenser with the quenching condenser increased the total TDO yield from 46.6 to 48.9 wt.%. For the BFBR it increased to 55.9 wt.% from 50.0 wt.%. This was attributed to the efficiency of the condensation of the hot volatiles by direct contact with the cooling water in the quenching condenser compared to indirect contact between the hot

volatiles and cooling medium in the tube-and-shell condenser. Nozzle sprayed chilled water in the quenching condenser improved mass and heat transfer when contacted with the hot volatiles from the pyrolysis reactor. The cooling rate of the hot volatiles is higher thus in the quenching condenser as compared to the tube-and-shell condenser.

8.4.2 Effect of condensation type the DL-limonene yield and benzothiazole content in the TDO

Exchanging the tube-and-shell condenser with the quenching condenser resulted in an increase in the DL-limonene yield, see Figure 8.2. The DL-limonene yield increased from 7.6 to 7.9 wt.% and from 8.04 to 8.13 wt.% in the FBR and BFBR, respectively. The observed improvements can be attributed to the efficient and rapid condensation of the hot gaseous DL-limonene to its liquid state in the quenching condenser.

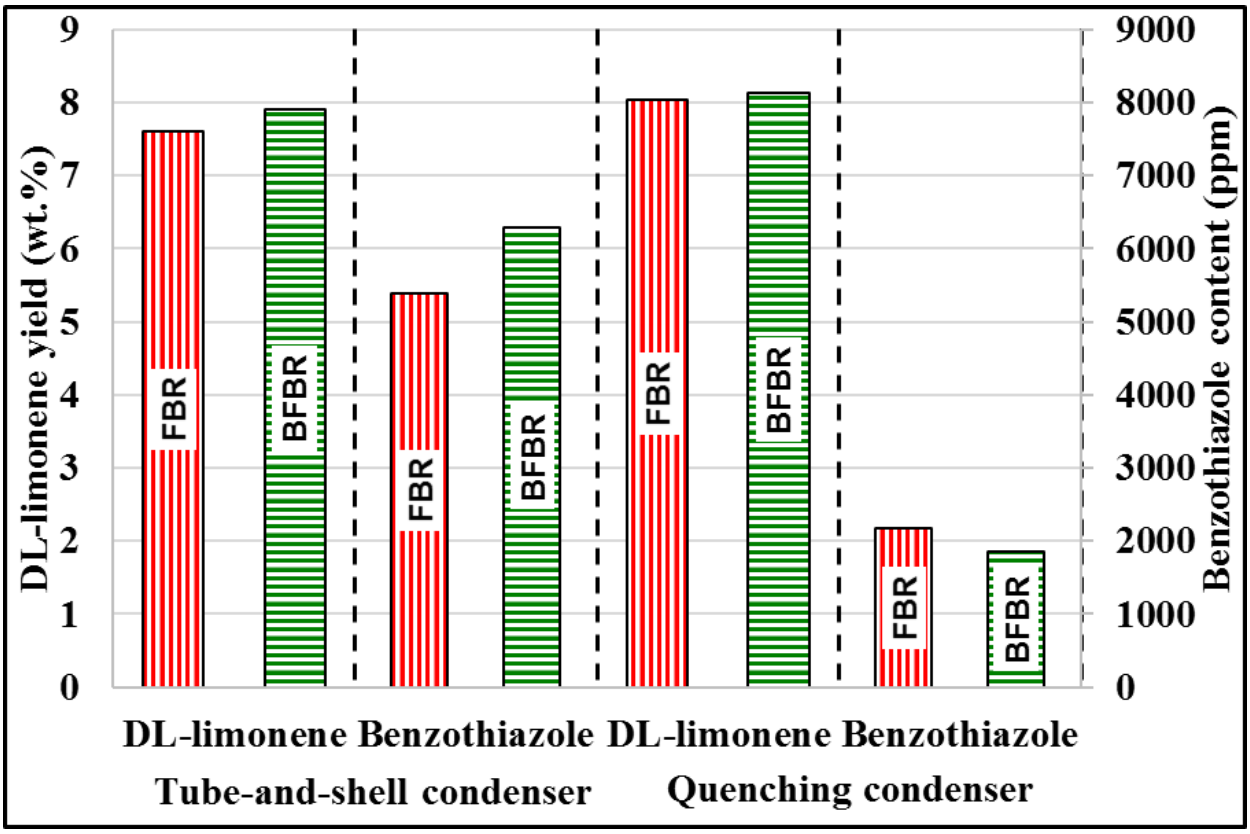

Figure 8.2: Schematic diagram showing effect of the condensation type (tube-and-shell or quenching condenser) on the DL-limonene yield and benzothiazole content in the TDO.

Benzothiazole is a high polar compound and is undesired in the TDO since it contains nitrogen and sulphur. It is associated with impediments in the processing of the TDO since it attacks TDO processing catalysts.

As the tube-and-shell condenser was replaced with the quenching condenser, the benzothiazole content in the TDO was reduced from 5382 to 2168 ppm and from 6287 to 1862 ppm in the FBR and BFBR, respectively. It is interesting to note that in the BFBR, exchanging the tube-and-shell condenser with the quenching condenser resulted in the reduction of the benzothiazole content in the TDO by 70%, while 60% in the FBR. The quenching condenser has the advantages that it increases the DL-limonene content in the TDO, while it significantly reduces the benzothiazole content in the TDO.

8.5 Conclusions

Increasing the heating rate, reducing the volatiles residence time in the reaction zones and exchanging tube-and-shell condenser with a quenching condenser all improved the total TDO yield and quality (lower benzothiazole content in the TDO) from waste tyre pyrolysis. A combination of the BFBR and the quenching condenser resulted in the high DL-limonene yield, while the benzothiazole content in the TDO was significantly reduced. A low benzothiazole content in the TDO indicates that the TDO has a high potential to be further upgraded towards fuels since the TDO refining processes will be less intensive and expensive once the sulphur and nitrogen contents are reduced. Waste tyre pyrolysis for valuable chemicals recovery and using the rest of the TDO for energy recovery is more practical and economically feasible than waste tyre pyrolysis to only recover energy.

CHAPTER 9. RECOMMENDATIONS

9.1 Introduction

Conventional waste tyre pyrolysis studies mainly focused on waste tyre pyrolysis for energy recovery. Waste tyre pyrolysis for merely energy recovery results in products that have limited market competitiveness. With current relatively low prices of crude oil and petroleum-derived fuels, waste tyre derived fuels experience challenges to be an alternative and secure market without financial support. Since waste tyres consist of high amounts of carbon and hydrogen, there is a high potential of valuable chemicals production from the waste tyre pyrolysis. Through waste tyre pyrolysis for valuable chemicals production, there is a potential that more revenue will be generated from the pyrolysis plant (mainly generated from chemicals), which should improve the economic viability of waste tyre pyrolysis. For example, the two main products from waste tyre pyrolysis for energy recovery, gasoline and diesel are each priced at less than 1 US$/kg, while the price of a kg of DL-limonene ranges between 2.5 and 25 US$/kg, depending on it purity. DL-limonene is a natural occurring compound and its concentration is high in citrus fruit peels oil at more than 80 %. DL-limonene is an important component in industrial formulations of solvents, resins, and adhesives.

The current study began by investigating the effect of the temperature and heating rate on DL-limonene production from waste tyre pyrolysis. The temperature and heating rate are mainly pyrolysis reactor related factors, and their influence was limited to the content of the DL-limonene in the hot volatiles evolving from polyisoprene devolatilisation. The study was expanded to include various reactors and the type of condensation and cooling rate of the hot volatiles to maximise the recovery of DL-limonene and TDO. This include techniques for removal of the hot volatiles from the pyrolysis reactor, then cooling and condensing of the hot volatiles. Incorporating production of the hot volatiles and treating of the hot volatiles to produce the TDO with a high content of DL-limonene has improved the understanding of waste tyre pyrolysis process for valuable chemicals and energy recovery.

9.2 Recommendations

To efficiently recover valuable chemicals from waste tyre pyrolysis, the overall recommendation will be subdivided into various interconnected stepwise sub-pyrolysis processes. The sub-processes include,

i. devolatilisation of the waste tyre crumb in the pyrolysis reactor (operating parameters mainly temperature and heating rate),
ii. hot volatiles handling (operating parameters mainly purging gas flow rate and hot volatiles residence time in the hot reaction zones), and
iii. cooling and condensation of the hot volatiles from the pyrolysis reactor (operating parameters mainly condensation type (direct or indirect contact between the hot volatiles and cooling fluid) and cooling rate of the hot volatiles).

Temperature based devolatilisation of the waste tyre crumb has been extensively investigated and reported in the literature. However, due to conventional waste tyre pyrolysis being focused on energy recovery, the heating rate has not been extensively investigated. The heating rate should be investigated and valuable products formation should be targeted in the investigations. From the instant the hot volatiles are evolved from the waste tyre crumb in the pyrolysis reactor to the point where a first drop of TDO is formed, a variety of reaction pathways are possible. When certain types of chemical compounds are targeted as the final product, the conditions under which the vapour phase of the compound is exposed can be monitored to improve the recovery of that compound, resulting in high yields of that valuable chemical. While it is common to separate waste pyrolysis from cooling and condensation of the hot volatiles, the two are actually interrelated and are required to be considered simultaneously. During the cooling and condensing of the hot volatiles into the TDO, much can be done to improve the yield of the TDO and valuable chemicals yield. A well-designed pyrolysis process can improve the TDO the quality, which is normally perceived as a downstream process after pyrolysis has been completed. For example, conventional TDO upgrading is conducted by cooling and condensing hot vapours to yield TDO and then heated up back to vapours in a separate operating unit(s). It is possible to treat the hot volatiles before they are cooled and condensed to the TDO to achieve a higher quality TDO. In the following subsections recommendations are discussed on each finding and the sub-processes are integrated for the overall recommendations.

9.2.1 Effect of the temperature

A temperature of 475 °C resulted in the highest total TDO and DL-limonene yield. No doubt this temperature is highly recommended for waste tyre pyrolysis to produce valuable chemicals, such as, DL-limonene. A variety of waste tyre pyrolysis reactors, fixed bed reactor (FBR) and bubbling fluidised bed reactor (BFBR) confirmed the temperature as the optimal for DL-limonene production. Although the results were satisfactory and consistent from the two reactors, other pyrolysis, such as, pilot-scale and industrial-scale reactors should be investigated at the same pyrolysis temperature of 475 °C.

9.2.2 Effect of the heating rate

Increasing the heating rate extensively (from 29 to > 10000 °C/min) might have been a bit audacious. A more moderate step-wise increment of the heating rate study, i.e., from 10s °C/min, 100s °C/min, 1000s °C/min and then to flash heating, may be a better approach. An optimal heating rate may be located at more moderate heating rates and can result in the reduction of the high flow rate purging gases required to remove the hot volatiles from the hot reaction zones as they are rapidly evolved during pyrolysis. Unlike temperature, heating rate control in waste tyre pyrolysis has many challenges and has not been extensively investigated. Designing of a pyrolysis reactor that can effectively control the heating rate should be considered.

Since the heating rate plays a major role in the kinetic mechanism of the waste tyre pyrolysis processes, the tracking of product formation compared to typical starting material devolatilization should be considered. This recommendation is based on the fact that recovery of the valuable chemicals from waste tyre is becoming interesting as compared to merely waste tyre pyrolysis for energy recovery.

9.2.3 Effect of the hot volatiles residence time in the hot reaction zones

Flash pyrolysis of waste tyres requires high purging gas flow rates which results in short residence time of the hot volatiles in the hot reaction zones. As recommended in subsection 9.2.2, a rather moderate reduction in the hot volatiles residence time in the hot reaction zones should be studied instead of a decrease in the residence time from 41 to 5 s in the FBR and BFBR, respectively.

Since conventional kinetic mechanism study of waste tyre pyrolysis has been mainly based on the devolatilization of the waste tyre crumb, it will be interesting to base such studies on the products formed and the effect of the residence time in the hot reaction zones. A combination of the operating conditions from the slow fixed-bed pyrolysis reactor (FBR) and flash pyrolysis reactor (BFBR) will be interesting to study. High flow rate of the hot volatiles from the pyrolysis reactor requires high efficient cooling and condensation system, the following subsection discusses recommendation on the condensation type and cooling rate.

9.2.4 Effect of condensation type and cooling rate of the hot volatiles

As various means of waste tyre pyrolysis for maximum DL-limonene production was discussed in CHAPTER 7, the main goal was to treat hot volatiles before cooling and condensation to upgrade TDO quality. Therefore, reducing the contents of heteroatom compounds, such as, nitrogenous, oxygenous and sulphurous compounds, in the TDO as the hot volatiles are being cooled and condensed into the TDO is recommended. Although using water (a relative cheap and readily available commodity) to investigate the condensation type of the hot volatiles was carried out in the current study, various other polar fluids should be investigated, such as, glycerol and acetonitrile. Additionally, water at various pHs, quality, physical state, etc can be used. Extensive investigation of the cooling liquid still needs to be carried out to improve the elimination of the heteroatoms from the TDO.

Used quenching water from the quenching condenser should also be investigated to determine the recycling feasibility. When pyrolysis is complete, the quenching water will be concentrated with heteroatom compounds, particularly benzothiazole. Recovery of the benzothiazole from the used quenching water should be investigated.

9.3 Overall remarks

The overall recommendations to potential waste tyre recyclers or processers by thermochemical treatment processes, particularly pyrolysis, mainly evolves around upgrading of the pyrolysis main fractions. By upgrading the main pyrolysis products (i.e., TDO and char) prior to selling them as final products will improve their market acceptance and increase revenue for the pyrolysis plant. Final products that should be targeted, are listed subsequently according to their priorities.

9.3.1 Pyrolysis for mainly DL-limonene

Among the primary compounds in the TDO, DL-limonene is the most predominant compound in the TDO [1] and has a relatively high market value of up to 25 US$/kg. In the current study, it has been shown that the content of DL-limonene in the TDO can be improved significantly. A study carried out by Ngwetjana (2016) concluded that, using enhanced distillation, high purity DL-limonene can be recovered from the TDO [2]. It was further pointed out that a minimum DL-limonene content in the TDO should be achieved, while a conventional distillation process can be used to recover the DL-limonene [2]. Therefore, this indicates that DL-limonene production from waste tyre pyrolysis is feasible.

9.3.2 Upgrading the remaining TDO (after DL-limonene recovery) to fuels

After the DL-limonene has been recovered from the TDO, the next potential product that should be targeted as part of waste tyre pyrolysis is upgrading of the remaining TDO to fuels, such as, gasoline, diesel or marine fuels (marine bunker oil). This modified waste tyre pyrolysis process results in a TDO consisting of low concentrations of heterogeneous compounds (benzothiazole) [3]. Therefore, it will easier to upgrade the remaining TDO to high-quality fuels. In addition to energy fuels, a fraction of the heavy TDO can be used as a feedstock in the production of carbon black.

9.3.3 Upgrading of the char to the intermediate products

The second product to the TDO in terms of the yields is the char. About 35 wt.% of the waste tyre is recovered as a char. To upgrade the char to the quality equivalent to carbon black and activated carbon is possible, however, it may not be economically viable. Therefore, partial upgrading of the char to products that can be used in various applications, such as, extenders in the manufacturing of adhesives, coatings and cements, is recommended. Henry (2015) observed that char can be upgraded by conventional techniques involving the use of the acid, alkali, and acid-alkali solvents [4].

9.3.4 Other techniques to improve waste tyre pyrolysis processes

Using the permanent gas fraction from waste tyre pyrolysis has been suggested by various researchers. Some researchers have pointed out that the permanent gases from waste tyre pyrolysis processes is sufficient to meet the energy requirement for the waste tyre pyrolysis process. Moreover, the permanent gases can be collected, compressed and stored for future use [5]. Finally, part of the waste tyre crumb should be diverted and directly recycled through devulcanization processes then used as a feedstock in the manufacturing of various products [6].

9.4 References

[1] S. Ngxangxa, Development of GC-MS methods for the analysis of tyre pyrolysis oils, Stellenbosch University. (2016).
[2] M.M. Ngwetjana, Fractionation of tyre derived oil, Stellenbosch University. (2017).
[3] N.M. Mkhize, B. Danon, P. van der Gryp, J.F. Görgens, Condensation of the hot volatiles from waste tyre pyrolysis by quenching, J. Anal. Appl. Pyrolysis. 124 (2017) 180-185.

[4] K.L. Henry, Upgrading pyrolytic tyre char through acid-alkali demineralisation, Stellenbosch University. (2015).

[5] N. Nkosi, E. Muzenda, A review and discussion of waste tyre pyrolysis and derived products, Lect. Notes Eng. Comput. Sci. 2 (2014) 979-985.

[6] D.W. Edwards, B. Danon, P. van der Gryp, J.F. Görgens, Quantifying and comparing the selectivity for crosslink scission in mechanical and mechanochemical devulcanization processes, J Appl Polym Sci. 133 (2016).

CHAPTER 10. APPENDIX

10.1 Patent: A system for processing waste rubber-derived hot volatiles

Patent journal: South Africa patents

Title: A system for processing waste rubber-derived hot volatiles

Patent application no.: 2016/05356

Date: 04 August 2016

Applicant: Stellenbosch University

Inventors: Mkhize, Ntandoyenkosi Malusi, Danon, Bart, Gorgens, Johann Ferdinand

Short summary

Quenching condenser was significantly better than the tube-and-shell condenser in cooling and condensing the hot volatiles from the pyrolysis reactor. Exchanging the tube-and-shell condenser with the quenching condenser highlighted innovative method of cooling and condensing the hot volatiles. Quenching condenser qualified for both innovation and (according to the findings from subsection 0) novelty. Merely publication of the findings on the research journal was not sufficient. The current subsection is part of objective 3 and summarises provisional patent application filed with the South African Patents. In the current subsection applicability and simplicity of the invention is highlighted. In the wake of the challenges in eliminating waste tyre piles which are increasing at a high rate, many local small business and government agencies (federal and local) are devising methods for waste tyre valorisation. Due to operation simplicity of the quenching condenser there is a potential that it can be adopted as a preferred method of cooling and condensing of the hot volatiles from pyrolysis reactor, it can also be suitable option for a variety of polymeric based materials in addition to the waste tyres. Although the current study focuses on the waste tyre processing, the effect of the quenching condenser to treat hot volatiles regardless of it nature is possible, including edible materials and their hot volatiles.

TITLE: A system for processing waste rubber-derived hot volatiles

N. M. Mkhize, B. Danon, J. F. Görgens*

Department of Process Engineering, Stellenbosch University, Private Bag X1, Matieland, 7602, Stellenbosch, South Africa

* Corresponding inventor: jgorgens@sun.ac.za

Abstract

Disclosed is a technique for cooling and condensing of hot volatiles from a waste tyre pyrolysis reactor by quenching condensation, entailing the use of direct contact (by e.g. spraying) between a polar cooling fluid (e.g. water, glycerol, acetonitrile etc.) and the hot volatiles from a pyrolysis reactor, in order to quickly condense the condensable gases fraction in the hot volatiles to form the tyre derived oil (TDO). The present technique improves the total TDO and DL-limonene yield (DL-limonene is a valuable chemical in the TDO) and decreases the benzothiazole concentration in the TDO (which is a nitrogen and sulphur containing 'smelly' compound). Moreover, elemental sulphur and char soot is extracted from the hot volatiles, thus not ending up in the TDO or permanent gases.

10.1.1 Background

High contents of C and H in waste tyres has characterised waste tyre pyrolysis as a potential source of energy, materials and chemicals [1]. Waste tyre pyrolysis entails thermal devolatilisation of the organic compounds present in the waste tyre under inert conditions to produce gaseous, liquid and solid products. Among these three products, i.e., (pyro) gas, tyre derived oil (TDO) and (pyro) char, the TDO is the most important fraction for energy recovery (engine fuel) and for the recovery of valuable chemical products (e.g. dipentene or DL-limonene) [2]. The TDO is separated from the gas by condensing the condensable fraction of the hot volatiles coming from the pyrolysis reactor.

Conventional methods and apparatus for cooling and condensing of the hot volatiles from waste tyre pyrolysis reactor is achieved by using a tube-and-shell type heat exchanger condensation train which has little effect on improving the quality of TDO [3-6]. Recently, there is interest in novel methods and apparatus of cooling and condensing hot volatiles from pyrolysis reactor by direct contact (spraying) with cooled TDO from previous waste tyre pyrolysis, as disclosed in the patents KR20120052210 and KR 20110138316 [7,8]. Direct contact of the hot volatiles from the pyrolysis reactor with the TDO from previous waste pyrolysis has no effect on the quality in terms of sulphurous and nitrogenous compounds as

well as impurities (sand, solids and char soot) in the TDO. In patent US 842731 B2, the method and apparatus used was similar to the conventional condensation train except that the hot volatiles were on the shell side of the heat exchange [9]. A disclosure of the permanent gases scrubbing in water containing scrubbing agents in an additional unit was claimed in patent KR20120052210 [7]. For the capturing of char soot from the permanent gases, patent CN104059396 discloses a method and apparatus that employs a separate additional unit (post condensation process) specifically for direct contact of permanent gases with water/detergent surfactant [10]. The method used entails bubbling of the permanent gases through a water bath.

10.1.2 Disclosure of invention

10.1.2.1 Technical problem

Although TDO is the most important waste tyre pyrolysis product for energy and valuable chemical products recovery, it is notoriously known as a low value pyrolysis product due to: i) high concentrations of nitrogenous and sulphurous compounds, ii) high concentrations of elemental sulphur, and iii) containing char soot. All of these properties are a result of the chemical composition of the tyre and the applied methods for waste tyre pyrolysis, particularly during cooling and condensation of the hot volatiles from waste tyre pyrolysis reactor.

High sulphur and nitrogen contents, high proportion of heavy molecules (gumming) and solid impurities in the TDO represent an obstacle for the application of the TDO as a fuel in combustion engines and for further processing to recover valuable chemicals [11]. Indeed, TDO has a higher viscosity and sulphur content [12] compared to petroleum derived diesel. Additionally, nitrogenous compounds in the TDO are undesirable because they can promote gum formation during TDO refining [13,14].

Sulphurous and nitrogenous compounds in the TDO have their origin in the thermal devolatilisation of the processing additives and vulcanisation agents used in the tyre formulation [13,15]. Even after upgrading of the low quality TDO (by e.g. moisture removal, sulphurous and nitrogenous compounds removal and distillation) to match the properties of petroleum derived fuels, economic competitiveness is still an impediment at the current prices of crude oil [16-19]. This is due to the cost associated with the processes required to upgrade the low-quality TDO [20].

10.1.2.2 Technical solution

The present invention is directed to a technique and apparatus for improving TDO in the process of cooling and condensing of the hot volatiles produced by performing pyrolysis on waste tyres that encompasses: rapid condensation of condensable gases to TDO by direct contact of the hot volatiles from the pyrolysis reactor with a polar cooling fluid (water, glycerol, acetonitrile, etc.) to improve TDO and DL-limonene yield.

The technique further encompasses: extraction of the nitrogenous and sulphurous compounds present in the hot volatiles from pyrolysis reactor by dissolving in the polar cooling fluid resulting into two phases, i) organic phase at the top, and ii) aqueous phase at the bottom. The technique further encompasses: selective separating of the top organic phase, containing the majority of the DL-limonene, using top exit point.

The technique further encompasses: circulating (reusing) the polar cooling fluid (aqueous phase containing the majority of the benzothiazole) and increasing nitrogenous and sulphurous compounds concentrations in the cooling fluid before blowdown of benzothiazole concentrated cooling fluid and then adding fresh make-up cooling fluid.

The technique further encompasses: wetting and capturing of the char soot from the hot volatiles from the pyrolysis reactor by direct contact with the polar cooling fluid. The preferred polar cooling fluid is liquid water.

The pyrolysis apparatus can be any kind of waste tyre pyrolysis reactor (i.e., continuous, semi-continuous or batch operated). The hot volatiles from the pyrolysis reactor are continuously fed in a quenching condensation tower. The quenching condensation unit allows periodical blowdown of benzothiazole concentrated polar cooling fluid from the TDO/cooling fluid tank and addition of fresh make-up polar cooling fluid either when pyrolysis is complete (no more volatiles evolving) or when the reuse of the benzothiazole concentrated polar cooling fluid is no longer practicable due to high benzothiazole concentration in the polar cooling fluid.

10.1.3 Advantageous effects

The present invention provides an effect of increasing total TDO yield due to the rapid condensation of hot volatiles from pyrolysis reactor using quenching condensation;

Further, the present invention improves DL-limonene yield due to the rapid condensation of hot volatiles from pyrolysis reactor using quenching condensation (DL-limonene is a valuable chemical in the TDO, estimated price around 2 US$ /kg) [2];

Further, the use of the present invention in cooling and condensation of the hot volatiles from the pyrolysis reactor results in the reduction of benzothiazole concentration in the TDO (which is a nitrogen and sulphur containing 'smelly' compound);

Further, the present invention provides extraction of the elemental sulphur from TDO and from the permanent gases; the elemental sulphur remains as solid particles in the aqueous fraction and can be readily separated;

Further, the use of the present invention eliminates the need for further scrubbing of the permanent gases since the permanent gases are immediately scrubbed in the quenching condensation tower, i.e., quenching condensation unit works also as a scrubber.

10.1.4 Best mode for carrying out the invention

In the subsequent paragraphs, a detailed description of the present invention is presented with reference to the accompanying drawings. Figure 10.1 and Figure 10.2 are a schematic process flow diagram and a schematic diagram showing process of the present invention and functionality of the quenching condensation, respectively.

Pyrolysis of waste tyre should be performed in a pyrolysis reactor by heating up the reactor in an inert atmosphere. As the hot volatiles evolve from the devolatilisation of the waste tyres, they are constantly purged out and separated from the solid residue (char) using flow of gas (for example by purging with an inert gas or by vacuum suction).

The hot volatiles from the pyrolysis reactor should be immediately introduced at the lower half of the quenching tower through an inlet pipe connecting the pyrolysis reactor with the lower half of the quenching tower. To prevent condensation of the hot volatiles in the pipe connecting the pyrolysis reactor to the quenching tower, this pipe should be maintained at an elevated temperature.

At the top of the quenching tower, a polar cooling fluid should be introduced using a spraying nozzle. The nozzle should be designed to form a full cone-spray profile covering the whole cross-sectional area of the quenching tower to maximise contact between the cooling fluid spray and the hot volatiles as the latter flow up the quenching tower.

Condensable gases then condense to form the tyre derived oil (TDO) by contact between the polar cooling fluid cone-spray flowing down counter-currently with the upward flow of the hot volatiles. The mixed liquid of TDO and polar cooling fluid is collected in the TDO/cooling fluid collecting tank at the bottom of the quenching tower. The two fluids are immiscible, thus the organic non-polar phase (i.e. TDO, containing the majority of the DL-limonene) floats over the polar phase cooling fluid (containing the majority of the benzothiazole) due to difference in polarity and densities.

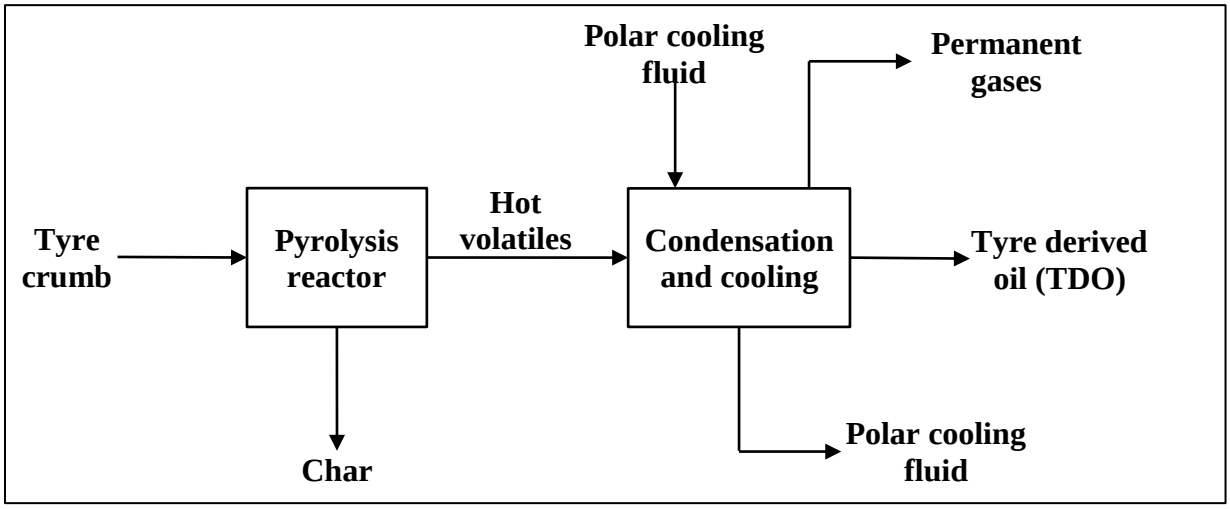

Figure 10.1: schematic process flow diagram of the present invention.

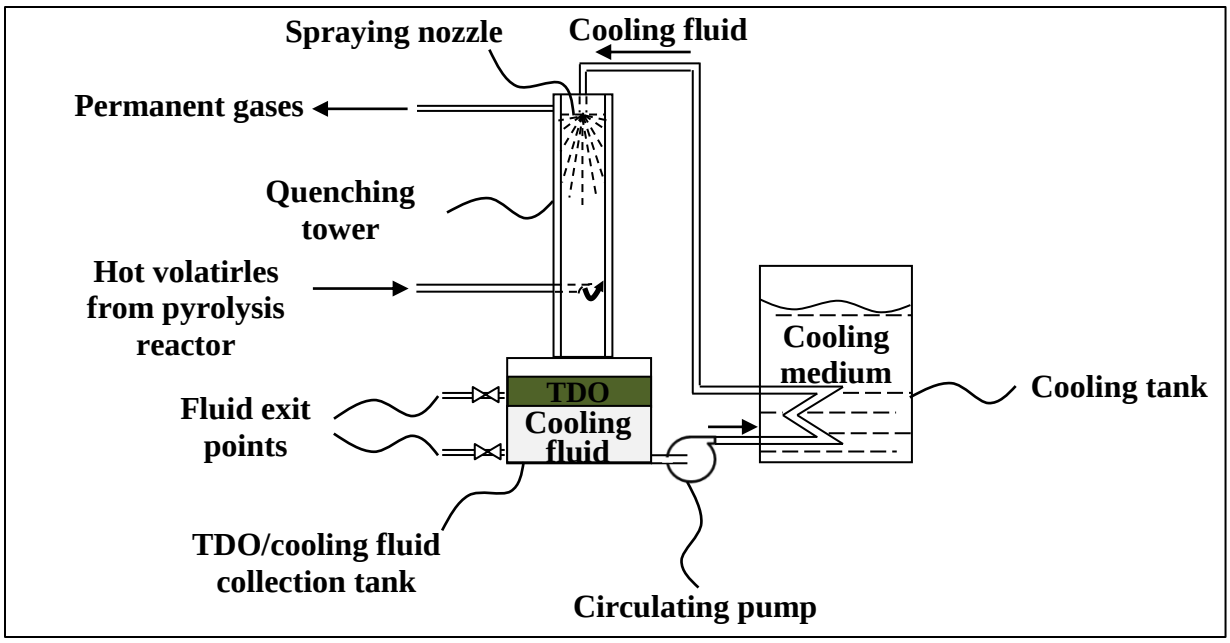

Figure 10.2: Schematic diagram depicting the functionality of the quenching condensation.

A known volume of polar cooling fluid should be initially added in the TDO/cooling fluid tank and then drawn out of the tank from the lower exit point at the bottom of the tank at a known flow rate using a circulating mechanism (e.g. a pump). The circulating mechanism should be employed to continuously circulate the polar cooling fluid through a heat removal and cooling unit to lower the temperature of the polar cooling fluid before being fed back into the quenching tower via the spraying nozzle at the top of the quenching tower. The cooling medium in the cooling tank can for example be ice/water slurry or by circulating cooling fluid using a chilling unit. The cycle should continue until the concentration of the nitrogenous and sulphurous compounds (mainly benzothiazole) in the cooling fluid has increased considerably or when the permanent gases exit the quenching tower via the top exit point.

Depending on the rate of the accumulation of the TDO, a higher exit point on the TDO/cooling fluid tank, corresponding to the level of the TDO phase, can be used to draw out TDO from the TDO/cooling fluid collecting tank. Therefore, there is no need for a post-separation process of the two products, TDO and cooling fluid, in the TDO/cooling fluid tank. DL-limonene in the TDO and benzothiazole in the cooling fluid can be extracted using existing technologies such as distillation and liquid-liquid extraction. Moreover, solid elemental sulphur can be readily separated from the cooling fluid.

10.1.5 Example

Two different experimental setups for condensation of hot volatiles from waste tyre pyrolysis were used to study the effect of quenching condensation by direct contact of hot volatiles from the pyrolysis reactor with a polar cooling liquid (water in this case). Both condensation setups were connected to a pyrolysis reactor, in the form of a horizontal (850 mm long, 60 mm OD) quartz tube, heated by six well-insulated and computer controlled elements. The first condensation setup consisted of a conventional condensation train (series of externally cooled vessels). The second setup is a quenching condensation tower.

A sample size of 40 g waste tyre was fed in a pyrolysis unit and heated up to the final temperature of 475 °C at a heating rate of 20 °C/min and held constant for 60 min. The hot volatiles evolving in the pyrolysis reactor were purged (and thus separated from the solid char product) by nitrogen gas at a flow rate of 1 L/min and subsequently introduced to either the condensation train (first setup) or quenching condensation tower (second setup). The products from both setups were weighed and the chemical composition of the obtained TDO's and the cooling water was determined, see Table 10.1.

As can be seen from Table 10.1, quenching condensation improved the total TDO yield by 4.7 % from 46.66 wt.% (condensation train) to 48.85 wt.% (quenching condensation). Moreover, the DL-limonene concentration in the TDO for the quenching condensation was higher at 31 990 ppm, compared to 28 178 ppm for condensation train. The benzothiazole concentration in the TDO decreased by 60 % when the condensation train was replaced by quenching condensation, from 5 382 to 2 168 ppm. Moreover, the benzothiazole concentration in the cooling water was high (1 333 ppm) compared to the concentration of DL-limonene (504 ppm) in that same cooling water.

In addition, it is shown that the two liquids (TDO and cooling water) separated well, which can be concluded from the low water content in the TDO from the quenching condenser (0.26 wt.%), see Table 10.1. Water content in the TDO from the quenching condenser is even lower than that of the TDO from the condensation train (the latter being 0.73 wt.%).

Table 10.1: Results of products from waste tyre pyrolysis with condensation train and quenching condenser.

Process	Parameters	Type of condensation	
		Condensation train	**Quenching condenser**
Waste tyre pyrolysis	Temperature (°C)	475	475
	Heating rate (°C/min)	20	20
Quenching condensation	Cooling water (l)	–	2.10
	Water spray flow (l/min)	–	0.96
Main products yield	Permanent gases (wt.%)	17.68	14.73
	Solid residue or char (wt.%)	35.66	36.42
	Tyre derived oil TDO (wt.%)	46.66	48.85
Organic phase (TDO)	DL-limonene (ppm)	28 178	31 990
	Benzothiazole (ppm)	5 382	2 168
	Water content (wt.%)	0.73	0.26
Aqueous phase (cooling water)	DL-limonene (ppm)	–	504
	Benzothiazole (ppm)	–	1 333

Acknowledgements

This research was supported by the Recycling and Economic Development Initiative of South Africa (REDISA) and the National Research Foundation (NRF). The authors acknowledge that opinions, findings and conclusions or recommendations expressed are those of the authors only, and the sponsors accept no liability whatsoever in this regard.

References

[1] I. Hita, M. Arabiourrutia, M. Olazar, J. Bilbao, J.M. Arandes, P. Castaño, Opportunities and barriers for producing high quality fuels from the pyrolysis of scrap tires, Renewable and Sustainable Energy Reviews. 56 (2016) 745-759.

[2] B. Danon, P. Van Der Gryp, C.E. Schwarz, J.F. Görgens, A review of dipentene (dl-limonene) production from waste tire pyrolysis, J. Anal. Appl. Pyrolysis. 112 (2015) 1-13.

[3] P.T. Williams, A.J. Brindle, Fluidised bed pyrolysis and catalytic prolysis of scrap tyres, Environmental Technology. 24 (2003) 921-929.

[4] M. Kyari, A. Cunliffe, P.T. Williams, Characterization of oils, gases, and char in relation to the pyrolysis of different brands of scrap automotive tires, Energy Fuels. 19 (2005) 1165-1173.

[5] M.F. Laresgoiti, B.M. Caballero, I. de Marco, A. Torres, M.A. Cabrero, M.J. Chomón, Characterization of the liquid products obtained in tyre pyrolysis, J. Anal. Appl. Pyrolysis. 71 (2004) 917-934.

[6] Y. Kar, Catalytic pyrolysis of car tire waste using expanded perlite, Waste Manage. 31 (2011) 1772-1782.

[7] C.H. Sun, Apparatus for extracting oil from used waste tire, (2012).

[8] C.H. Sun, Apparatus for extracting oil from used waste tire and method thereof, (2011).

[9] M. Ali, S.F.M. Shariff, C.J. Webb, Pyrolysis process for decomposing rubber products, (2013).

[10] H. Zhirongi, C. Dongsheng, Waste tire continuous segmentation pyrolysis process and equipment for carbon black capture, (2014).

[11] A.A. Zabaniotou, G. Stavropoulos, Pyrolysis of used automobile tires and residual char utilization, J. Anal. Appl. Pyrolysis. 70 (2003) 711-722.

[12] S. Murugan, M.C. Ramaswamy, G. Nagarajan, The use of tyre pyrolysis oil in diesel engines, Waste Manage. 28 (2008) 2743-2749.

[13] S. Mirmiran, H. Pakdel, C. Roy, Characterization of used tire vacuum pyrolysis oil: Nitrogenous compounds from the naphtha fraction, J. Anal. Appl. Pyrolysis. 22 (1992) 205-215.

[14] X. Chen, G. Clet, K. Thomas, M. Houalla, Correlation between structure, acidity and catalytic performance of WOx/Al2O3 catalysts, Journal of Catalysis. 273 (2010) 236-244.

[15] S. Murugan, M.C. Ramaswamy, G. Nagarajan, Assessment of pyrolysis oil as an energy source for diesel engines, Fuel Process Technol. 90 (2009) 67-74.

[16] H. Aydın, C. İlkılıç, Optimization of fuel production from waste vehicle tires by pyrolysis and resembling to diesel fuel by various desulfurization methods, Fuel. 102 (2012) 605-612.

[17] C. İlkılıç, H. Aydın, Fuel production from waste vehicle tires by catalytic pyrolysis and its application in a diesel engine, Fuel Process Technol. 92 (2011) 1129-1135.

[18] M. Rofiqul Islam, H. Haniu, M. Rafiqul Alam Beg, Liquid fuels and chemicals from pyrolysis of motorcycle tire waste: Product yields, compositions and related properties, Fuel. 87 (2008) 3112-3122.
[19] S. Murugan, M.C. Ramaswamy, G. Nagarajan, Performance, emission and combustion studies of a DI diesel engine using Distilled Tyre pyrolysis oil-diesel blends, Fuel Process Technol. 89 (2008) 152-159.
[20] S.H. Chung, J.G. Na, Method for upgrade-processing carbon black produced by performing a pyrolysis process on waste tires, (2014).

10.2 Published paper: Waste truck-tyre processing by flash pyrolysis in a conical spouted bed reactor

Journal: Energy Conversion and Management

Issue: 142

Pages: 523 - 532

Waste truck-tyre processing by flash pyrolysis in a conical spouted bed reactor

G. Lopez[a*], J. Alvarez[a], M. Amutio[a], N. M. Mkhize[b], B. Danon[b], P. van der Gryp[b], J. F. Görgens[b], J. Bilbao[a], M. Olazar[a]

[a]Department of Chemical Engineering, University of the Basque Country UPV/EHU, P.O. Box 644-E48080 Bilbao, Spain

[b]Department of Process Engineering, Stellenbosch University, Private Bag X1, Matieland, 7602, Stellenbosch, South Africa

* Corresponding author: gartzen.lopez@ehu.es

Abstract

The flash pyrolysis of waste truck-tyres was studied in a conical spouted bed reactor (CSBR) operating in continuous regime. The influence of temperature on product distribution was analysed in the 425 – 575 °C range. A detailed characterization of the pyrolysis products was carried out in order to assess their most feasible application. Moreover, special attention was paid to the sulphur distribution among the products. The analysis of gaseous products was carried out using a micro-GC and the tyre pyrolysis oil (TPO) by means of GC-FID using peak areas for quantification, with GC/MS for identification and elemental analysis. Finally, the char was subjected to elemental analysis and surface characterization. According to the results, 475 °C is an appropriate temperature for the pyrolysis of waste tyres, given that it ensures total devolatilisation of tyre rubber and a high TPO yield, 58.2 wt.%. Moreover, the quality of the oil is optimum at this temperature, especially in terms of high concentrations of valuable chemicals, such as limonene. An increase in temperature to 575 °C reduced the TPO yield to 53.9 wt.% and substantially changed its chemical composition by increasing the aromatic content. However, the quality of the recovered char was improved at high temperatures.

10.2.1 Introduction

Polymers have become a basic product that guarantee the current standard quality of living. Among them, and due to the growing transport necessities of modern societies, a continuous increase in the use of rubbers for tyre production has been reported [1]. According to recent estimations, the annual global tyre production is around 1.4 billion units [2], which means one car tyre is approximately discarded per inhabitant per year in developed countries. Moreover, around 4 billion waste tyres are currently in landfills worldwide [3]. Therefore, proper waste tyre management represents a major environmental challenge, since the inappropriate disposal of this non-biodegradable polymer could lead to significant issues. Accidental fires are especially risky due to the emissions of hazardous compounds and the great difficulty of their extinction [3]. Moreover, dumped waste tyres promote breeding of various pests and insects. Due to the relatively high heating value of waste tyres, direct combustion may be a promising energy recovery route, but this alternative faces significant restrictions due to the emissions of polycyclic aromatic hydrocarbons (PAHs), dioxins and particulate matter [4]. Accordingly, valorisation of waste tyres by pyrolysis has gained increasing attention over the last years due to its environmental and economic advantages [5]. More recently, the copyrolysis of waste tyres with other residues has also been regarded as a promising valorisation route [6,7].

The pyrolysis or thermal degradation under inert conditions of waste tyres gives way to three main products; gases, tyre pyrolysis oil (TPO) and residual pyrolysis char. The gases produced from waste tyres are mainly made up of hydrocarbons and some H_2, CO_2, CO and H_2S. Consequently, their main interest is energy production given that their heating value is high, usually above 35 $MJ.m^{-3}$ [1]. Gas fraction yield is enhanced at high temperatures and long residence times, as these conditions maximize secondary cracking at the expense of TPO. The main product obtained in the pyrolysis of waste tyres is the TPO, being a complex mixture of aliphatic and aromatic hydrocarbons and heteroatomic compounds [8]. This oil contains interesting chemicals in high concentration, in particular dl-limonene, if produced under suitable pyrolysis conditions [9]. Limonene is a valuable chemical and its market price is estimated at US$ 2 kg^{-1} [9]. The TPO can be used directly as a fuel, be it with some minor limitations, mostly related to its sulphur and aromatics content. However, its upgrading in existing refinery units allows overcoming these limitations [5]. The char derived from waste tyres consists of the carbon black added to tyre formulation, with varying adulteration degrees, depending on the pyrolysis conditions. In spite of the fact that its direct reutilization is an attractive option, its sulphur and ash contents, as well as its morphology, particle size distribution and porosity, are far from commercial carbon black specifications [10].

A wide range of reactor configurations have been applied to the pyrolysis of waste tyres. Fixed bed reactors operating in batch regime have been commonly used in the literature [11–14]. Despite their simple design and operation, this technology involves serious drawbacks for its large-scale development. Fluidised bed reactors are a more appropriate alternative for waste tyre pyrolysis, as they ease continuous operation and process scale-up. Moreover, their operation under fast pyrolysis conditions improves TPO yield [1,3]. Therefore, this technology has been widely used in the literature [15–17]. Another commonly proposed reactor design is rotary kiln since it allows good control of the process variables, especially waste tyre residence time in the reactor [18–20].

The conical spouted bed reactor (CSBR) has demonstrated adequate performance in the pyrolysis of different waste materials [21–25]. This reactor is characterized by its vigorous solid circulation, which allows operating under isothermal condition, with almost perfectly mixed regime for the solid and high heat and mass transfer rates. Accordingly, the CSBR allows for handling sticky and irregular materials without operational problems. This versatility for handling solids of different nature makes the CSBR suitable for the utilization of a catalyst in situ, as was demonstrated in previous studies dealing with catalytic pyrolysis of waste tyres [26,27]. Moreover, its short residence time for volatiles minimises secondary reactions in the gas phase, which enhances oil production in pyrolysis processes [21,25]. The main advantages and drawbacks of the CSBR in relation to other pyrolysis technologies have been discussed in detail elsewhere [28].

In the present study, continuous pyrolysis of waste truck-tyres was performed in a CSBR fitted with a non-porous draft tube. The use of the draft tube significantly improved spouting regime performance, given that bed stability was increased and fluidizing gas requirements reduced [29]. In fact, its use is critical for the full-scale application of the spouted bed technology. The main aim was to determine the influence of temperature on product yields and their composition, with the intention of determining their most suitable application. Thus, a sulphur mass balance has been carried out to determine its distribution among pyrolysis products and the limitations caused by its content on their possible uses. In addition, the results were compared with those in a previous study carried out in a fixed bed reactor operated at the same pyrolysis temperature [13]. Given that in both studies the same tyre material was used, the influence of pyrolysis conditions, specially heating rate and residence time, on process performance can be determined. Furthermore, the interest and originality of the study lies in the use of waste truck-tyre as they have a different composition in relation to the more studied light vehicle tyres.

10.2.2 Experimental section

10.2.2.1 Equipment

Continuous tyre pyrolysis runs were carried out in a bench scale plant, whose scheme is shown in Figure 10.3. The main component of the plant is the CSBR, whose design is based on the prior application of this technology to the pyrolysis and gasification of different solid wastes, such as biomass [21,22,30], plastics [23,31] and waste tyres [24,25]. The spouted bed reactor was heated by a two-independent section radiant oven that provides the heat to operate up to 900 °C. The lower section of the oven was used to preheat the gas and the upper section to heat the CSBR. The temperature in each section was controlled by means of thermocouples located inside the gaseous stream and in the silica sand bed, in the lower and higher sections, respectively.

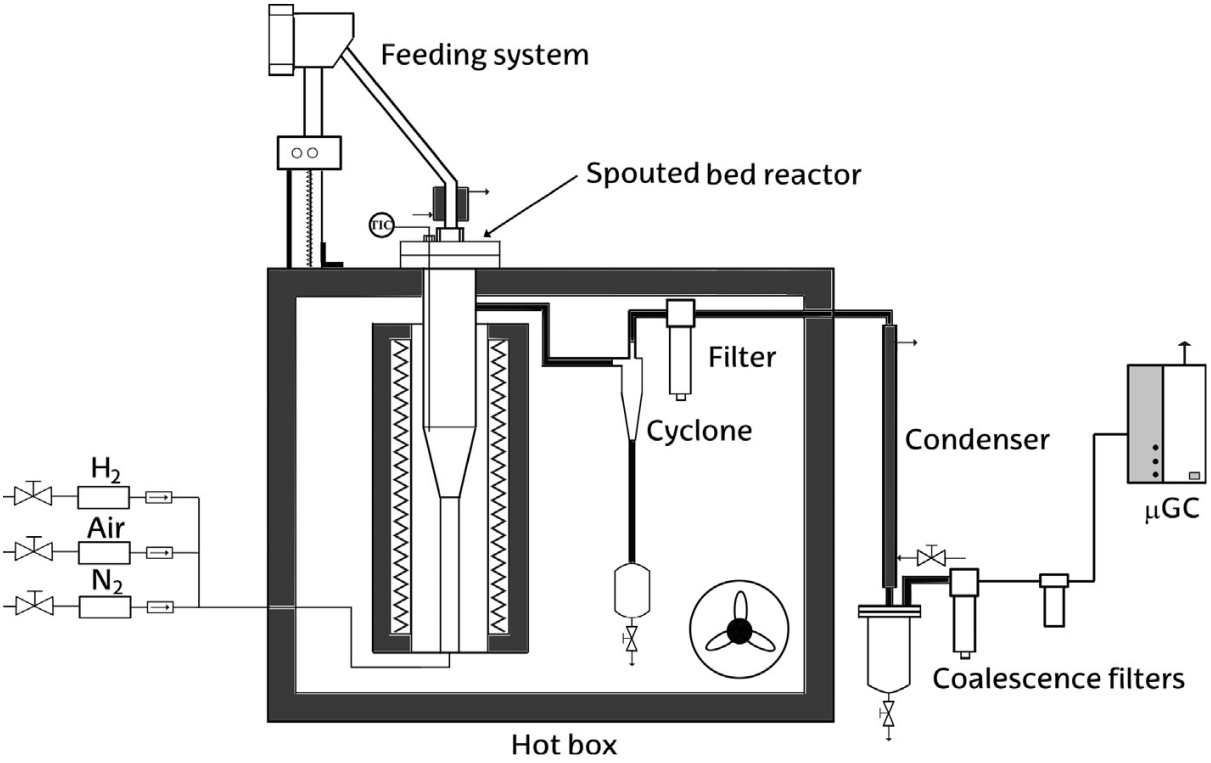

Figure 10.3: Scheme of the conical spouted bed bench scale plant.

The detailed design and dimensions of the CSBR are shown in Figure 10.4 and are as follows: an upper diameter of 95 mm, a cone height of 150 mm, a conical angle of 30 ° and a reactor total height of 430 mm. The base diameter is 20 mm and that of the gas inlet is 8 mm. The reactor allows for using draft tubes of different designs in order to fine-tune the spouting regime characteristics and improve its stability [32,33].

The design and main dimensions of that used in the present study are shown in Figure 10.4. The draft tube used in this study has an internal diameter of 10 mm, a total height of 85 mm and the height of the entrainment zone is 15 mm. This latter parameter is particularly important as it controls the solid circulation rate in the reactor [29,33].

The reactor together with the gas stream cleaning devices is located within a forced convection oven maintained at 300 °C to avoid the condensation of pyrolysis products before the condensation system. The gas cleaning system is made up of a high efficiency cyclone and a sintered steel filter (5 μm), which ensure the retention of fine char entrained from the bed. The fluidizing gas used in the experiments was nitrogen in order to ensure inert conditions, and its flow rate was measured by means of a mass flow meter (Brooks SLA5800).

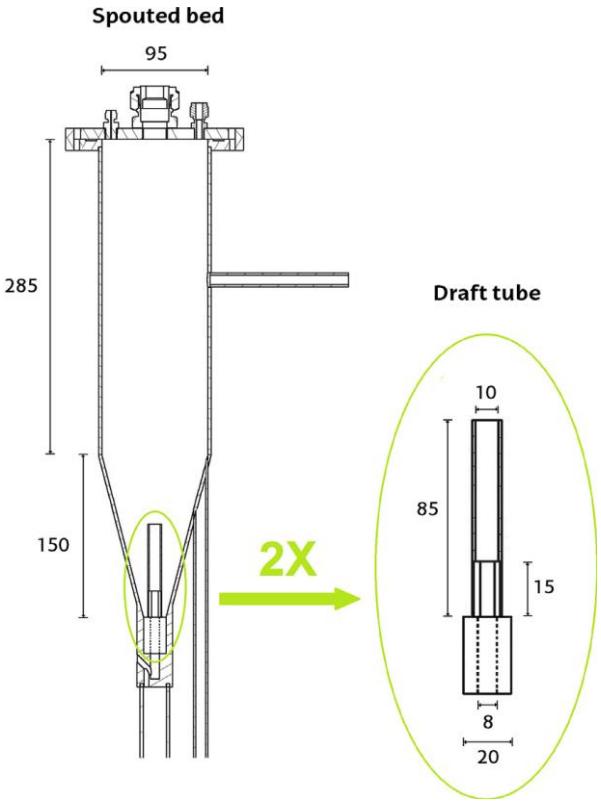

Figure 10.4: Dimensions (expressed in mm) of the conical spouted bed reactor and of the draft tube (enlarged two times).

The plant is provided with a system for continuous tyre rubber feeding, which consists of a cylindrical vessel equipped with a vertical shaft connected to a piston placed below the tyre material. The tyre was fed into the reactor by raising the piston at the same time as the whole system was vibrated by an electric engine.

In order to avoid pyrolysis vapours entering into the feeding system, a small nitrogen flow rate was introduced into the feeder. The feed rate can be adjusted from 0.5 to 8 $g.min^{-1}$, by varying the piston raising velocity, while the total feeding capacity is around 1 kg of tyre rubber. The feeding pipe was cooled with tap water to avoid premature pyrolysis of the feed material, which could lead to pipe clogging.

The product stream leaving the forced convection oven circulated through the volatile condensation system consisting of a condenser connected to a stainless steel filter. The condenser is a double-shell tube cooled by tap water. The condensed stream was then introduced into a steel filter that allows retaining fine TPO droplets from the gas. The TPO was collected in the tank where the filter is located. Finally the gases were filtered by coalescence filters in order to ensure they were clean prior to micro gas chromatograph (micro-GC) analysis.

10.2.2.2 Experimental conditions

In the pyrolysis runs, the CSBR contained 150 g of silica sand in order to ensure suitable heat transfer to the tyre rubber, with the sand particle size being between 0.3 and 0.8 mm. Nitrogen flow rate was 8 $L.min^{-1}$ in all the experiments, which is approximately 1.5 times that corresponding to the minimum spouting velocity [32]. These conditions guarantee a vigorous solid circulation in the reactor and accordingly suitable heat transfer conditions. The pyrolysis runs were carried out in continuous regime by feeding 1.3 $g.min^{-1}$ of tyre rubber. The effect of temperature on pyrolysis product distribution was studied in the 425 – 575 °C range. The duration of each experiment was of around 30 min in order to ensure operation under steady state conditions and reproducibility of gaseous product analysis. Moreover, the runs were repeated at least 3 times under the same experimental conditions to guarantee
the soundness of the results.

Once continuous pyrolysis had been carried out for 30 min, the tyre rubber feeder was stopped and the reactor was cooled under nitrogen atmosphere. The amount of char or residual carbon black formed was determined by weighting the mass remaining in the reactor and that retained in the cyclone and in the sintered steel filter located downstream the reactor. Its yield was calculated based on the mass obtained in the different places mentioned and the amount of tyre fed into the reactor in each run.

10.2.2.3 Product analysis

The gaseous pyrolysis products were analysed in-line in a micro-GC (Varian 4900) equipped with four modules, namely, Molecular sieve 5, Porapak (PPQ), CPSil and Plot Alumina. Molecular sieve column operated at 80 °C and 20 psi, Porapak at 90 °C and 25 psi and both CPSil and Plot at 110 °C and 25 psi.

In order to determine the gas yield, cyclohexane was used as external reference because it is not formed in the process. Given that the pyrolysis process operated in continuous regime with a steady tyre feed rate, the gas products yields could be assessed by comparing their concentration with that of cyclohexane. A constant flow of 0.05 $ml.min^{-1}$ was injected downstream the condensation system and was analysed in the micro-GC together with the other gaseous products formed.

The TPO obtained in the condensation system was analysed in a gas chromatograph (GC, Agilent 6890) and in a chromatograph/mass spectrometer (GC/MS, Shimadzu UP-2010S), with the former being used for its quantification and the latter for the identification of individual compounds in the TPO. The Agilent 6890 gas chromatograph was equipped with a HP PONA column (50 m, 0.22 mm, 0.25 mm) and the temperature programme was as follows: a heating ramp of 3 $°C.min^{-1}$ from 40 °C to 320 °C followed by an isothermal one at 320 °C for 8 min in order to ensure total removal of all products from the column. In the case of GC/MS Shimadzu QP-2010S, the column used was a BPX-5 (50 m, 0.22 mm, 0.25 mm) and the temperature sequence of the oven was the same previously described for the GC. The column was connected to a mass spectrometer and operated under the following conditions: ion source and interface temperatures were 200 °C and 300 °C, respectively, operating in the 33–330 m/z range.

The gaseous product heating value has been determined based on the N_2 free basis composition and the heating values of individual compounds. The elemental analysis of waste truck-tyre, the TPO and the char was carried out in a LECO CHNS-932 elemental analyzer, while their higher heating value (HHV) was determined using a Parr 1356 isoperibolic bomb calorimeter. Finally, proximate analysis of the truck-tyre and char was performed using a TGA Q500IR thermobalance. The water content of the TPO was determined by Karl-Fischer Titration (ASTM D1744).

The pyrolysis process mass balance was closed by considering the amount of tyre rubber fed in each run, the volume of gases produced, which was determined using cyclohexene as internal standard, and the mass of TPO and char produced.

10.2.2.4 Tyre material characterization

The waste truck-tyre rubber used in this study was supplied by a tyre recycling company of South Africa (Enviroserv (Pty) Ltd), being almost completely free of steel and textiles. The particle size of this material was from below 1 mm to 5 mm and, although this size is suitable for the feeding system of the plant and the CSBR allows for handling coarse materials, it was sieved to between 2.8 and 3.3 mm prior its utilization. The results of the proximate, ultimate and HHV analyses are summarized in Table 10.2.

Table 10.2: Characterization of the truck tyre rubber used in the present study.

Ultimate analysis (wt.%)[a]	
Carbon	84.3
Hydrogen	7.7
Nitrogen	0.8
Sulphur	2.5
Oxygen	4.7[*]
Proximate analysis (wt.%)[b]	
Volatile matter	65.1
Fixed carbon	29.9
Ash	4.9
HHV ($MJ.kg^{-1}$)	38.2

[a] Ash free basis

[b] On dry basis

[*] Calculated by difference

Moreover, around 25 g of waste truck-tyre were calcined in a muffle furnace in order to obtain a representative ash sample. Subsequently, the ashes were analysed by means of X-ray fluorescence (model AXIOS, PANalytical). The detailed composition of the ash is reported in Table 10.3.

Table 10.3: Chemical composition of tyre rubber ashes.

Compound	wt.%
ZnO	48.01
SO_2	36.17
SO_3	4.59
Al_2O_3	3.91
CaO	1.84
K_2O	1.13
Fe_2O_3	0.89
P_2O_5	0.85
MgO	0.68
TiO_2	0.17

The thermal degradation behaviour of waste truck-tyre was analysed in a thermogravimetric analyzer, TGA Q500IR. Prior to TGA experiments, the tyre material was subjected to a cryogenic grinding (Retsch ZM 100) in order to obtain a particle size below 0.5 mm and avoid heat transfer limitations throughout their degradation. The mass used in each run was of around 10 mg, and the heating rate used was of 10 °C.min^{-1}. Each experiment was repeated three times in order to ensure the reproducibility of the results. Moreover, the interest of the thermogravimetric analysis results lies in the possibility to use differential thermogravimetric (DTG) curve to assess the tyre material composition [34–37]. Thus, DTG results have been fitted to a multi-component model that describes the rubber degradation by considering the volatile formation by means of three concurrent independent and parallel reactions. The pseudo-components considered are the additives and the rubbers typically contained in the truck tyres, i.e., natural and synthetic rubbers (see Figure 10.5). Natural rubber decomposition usually takes place between 300 and 480 °C. Finally, styrene-butadiene rubber is characterized by its higher thermal stability and pyrolyzes in the 360–500 °C range, appearing as a shoulder of the natural rubber degradation peak. Other authors have observed similar degradation behaviours of tyre rubber components in thermogravimetric studies [35,36,38,39].

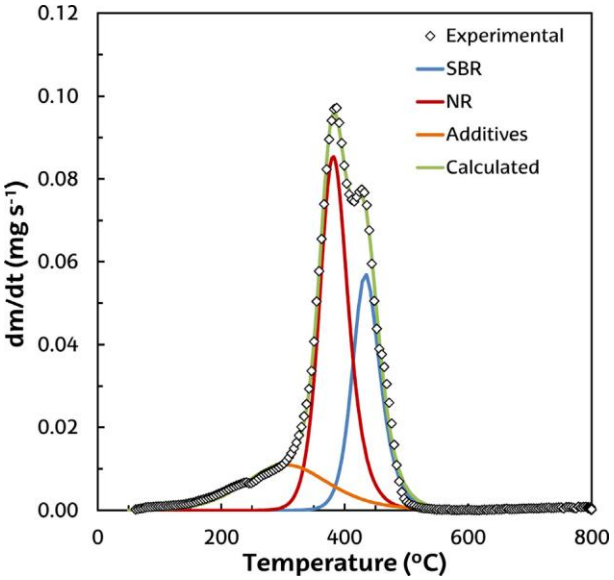

Figure 10.5: Comparison of DTG experimental results (points) and those estimated usingthe model proposed (lines).

Therefore, the model proposed considers three parallel independent reactions of n-th order, with the overall kinetic equation being as follows;

$$\left(-\frac{1}{w_0-w_\infty}\right)\left(\frac{dw}{dt}\right) = \sum_{i=1}^{3} c_i k_i \left[\frac{w_i-w_{\infty i}}{w_{0i}-w_{\infty i}}\right]^{n_i} \quad (1)$$

The following definition of conversion was considered;

$$X = \frac{w_0-w}{w_0-w_\infty} \quad (2)$$

where w, w_0, and w_∞ are the tyre rubber mass at time t, initially and at the end of the thermal degradation, respectively. According to the conversion definition shown in Eqs. (2) and (1) can be expressed as;

$$\frac{dX}{dt} = c_1 k_1 (X_{\infty 1} - X_1)^{n_1} + c_2 k_2 (X_{\infty 2} - X_2)^{n_2} + c_3 k_3 (X_{\infty 3} - X_3)^{n_3} \quad (3)$$

where X_i and $X_{1,i}$ are the conversion at time t and the final conversion of each pseudo-component, c_i the mass concentrations of additives, natural and synthetic rubber and n_i the reaction order with respect to each pseudo-component.

By fitting the DTG experimental results to the kinetic model proposed the concentration of each tyre component (c_i) has been determined. In addition, the kinetic parameters, reaction order, frequency factor and activation energy corresponding to each component have also been estimated. The theoretical DTG curve is obtained as the addition of those corresponding to the individual components and has been fitted by minimizing the following error objective function;

$$EOF = \frac{\sum_{j=1}^{L}\left[(DTG)_{calculated} - (DTG)_{experimental}\right]^2}{L} \quad (4)$$

where L is the number of data points used for the fitting.

Figure 10.5 shows the comparison of DTG experimental curve and that calculated with the model as the addition of individual compound degradation. As observed, the three independent reaction model provides an excellent fitting to the experimental results. Table 3 shows the kinetic parameters obtained for the thermal degradation of each pseudo-component and their content. The ci values shown in Table 3 are the relative contents of each component, and the actual contents are the values based on the tyre volatile matter, that is, without fixed carbon and ashes. Therefore, the waste truck-tyre used in this study is approximately made up of 32 wt.% natural rubber, 21 wt.% synthetic rubber and 12 wt.% additives, with the balance being 35 wt.% ashes and carbon black.

Table 10.4: Tyre rubber component contents and kinetic parameters of the thermal degradation of the pseudo-components determined by DTG curve fitting.

	Log k_0 (s^{-1})	**E ($kJ.mol^{-1}$)**	**n**	**c_i (wt.%)**	**Actual content (wt.%)**
Additives	1.87	45.2	1.52	18.3	11.9
Natural rubber	16.89	231.8	2.24	49.6	32.3
Synthetic rubber	19.62	283.6	2.17	32.1	20.3

10.2.3 Results

10.2.3.1 Effect of temperature on product distribution in the CSBR

The influence of temperature on the product distribution obtained from the continuous pyrolysis of waste truck-tyres was studied in the 425–575 °C range. The products were grouped into three fractions; (i) the gaseous products, including C_1 to C_5 hydrocarbons, CO, CO_2 and H_2S, (ii) the liquid fraction or TPO, which is made up of hydrocarbons heavier than C6, and (iii) char or residual carbon black.

Figure 10.6 shows the evolution of the yields of pyrolysis products in the 425 – 575 °C range. The main product obtained was the TPO, whose yield kept almost at a constant value slightly above 58 wt.% at 425 and 475 °C, but was significantly reduced to 53.9 wt.% at 575 °C. On the other hand, the gas fraction yield increased linearly from 3.6 to 10.2 wt.% in the studied temperature range. The same trend of gas and TPO yield evolution with temperature was reported by several authors using different pyrolysis technologies [15,40–43], and temperatures of around 500 °C were regarded as the most suitable for tyre pyrolysis process [3,42,44]. This behaviour is related to the promotion of secondary cracking reactions at higher temperatures which gives way to gas production at the expense of liquid hydrocarbons [3]. The extent of these reactions is highly influenced by the residence time of primary pyrolysis products in the reactor. Accordingly, the low residence times in the CSBR results in a relatively modest increase in gas yield with temperature.

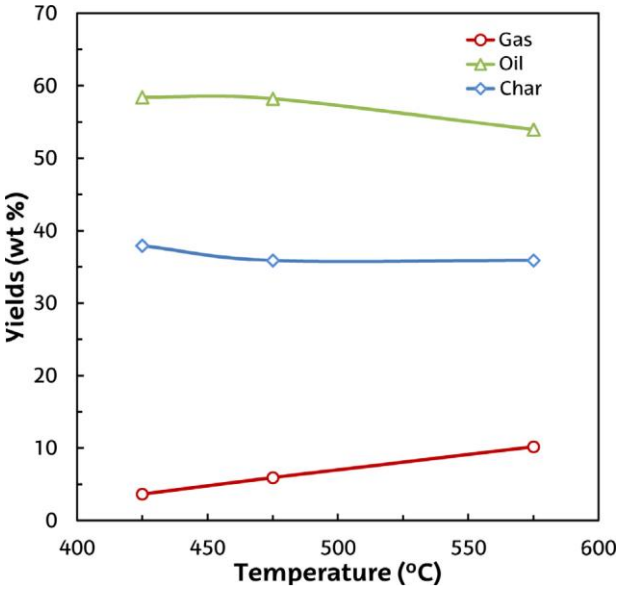

Figure 10.6: Effect of temperature on pyrolysis products yields in the 425 – 575 °C range.

The char yield was reduced from 37.9 wt.% at 425 °C to 35.9 wt.% at 475 °C, while this value remained constant when the temperature was further increased to 575 °C. Accordingly, it can be concluded that tyre rubber devolatilization is complete at 475 °C, with this point being confirmed by the proximate analyses of the chars obtained at different temperatures. This fact is due to the high heat and mass transfer rates attained in the CSBR, which eases the full conversion of tyre rubber even at low temperatures. Thus, even considering the relatively low heating rate used (10 °C.min^{-1}) in the thermobalance, a remarkable difference in the pyrolysis behaviour is observed when both results are compared, in fact, a temperature of around 500

°C was required for the complete devolatilization of the same tyre rubber in the pyrolysis carried out in thermobalance (see Figure 10.5).

Interestingly, the possibility to achieve complete pyrolysis of the sample at low temperatures together with short residence times of the gaseous products in the CSBR minimizes secondary cracking reactions, and therefore leads to high TPO yields [8,24,25,42]. The maximum TPO yields reported in the literature vary considerably depending on the pyrolysis conditions, being those usually obtained in the fixed bed reactors and rotary kilns below those obtained in the present study. Thus, the TPO yields obtained in fixed bed reactors are in the 30 to 55 wt.% range [43–46] and those typically reported in rotary kilns and screw kilns are of around 40 wt.% [18,20,47]. On the other hand, fast pyrolysis conditions in fluidised bed reactors improve the TPO yield leading to values above 50 wt.% [15,16,40]. The application of microwave assisted pyrolysis is gaining growing interest, and the conditions attained in this technology are characterized by relatively low heating rates and long residence times, thereby the TPO yields are usually in the 30 to 45 wt.% range [48,49]. It is of particular interest here to compare the results of this study with those reported by Mkhize et al. [13], given that this study was carried out with the same waste truck-tyre and consequently, any influence of the material composition on product yields is avoided. These authors reported a maximum TPO yield of around 45 wt.% in a fixed bed batch reactor using heating rates between 1 and 29 °C.min^{-1} and final temperatures between 450 and 591 °C. These results therefore stipulate the performance of flash pyrolysis conditions attained in a CSBR for maximization of TPO production.

10.2.3.2 Properties of pyrolysis products

Gas product

The gas product obtained in the pyrolysis of waste tyres is a mixture of C_1 to C_5 alkanes and alkenes, with varying contents of H_2, CO, CO_2 and sulphurous gases. The composition of the gases and the individual product yields obtained at different temperatures was determined by micro-GC analysis (see Section 10.2.2.3) and is shown in Table 10.5. As observed, at low temperatures the gases were mainly made up of olefins of 4 and 5 carbon atoms. These hydrocarbons can be directly formed from natural or synthetic rubber depolymerisation [8,9]. However, at higher temperatures a significant increase in methane and C_2 hydrocarbons was observed [50], with these compounds being mainly formed by secondary cracking reactions [1].

The main component in the pyrolysis gases at low temperatures is 1,3-butadiene, which is produced by the thermal degradation of synthetic rubber [15,42]. Despite the fact that its yield increased with temperature, its concentration in the gas was remarkably reduced, which is due to the increasing quantities of light compounds in the C_1-C_3 range. The concentration and yield of isoprene, a monomer of natural rubber, followed a similar trend as that observed for 1,3-butadiene.

Additionally, the H_2 concentration in the gas increased with temperature (Table 10.5), which was attributed to the intensification of aromatization and cyclization reactions [51]. The presence of CO and CO_2 in the tyre pyrolysis gases was attributed to the thermal degradation of oxygenated additives (i.e., extender oils or stearic acid) and charges (as $CaCO_3$) [1]. The only sulphur compound measured in the gas was H_2S, whose concentration was sharply reduced with temperature.

Table 10.5: Gas fraction products yields and composition in the studied temperature range.

	Concentration (% vol.)			Yields (% wt)		
Temperature (ºC)	**425**	**475**	**575**	**425**	**475**	**575**
H_2	17.6	14.6	18.4	0.03	0.04	0.10
CH_4	2.8	18.9	16.9	0.04	0.45	0.77
CO	2.3	1.9	1.8	0.06	0.08	0.14
CO_2	7.9	5.6	2.7	0.30	0.37	0.34
C_2	3.0	4.0	14.6	0.10	0.20	1.20
Ethylene	1.5	2.5	8.0	0.04	0.10	0.64
Ethane	1.5	1.6	6.6	0.04	0.07	0.56
C_3	3.5	3.4	7.3	0.10	0.20	0.9
Propylene	1.8	1.6	5.1	0.06	0.10	0.61
Propane	1.7	1.8	2.2	0.06	0.12	0.28
C_4	33.0	23.6	16.7	1.53	1.91	2.59
butane	1.1	0.9	0.7	0.06	0.07	0.12
1,3-butadiene	28.7	19.5	11.1	1.32	1.57	1.70
butenes	3.1	3.3	4.9	0.15	0.27	0.78
C_5	25.5	24.7	20.7	1.36	2.51	4.04
isoprene	20.4	19.8	11.3	1.18	2.00	2.19
2-pentene	2.7	3.1	6.1	0.16	0.32	1.21
methyl-butenes	0.2	1.8	3.3	0.01	0.19	0.65
H_2S	4.3	3.1	0.9	0.12	0.16	0.08
Total	100	100	100	3.64	5.91	10.16

Several authors have remarked that the main interest of the gas produced in the pyrolysis of waste tyres is energy production [3], in fact its burning can meet the pyrolysis reactor heat necessities. Thus, the higher

heating values (calculated on a N_2 free basis) of the gas obtained in the present study ranged between 44.4 $MJ.kg^{-1}$ obtained at 425 °C and 48.7 $MJ.kg^{-1}$ at 575 °C, and these values are of the same order as those reported by other authors [44,52,53].

TPO properties

The TPO obtained in the pyrolysis of tyres was a dark oil of medium viscosity mainly made up of hydrocarbons of different nature, such as olefins, paraffins and aromatics. In addition, the presence of sulphur containing compounds was also remarkable. The TPO was analysed by GC and GC–MS techniques, to determine the main chemical compounds and chemical families present. As observed in Table 10.6, the prevailing compounds in the TPO at low temperatures were aliphatics, with a maximum yield of 25.7 wt.% at 475 °C, with almost 90% of them being olefins. This fact is related to the unsaturated nature of the polymers contained in waste tyres. The increase of pyrolysis temperature resulted in a modification of TPO composition, given that the yield in aromatic hydrocarbons increased at the expense of aliphatics, from 7.4 wt.% at 475 °C to 27.3 wt.% at 575 °C. Thus, the relative aromatic content in the TPO increased from 12.7 to 50.6 wt.% in the mentioned range. The aromatisation of TPO with temperature has been observed by several authors [12,15,24,54,55], being a process associated with the enhancement of secondary reactions of cyclization of olefins, dehydrogenation and Diels-Alder reactions taking place in the gas phase [42,44,53,56]. It should be noted that the aromatic hydrocarbons yield is also affected by the original tyre composition; a higher presence of SBR in the tyre formulation leads to a higher aromatic content in the TPO [3,24,44]. Among aromatics, the yield of xylenes and styrene derived products was remarkable at the highest temperature studied, 575 °C. In spite of the fact that the yield of polyaromatics was significant at this temperature, 8.4 wt.%, their presence was very low at 425 and 475 °C, and this fact improves the perspectives of TPO direct utilization as fuel.

The most important individual compound obtained in the TPO was limonene, which is formed by intramolecular cyclization of the allylic radicals produced by random scission of polyisoprene chain [9]. The interest of this product lies in its wide applications as solvent, in the production of resins and adhesives, as well as in the cosmetic industry. A maximum limonene yield of 14.1 wt.%, including d- and l- isomers, was obtained at 475 °C, while a further increase of temperature to 575 °C decreased its yield to 4.5 wt.%. Indeed, Danon et al. [9], reviewing limonene production from waste tyre pyrolysis, suggested the range between 400 and 500 °C as optimal for limonene production maximization. The yield of limonene is strongly influenced by pyrolysis conditions, especially temperature, residence time and pressure; due to its unstable nature under pyrolysis conditions it can be easily transformed into isoprene or aromatic

hydrocarbons, such as indane, cymene, trimethyl benzene [3]. In order to compare the limonene yields obtained with the same tyre material from the fixed bed reactor (FBR) [13], the different quantification method used should also be considered, i.e. internal standard calibration curve was used in the FBR study and GC/FID peak areas in the present study. Thus, the limonene yield at 475 °C in the CSBR was higher (14.1 wt.%) than that in the FBR (7.6 wt.%). The difference in limonene yield between the FBR [13] and the CSBR indicates the potential of flash pyrolysis conditions, namely, very short residence time and very high heating rates, attained in the CSBR for obtaining higher limonene yields. A more detailed discussion of the main features of the CSBR in relation to other pyrolysis technologies can be found elsewhere [28].

The concentration of oxygen containing compounds was low (Table 10.6), being these compounds derived from the degradation of oxygenates present in the waste tyre composition, such as stearic acid and extender oils [57]. The most relevant nitrogen and sulphur containing compound detected in the TPO was benzothiazole, (Table 10.6), which is added to tyre formulation as a vulcanization agent [55]. Similarly, the origin of other nitrogenous and sulphurous compounds is also related with the degradation of vulcanization additives [58]. The presence of these sulphur containing compounds lead to a sulphur content above 1 wt.%, as determined by ultimate analysis. This content increased slightly from 1.15 wt.% at 475 °C to 1.27 wt.% at 575°C. These values are consistent with those previously reported in the literature [12,44,53–55]. The ultimate analyses of the TPOs obtained at different temperatures and their heating values are reported in Table 6. As observed in Table 10.7, the carbon content of the TPO is above 85 wt.%. In addition, pyrolysis temperature led to an increase in this content, but to a decrease in hydrogen content, with both facts being consistent with the previously mentioned aromatisation caused by temperature. The unstable nature of oxygenates caused a reduction in the oxygen content as temperature is raised. However, the sulphur content remained almost constant in the studied temperature range.

Table 10.6: Yields of TPO individual compounds and chemical families (in bold) obtained at different temperatures (by mass unit of the tyre).

		Temperature (°C)		
Compounds, families (wt. % tyre)	**Formula**	**425**	**475**	**575**
Aromatics		**7.02**	**7.43**	**27.32**
o-Xylene	C_8H_{10}	0.32	0.44	1.98
α-Methylstyrene	C_9H_{10}	0.01	0.01	1.25
1,3,5-Trimethyl-benzene	C_9H_{12}	-	-	1.44
1-Ethenyl-4-methyl-benzene	C_9H_{10}	-	-	1.61
α-Dimethylstyrene	$C_{10}H_{12}$	0.54	0.58	2.28
1,2,3,5-Tetramethyl-benzene	$C_{10}H_{14}$	0.11	0.11	0.88
1-Ethyl-4-(1-methylethyl)-benzene	$C_{11}H_{16}$	0.25	0.16	0.91
Aliphatics		**23.87**	**25.70**	**11.59**
Alkanes		*2.70*	*2.91*	*1.74*
2,2,4,4-Tetramethyl-pentane	C_9H_{20}	0.45	0.53	0.04
1-Butenylidenecyclohexane	$C_{10}H_{16}$	0.27	0.37	0.52
n-Pentadecane	$C_{15}H_{32}$	0.21	0.52	0.12
n-Octadecane	$C_{18}H_{38}$	0.51	0.44	0.07
Alkenes		21.17	22.79	9.85
5,5-Dimethyl-2-propyl-1,3-cyclopentadiene	$C_{10}H_{16}$	0.12	0.10	0.93
3,3,6,6-Tetramethyl-1,4-cyclohexadiene	$C_{10}H_{16}$	0.33	0.32	0.54
2,5-Dimethyl-3-methylene-1,5-heptadiene	$C_{10}H_{16}$	0.46	0.50	-
1-Methyl-4-isopropyl-1-cyclohexene	$C_{10}H_{18}$	0.45	0.55	-
2,4,4,6-Tetramethyl-2-heptene	$C_{11}H_{22}$	0.66	0.65	-
L-Limonene	$C_{10}H_{16}$	0.48	0.84	0.68
D-Limonene	$C_{10}H_{16}$	12.30	13.30	3.80
Heteroaromatics		**9.03**	**8.35**	**3.32**
Benzothiazole	C_7H_5NS	0.59	0.90	0.98
2,2,4-Trimethyl-1,2-dihydroquinoline	$C_{12}H_{15}N$	0.66	0.48	0.03
Tetradecanoic acid	$C_{14}H_{28}O_2$	3.41	2.68	-
Water	H_2O	**0.86**	**0.45**	**0.28**
Undentified		**17.65**	**16.30**	**11.45**
Total		**58.43**	**58.22**	**53.96**

Table 10.7: Ultimate analysis and HHV of the TPOs obtained at different temperatures.

Ultimate analysis (wt %)						**HHV ($MJ.kg^{-1}$)**
Temperature (°C)	Carbon	Hydrogen	Nitrogen	Sulphur	Oxygen	
425	85.0	11.0	0.1	1.2	2.8	42.5
475	86.0	10.8	0.3	1.2	1.7	42.7
575	88.0	10.2	0.2	1.3	0.3	42.8

The TPO is characterized by a HHV much higher than that of biomass pyrolysis oils, being of the same order of magnitude as those of petroleum derived fuels. Those obtained in the present study range from 42.5 $MJ.kg^{-1}$ at 425 °C to 42.8 $MJ.kg^{-1}$ at 575 °C. However, the rather high sulphur and aromatic contents of TPO may limit its direct application as fuel in internal combustion engines [3]. In order to overcome this limitation, different hydrotreating strategies have been proposed in the literature yielding promising results [59,60]. Additionally, TPO compete with petroleum derived fuels at current relatively low prices. However, high concentration of limonene in the TPO and its high market value of US$ 2 kg^{-1} increase TPO potential as a source of limonene, while using the remaining TPO as a fuel [9]. Therefore, operating a CSBR at a temperature of 475 °C is more attractive as it results into high limonene yield even without improvement in TPO yield compared to 425 °C. A slightly higher pyrolysis temperature at a higher heating rate, such as happens in the CSBR compared to the heating rate attained in the FBR, is consistent with higher temperature requirements corresponding to maximum limonene formation rate during devolatilisation of polyisoprene or NR [13].

Char properties

The char obtained in the pyrolysis of waste tyres is mainly made up of the carbon black added to tyre formulation to improve its anti-abrasive performance. Moreover, the ashes are derived from its inorganic additives. In fact, the individual pyrolysis of rubber components of the tyre, i.e. styrene-butadiene, natural and polybutadiene rubbers, allows very low char yields [61]. The quality of char plays a key role over the overall economic feasibility of tyre pyrolysis process [62], the quality of this material being strongly dependent on the pyrolysis conditions. In order to assess the main valorisation routes of the char produced by continuous pyrolysis in a CSBR, it was subjected to a detailed characterization. Table 10.8 summarizes the main properties of the char obtained at different temperatures. As observed in Table 10.8, tyre pyrolysis char was characterized by its high carbon content, between 83 and 86 wt.%. The sulphur content was also remarkable, increasing from 2.9 wt.% at 425 °C to 3.6 wt.% at 575 °C. Similarly, other authors reported values of the same order [18,24,40,44,53,54,63]. The fixed carbon content remarkably increased from 77.1 to 87.5 wt.% in the 425 to 475 °C range, however, a further increase to 575 °C did not affect its content. This result confirms that 475 °C is a high enough temperature to ensure the complete degradation of tyre rubber. Interestingly, the volatile matter in the char was very low at 475 °C and 575 °C, with this factor being a good indicator of a very low presence of tars adsorbed in the char porous structure, which was also confirmed by the lack of a greasy texture.

The ash content of the char somewhat increased with temperature and the ash composition could be similar to that previously reported in Table 2, that is, their main component was ZnO. The proximate analyses of tyre chars reported in the literature are similar to those of the present study. Thus, the fixed carbon values are of around 90 wt.% [53,64], but their ash content vary in a wide range, between 5 and 20 wt.% [1,48], given that it strongly depends on the original tyre composition.

Table 10.8: Characterization of the char or residual carbon black obtained at different temperatures.

	Ultimate analysis (wt %)					Proximate analysis (wt %)*		
Temperature (ºC)	Carbon	Hydrogen	Nitrogen	Sulphur	Oxygen	Volatile matter	Fixed carbon	Ash
425	83.81	1.99	0.65	2.96	2.8	13.86	77.1	9.04
475	85.71	0.86	0.67	3.28	1.7	3.17	87.54	9.29
575	84.98	0.83	0.69	3.63	0.3	2.72	87.66	9.62

*On dry basis

Pyrolysis temperature had a considerable effect on char surface properties resulting in an increase in BET surface area to a maximum value of 80 $m^2.g^{-1}$ at 575 °C, with this effect being similar to that observed in previous studies [1]. The surface properties of the chars obtained at different temperatures are set out in Table 10.9. This improvement of char porosity was related with the loss of high molecular weight solid hydrocarbons, which promotes pore opening and widening [8].

Table 10.9: Surface properties of the chars obtained at different temperatures.

Temperature (ºC)	Area BET ($m^2.g^{-1}$)	Pore vol. ($cm^3.g^{-1}$)	Micropore vol. ($m^3.g^{-1}$)
425	45.6	11.0	0.1
475	63.3	10.8	0.3
575	80.5	10.2	0.2

The most straightforward application is the direct re-utilization of char as carbon black. However, this option faces important limitations due to the characteristics of the residual carbon black. Thus, the high ash and sulphur contents are a serious drawback, i.e., their contents are limited in commercial carbon blacks to values below 0.5 wt.% in the case of ashes [65] and to around 1 wt.% for sulphur [1]. The demineralisation by acid/base treatment was proposed as a method for ash content reduction [66]. Similarly, steam activation seems to be a reasonable solution for sulphur removal [67]. In spite of the good surface characteristics of the tyre pyrolysis char under suitable conditions, especially at high temperatures [15,42] or under vacuum [25,68], the problems related to particle structure for char re-utilization as carbon black have already been reported [69]. Even with that all, there are also promising re-utilization results in the literature [70],

probably further studies are required to analyse this interesting valorisation route for tyre pyrolysis char. Moreover, the remarkable surface properties of tyre derived char make them a suitable precursor for the production of high quality adsorbents [10]. Regarding the possibility of using it as solid fuel, despite its high energy content, it has been usually discarded due to its high sulphur content and the problems related with its handling because it is a solid with low density, volatile content and particle size [3].

10.2.3.3 Sulphur mass balance

The sulphur content of the pyrolysis products involves a significant challenge for their final applications. Accordingly, the sulphur distribution among the pyrolysis products was analysed. The sulphur content of the gaseous fraction was determined based on the H_2S yield, which was the single sulphur compound detected by micro-chromatography technique. Both the TPO and char sulphur content were measured by ultimate analysis, as explained in Section 10.2.2.3, and the results are reported in Table 10.7 and Table 10.8, respectively. Considering the sulphur contents of the waste truck-tyre, and those obtained for the pyrolysis products, a sulphur mass balance was carried out. The mass balance closure was above 80% at the three temperatures studied.

Figure 10.7 shows the sulphur distribution obtained among tyre pyrolysis products. Moreover, the yields of these products have also been plotted in the same figure. In spite of the fact that TPO was the prevailing product it contains only around 35% of the sulphur included in the original waste truck-tyre material with limited temperature influence. This can be attributed to the fact that the sulphur content in the TPO is mainly due to the processing oils and they volatilise at relatively low temperatures. As observed in Figure 10.7, around 60% of the total sulphur contained in the waste tyres is retained in the char, being the highest (above 63%) at 575 °C. The high sulphur content in the char is related with the high thermal stability of organic and inorganic sulphur containing compounds [71]. The sulphur contained in the gas product increased slightly to its maximum value of 7.4% at 475 °C, however at 575 °C it again decreased; the same effect was reported by Hu et al. [71], although at higher temperatures. Lanteigne et al. [72] analysed the sulphur release in waste tyre pyrolysis and they concluded that this complex process is influenced by process conditions, such as temperature or mass transfer limitations, and the presence of metals, such as steel or Zn, in the tyre material. In general the distribution obtained in the present study is consistent with that reported by other authors [71,73].

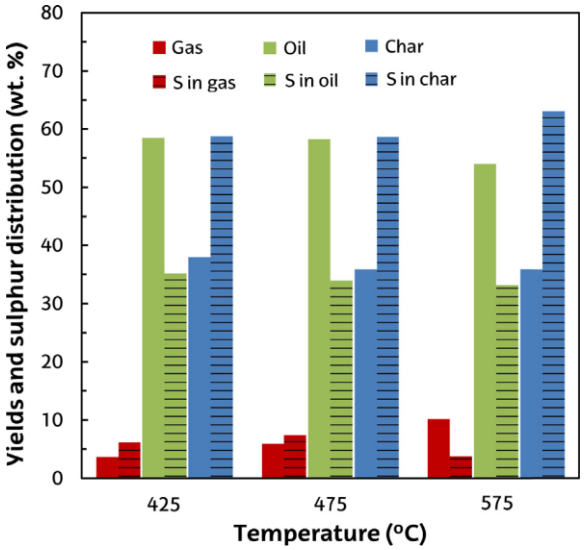

Figure 10.7: Sulphur distribution obtained among tyre pyrolysis products and their yields at different temperatures.

10.2.4 Conclusions

The continuous pyrolysis of waste truck-tyres was studied in a bench scale plant provided with a conical spouted bed reactor in the 425 – 575 °C range. This reactor is an interesting alternative for waste tyre valorisation given that it allows attaining flash pyrolysis conditions (high heating rates and short residence times), and consequently obtain high TPO yields. This fact was pointed out when the results were compared with a previous study performed with the same tyre rubber but under slow pyrolysis conditions. A temperature of 475 °C was required to completely devolatilize waste tyre rubber, in fact the char produced at 425 °C contained a significant amount of volatile matter. The maximum TPO yield of 58 wt.% was obtained between 425 and 475 °C. In addition, the highest limonene production of 14.1 wt.% was obtained at 475 °C, which remarks the interest of this pyrolysis temperature. A further temperature increase to 575 °C increased the gas yield at the expense of TPO, whose yield was reduced to 54 wt.%, as well as that of limonene to 7.1 wt.%. Moreover, the TPO undergoes a remarkable aromatisation, i.e., the aromatic content in the TPO is 12.7 wt.% at 475°C and this value was increased to 50.6 wt.% at 575 °C. Furthermore, temperature plays an interesting role in the residual carbon black properties, improving surface area to 80 $m^2.g^{-1}$ at 575 °C. The sulphur distribution between pyrolysis products was not affected by temperature in the studied range. Around 60% of the sulphur contained in waste tyres was retained in the solid product after the pyrolysis process, with the remaining 35 and 5% being retained in the TPO and gaseous products, respectively.

Acknowledgements

This work was carried out with financial support from the Ministry of Economy and Competitiveness of the Spanish Government (CTQ2016-75535-R and CTQ2014-59574-JIN), the European Regional Development Fund (ERDF), the Basque Government (IT748-13) and the University of the Basque Country (UFI 11/39). Jon Alvarez also thanks the University of the Basque Country UPV/EHU for his postgraduate Grant (ESPDOC 2015). This work was also supported by the Recycling and Economic Development Initiative of South Africa (REDISA) and the National Research Foundation (NRF).

References

[1] Antoniou N, Zabaniotou A. Features of an efficient and environmentally attractive used tyres pyrolysis with energy and material recovery. Renew Sustain Energy Rev 2013;20:539–58.

[2] Ramarad S, Khalid M, Ratnam CT, Chuah AL, Rashmi W. Waste tire rubber in polymer blends: a review on the evolution, properties and future. Progr Mater Sci 2015;72:100–40.

[3] Martinez JD, Puy N, Murillo R, Garcia T, Navarro MV, Mastral AM. Waste tyre pyrolysis: a review. Renew Sustain Energy Rev 2013;23:179–213.

[4] Conesa JA, Gálvez A, Mateos F, Martín-Gullón I, Font R. Organic and inorganic pollutants from cement kiln stack feeding alternative fuels. J Hazard Mater 2008;158:585–92.

[5] Hita I, Arabiourrutia M, Olazar M, Bilbao J, Arandes JM, Castaño Sánchez P. Opportunities and barriers for producing high quality fuels from the pyrolysis of scrap tires. Renew Sustain Energy Rev 2016;56:745–59.

[6] Abnisa F, Wan Daud WMA. Optimization of fuel recovery through the stepwise co-pyrolysis of palm shell and scrap tire. Energy Convers Manage 2015;99:334–45.

[7] Bicáková O, Straka P. Co-pyrolysis of waste tire/coal mixtures for smokeless fuel, maltenes and hydrogen-rich gas production. Energy Convers Manage 2016;116:203–13.

[8] Williams PT. Pyrolysis of waste tyres: a review. Waste Manage 2013;33:1714–28.

[9] Danon B, Van Der Gryp P, Schwarz CE, Görgens JF. A review of dipentene (dllimonene) production from waste tire pyrolysis. J Anal Appl Pyrolysis 2015;112:1–13.

[10] Antoniou N, Stavropoulos G, Zabaniotou A. Activation of end of life tyres pyrolytic char for enhancing viability of pyrolysis – critical review, analysis and recommendations for a hybrid dual system. Renew Sustain Energy Rev 2014;39:1053–73.

[11] Diez C, Martinez O, Calvo L, Cara J, Moran A. Pyrolysis of tyres. Influence of the final temperature of the process on emissions and the calorific value of the products recovered. Waste Manage 2004;24:463–9.

[12] Cunliffe A, Williams P. Composition of oils derived from the batch pyrolysis of tyres. J Anal Appl Pyrolysis 1998;44:131–52.

[13] Mkhize NM, van der Gryp P, Danon B, Görgens JF. Effect of temperature and heating rate on limonene production from waste tyre pyrolysis. J Anal Appl Pyrolysis 2016;120:314–20.

[14] Kan T, Strezov V, Evans T. Fuel production from pyrolysis of natural and synthetic rubbers. Fuel 2017;191:403–10.

[15] Kaminsky W, Mennerich C. Pyrolysis of synthetic tire rubber in a fluidised-bed reactor to yield 1,3-butadiene, styrene and carbon black. J Anal Appl Pyrolysis 2001;58:803–11.

[16] Williams P, Brindle A. Fluidised bed pyrolysis and catalytic pyrolysis of scrap tyres. Environ Technol 2003;24:921–9.

[17] Edwin Raj R, Robert Kennedy Z, Pillai BC. Optimization of process parameters in flash pyrolysis of waste tyres to liquid and gaseous fuel in a fluidized bed reactor. Energy Convers Manage 2013;67:145–51.

[18] Aylon E, Fernandez-Colino A, Navarro M, Murillo R, Garcia T, Mastral A. Waste tire pyrolysis: comparison between fixed bed reactor and moving bed reactor. Ind Eng Chem Res 2008;47:4029–33.

[19] Ayanoɨlu A, Yumrutas_ R. Rotary kiln and batch pyrolysis of waste tire to produce gasoline and diesel like fuels. Energy Convers Manage 2016;111:261–70.

[20] Luo S, Feng Y. The production of fuel oil and combustible gas by catalytic pyrolysis of waste tire using waste heat of blast-furnace slag. Energy Convers Manage 2017;136:27–35.

[21] Alvarez J, Amutio M, Lopez G, Barbarias I, Bilbao J, Olazar M. Sewage sludge valorization by flash pyrolysis in a conical spouted bed reactor. Chem Eng J 2015;273:173–83.

[22] Amutio M, Lopez G, Alvarez J, et al. Flash pyrolysis of forestry residues from the Portuguese Central Inland Region within the framework of the BioREFINA-Ter project. Biores Technol 2013;129:512–8.

[23] Artetxe M, Lopez G, Amutio M, Elordi G, Bilbao J, Olazar M. Cracking of high density polyethylene pyrolysis waxes on HZSM-5 catalysts of different acidity. Ind Eng Chem Res 2013;52:10637–45.

[24] Lopez G, Olazar M, Amutio M, Aguado R, Bilbao J. Influence of tire formulation on the products of continuous pyrolysis in a conical spouted bed reactor. Energy Fuels 2009;23:5423–31.

[25] Lopez G, Olazar M, Aguado R, et al. Vacuum pyrolysis of waste tires by continuously feeding into a conical spouted bed reactor. Ind Eng Chem Res 2010;49:8990–7.

[26] Olazar M, Aguado R, Arabiourrutia M, Lopez G, Barona A, Bilbao J. Catalyst effect on the composition of tire pyrolysis products. Energy Fuels 2008;22:2909–16.

[27] Arabiourrutia M, Olazar M, Aguado R, Lopez G, Barona A, Bilbao J. HZSM-5 and HY zeolite catalyst performance in the pyrolysis of tires in a conical spouted bed reactor. Ind Eng Chem Res 2008;47:7600–9.
[28] Lopez G, Artetxe M, Amutio M, Bilbao J, Olazar M. Thermochemical routes for the valorization of waste polyolefinic plastics to produce fuels and chemicals. A review. Renew Sustain Energy Rev 2017;73:346–68.
[29] Makibar J, Fernandez-Akarregi AR, Diaz L, Lopez G, Olazar M. Pilot scale conical spouted bed pyrolysis reactor: draft tube selection and hydrodynamic performance. Powder Technol 2012;219:49–58.
[30] Erkiaga A, Lopez G, Amutio M, Bilbao J, Olazar M. Steam gasification of biomass in a conical spouted bed reactor with olivine and g-alumina as primary catalysts. Fuel Process Technol 2013;116:292–9.
[31] Lopez G, Erkiaga A, Amutio M, Bilbao J, Olazar M. Effect of polyethylene cofeeding in the steam gasification of biomass in a conical spouted bed reactor. Fuel 2015;153:393–401.
[32] Altzibar H, Lopez G, Bilbao J, Olazar M. Minimum spouting velocity of conical spouted beds equipped with draft tubes of different configuration. Ind Eng Chem Res 2013;52:2995–3006.
[33] Ishikura T, Nagashima H, Ide M. Hydrodynamics of a spouted bed with a porous draft tube containing a small amount of finer particles. Powder Technol 2003;131:56–65.
[34] Lah B, Klinar D, Likozar B. Pyrolysis of natural, butadiene, styrene-butadiene rubber and tyre components: modelling kinetics and transport phenomena at different heating rates and formulations. Chem Eng Sci 2013;87:1–13.
[35] Danon B, Görgens J. Determining rubber composition of waste tyres using devolatilisation kinetics. Thermochim Acta 2015;621:56–60.
[36] Lopez G, Aguado R, Olazar M, Arabiourrutia M, Bilbao J. Kinetics of scrap tyre pyrolysis under vacuum conditions. Waste Manage 2009;29:2649–55.
[37] Yang J, Kaliaguine S, Roy C. Improved quantitative determination of elastomers in tire rubber by kinetic simulation of DTG curves. Rubber Chem Technol 1993;66:213–29.
[38] Aylon E, Callen M, Lopez J, et al. Assessment of tire devolatilization kinetics. J Anal Appl Pyrolysis 2005;74:259–64.
[39] Mui ELK, Lee VKC, Cheung WH, McKay G. Kinetic modeling of waste tire carbonization. Energy Fuels 2008;22:1650–7.
[40] Choi G, Oh S, Kim J. Non-catalytic pyrolysis of scrap tires using a newly developed two-stage pyrolyzer for the production of a pyrolysis oil with a low sulfur content. Appl Energy 2016;170:140–7.
[41] Choi G, Jung S, Oh S, Kim J. Total utilization of waste tire rubber through pyrolysis to obtain oils and CO2 activation of pyrolysis char. Fuel Process Technol 2014;123:57–64.
[42] Lopez G, Olazar M, Aguado R, Bilbao J. Continuous pyrolysis of waste tyres in a conical spouted bed reactor. Fuel 2010;89:1946–52.

[43] Islam M, Haniu H, Beg M. Liquid fuels and chemicals from pyrolysis of motorcycle tire waste: product yields, compositions and related properties. Fuel 2008;87:3112–22.

[44] Ucar S, Karagoz S, Ozkan A, Yanik J. Evaluation of two different scrap tires as hydrocarbon source by pyrolysis. Fuel 2005;84:1884–92.

[45] Banar M, Akyıldız V, Özkan A, Çokaygil Z, Onay Ö. Characterization of pyrolytic oil obtained from pyrolysis of TDF (Tire Derived Fuel). Energy Convers Manage 2012;62:22–30.

[46] Akkouche N, Balistrou M, Loubar K, Awad S, Tazerout M. Heating rate effects on pyrolytic vapors from scrap truck tires. J Anal Appl Pyrolysis 2017;123:419–29.

[47] Martínez JD, Murillo R, García T, Veses A. Demonstration of the waste tire pyrolysis process on pilot scale in a continuous auger reactor. J Hazard Mater 2013;261:637–45.

[48] Song Z, Yang Y, Zhao X, et al. Microwave pyrolysis of tire powders: evolution of yields and composition of products. J Anal Appl Pyrolysis 2017;123:152–9.

[49] Undri A, Rosi L, Frediani M, Frediani P. Upgraded fuel from microwave assisted pyrolysis of waste tire. Fuel 2014;115:600–8.

[50] Arion A, Baronnet F, Lartiges S, Birat J. Characterization of emissions during the heating of tyre contaminated scrap. Chemosphere 2001;42:853–9.

[51] Cypres R. Aromatic hydrocarbons formation during coal pyrolysis. Fuel Process Technol 1987;15:1–15.

[52] Fernandez AM, Barriocanal C, Alvarez R. Pyrolysis of a waste from the grinding of scrap tyres. J Hazard Mater 2012;203–204:236–43.

[53] Lopez FA, Centeno TA, Alguacil FJ, Lobato B. Distillation of granulated scrap tires in a pilot plant. J Hazard Mater 2011;190:285–92.

[54] Li S, Yao Q, Chi Y, Yan J, Cen K. Pilot-scale pyrolysis of scrap tires in a continuous rotary kiln reactor. Ind Eng Chem Res 2004;43:5133–45.

[55] Laresgoiti M, Caballero B, de Marco I, Torres A, Cabrero M, Chomon M. Characterization of the liquid products obtained in tyre pyrolysis. J Anal Appl Pyrolysis 2004;71:917–34.

[56] Unapumnuk K, Lu M, Keener T. Carbon distribution from the pyrolysis of tirederived fuels. Ind Eng Chem Res 2006;45:8757–64.

[57] Boxiong S, Chunfei W, Cai L, Binbin G, Rui W. Pyrolysis of waste tyres: the influence of USY catalyst/tyre ratio on products. J Anal Appl Pyrolysis 2007;78:243–9.

[58] Pakdel H, Pantea D, Roy C. Production of dl-limonene by vacuum pyrolysis of used tires. J Anal Appl Pyrolysis 2001;57:91–107.

[59] Jantaraksa N, Prasassarakich P, Reubroycharoen P, Hinchiranan N. Cleaner alternative liquid fuels derived from the hydrodesulfurization of waste tire pyrolysis oil. Energy Convers Manage 2015;95:424–34.

[60] Hita I, Rodríguez E, Olazar M, Bilbao J, Arandes JM, Castaño P. Prospects for obtaining high quality fuels from the hydrocracking of a hydrotreated scrap tires pyrolysis oil. Energy Fuels 2015;29:5458–66.

[61] Williams PT, Besler S. Pyrolysis-thermogravimetric analysis of tyres and tyre components. Fuel 1995;74:1277–83.

[62] Zhang X, Wang T, Ma L, Chang J. Vacuum pyrolysis of waste tires with basic additives. Waste Manage 2008;28:2301–10.

[63] Kyari M, Cunliffe A, Williams P. Characterization of oils, gases, and char in relation to the pyrolysis of different brands of scrap automotive tires. Energy Fuels 2005;19:1165–73.

[64] Munillo R, Aylon E, Navarro M, Callen M, Aranda A, Mastral A. The application of thermal processes to valorise waste tyre. Fuel Process Technol 2006;87:143–7.

[65] Tang L, Huang H. Thermal plasma pyrolysis of used tires for carbon black recovery. J Mater Sci 2005;40:3817–9.

[66] Chaala A, Darmstadt H, Roy C. Acid-base method for the demineralization of pyrolytic carbon black. Fuel Proces Technol 1996;46:1–15.

[67] Lopez G, Olazar M, Artetxe M, Amutio M, Elordi G, Bilbao J. Steam activation of pyrolytic tyre char at different temperatures. J Anal Appl Pyrolysis 2009;85:539–43.

[68] Roy C, Chaala A, Darmstadt H. The vacuum pyrolysis of used tires - End-uses for oil and carbon black products. J Anal Appl Pyrolysis 1999;51:201–21.

[69] Gonzalez J, Encinar J, Canito J, Rodriguez J. Pyrolysis of automobile tyre waste. Influence of operating variables and kinetics study. J Anal Appl Pyrolysis 2001;58:667–83.

[70] Faulkner BP, Weinecke M. Carbon black production from waste tires. Miner Metall Process 2001;18:215–20.

[71] Hu H, Fang Y, Liu H, et al. The fate of sulfur during rapid pyrolysis of scrap tires. Chemosphere 2014;97:102–7.

[72] Lanteigne J, Laviolette J, Chaouki J. Behavior of sulfur during the pyrolysis of tires. Energy Fuels 2015;29:763–74.

[73] Susa D, Haydary J. Sulphur distribution in the products of waste tire pyrolysis. Chem Pap 2013;67:1521–6.

10.3 Published paper: Evaluation of the properties of tyre pyrolysis oils obtained in a conical spouted bed reactor

Journal: Energy

Issue: 128

Pages: 463 – 474

Evaluation of the properties of tyre pyrolysis oils obtained in a conical spouted bed reactor

J. Alvarez[a], G. Lopez[a*], M. Amutio[a], N. M. Mkhize[b], B. Danon[b], P. van der Gryp[b], J. F. Görgens[b], J. Bilbao[a], M. Olazar[a]

[a]Department of Chemical Engineering, University of the Basque Country UPV/EHU, P.O. Box 644-E48080 Bilbao, Spain

[b]Department of Process Engineering, Stellenbosch University, Private Bag X1, Matieland, 7602, Stellenbosch, South Africa

* Corresponding author: gartzen.lopez@ehu.es

Abstract

Waste truck tyre valorization by fast pyrolysis has been performed in a conical spouted bed reactor in the 425 – 575 °C range. The tyre pyrolysis oil (TPO) yield was found to decrease with increasing temperature whilst the yield of gas increased. The effect of temperature on TPO properties has been studied in order to establish the best possible valorization route. FTIR and chromatographic analysis revealed the presence of some undesired compounds with sulphur, nitrogen or oxygen functionalities (benzothiazoles, nitriles and carboxylic acids amongst others) and an increase of TPO aromaticity with increasing temperature. The carbon and sulphur content and the heating value of the TPO increased with temperature. The simulated distillation showed that approximately 70% of the TPOs produced at 425 and 475 °C correspond to diesel range, whereas that TPO obtained at 575 °C is between diesel and gasoline range. The properties of the TPOs evidenced their potential to substitute conventional fuels. However, some of them need to be improved, i.e., by reduction of the sulphur, nitrogen and aromatic content. Additionally, the TPO obtained at 425 and 475 °C could be an important source of limonene and that at 575 °C of xylenes, although current removal methods present some limitations.

10.3.1 Introduction

Currently the total annual production of tyres in the worldwide is around 1.5 billion units and approximately a quarter of that manufacture (355 million per year) corresponds to the EU [1,2]. In addition, the increase in the demand of new vehicles in developing countries in the last years, mainly in Asia, leads to a further significant increase of tyre consumption [3]. Tyres that are used, rejected or unwanted are classified as 'waste tyres' (WT) and need to be managed responsibly, following a hierarchical approach (reuse, recycling, energy or chemical recovery and landfilling) in order to minimize their environmental impact [4]. With the banning of tyre disposal in landfills in the EU due to their potential risk of provoking fires, the main strategies followed in the last years for treating WT have been energy recovery (mainly using them as fuel in cement kilns) and material recycling through the production of rubberised flooring in sport tracks and playgrounds [5].

Abbrebiation box	
BP	boiling point
BTX	benzene, toluene and xylene
CSBR	conical spouted bed reactor
FTIR	fourier transform infrared spectrometer/spectroscopy
HHV	higher heating value
MAH	monocyclic aromatic hydrocarbons
NBR	nitrile rubber
NR	natural rubber
PAH	polycyclic aromatic hydrocarbons
PCT	passenger car tyre
SBR	styrene butadiene rubber
SR	synthetic rubber
TPO	tyre pyrolysis oil
TT	truck tyres
VGO	vacuum gas oil
WT	waste tyres

Nevertheless, recycling cannot mitigate completely the disposal problems and direct use as fuel also involves some drawbacks related to air pollution due to the high sulphur content of WT [4]. Accordingly, promising recycling alternatives, such as chemical recovery, are gaining major attention in order to recover

valuable chemical products from the WT, especially using fast pyrolysis due to its benefits from an energetic, environmental and economical point of view [3]. Furthermore, this technology is an easily scalable process, which has been successfully integrated in existing refinery plants in order to co-process some of the products [3].

Pyrolysis is described as the thermal breakdown of the volatile tyre components under a non-oxidative atmosphere to produce gaseous, liquid and solid (char) products. The liquid, also known as tyre pyrolysis oil (TPO), is the main product of WT fast pyrolysis and it is composed of a complex mixture of aromatic, aliphatic and polar compounds with a high heating value (40 – 44 $MJ.kg^{-1}$) and comparable physicochemical properties to those of fossil fuels [6,7]. Nevertheless, the viscosity is depending on the tyre composition and process conditions adopted, but can vary significantly from that of conventional fuels [8]. Moreover, nitrogen and sulphur contents in the TPOs are in the 1 – 2 wt.% and 0.5 – 1 wt.% range, respectively, whilst their content in diesel fuel are typically lower than 0.05 wt.% and 0.2 wt.%, respectively [4]. These TPO properties, together with its low cetane number, hinder its direct utilization in diesel engines. However, in order to meet the required specifications and stringent SO_2 exhaust limits, TPO can be mixed with diesel fuel [6], complemented by a cetane improver such as diethyl ether [9], or its sulphur content can be reduced using appropriate desulphurization methods [10], respectively. It is noteworthy that TPO also contains valuable molecules with economic interest, including e.g. limonene [11], which is useful in the formulation of industrial products (solvents, resins, adhesives), and light aromatics (benzene, toluene, xylene; BTX), which are valued commodities with various uses [12]. Therefore, in view of the different applications available and with the objective to assess the most suitable one, it is essential to analyse in depth the chemical composition and, more importantly, the physicochemical properties of the TPOs.

The compounds that make up the TPO mainly come from the synthetic and natural rubbers as well as the additives such as fillers and accelerators used in the tyre formulation, while their contents differ depending on the tyre type [13]. For example, truck tyres (TT) present approximately a two to one ratio of natural rubber (NR) to synthetic rubber (SR), which will lead to relatively high proportions of isoprene in the gas, and limonene and xylene in the TPO. At the same time, passenger car tyres (PCT) consist of considerably higher amounts of SR, thus favouring the formation of degradation products such as ethylbenzene, styrene and cumene [3,5]. Furthermore, according to Ucar et al. [14], the TPO derived from PCT and TT showed remarkable differences in the aromatic and sulphur content, being in both cases lower for the latter, which was mainly ascribed to the feedstock composition. However, as previously stated, the yield and the properties of the TPO not only depend on tyre type, but also on the pyrolysis conditions and the technology used.

Typical reactors used for tyre pyrolysis include fixed bed, screw and rotator kiln and fluidized bed reactors, the latter being the most employed technology especially due to its high heat and mass transfer rates and bed isothermicity [2,5]. However, other reactor types, such as conical spouted bed reactors (CSBR), have proven to perform satisfactorily for the pyrolysis of waste PCT in a continuous mode [15], not only due to the high heat and mass transfer rates, but also due to the reduced gas residence time, which minimizes secondary reactions and allows higher TPO yields and products with higher quality to be attained [3]. Furthermore, CSBR has several advantages over traditional fluidized bed reactors; it has a simpler design because no distribution plate is required, it has a lower pressure drop and it is particularly suitable for handling solids with irregular texture [15,16]. Fluidized bed reactors have operating problems when coarse particles or those with irregular and/or sticky nature have to be treated. In these cases, spouted bed reactors have been successfully applied by several research groups in thermochemical processes, such as are the gasification of vegetable biomass or coal [17–19] and the pyrolysis of biomass and plastics [20,21].

It is noteworthy that the most interesting fraction for its energetic and economic value is the TPO and CSBR technology allows for obtaining very high TPO yields [22]. Hence, the aim of this work is to study the effect of temperature on the properties of the TPOs obtained by fast pyrolysis of waste TT in a CSBR and how these properties would influence the best routes for their valorization. Concretely, this paper analyses the chemical composition, water content, calorific value and ultimate analysis of the TPOs obtained at 425, 475 and 575 °C. Additionally, in order to evaluate the feasibility of their application as a fuel, simulated distillation curves of the three TPOs are also determined.

10.3.2 Experimental

10.3.2.1 Characterization of the feedstock

The feedstock material used in this work is a waste truck tyre (steel and other carcass elements free) supplied by a South African waste tyre recycler, Enviroserv (Pty) Ltd. The original sample has a particle size of up to 5 mm. Although the CSBR has very good capabilities of handling materials of irregular texture and wide particle size distributions, the tyre sample was nevertheless sieved down to a particle size range between 2.8 and 3.3 mm before feeding it into the reactor.

The main properties of the tyres are displayed in Table 10.10. The ultimate and proximate analyses have been carried out in a LECO CHNS-932 elemental analyser and in a TGA Q500IR thermogravimetric

analyser, respectively. The higher heating value (HHV) has been determined in a Parr 1356 isoperibolic bomb calorimeter.

Table 10.10: Characterization of the feedstock material.

Elemental analysis	
C (wt.%)	84.3
H (wt.%)	7.7
N (wt.%)	0.8
S (wt.%)	2.5
O (wt.%)[a]	4.7[*]
Proximate analysis (wt.%)[b]	
Volatile (wt.%)	65.1
Fixed carbon (wt.%)	29.9
Ash (wt.%)	4.9
HHV ($MJ.kg^{-1}$)	38.2

[a] by different

[b] On dry basis

10.3.2.2 Pyrolysis bench scale plant

The conical spouted bed bench-scale plant used for waste tyre pyrolysis is shown in Figure 10.8. This plant has been set up and finetuned on the basis of the knowledge acquired in previous pyrolysis studies of other waste tyres [22] and different types of waste materials such as lignocellulosic biomasses [23,24], sewage sludge [16] and plastics [25]. The setup is suitable for attaining high oil yields using fast pyrolysis due to the cyclic and vigorous movement of the solids which results in high heat and mass transfer rates (for the particle sizes used in this work, the heating rate is in the 103 – 104 $°C.s^{-1}$ range), low residence times of the hot volatiles (from approximately 30 ms in the spout zone to 500 ms in the annulus [16]) and the rapid removal of char from the reaction environment which minimizes undesired secondary reactions.

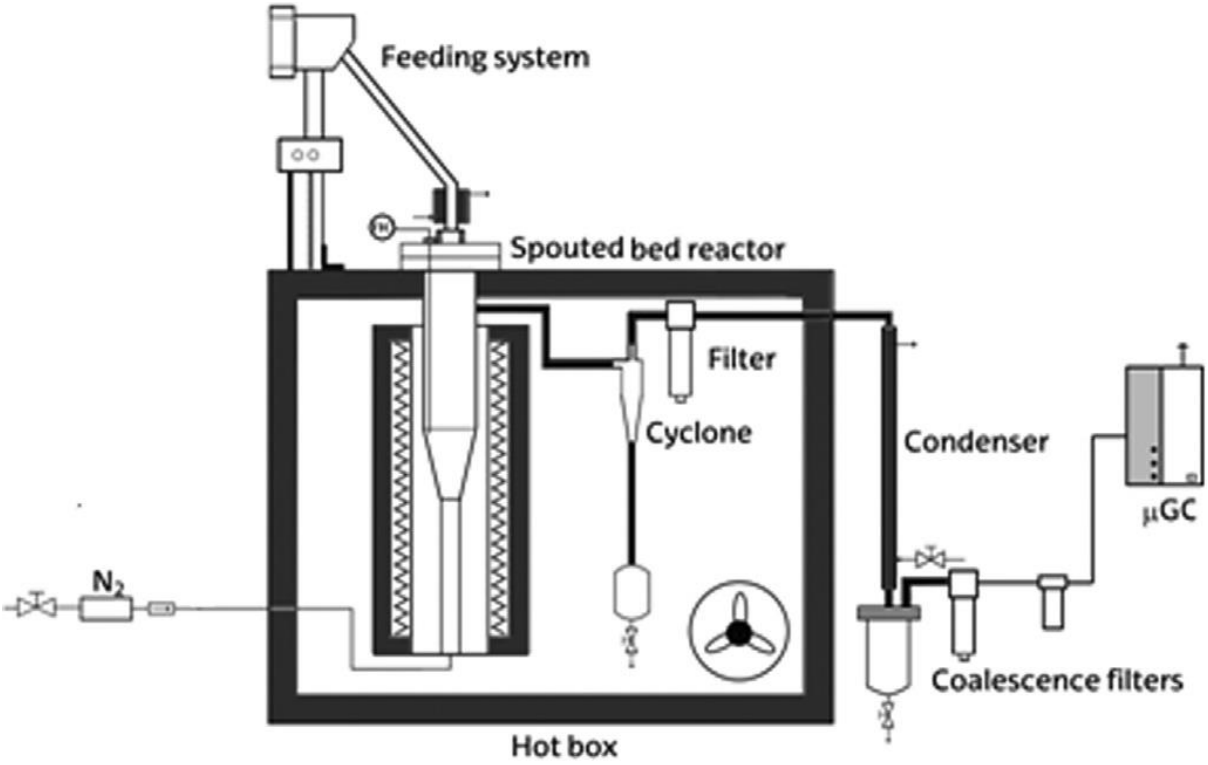

Figure 10.8: Schematic diagram of the bench-scale pyrolysis plant.

The plant (Figure 10.8) is composed of a solid and gas feeding device, a CSBR reactor, a fine particle retention system (i.e. a high efficiency cyclone followed by a sintered steel filter with a sieving size of 5 mm), a condensation system (i.e. a double-shell tube condenser cooled by tap water followed by a stainless steel filter, where the TPO is collected) and a gaseous product analysis system. The solid feeding system consists of a vessel equipped with a vertical shaft connected to a piston placed below the material, allowing the continuous feeding of the tyre rubber between 0.5 and 8 $g.min^{-1}$. Nitrogen was used as the fluidizing agent in order to work under inert conditions and its flow rate was controlled by means of a mass flow meter (Brooks SLA5800). The CSBR is heated by a two independent section radiant oven that provides the heat to operate up to 900 °C. Pyrolysis temperature has been measured and recorded by means of two K-type thermocouples located inside the reactor, one in the bed annulus and the other one close to the wall. It is noteworthy that the gases leaving the condensation system are filtered by means of two coalescence filters located before the micro-GC analysis.

10.3.2.3 TPO analysis

The collected TPO has been analysed by means of a GC/MS Shimadzu QP-2010S in order to identify individual compounds in the TPO. The gas chromatograph was equipped with a BPX-5 column (50 m x

0.22 mm x 0.25 mm) and the temperature programme was as follows: a steady heating ramp of 3 °C.min^{-1} from 40 °C up to 320 °C for separating the volatile products was followed by an isothermal (at 320 °C) period of 8 min in order to ensure total removal of all products from the column. Pressure was kept at 168.9 kPa with a He flow rate of 1.15 ml.min^{-1} and a total flow rate of 60.8 ml.min^{-1} in a split ratio of 50:1. The column was connected to a mass spectrometer and the parameters were as follows: ion source and interface temperatures were kept at 200 and 300 °C, respectively, operating in the 33 – 330 m/z range with a solvent cut time of 4.05 min.

The content of each compound in the TPO has additionally been quantified by means of a gas chromatograph (Agilent 6890) equipped with a flame ionization detector (FID). The column used was a HP-PONA (50 m x 0.22 mm x 0.25 mm) and the temperature sequence of the oven was the same as that used in the GC/MS Shimadzu QP-2010S. As most products obtained in the tyre pyrolysis process are hydrocarbons and the response factors of the FID detector for these compounds are approximately unity, a one-to-one relationship was assumed between mass and peak area.

The water content of the TPO was determined by Karl-Fischer Titration (Metrohm 870 KF Titrino plus, ASTM D1744), whereas the surface organic functional groups contained in each TPO have been determined by Fourier transform infrared spectrometer (FTIR, Thermo Nicolet 6700). Ultimate analysis of the TPO produced at different temperatures was carried out in a LECO CHNS-932 elemental analyser. Additionally, in order to assess the similitude of the TPOs with conventional fuels (such as gasoline or diesel), the TPOs have been fractionated using simulated distillation. The equipment used for this consisted of an Agilent 6990 chromatograph provided with a FID detector and the procedure performed was according to ASTM-D2887-84 (boiling range distribution of petroleum fraction by gas chromatography). Finally, the HHV of the TPO samples were determined using a Parr 1356 isoperibolic bomb calorimeter.

10.3.2.4 Experimental procedure

The continuous operation for TPO production has been carried out at three different temperatures: 425, 475 and 575 °C. An initial bed of 150 g of sand (particle size between 0.3 and 0.8 mm) was deposited inside the reactor and the fluidizing gas (nitrogen) rate was 8 NL.min^{-1} (i.e. 1.5 times that corresponding to the minimum spouting velocity to ensure stable spouting [26]) which guarantees good heat transfer and bed isothermicity during the pyrolysis runs.

In each run, 65 g of truck tyre have been continuously fed (1.3 $g.min^{-1}$) into the reactor for 50 min. The microchromatographic analysis of volatile and gaseous streams was conducted after at least 10 min of operation under the same conditions. To ratify the reproducibility, the experiments performed at each temperature have been repeated three or four times. The mass balance is closed using the information obtained at the end of each experiment by: i) weighing the mass of the TPO gathered in the condensation system; ii) weighing the char collected in the filter, the cyclone and the reactor, and; iii) determining the volume of gases formed during the pyrolysis reaction by means of an internal standard (cyclohexane) introduced to the micro-chromatograph with a specific flow rate of 0.05 $ml.min^{-1}$. The mass balance closure attained in all the cases was higher than 94%. Finally, at the end of each experiment the TPO was subjected to the characterization techniques as described above.

10.3.3 Results and discussion

10.3.3.1 TPO yields

The products obtained from tyre pyrolysis have been grouped into three fractions: the gas which contains permanent gases such as CO, CO_2, H_2, and C_1 – C_5 hydrocarbons as well as H_2S traces, the TPO which includes hydrocarbons from C_6 up to C_{23} and the char or solid residue which consists mainly of the carbon black and the ashes present in the original tyre. Table 10.11 shows the TPO yields obtained at 425, 475 and 575 °C, respectively.

Table 10.11: Effect of temperature on the yields of TT pyrolysis products.

Yield (wt.%)	425 °C	475 °C	575 °C
Gas	3.7±0.2	5.9±0.6	10.1±0.3
TPO	58.4±2.1	58.2±2.6	54.0±1.7
Char	37.9±1.5	35.9±1.6	35.9±1.1

The gradual increase in the gas yield with temperature is mainly attributed to a more severe cracking of the volatiles at higher temperatures, which at the same time contributes to a decrease of the TPO yield. In addition, gas and TPO formation is also favoured between 425 and 475 °C by devolatilization and cracking reactions of some solid hydrocarbons present on the surface of the char, thus decreasing its yield [27,28]. Above 475 °C the char yield remained constant at a value of 35.9 wt.% which corresponds well with the fixed carbon and inorganic material content of the tyre sample (Table 10.11), as it was also observed by Mkhize et al. [11] who pyrolyzed the same TT in a fixed bed reactor.

These results are consistent with those reported previously using the CSBR technology given that similar product distributions were obtained from the pyrolysis of a different type of tyre. For example, between 400 and 500 °C very low gas yields were obtained while the TPO yield remained fairly constant. At higher temperatures, gas yields increased considerably whereas that of TPO decreased due to the promotion of secondary cracking reaction [15,22,29]. Moreover, the TPO yields in this work (54 – 58 wt.%) are relatively high as compared to values reported in the literature with other technologies, such as fixed beds (38 – 58 wt.%), screw/rotator kiln reactors (38 – 45 wt.%) or fluidized beds (27 – 55 wt.%), the latter also operating under isothermal conditions and short residence times [3,5,30,31]. It is stressed that the high TPO and low gas yields in the CSBR are due to i) very high heat and mass transfer rates [32] and ii) reduced residence times of the hot volatiles, ranging from approximately 30 ms in the spout zone to 500 ms in the annulus [16] (the residence time in fluidized beds is usually an order of magnitude higher, while in other common fast pyrolysis technologies, such as screw kiln or auger rectors, is higher than 5 s). These characteristics minimize secondary cracking reactions which enhance gas production [33].

10.3.3.2 TPO characterization

The TPO collected from the condensation system is a dark brown coloured product that resembles crude oil. The effect of pyrolysis temperature on the TPO has been assessed by means of the characterization of the chemical composition (FTIR and chromatographic analysis), elemental composition, water content, HHV as well as simulated distillation. Given that the TPO fraction is the most abundant fraction and its final market value could therefore significantly improve the economic viability of the pyrolysis process, these characteristics will help to establish its potential for being used as an alternative fuel or as a source of chemicals.

FTIR analysis

The FTIR analysis allowed the evaluation of the functional groups present in the TPOs, which would help revealing their main chemical properties. Figure 10.9 shows the transmittance spectrums of the TPOs obtained at 425, 475 and 575 °C, respectively, while Table 10.12 summarizes the main absorption bands identified in these spectra (the numbers correspond to the different bands described in Figure 10.9). As observed in Figure 10.9, the three spectrums are quite similar although some differences can be appreciated in the absorbance strength of some peaks. The weak absorption band between 3500 and 3200 cm^{-1} (1) is assigned to O–H stretching vibrations, indicating limited presence of water and hydroxyl groups, such as alcohols, phenols or carboxylic acids [34]. The bands in the range from 3100 to 2800 cm^{-1} (2 – 3) are due

to C–H stretching, those around 3050 cm^{-1} are related to aromatic compounds whereas those from 3000 to 2700 cm^{-1} corresponds to aliphatic compounds [35]. In addition, the peaks around 1750 – 1675 cm^{-1} (4) corresponded to C–O stretching vibration attributed to carbonyl/carboxyl groups mainly derived from the additives of the tyres [28,36]. The bands observed between 1650 and 1605 cm^{-1} (5) and 1600–1550 cm^{-1} (6) are due to C–C stretching vibrations indicative of the presence of alkenes and aromatics, respectively [34]. The peak at 1450 cm^{-1} (7) is associated with sulphur containing compounds, whereas that at 1370 cm^{-1} (8) is assigned to CH_2 and CH_3 groups or to the contribution of some nitrogenated species [28,35]. Finally, the region between 900 and 675 cm^{-1} (9) corresponds to the C–H out-of-plane bending peaks derived from aromatic compounds. Thus, band (9) together with (1) and (6) indicates the presence of aromatic structures. The intensities of these peaks increased considerably for the TPOs produced at increasing pyrolysis temperatures, indicating that the aromatic content in these TPOs is increased [4].

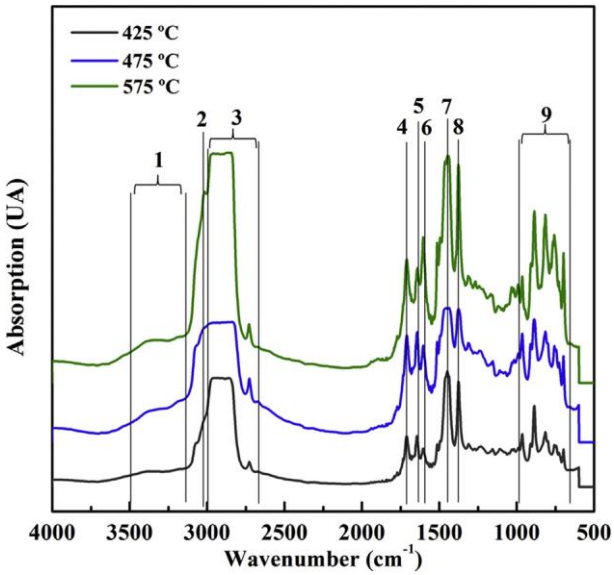

Figure 10.9: FTIR spectra of the TPOs obtained at 425, 475, 575 °C, respectively.

Table 10.12: FTIR functional groups and the indicated compounds in the TPOs.

Band	Frequency range (cm^{-1})	Functional group	Class of compound
1	3500-3200	O-H stretching	Phenols, alcohols or carboxylic acids
2	3050	C-H stretching	Aromatic
3	3000-2700	C-H stretching	Alkanes
4	1750-1675	C=O	Carbonyl/Carboxyl
5	1650-1605	C=C stretching	Aromatic
6	1600-1550	C=C stretching	Alkenes
7	1450	CH_2-S	Sulfur containing compounds
8	1370	-CH_2- or -CH_3	Alkanes
		N-CH_2	Nitrogenated compounds
9	900-700	C-H out of plane blending	Aromatic

Chromatographic analysis

The chemical composition of the TPOs obtained at different temperatures (Table 10.13) confirms the presence of the functional groups detected in the FTIR analysis. Furthermore, the chromatographic technique also reveals components with other functional groups which were not detected in the FTIR analysis. The chromatograms of the three TPOs obtained by GC/MS analysis are shown in Figure 10.10. More than 100 compounds have been identified by GC/MS using the NIST 147 library and they have been classified into four chemical classes in Table 10.13, namely, water, aromatic, aliphatic and heteroaromatic compounds. The aromatic compounds have been further classified according to monocyclic aromatic hydrocarbons (MAH) and polycyclic aromatic hydrocarbons (PAH). Besides, the aliphatic family has also been subdivided according to alkanes, alkenes and terpenes. It is noteworthy that there is such a plethora of compounds in the TPOs that their individual concentrations are typically very low.

Table 10.13: Detailed TPO composition (wt.%) at different pyrolysis temperatures.

Compounds (wt.%)	Formula	425 °C	475 °C	575 °C
Aromatics		**12.01**	**12.76**	**50.64**
MHA		*7.44*	*8.08*	*38.00*
Bencene	C_6H_6	0.11	0.12	0.26
Toluene	C_7H_8	0.08	0.14	1.40
Ethylbenzene	C_8H_{10}	0.14	0.16	0.48
o-Xylene	C_8H_{10}	0.55	0.76	3.67
1,3-dimethyl benzene	C_8H_{10}	-	-	0.03
Isopropylbenzene	C_9H_{12}	0.06	0.09	0.17
1,2,4-Trimethylbenzene	C_9H_{12}	0.13	0.23	0.66
1-ethyl-2-methyl-benzene	C_9H_{12}	0.34	0.39	0.84
1-ethyl-3-methyl-benzene	C_9H_{12}	0.77	0.88	1.19
α-Methylstyrene	C_9H_{10}	0.01	0.02	2.31
Indane	C_9H_{10}	0.07	0.13	0.33
1-ethyl-4-methyl-benzene	C_9H_{12}	-	-	0.81
2-propenyl-benzene	C_9H_{10}	0.12	0.24	0.34
Indene	C_9H_8	0.26	0.30	1.09
1,3,5-trimethyl-benzene	C_9H_{12}	-	-	2.67
1-ethenyl-4-methyl-benzene	C_9H_{10}	-	-	2.99
1-ethenyl-3-methyl-benzene	C_9H_{10}	-	-	0.37
tert-butyl-benzene	$C_{10}H_{14}$	-	-	0.35
1-methyl-4-(1-methylethyl)-benzene	$C_{10}H_{14}$	0.89	0.54	0.44
α-Dimethylstyrene	$C_{10}H_{12}$	0.92	1.00	4.23
1-methyl-3-propyl-benzene	$C_{10}H_{14}$	-	-	0.45
5-Ethyl-m-xylene	$C_{10}H_{14}$	-	-	1.15
1,2,3,5-tetramethyl-benzene	$C_{10}H_{14}$	0.19	0.19	1.64
5-Methylindane	$C_{10}H_{12}$	0.11	0.12	0.21
3-Methylindene	$C_{10}H_{10}$	0.09	0.13	0.54
1-Methylindene	$C_{10}H_{10}$	-	-	0.95
2-Methylindene	$C_{10}H_{10}$	-	-	0.85
1,2-Dimethylindane	$C_{11}H_{12}$	0.22	0.29	0.33
1,3-Dimethyl-1H-indene	$C_{11}H_{12}$	-	-	1.33
1,1-dimethyl-1H-Indene	$C_{11}H_{12}$	-	-	0.56
2,3-Dimethyl-1H-indene	$C_{11}H_{12}$	-	-	0.30
2,4-Diethyl-1-methylbenzene	$C_{11}H_{16}$	0.82	1.00	0.67
1-ethyl-4-(1-methylethyl)-benzene	$C_{11}H_{16}$	0.43	0.28	1.68
1-Methyl-3-(1-methyl-2-propenyl)benzene	$C_{11}H_{14}$	0.19	0.31	0.11

Table 10:13 (continue)

Compounds (wt.%)	Formula	425 °C	475 °C	575 °C
2,4,6-Trimethylstyrene	$C_{11}H_{14}$	0.13	0.10	0.25
1-Methyl-4-(1-methyl-2-propenyl)benzene	$C_{11}H_{14}$	-	-	0.56
1-Methyl-4-(3-methyl-3-butenyl)benzene	$C_{12}H_{16}$	-	-	0.23
1,2,3-Trimethylindene	$C_{12}H_{14}$	0.26	0.26	0.65
1,1,3-Trimethyl-1H-indene	$C_{12}H_{14}$	0.23	0.13	0.37
1-(1,5-Dimethyl-4-hexenyl)-4-methylbenzene	$C_{15}H22$	0.33	0.29	0.56
PAH		*4.57*	*4.68*	*12.64*
Naphthalene	$C_{10}H_8$	-	-	0.24
6-Methyl-1,2-dihydronaphthalene	$C_{11}H_{12}$	0.15	0.21	1.05
1,2,3,4-tetrahydro-1-methyl-naphthalene	$C_{11}H_{14}$	0.24	0.27	1.07
3-Methyl-1,2-dihydronaphthalene	$C_{11}H_{12}$	0.26	0.42	0.92
2-methyl-naphthalene	$C_{11}H_{10}$	0.40	0.33	0.65
1-methylnaphthalene	$C_{11}H_{10}$	-	-	0.60
1,5-dimethyl-naphthalene	$C_{12}H_{12}$	0.38	0.35	0.53
1,7-dimethyl-naphthalene	$C_{12}H_{12}$	-	-	0.53
Phenylbenzene	$C_{12}H_{10}$	-	-	0.26
1,8-dimethyl-naphthalene	$C_{12}H_{12}$	-	-	1.03
2,6-dimethyl-naphthalene	$C_{12}H_{12}$	-	-	0.04
1,2-dihydro-2,5,8-trimethyl-naphthalene	$C_{13}H_{16}$	0.22	0.19	0.24
1,2-dihydro-3,5,8-trimethyl-naphthalene	$C_{13}H_{16}$	0.12	0.16	-
Diphenylmethane	$C_{13}H_{12}$	-	-	0.31
4-methyl-1,1'-Biphenyl,	$C_{13}H_{12}$	0.29	0.33	0.34
1,6,7-trimethyl-naphthalene	$C_{13}H_{14}$	0.27	0.49	0.46
2,3,6-trimethyl-naphthalene	$C_{13}H_{14}$	0.55	0.51	1.02
1,4,6-Trimethyl-naphthalene	$C_{13}H_{14}$	-	-	0.33
1,4,5-Trimethyl-naphthalene	$C_{13}H_{14}$	-	-	0.24
4,6,8-Trimethylazulene	$C_{13}H_{14}$	-	-	0.11
1,2,3,4-Tetramethylnaphthalene	$C_{14}H_{16}$	0.29	0.25	0.10
3,3'-Dimethylbiphenyl	$C_{14}H_{14}$	-	-	0.19
1-methyl-7-(1-methylethyl)-naphthalene	$C_{14}H_{16}$	-	-	0.18
1,4-Dimethyl-7-ethylazulene	$C_{14}H_{16}$	-	-	0.09
1,4,5,8-Tetramethylnaphthalene	$C_{14}H_{16}$	0.21	0.17	0.10
2,4'-dimethyl-1,1'-biphenyl	$C_{14}H_{14}$	-	-	0.16
2-methyl-9H-fluorene	$C_{14}H_{12}$	-	-	0.16
1-methyl-9H-fluorene	$C_{14}H_{12}$	-	-	0.09
9-methyl-9H-fluorene	$C_{14}H_{12}$	-	-	0.17

Table 10:13 (continue)

Compounds (wt.%)	Formula	425 °C	475 °C	575 °C
1,2,3,4,5,6-Hexahydroanthracene	$C_{14}H_{16}$	-	-	0.29
9,10-dihydro-anthracene	$C_{14}H_{12}$	-	-	0.13
1-Ethyl-4-phenylbenzene	$C_{14}H_{14}$	-	-	0.10
Phenanthrene	$C_{14}H_{10}$	-	-	0.11
Ledane	$C_{15}H_{26}$	0.20	0.11	0.15
1,1'-(1,3-propanediyl)bis-benzene	$C_{15}H_{16}$	0.12	0.19	0.16
1,4-dimethyl-7-(1-methylethyl)-azulene	$C_{15}H_{18}$	-	-	0.15
1-Methyl-2-(4-methylbenzyl)benzene	$C_{15}H_{16}$	-	-	0.30
(3,4-Divinylcyclohexyl)benzene	$C_{16}H_{20}$	0.10	0.13	0.04
1,2,3,5,6,7,8,8a-octahydro-1,4-dimethyl-7-(1-methylethenyl)-azulene	$C_{15}H_{24}$	0.76	0.57	-
Aliphatics		**40.85**	**44.14**	**21.48**
Alkanes		*4.62*	*5.00*	*3.23*
n-Hexane	C_6H_{14}	0.16	0.08	0.03
Cyclohexane	C_6H_{12}	0.02	0.02	0.04
1,4-bis(methylene) cyclohexane	C_8H_{12}	-	-	0.04
1,1-Dimethyl-2-(2-methyl-2-propenyl)cyclopropane	C_9H_{16}	-	-	0.07
1-Methylene-3-(1-methylethylidene)cyclopentane	C_9H_{14}	-	-	0.04
1,1-Dimethyl-4-methylenecyclohexane	C_9H_{16}	0.01	0.11	0.05
2,2,4,4-tetramethyl-pentane	C_9H_{20}	0.77	0.90	0.08
1-Butenylidenecyclohexane	$C_{10}H_{16}$	0.46	0.63	0.97
4-propyl-heptane	$C_{10}H_{22}$	0.16	0.26	-
n-Tridecane	$C_{13}H_{28}$	0.09	-	0.18
n-Tetradecane	$C_{14}H_{30}$	-	-	0.21
n-Pentadecane	$C_{15}H_{32}$	0.35	0.89	0.23
n-Hexadecane	$C_{16}H_{34}$	0.25	0.08	0.14
2,2,4,4,6,8,8-heptamethyl-nonane	$C_{16}H_{34}$	0.48	0.51	-
n-Heptadecane	$C_{17}H_{36}$	0.22	0.30	0.67
n-Octadecane	$C_{18}H_{38}$	0.88	0.76	0.13
n-Nonadecane	$C_{19}H_{40}$	0.21	0.11	0.15
n-Eicosane	$C_{20}H_{42}$	0.30	0.10	0.08
n-Heneicosane	$C_{21}H_{44}$	0.25	0.26	0.12
Alkenes		*11.48*	*12.00*	*9.71*
2,4-dimethyl-1,3-pentadiene	C_7H_{12}	-	0.02	0.04
1,5-Dimethyl-1-cyclopentene	C_7H_{12}	0.02	0.02	0.03
2-Methyl-1,3,5-hexatriene	C_7H_{10}	0.01	0.02	0.07

Table 10:13 (continue)

Compounds (wt.%)	Formula	425 °C	475 °C	575 °C
3-Methyl-1,3,5-hexatriene	C_7H_{10}	0.03	0.04	0.07
2,3-dimethyl-1-pentene	C_7H_{14}	0.01	0.01	0.07
1,3-Cycloheptadiene	C_7H_{10}	0.02	0.02	0.03
2,4,4-trimethyl-1-pentene	C_8H_{16}	0.00	-	-
2,3,3-trimethyl-1,4-pentadiene	C_8H_{14}	0.03	0.02	-
1,2-dimethyl-cyclohexene	C_8H_{14}	0.01	0.02	0.03
4-ethenyl-cyclohexene	C_8H_{12}	0.25	0.15	0.08
2,5,5-Trimethyl-1,3-cyclopentadiene	C_8H_{12}	0.02	0.05	0.05
1,3-Dimethyl-1-cyclohexene	C_8H_{14}	-	-	0.03
1,5-Dimethyl-1,4-cyclohexadiene	C_8H_{12}	-	-	0.05
1,2-Dimethyl-4-methylene-1-cyclopentene	C_8H_{12}	0.02	0.04	0.11
2,5-dimethyl-2,4-Hexadiene	C_8H_{14}	-	-	0.04
2,4,6-Octatriene	C_8H_{12}	0.11	0.10	0.13
1,3,5,7-Cyclooctatetraene	C_8H_8	0.35	0.41	0.95
3-(1-methylethyl) cyclohexene	C_9H_{16}	0.04	0.05	0.08
2,5-Dimethyl-3-methylene-1,5-hexadiene	C_9H_{14}	0.12	0.18	0.80
2,6-Dimethyl-1,3,5-heptatriene	C_9H_{14}	0.05	0.10	0.08
1,6-Dimethyl-2,3,5-heptatriene	C_9H_{15}	0.04	0.05	-
1,2,5,5-Tetramethyl-1,3-cyclopentadiene	C_9H_{14}	0.06	0.07	0.10
1,3,5,5-Tetramethyl-1,3-cyclohexadiene	$C_{10}H_{16}$	0.07	0.27	0.19
2,5,6-Trimethyl-1,3,6-heptatriene	$C_{10}H_{16}$	0.32	0.41	0.34
5,5-Dimethyl-2-propyl-1,3-cyclopentadiene	$C_{10}H_{16}$	0.20	0.17	1.71
2,4,6-Trimethyl-1,3,6-heptatriene	$C_{10}H_{16}$	0.17	0.22	-
2,6-Dimethyl-1,6-octadiene	$C_{10}H_{18}$	0.19	0.55	0.15
2,7-Dimethyl-1,7-octadiene	$C_{10}H_{18}$	0.31	0.46	-
1-Decene	$C_{10}H_{20}$	0.04	0.12	0.68
5-methyl-3-(1-methylethenyl)-cyclohexene	$C_{10}H_{16}$	0.38	0.14	0.32
3,3,6,6-Tetramethyl-1,4-cyclohexadiene	$C_{10}H_{16}$	0.56	0.55	0.99
2,5-Dimethyl-3-methylene-1,5-heptadiene	$C_{10}H_{16}$	0.79	0.87	-
4-Methyl-3-(1-methylethylidene)-1-cyclohexene	$C_{10}H_{16}$	0.13	0.23	-
1-Methyl-4-isopropyl-1-cyclohexene	$C_{10}H_{18}$	0.77	0.94	-
4-methyl-1-(1-methylethenyl)-cyclohexene	$C_{10}H_{16}$	0.25	0.28	-
3,7-dimethyl-1,3,6-Octatriene	$C_{10}H_{16}$	0.21	0.27	-
1,3-Butadienylidenecyclohexane	$C_{10}H_{14}$	0.12	0.20	-
2,5,5-Trimethyl-1,3,6-heptatriene	$C_{10}H_{16}$	0.14	0.20	-
4-Ethyl-3-ethylidene-1-cyclohexene	$C_{10}H_{16}$	0.19	0.25	-

Table 10:13 (continue)

Compounds (wt.%)	Formula	425 °C	475 °C	575 °C
1-Methyl-4-(1-methylethylidene)-1-cyclohexene	$C_{10}H_{16}$	0.34	0.32	-
4-Ethyl-3-ethylidene-1-cyclohexene	$C_{10}H_{16}$	0.20	0.18	-
5-Methyl-3-(1-methylethylidene)-1,4-hexadiene	$C_{10}H_{16}$	0.29	0.35	-
2,6-dimethyl-2,4,6-octatriene	$C_{10}H_{16}$	0.38	0.39	-
2,4,4,6-Tetramethyl-2-heptene	$C_{11}H_{22}$	1.13	1.12	-
1-Dodecene	$C_{12}H_{24}$	0.09	0.12	0.15
1-Tridecene	$C_{13}H_{26}$	0.10	-	0.72
2,6,10-Trimethyl-1,5,9-undecatriene	$C_{14}H_{24}$	0.47	0.53	0.07
2,3,5,8-Tetramethyl-1,5,9-decatriene	$C_{14}H_{24}$	0.41	0.26	0.07
1-Tetradecene	$C_{14}H_{28}$	-	-	0.11
2,3,5,8-Tetramethyl-1,5,9-decatriene	$C_{14}H_{24}$	0.57	0.45	-
1-Pentadecene	$C_{15}H_{30}$	0.46	0.35	0.23
1-Hexadecene	$C_{16}H_{32}$	0.46	0.08	0.13
1-Octadecene	$C_{18}H_{36}$	0.42	0.23	1.01
2,4a,5,6,7,8,9,9a-octahydro-3,5,5-trimethyl-9-methylene-1H-benzocycloheptene	$C_{15}H_{24}$	0.12	0.11	-
Terpenes		*24.78*	*27.16*	*8.54*
Isolimonene	$C_{10}H_{16}$	0.01	0.05	0.16
Camphene	$C_{10}H_{16}$	0.02	0.03	0.09
L-Limonene	$C_{10}H_{16}$	0.82	1.45	1.25
1,3,8-p-Menthatriene	$C_{10}H_{14}$	0.40	0.42	-
D-Limonene	$C_{10}H_{16}$	21.05	22.84	7.04
1,2,8-p-Menthatriene	$C_{10}H_{14}$	0.35	0.65	-
α-Selinene	$C_{15}H_{24}$	0.41	0.29	-
Thujopsene	$C_{15}H_{24}$	0.79	0.66	-
Aromadendrene	$C_{15}H_{24}$	0.58	0.47	-
α-Farnesene	$C_{15}H_{24}$	0.31	0.27	-
Heteroaromatics		**15.45**	**14.34**	**6.15**
2-methyl-thiophene	C_5H6_S	0.02	0.03	-
4-Hydroxy-4-methylpentanone	$C_6H_{12}O_2$	0.16	0.25	0.22
Benzothiazole	C_7H_5NS	1.01	1.54	1.82
2(3H)-Benzothiazolone	C_7H_5NOS	0.12	0.08	-
4-ethyl-phenol	$C_8H_{10}O$	-	-	0.12
3-(2-butenyl)-thiophene	$C_8H_{10}S$	0.10	0.16	-
2,2-Dimethylhexanol	$C_8H_{18}O$	0.65	0.52	0.07
Benzenepropanol	$C_9H_{12}O$	0.05	0.06	-
2,7-Dimethyl-1-benzothiophene	$C_{10}H_{10}S$	0.18	0.12	0.29

Table 10:13 (continue)

Compounds (wt.%)	Formula	425 °C	475 °C	575 °C
4-tert-Butylphenol	$C_{10}H_{14}O$	-	-	0.22
2,8-Dimethylquinoline	$C_{11}H_{11}N$	0.57	0.46	1.04
2,2,4-Trimethyl-1,2-dihydroquinoline	$C_{12}H_{15}N$	1.14	0.83	0.05
Diphenylamine	$C_{12}H_{11}N$	0.18	0.18	0.14
3-Acetyl-2,5-dimethylbenzo(b)thiophene	$C_{12}H_{12}OS$	0.09	0.16	0.25
2-Phenylbenzothiazole	$C_{13}H_9NS$	0.19	0.17	0.14
4-(1,1,3,3-tetramethylbutyl)-phenol	$C_{14}H_{22}O$	0.80	0.71	0.24
Tetradecanoic acid	$C_{14}H_{28}O_2$	5.84	4.61	-
6,11-Dimethyl-2,6,10-dodecatrien-1-ol	$C_{14}H_{24}O$	0.27	0.29	-
2-methyl-4-(1,1,3,3-tetramethylbutyl)-phenol	$C_{15}H_{24}O$	0.18	0.16	0.08
3,7,11-Trimethyl-1,6,10-dodecatriene-3-ol	$C_{15}H_{26}O$	0.20	0.12	-
Pentadecanoic acid	$C_{15}H_{30}O_2$	2.78	2.96	1.01
Hexadecanenitrile	$C_{16}H_{31}N$	0.39	0.34	0.11
4-(1,3-Dimethylbutyl)amino-diphenylamine	$C_{18}H_{24}N_2$	0.54	0.61	-
Heptadecanenitrile	$C_{17}H_{33}N$	-	-	0.21
Hexadecanoic acid	$C_{16}H_{32}O_2$	-	-	0.12
Water	H_2O	**1.48**	**0.77**	**0.51**
Undifined		**30.22**	**27.99**	**21.22**
Total		**100.00**	**100.00**	**100.00**

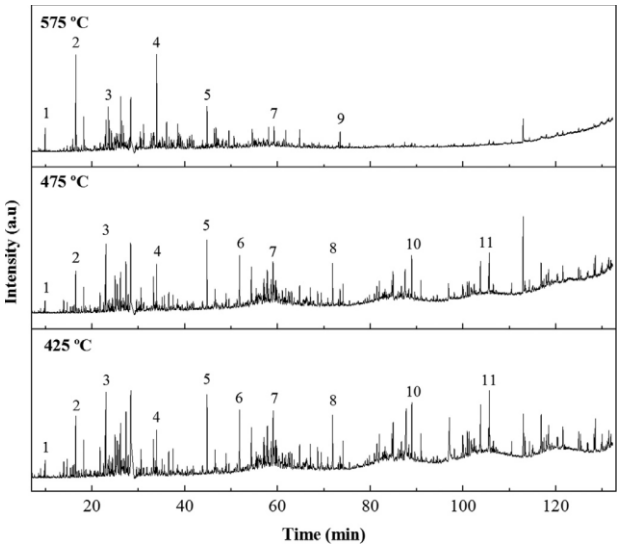

Figure 10.10: Chromatograms of the three TPOs obtained by GC/MS analysis (Peaks: 1) toluene; 2) o-xylene; 3) D-limonene; 4) a-methylstyrene; 5) Benzothiazole; 6) 2,2,4,4-tetramethylpentane; 7) 2,4,4,6-tetramethyl-2-heptene; 8) Tridecene; 10) tetranoic acid; 11) 4-(1,3-dimethylbutyl)amino-diphenylamine).

As observed in Table 10.13, GC/MS analysis revealed that the TPO was a mixture of $C_6 - C_{20+}$ compounds and that it contained mainly aliphatic and aromatic compounds, the former being predominant in the TPOs obtained at 425 and 475 °C and the latter at 575 °C. Thus, it can be seen that the proportion of aromatics increased with temperature, which is in agreement with the results observed by other researchers [3,5]. The aromaticity of TPOs is due, on the one hand, to the aromatic nature of the source polymeric material, specifically SBR, which already contains aromatic rings and hence chain splitting may easily lead to the formation of aryl chain fragments [4,28], and on the other hand, to the following secondary recombination reactions: (i) cyclisation of aliphatic chains, (ii) cyclisation of olefin structures followed by dehydrogenation and, (iii) Dies-Alder condensation reactions of alkenes [2,37]. These results that confirm the aromatization of the TPOs at higher temperature agree well with the FTIR analysis (Figure 10.9), where a clear increase of aromatic peaks intensity in the 575 °C TPO was observed.

The volatile or light aromatics such as benzene, toluene, xylenes (dimethylbenzenes) or ethylbenzene (BTXE) as well as styrene and indene are interesting products of the TPO given their high added value for the plastics/polymer industry. Some of these volatile aromatic hydrocarbons and their alkylated homologues reach significant concentration at 575 °C, e.g. toluene (1.40 wt.%), total xylenes (4.82 wt.%), alkylated styrenes (6.79 wt.%) and indenes (3.97 wt.%).

Among the different aromatics detected in the TPO obtained at 575 °C, around 12.64 wt.% were PAHs, being largely formed by alkylated naphthalenes, fluorenes and phenathrenes. It can be seen in Table 10.13 that some of the PAHs are not present in the TPOs produced at lower temperatures, while at 575 °C all of them are present and mostly in a higher concentrations. The formation of these compounds is favoured by secondary cracking of volatiles and Dies-Alder condensation type reactions at high temperatures, as confirmed by Cunliffe and Williams [37]. According to the literature [4], aliphatic compounds are aromatised to PAHs as temperature is increased and their formation seems to be unavoidable. However, the low yield of this fraction at low temperatures, compared to other works developed in rotator kiln [38] or fixed bed reactors [39], highlights the efficient performance of the CSBR reactor regarding the limited residence time of volatiles and high heat and mass transfer, which hinders the formation of these compounds, as also demonstrated by Arabiourrutia et al. [40].

With respect to the aliphatic fraction yield, its decrease at 575 °C is not only due to the recombination reactions (mainly from the olefins, whose yield is much higher than alkanes at 425 and 475 °C), which enhances the formation of aromatics, but also to the increase of thermal cracking at high temperatures, thus, promoting the formation of gaseous products [13]. The main alkanes compounds are straight chain hydrocarbons from C_{13} to C_{20}, whereas alkenes predominantly contain a mixture of $C_8 – C_{14}$ hydrocarbons. Rathsack et al. [2] suggested that the formation of i- and n-alkanes were not only derived from rubber polymers, but also from the mineral oils added as plasticizers.

The largest individual component in the aliphatic fraction and also in the whole TPO is D-limonene, which attains its maximum concentration of 22.84 wt.% at 475 °C (being the total yield of 13.30 wt.% based on tyre weight). Limonene is a cyclic terpene ($C_{10}10H_6$) that exists in its D- and L-form and its main source is the polyisoprene (NR) content of the tyre. Its formation during fast pyrolysis mainly occurs by depolymerisation reactions of polyisoprene through a b-scission mechanism and subsequent intramolecular cyclisation [41,42]. Additionally, isoprene could also dimerize through a Dies-Alder pathway and be transformed into D,L-limonene [42]. As observed in Table 10.13, both, D- and L-limonene yields decreases sharply at 575 °C due to secondary reactions (mainly that of dehydrogenation), which take place at high temperatures. It has been suggested that limonene decomposes above 500 °C to form a range of products, including BTX, trimethylbenzenes, methylstyrene and indanes among others [38,41]. Other authors have observed a similar trend of limonene with temperature, attaining maximum yields between 400 and 500 °C [15,40,43,44]. Moreover, Mkhize et al. [11] working with the same TT sample, also reported that the maximum D,L-limonene yield was obtained within the temperature range of 450–500 °C. It is believed that D,L-limonene is very unstable and it will decompose above 450 °C if it is not quickly removed from the

reaction zone [41], thus, the short residence time of volatiles in the CSBR will prevent limonene degradation. Furthermore, working under vacuum conditions in a CSBR is possible to obtain even higher limonene yields by further reducing the gas residence time [22,42].

These results are in accordance with those reported in the literature where the yields of non-aromatics are higher than aromatic compounds at 400 – 500 °C [2,8,45]. Likewise, similar trends of different families yield with temperature have been reported in the literature with the CSBR technology and working in a continuous mode [13,15]. Nevertheless, the previous research group obtained higher concentration of aromatics and lower of aliphatics in their TPOs produced from PCT at 425 °C and 500 °C. This difference might be attributed to the distinct tyre composition, i.e, the higher content of SBR used in PCT manufacturing (approximately 60 %) compared to that in TT (20 – 30 %) will lead to higher amount of aromatics. The same trend was observed by Ucar et al. [14] where the TPO from PCT pyrolysis contained a higher amounts of aromatics than the TPOs from TT pyrolysis. Similarly, Islam et al. [28] found that the concentration of aliphatic compounds was higher than that of aromatic compounds, and concretely, the alkene group was predominant in the aliphatic family in the pyrolysis of motorcycle tyre waste because the content of NR in this type of tyre formulation is higher than that of SBR.

Besides, oxygen functionalized compounds like alkylphenols and carboxylic acids, nitrogenated species, such as quinolines or nitriles, and sulphur containing compounds, such as thiophenes and benzothiophenes were also identified in the TPOs be it with lower concentrations. Concretely, benzothiazole increases in the TPO with temperature from 0.58 wt.% at 425 °C to 0.98 wt.% at 575 °C. The presence of oxygenated compounds is probably due to the thermal degradation of some additives of the tyre such as stearic acid or extender oils that contain oxygen in their molecular structure. Likewise, nitrogenated and nitro-sulphurated species are derived from the accelerators used for the vulcanization of rubber, which are frequently sulphur and/or nitrogen based organic compounds, for instance 2-mercaptobenzothiozole, benzothiozolyl disulphide and so on [28]. Furthermore, the origin of some nitrogenated compounds would also be the presence of some nitrile rubber (NBR) in the tyre [46]. Table 10.13 shows that the main heteroatomic compounds are carboxylic acids, such as tetranoic and pentanoic acid. These carboxylic acids are highly affected when the pyrolysis temperature is raised given that cracking reactions are more severe, and therefore lighter compounds are formed. The same tendency was reported by Choi et al. [45], where the yield of heteroatomic compounds decreased from 8.98 wt.% at 496 °C to 5.77 wt.% at 614 °C. Moreover, in their study the concentration of carboxylic acids in the TPO also diminished greatly with temperature. Besides, Lopez et al. [15] also determined that the main nitro-sulphurated compound was benzothiazole, whose yield also increased slightly with temperature.

Ultimate analysis, water content and HHV

Table 10.14 shows the HHV, water content and the ultimate analysis of the TPOs obtained at different temperatures. These properties are also compared in Table 10.14 with those of diesel and gasoline.

Table 10.14: Ultimate analysis, high heating values of the TPOs obtained at different temperatures and their comparison with those of diesel and gasoline.

Ultimate analysis (wt.%)	425 °C	475 °C	575 °C	Diesel [6]	Gasoline [30]
Carbon	85	86	88	86.1	85.4
Hydrogen	11	10.8	10.2	13.2	14.1
Nitrogen	0.1	0.3	0.2	0	200 ppm
Sulphur	1.15	1.17	1.27	0	280 ppm
Oxygen*	2.75	1.73	0.33	0.7	-
Water	1.48	0.77	0.51	55 ppm	-
HHV (MJ kg-1)	42.5	42.7	42.8	45.1	44
H/C	1.55	1.51	1.39	1.9	2

* By difference

As observed, the content of C and H increases, while that of N, S and O decreases with respect to the initial tyre (Table 10.11). As reported for other TPOs [3], the present ones contain carbon and hydrogen contents around 85–89 wt.% and 10 – 11 wt.%, respectively, with these values being similar to those of refined petroleum fuels. It is noteworthy that the sulphur content in the TPOs slightly increases with increasing the temperature, however, in the three cases the sulphur is out of specification according to the diesel and gasoline fuel standards. These results are consistent with those reported by Unapumnuk et al. [47], who specified that the initial S percentage of the TPO was less than 0.2 wt.% at 400 °C and it was increased rapidly to about 2 wt.% with the increase in temperature. Similarly, Cunliffe and Williams [15] reported sulphur concentrations of 1.3 – 1.4 % in the TPO in the range 450–600 °C. Additionally, the increase of aromaticity in the TPOs with increasing temperature is again confirmed with the decrease of H/C molar ratio from 1.55 to 1.39. The drop between 475 and 575 °C is sharper given that secondary reactions of the vapours, including chain cracking, dehydrocyclization, and aromatization, become more important [38]. The H/C values are lower than that for diesel (1.9) and gasoline (2), which contain more paraffinic compounds and have therefore higher H/C ratios.

The HHV of all the TPOs is higher than of the raw TT (38.1 $MJ.kg^{-1}$) and is close to that of diesel and gasoline, which reflects their potential to be used as liquid fuels. In this work, the HHV increases slightly with pyrolysis temperature attaining a maximum value of 42.8 $MJ.kg^{-1}$ at 575 °C. Conversely, other works

have reported a slight decrease of HHV with increasing temperature, given that longer chain hydrocarbons are cracked into gaseous products [39,46]. However, the suitable features of the CSBR hinder secondary cracking reactions, thus, attaining a TPO with higher C content and HHV.

Moreover, the content of water in the TPOs obtained at different temperatures has also been measured because it significantly affects combustion. This water comes from the initial moisture of the feedstock and that produced during the reaction. Despite its low content (1.5 – 0.5 wt.%), the amount of water specified for gasoline and diesel is lower, thus, it should be removed before using the TPO as alternative fuel. Nevertheless, according to Martinez et al. [6], modest water content in the TPO can reduce the combustion temperature in diesel engines and thereby reduce NO_x emissions. Despite the tyre types (different compositions) and the different reactor configurations utilized, the results shown in Table 10.14 are consistent with those obtained in the literature. In fact, the carbon content in all the studies is in the 82 – 88 wt.% range, HHV is always between 40 and 44 $MJ.kg^{-1}$, and similarly, low water content (up to 4 wt.%) was measured in most TPOs [6,36,37].

Simulated distillation

Figure 10.11 shows the simulated distillation curves of the TPOs obtained at 425, 475 and 575 °C and compares them with those of vacuum gasoil, gasoline and diesel fuel in order to better assess the potential uses of TPOs. As observed, the distillation range of the TPOs reflects their unrefined nature due to the presence of a wide variety of products (Table 10.13) with different boiling points. The distillation curves obtained for the TPOs of 425 and 475 °C are quite similar. Severe thermal cracking at higher temperatures gives higher concentration of light compounds, thus, resulting in an increase of the gasoline fraction (<160 °C) from 39.4 % at 425 °C to 86.4 % at 575 °C.

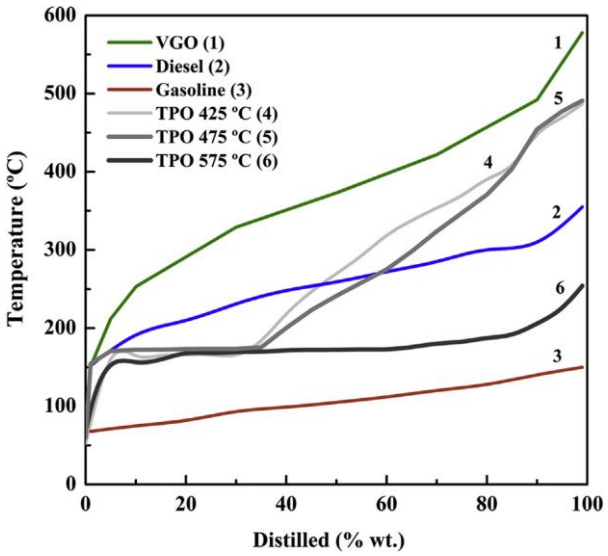

Figure 10.11: Comparison of the simulated distillation curves of the TPOs obtained at 425, 475 and 575 °C with those of commercial fuels.

As shown in Figure 10.11, the initial boiling points of the TPOs are lower than that of diesel fuel. Approximately 60 % of the TPO of 425 and 475 °C corresponds to the diesel boiling range, while the remaining heavier organic compounds (40%) distillate at higher temperatures, corresponding to those of VGO. It should be noted that the boiling point of the TPO obtained at 575 °C is between diesel fuel and gasoline. This same trend was observed by Rofiqul et al. [28], i.e., up to 90 % of their TPO was in the diesel-gasoline range. According to some authors [14,28], the conclusion from these curves is that TPOs from PCT and TT can be blended with gasoline or diesel fuels after performing treatments such as desulphurization and hydrogenation or blending them with petroleum refinery streams.

10.3.3.3 TPO applications and future perspectives

In view of the properties of the TPOs obtained in this work, some conclusions about their possible applications can be drawn. It is clear that pyrolysis temperature changes the product characteristic and therefore this parameter can be fixed depending on the targeted application for the TPO.

Considering their high HHV (Table 10.14), boiling points (Figure 10.11) and storage stability (the properties remained unaltered with time), the TPOs obtained at different temperatures might be an interesting alternative to commercial fuels. The TPOs obtained at 425 and 475 °C seem to be a better substitute for diesel (BP = 150 – 360 °C) or fuel-oil (BP = 150 – 390 °C), whereas that at 575 °C is a more convenient alternative for gasoline (BP = 140 – 216 °C). However, the high content of sulphur, nitrogen

and moisture (Table 10.14), as well as the presence of aromatic compounds indicate that their upgrading/purification is crucial to be used directly as liquid fuel. Thus, the selection of pyrolysis temperature must be a balance between different parameters, i.e, the specifications of a country/region, the current price of fuels and the economy of the whole process (pyrolysis and upgrading step), which would define the type of fuel that should be produced.

Towards upgrading alternatives, several researchers have proposed different processes in order to increase the value of the feedstock [27]. For example, Hita el al [10]. concluded that the most interesting reaction pathways for TPO upgrading were hydrodesulphuration, hydrodearomatization and hydrocracking. However, utilization of catalysts to upgrade TPO is fraught with challenges since nitrogenous compounds present in the TPO can attack catalysts and promote gum formation [48,49]. Moreover, Murugan et al. [50] improved the viscosity and the sulphur content of the TPO through a refining process which included 3 stages: removal of moisture, desulphuration and vacuum distillation. Chen et al. [51] developed an Ultrasound Assisted Oxidative Desulphuration process attaining a sulphur removal of 89 %, although high investments were required at large scale operation.

Alternatively, some studies recommended blending TPOs with different petroleum refinery streams, where mixing it with diesel being the most successful [30]. It has been reported that TPO is completely miscible with diesel and some examples of using diesel/TPO blends in real compression ignition engines have been reported in the literature [8,50,52]. However, high aromatic contents have poor ignition quality and the presence of cycloalkanes also reduces the cetane number, thus, the TPOs obtained in this work could represent a feasible alternative to fossil derived liquid fuels as long as it is blended with diesel in low concentrations.

Moreover, some of the compounds detected in the TPOs (Table 10.13) are high value added products in the chemical industry and they could constitute some economic benefit to the pyrolysis process. Indeed, the major compound in the TPOs obtained at 425 and 475 °C was limonene, with a maximum potential production of 0.22 g and 0.24 g of limonene/g of TPO, respectively. This compound is commonly used in the formulation of industrial solvents, resins, adhesives, and a dispersing agent for pigments [4], however, it needs to be separated from the multitude of components contained in the TPO. While it is relatively easy to obtain a dipentene enriched light naphtha (or similar) fraction by either TPO distillation (boiling points close to 170 °C) or selective condensation, further purification is not so simple [42]. Although Pakdel et al. [41] have obtained promising results recovering limonene from TPO with a purity of 95%, the methods used are not easily transferable to large scale. In fact, the main challenges for future research lies in the

separation of limonene from other compounds. On the one hand, the compounds with boiling points close to that of limonene such as 1,2,4- trimethylbenzene, 1-methyl-4-(1-methylethyl)-benzene (p-cymene), indane and, on the other hand, the sulphur-containing compounds (even in very low concentrations) can result in a foul odor to the oil, thus reducing the quality and economic value [42]. In this work, the sulphur content in both TPO (475 and 425 °C) is almost the same (Table 10.14) and the total concentration of those compounds difficult to separate (trimethylbenzene, p-cymene and indane) is lower in the TPO obtained at 475 °C (0.9 wt.%) than that at 425 °C (1.1 wt.%). These facts added to the higher limonene yield suggest that the pyrolysis temperature for limonene production should be close to 475 °C.

In addition, some other valuable chemicals can be also recovered from the TPO. For example, the TPO from 575 °C have revealed considerable amounts of xylenes (Table 10.13), which have applications in the plastics industry to produce plasticizers, polyester resins and fibres. Besides, at this temperature the maximum yield of 0.75 wt.% was also obtained for toluene, which is commonly used in the production of pesticides, dyestuffs, surfactants and solvents. In the literature, significant concentrations have been reported for other useful compounds, such as benzene, ethylbenzene or styrene [5], but their content was almost negligible in the TPOs obtained in this work mainly due to the TT containing lesser synthetic rubber. It should be noted that these compounds are not easily recovered from the TPO and future research should focus on overcoming these limitations.

The possible direct applications of TPO and post-treatment methods for its valorization are very similar to those reported in the literature for other wastes, such as waste plastics [53–55]. Thus, the pyrolysis liquid from different types of plastics could be improved by techniques, such as filtration, chemical treatment, blending with diesel and other fuels, and distillation and refining to remove heavy hydrocarbons and impurities. This fact could be of great interest, as the pyrolysis oils from plastics and tyres could be jointly treated for improving their properties.

Accordingly, the great market potential of TPO and the wide range of valorization possibilities for the produced gas and char (as a fuel to reduce energy requirements or as raw material for producing higher value-added products) make pyrolysis especially interesting for large-scale implementation. In fact, the high level of process technological development reported in the literature, the versatility of the process, the simple equipment required (and therefore low investment) and the minimization of environmental concerns, as well as the commercial interest of the products make pyrolysis an interesting alternative for tyre valorization. According to Ouda et al. [56] and Nizami et al. [57], the pyrolysis process has lower annual

capital investment and net operational costs per ton of waste produced in comparison to other waste-to-energy technologies (WTE), such as transesterification technology.

Therefore, in view of the results presented in this work and the technological development of fast pyrolysis process for attaining very high oil yields, the future perspectives in this field should focus on exploring further TPO applications and improving the energy efficiency of the process to make it economically sustainable. Energy requirements would be greatly reduced by burning the gas and char in auxiliary units, but this choice depends on the marketability of these by-products for attaining higher value added products (activated carbons in the case of char) or for recovering the isoprene from the gas. Likewise, improving the separation efficiency of the most valuable compounds (limonene and BTX) is also a key factor for the large-scale implementation of pyrolysis. In addition, a comprehensive life cycle assessment of waste tyre pyrolysis would also be necessary to fully understand the economic, environmental and overall sustainability of this technology [55].

10.3.4 Conclusions

The TPO produced in a CSBR has been characterized and the effect of temperature on its properties and composition has been studied. This reactor is suitable for attaining high liquid yields, which is mainly due to the low residence time of the volatiles hindering secondary gas formation. The FTIR analysis revealed that TPO was composed of aliphatic, aromatic and sulphur and oxygen containing compounds among others. The GC-MS analysis identified hundreds of those compounds and revealed that their concentrations changed with increasing temperature. Thus, the production of aromatics was promoted at high temperatures due to secondary recombination reactions, whereas limonene was the major compound in the 425 – 475 °C range.

The ultimate analysis and simulated distillation showed that the TPOs obtained at 425 °C and 475 °C share certain similarities with diesel fuels, while that obtained at 575 °C is closer to gasoline. It is noteworthy that the high sulphur, nitrogen and moisture content would hinder the direct combustion of TPO, although mixing it with diesel have resulted in satisfactory results in terms of engine performance and exhaust emissions. Moreover, the relatively high concentrations of certain valuable compounds (limonene, xylene, toluene, etc.) indicate that there is potential for chemicals production, despite the fact that the recovery of these compounds from TPO is not straightforward.

Acknowledgements

This work was carried out with financial support from the Ministry of Economy and Competitiveness of the Spanish Government (CTQ2016-75535-R and CTQ2014-59574-JIN), the European Regional Development Fund, the Basque Government (IT748-13) and the University of the Basque Country (UFI 11/39). Jon Alvarez also thanks the University of the Basque Country UPV/EHU for his post-graduate Grant (ESPDOC 2015). This research was also supported by the Recycling and Economic Development Initiative of South Africa (REDISA) and the National Research Foundation.

References

[1] Torretta V, Rada EC, Ragazzi M, Trulli E, Istrate IA, Cioca LI. Treatment and disposal of tyres: two EU approaches. A review. Waste Manage 2015;45: 152–60.

[2] Rathsack P, Riedewald F, Sousa-Gallagher M. Analysis of pyrolysis liquid obtained from whole tyre pyrolysis with molten zinc as the heat transfer media using comprehensive gas chromatography mass spectrometry. J Anal Appl Pyrolysis 2015;116:49–57.

[3] Hita I, Arabiourrutia M, Olazar M, Bilbao J, Arandes JM, Casta~no P. Opportunities and barriers for producing high quality fuels from the pyrolysis of scrap tires. Renew Sustain Energy Rev 2016;56:745–59.

[4] Martínez JD, Puy N, Murillo R, García T, Navarro MV, Mastral AM. Waste tyre pyrolysis e a review. Renew Sustain Energy Rev 2013;23:179–213.

[5] Williams PT. Pyrolysis of waste tyres: a review. Waste Manage 2013;33: 1714e28.

[6] Martínez JD, Lapuerta M, García-Contreras R, Murillo R, García T. Fuel properties of tire pyrolysis liquid and its blends with diesel fuel. Energy Fuels 2013;27:3296–305.

[7] Ayano_glu A, Yumrutas¸ R. Production of gasoline and diesel like fuels from waste tire oil by using catalytic pyrolysis. Energy 2016;103:456–68.

[8] Frigo S, Seggiani M, Puccini M, Vitolo S. Liquid fuel production from waste tyre pyrolysis and its utilisation in a diesel engine. Fuel 2014;116:399–408.

[9] Hariharan S, Murugan S, Nagarajan G. Effect of diethyl ether on tyre pyrolysis oil fueled diesel engine. Fuel 2013;104:109–15.

[10] Hita I, Rodríguez E, Olazar M, Bilbao J, Arandes JM, Casta~no P. Prospects for obtaining high quality fuels from the hydrocracking of a hydrotreated scrap tires pyrolysis oil. Energy Fuels 2015;29:5458–66.

[11] Mkhize NM, van der Gryp P, Danon B, G€orgens JF. Effect of temperature and heating rate on limonene production from waste tyre pyrolysis. J Anal Appl Pyrolysis 2016;120:314–20.

[12] Weitkamp J, Raichle A, Traa Y. Novel zeolite catalysis to create value from surplus aromatics: preparation of C2 þ-n-alkanes, a high-quality synthetic steamcracker feedstock. Appl Catal A 2001;222:277–97.

[13] Lopez G, Olazar M, Amutio M, Aguado R, Bilbao J. Influence of tire formulation on the products of continuous pyrolysis in a conical spouted bed reactor. Energy Fuels 2009;23:5423–31.

[14] Ucar S, Karagoz S, Ozkan AR, Yanik J. Evaluation of two different scrap tires as hydrocarbon source by pyrolysis. Fuel 2005;84:1884–92.

[15] L_opez G, Olazar M, Aguado R, Bilbao J. Continuous pyrolysis of waste tyres in a conical spouted bed reactor. Fuel 2010;89:1946–52.

[16] Alvarez J, Amutio M, Lopez G, Barbarias I, Bilbao J, Olazar M. Sewage sludge valorization by flash pyrolysis in a conical spouted bed reactor. Chem Eng J 2015;273:173–83.

[17] McCullough DP, Van Eyk PJ, Ashman PJ, Mullinger PJ. Impact of sodium and sulfur species on agglomeration and defluidization during spouted bed gasification of south Australian lignite. Energy Fuels 2015;29:3922–32.

[18] Bernocco D, Bosio B, Arato E. Feasibility study of a spouted bed gasification plant. Chem Eng Res Des 2013;91:843–55.

[19] Spiegl N, Sivena A, Lorente E, Paterson N, Millan M. Investigation of the oxyfuel gasification of coal in a laboratory-scale spouted-bed reactor: reactor modifications and initial results. Energy Fuels 2010;24:5281–8.

[20] Park HC, Lee B, Yoo HS, Choi HS. Fast pyrolysis characteristics of biomass in a conical spouted bed reactor. Environ Prog Sustain Energy 2016. http://dx.doi.org/10.1002/ep.12476. In Press.

[21] Niksiar A, Faramarzi AH, Sohrabi M. Kinetic study of polyethylene terephthalate (PET) pyrolysis in a spouted bed reactor. J Anal Appl Pyrolysis 2015;113:419–25.

[22] Lopez G, Olazar M, Aguado R, Elordi G, Amutio M, Artetxe M, et al. Vacuum pyrolysis of waste tires by continuously feeding into a conical spouted bed reactor. Ind Eng Chem Res 2010;49:8990–7.

[23] Alvarez J, Lopez G, Amutio M, Bilbao J, Olazar M. Bio-oil production from rice husk fast pyrolysis in a conical spouted bed reactor. Fuel 2014;128:162–9.

[24] Amutio M, Lopez G, Alvarez J, Moreira R, Duarte G, Nunes J, et al. Flash pyrolysis of forestry residues from the Portuguese Central Inland Region within the framework of the BioREFINA-Ter project. Bioresour Technol 2013;129: 512–8.

[25] Artetxe M, Lopez G, Amutio M, Barbarias I, Arregi A, Aguado Bilbao J, et al. Styrene recovery from polystyrene by flash pyrolysis in a conical spouted bed reactor. Waste Manage 2015;45:126–33.

[26] Altzibar H, Lopez G, Bilbao J, Olazar M. Minimum spouting velocity of conical spouted beds equipped with draft tubes of different configuration. Ind Eng Chem Res 2013;52:2995–3006.

[27] Antoniou N, Zabaniotou A. Experimental proof of concept for a sustainable end of life tyres pyrolysis with energy and porous materials production. J Clean Prod 2015;101:323–36.

[28] Rofiqul Islam M, Haniu H, Rafiqul Alam Beg M. Liquid fuels and chemicals from pyrolysis of motorcycle tire waste: product yields, compositions and related properties. Fuel 2008;87:3112–22.

[29] Olazar M, Aguado R, Arabiourrutia M, Lopez G, Barona A, Bilbao J. Catalyst effect on the composition of tire pyrolysis products. Energy Fuels 2008;22: 2909–16.

[30] Kumaravel ST, Murugesan A, Kumaravel A. Tyre pyrolysis oil as an alternative fuel for diesel engines e a review. Renew Sustain Energy Rev 2016;60: 1678–85.

[31] Choi G, Oh S, Kim J. Scrap tire pyrolysis using a new type two-stage pyrolyzer: effects of dolomite and olivine on producing a low-sulfur pyrolysis oil. Energy 2016;114:457–64.

[32] Makibar J, Fernandez-Akarregi AR, Alava I, Cueva F, Lopez G, Olazar M. Investigations on heat transfer and hydrodynamics under pyrolysis conditions of a pilot-plant draft tube conical spouted bed reactor. Chem Eng Process 2011;50:790–8.

[33] Alvarez J, Amutio M, Lopez G, Bilbao J, Olazar M. Fast co-pyrolysis of sewage sludge and lignocellulosic biomass in a conical spouted bed reactor. Fuel 2015;159:810–8.

[34] Gonz_alez JF, Encinar JM, Canito JL, Rodrıguez JJ. Pyrolysis of automobile tyre waste. Influence of operating variables and kinetics study. J Anal Appl Pyrolysis 2001;58e59:667–83.

[35] Fern_andez AM, Barriocanal C, Alvarez R. Pyrolysis of a waste from the grinding of scrap tyres. J Hazard Mater 2012;203e204:236–43.

[36] Banar M, Akyıldız V, €Ozkan A, Çokaygil Z, Onay €O. Characterization of pyrolytic oil obtained from pyrolysis of TDF (tire derived fuel). Energy Conver Manage 2012;62:22–30.

[37] Cunliffe AM, Williams PT. Composition of oils derived from the batch pyrolysis of tyres. J Anal Appl Pyrolysis 1998;44:131–52.

[38] Li S, Yao Q, Chi Y, Yan J, Cen K. Pilot-scale pyrolysis of scrap tires in a continuous rotary kiln reactor. Ind Eng Chem Res 2004;43:5133–45.

[39] Laresgoiti MF, Caballero BM, de Marco I, Torres A, Cabrero MA, Chom_on MJ. Characterization of the liquid products obtained in tyre pyrolysis. J Anal Appl Pyrolysis 2004;71:917–34.

[40] Arabiourrutia M, Lopez G, Elordi G, Olazar M, Aguado R, Bilbao J. Product distribution obtained in the pyrolysis of tyres in a conical spouted bed reactor. Chem Eng Sci 2007;62:5271–5.

[41] Pakdel H, Pantea DM, Roy C. Production of dl-limonene by vacuum pyrolysis of used tires. J Anal Appl Pyrolysis 2001;57:91–107.

[42] Danon B, van der Gryp P, Schwarz CE, Gorgens JF. A review of dipentene (dllimonene) production from waste tire pyrolysis. J Anal Appl Pyrolysis 2015;112:1–13.

[43] Rofiqul IM, Haniou H, Rafiqul ABM. Limonene-rich liquids from pyrolysis of heavy automotive tire wastes. J Environ Eng 2007;2:681–95.

[44] Dai X, Yin X, Wu C, Zhang W, Chen Y. Pyrolysis of waste tires in a circulating fluidized-bed reactor. Energy 2001;26:385–99.

[45] Choi G, Oh S, Kim J. Non-catalytic pyrolysis of scrap tires using a newly developed two-stage pyrolyzer for the production of a pyrolysis oil with a low sulfur content. Appl Energy 2016;170:140–7.

[46] de Marco Rodriguez I, Laresgoiti MF, Cabrero MA, Torres A, Chom_on MJ, Caballero B. Pyrolysis of scrap tyres. Fuel Process Technol 2001;72:9–22.

[47] Unapumnuk K, Keener TC, Lu M, Liang F. Investigation into the removal of sulfur from tire derived fuel by pyrolysis. Fuel 2008;87:951–6.

[48] Mirmiran S, Pakdel H, Roy C. Characterization of used tire vacuum pyrolysis oil: nitrogenous compounds from the naphtha fraction. J Anal Appl Pyrolysis 1992;22:205–15.

[49] Chen X, Clet G, Thomas K, Houalla M. Correlation between structure, acidity and catalytic performance of WOx/Al2O3 catalysts. J Catal 2010;273:236–44.

[50] Murugan S, Ramaswamy MC, Nagarajan G. Performance, emission and combustion studies of a DI diesel engine using distilled tyre pyrolysis oil-diesel blends. Fuel Process Technol 2008;89:152–9.

[51] Chen T, Shen Y, Lee W, Lin C, Wan M. An economic analysis of the continuous ultrasound-assisted oxidative desulfurization process applied to oil recovered from waste tires. J Clean Prod 2013;39:129–36.

[52] _Ilkılıç C, Aydın H. Fuel production from waste vehicle tires by catalytic pyrolysis and its application in a diesel engine. Fuel Process Technol 2011;92: 1129–35.

[53] Miandad R, Nizami AS, Rehan M, Barakat MA, Khan MI, Mustafa A, et al. Influence of temperature and reaction time on the conversion of polystyrene waste to pyrolysis liquid oil. Waste Manage 2016;58:250–9.

[54] Miandad R, Barakat MA, Aburiazaiza AS, Rehan M, Ismail IMI, Nizami AS. Effect of plastic waste types on pyrolysis liquid oil. Int Biodeterior Biodegr 2017;119:239–52.

[55] Miandad R, Barakat MA, Aburiazaiza AS, Rehan M, Nizami AS. Catalytic pyrolysis of plastic waste: a review. Process Saf Environ Prot 2016;102:822–38.

[56] Ouda OKM, Raza SA, Nizami AS, Rehan M, Al-Waked R, Korres NE. Waste to energy potential: a case study of Saudi Arabia. Renew Sustain Energy Rev 2016;61:328–40.

[57] Nizami AS, Shahzad K, Rehan M, Ouda OKM, Khan MZ, Ismail IMI, et al. Developing waste biorefinery in Makkah: a way forward to convert urban waste into renewable energy. Appl Energy 2017;186(Part 2):189–96.